5 May 2006 | $10

Science

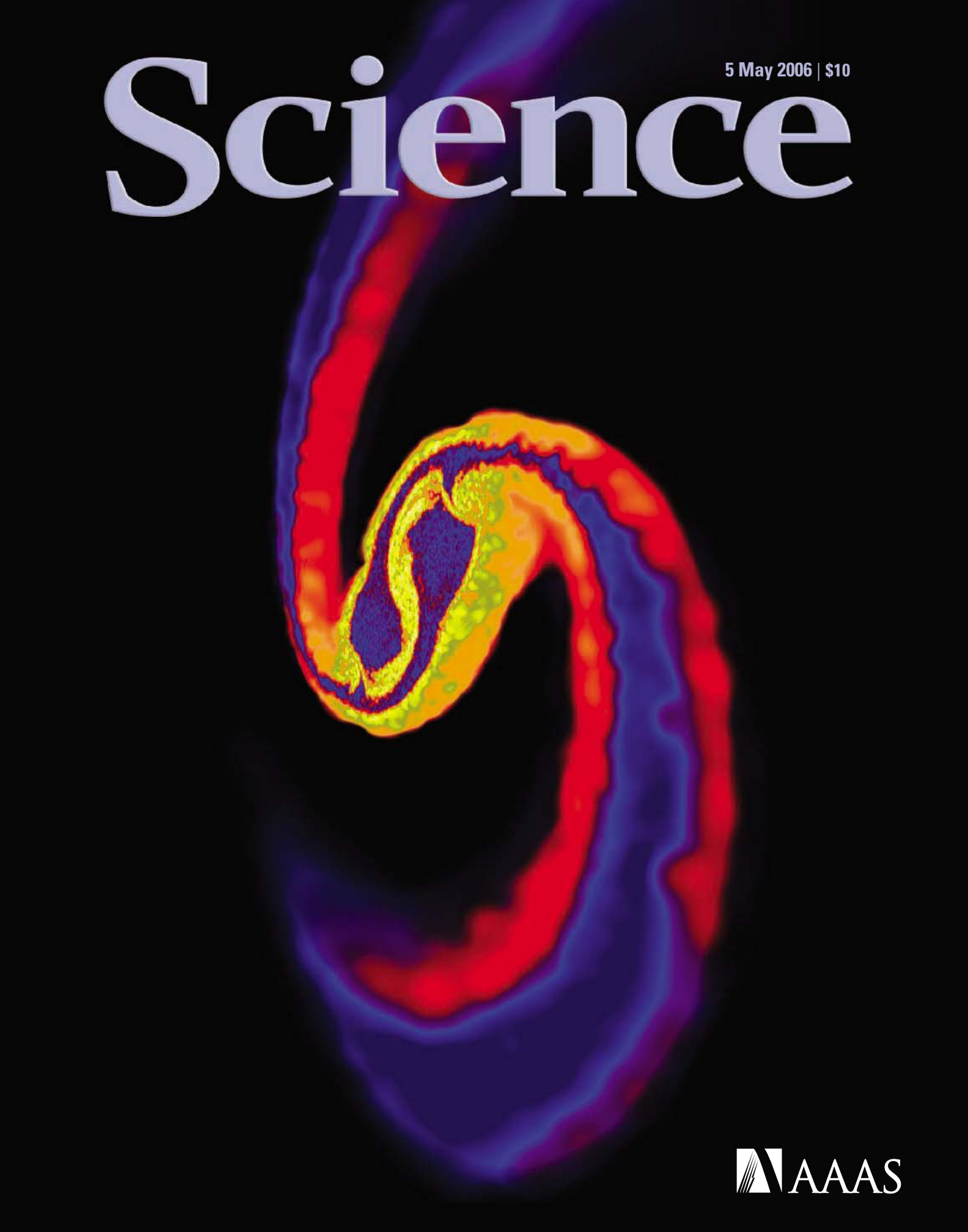

AAAS

Don't let temperature hold you back.

Only StrataScript® 5.0 RT delivers reliable results at any temperature.

Our new StrataScript® 5.0 Multi-Temperature Reverse Transcriptase (RT) delivers high cDNA yield over a broader cDNA synthesis temperature range (37–60°C). This unique, multi-temperature capability allows you to use the optimal reaction temperature for your template and primers without having to change your reverse transcriptase. Achieve 10-fold greater yield of amplifiable cDNA from lower RNA input levels and up to four-fold better yields of full-length cDNA.

Choose the Temperature You Need

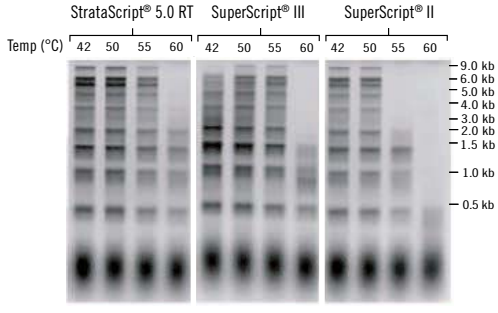

Need More Information? Give Us A Call:

Stratagene US and Canada
Order: 800-424-5444 x3
Technical Service: 800-894-1304 x2

Stratagene Europe
Order: 00800-7000-7000
Technical Service: 00800-7400-7400

Stratagene Japan K.K.
Order: 3-5821-8077
Technical Service: 3-5821-8076

www.stratagene.com

Ask Us About These Great Products:

StrataScript® 5.0 Multi-Temperature Reverse Transcriptase	**2,000U**	**600098**
	10,000U	**600100**

STRATAGENE®

Believe it!

DNA Sequencing for $2.50 per reaction.

- Read length up to 900 bases.
- High quality electropherograms.
- Fast turnaround.
- Plasmid and PCR purification available.

POLYMORPHIC
Polymorphic DNA Technologies, Inc.℠

www.polymorphicdna.com
info@polymorphicdna.com

1125 Atlantic Ave., Ste. 102
Alameda, CA 94501

Polymorphic exclusively uses ABI 3730XL sequencers.
Data delivered via secure FTP, email or CD.
No charge for standard sequencing primers.
384 sample minimum order.
96 well plates only—no tubes.

888.362.0888

For more information please visit
www.polymorphicdna.com

GE Healthcare

Faster protein purification? It's not rocket science.

HiTrap™ columns give you pure proteins with less effort. They come prepacked with the widest choice of media, ensuring results you can depend on in a broad range of applications, and the highest level of convenience.

But we're never content to stand still. We constantly strive for new innovations for tomorrow's research and drug development. And thanks to our technological achievements and global presence, we're able to help you turn your scientific ideas into reality – bringing science to life and helping transform healthcare.

We call it Life Science Re-imagined.

Discover how HiTrap columns can help power your protein purification.
Visit www.gehealthcare.com/life

imagination at work

GE Healthcare Bio-Sciences AB, a General Electric Company.
Björkgatan 30, 751 84 Uppsala, Sweden.

GE05-06

Volume 312, Issue 5774

COVER

A snapshot from computer simulations of the collision of two neutron stars, about 3 milliseconds after impact. Spiral arms form as the stars shred each other by their strong tidal forces. The colors represent the strength of the magnetic fields produced in the merger, here already amplified in the central regions to values exceeding any previously known in the universe (yellow-white regions). See page 719.

Image: D. J. Price and S. Rosswog

DEPARTMENTS

EDITORIAL

NEWS OF THE WEEK

NEWS FOCUS

LETTERS

BOOKS *ET AL.*

POLICY FORUM

PERSPECTIVES

CONTENTS continued **>>**

Systems Biology — RNA Purification

Standardized RNA solutions guarantee comparable results

Convenient RNA purification

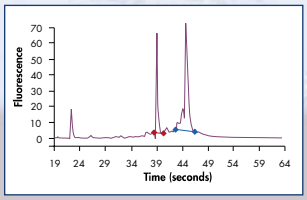

Purification of high-quality RNA

Advance your gene expression research with standardized solutions for RNA purification!

QIAGEN RNA solutions standardize the purification of RNA from biological samples.

Benefits include:

- **Reliability** — highly pure, intact RNA for standardized results in all downstream applications
- **Convenience** — easy-to-use kits with minimal protocol steps
- **Speed** — ready-to-use RNA purified in as little as 25 minutes
- **Versatility** — manual and automated kits for a wide range of sample types, sizes, and throughputs

Visit www.qiagen.com/goto/RNAsolutions to find out more!

QIAGEN

Science

SCIENCE EXPRESS

www.sciencexpress.org

ASTRONOMY

Why the Cosmological Constant Is Small and Positive
P. J. Steinhardt and N. Turok
Models in which our universe repeatedly grows from a big bang and then collapses produce a small cosmological constant consistently, not only as a special case.
>> Science *Express Perspective by A. Vilenkin*
10.1126/science.1126231

PERSPECTIVE: The Vacuum Energy Crisis
A. Vilenkin
>> Science *Express Research Article by P. J. Steinhardt and N. Turok*
10.1126/science.1128570

STRUCTURAL BIOLOGY

Structure of the Eukaryotic Thiamine Pyrophosphate Riboswitch with Its Regulatory Ligand
S. Thore, M. Leibundgut, N. Ban
The structure of a common metabolite bound to a ubiquitous riboswitch shows how its ligand turns it off, suppressing translation of genes for the metabolite's synthesis.
10.1126/science.1128451

PLANT SCIENCE

***CO/FT* Regulatory Module Controls Timing of Flowering and Seasonal Growth Cessation in Trees**
H. Böhlenius et al.
Poplar, a perennial tree, contains genes controlling flowering and the onset of dormancy that are homologs of flowering time genes in *Arabidopsis*.
10.1126/science.1126038

BREVIA

ATMOSPHERIC SCIENCE

RESEARCH ARTICLE

CHEMISTRY

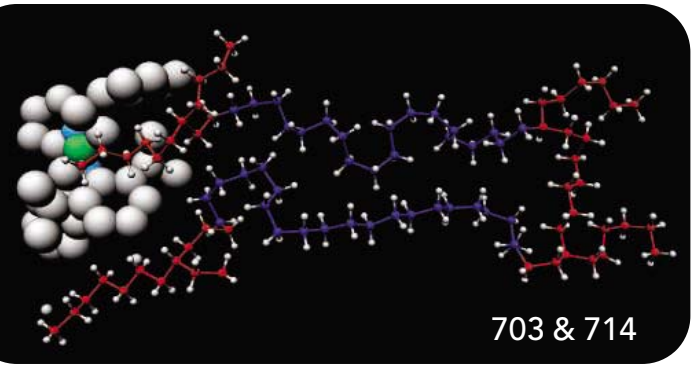

REPORTS

ASTROPHYSICS

CHEMISTRY

PLANETARY SCIENCE

GEOCHEMISTRY

CONTENTS continued >>

"I think the dosage needs adjusting. I'm not nearly as happy as the people in the ads."

It's time for genetics.

What if you could use DNA to identify patients who respond well to your drug? You might use that knowledge to reach more patients and expand your market, or to get a drug to market faster. Either way – patients win. Perlegen is helping drug companies do just that – today.

Working with you, we can comprehensively analyze the DNA from hundreds of patients taking your drug. Out of the millions of genetic variations between patients, we help you identify the ones that are associated with strong efficacy, poor efficacy, or side effects. Perlegen's unparalleled coverage of the genome and experienced team of analysts mean you get clinically relevant answers, not just data, in a matter of months.

We partner with the top pharmaceutical companies around the world. We also license late-stage drugs. If you have a drug that can benefit from our approach, please contact us.

Patients are waiting.

genetics@perlegen.com
Mountain View, California • 650-625-4500
Tokyo, Japan • +81 (0)3 3444-6080
www.perlegen.com

Targeting today's drugs. Discovering tomorrow's.™

PERLEGEN SCIENCES®

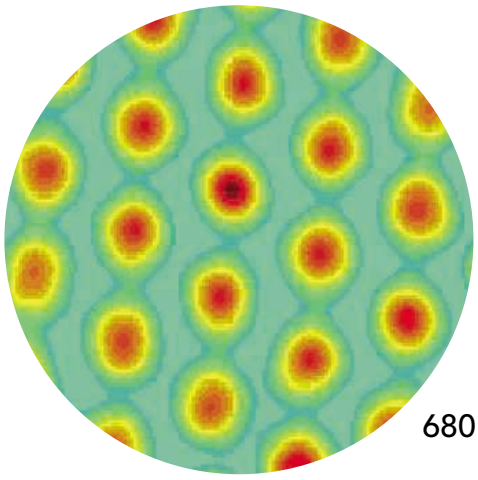

680 & 758

REPORTS *CONTINUED...*

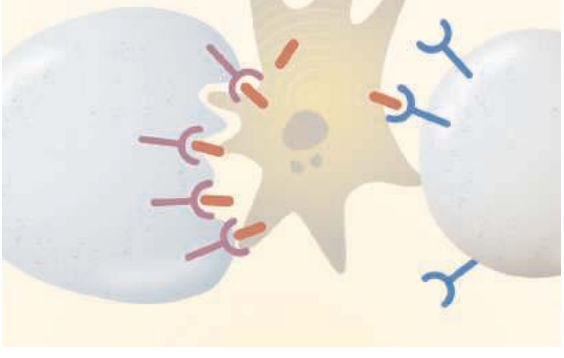

709 & 738

AAAS
ADVANCING SCIENCE, SERVING SOCIETY

SCIENCE (ISSN 0036-8075) is published weekly on Friday, except the last week in December, by the American Association for the Advancement of Science, 1200 New York Avenue, NW, Washington, DC 20005. Periodicals Mail postage (publication No. 484460) paid at Washington, DC, and additional mailing offices. Domestic individual membership and subscription (51 issues): $139 ($74 allocated to subscription). Domestic institutional subscription (51 issues): $650; Foreign postage extra: Mexico, Caribbean (surface mail) $55; other countries (air assist delivery) $85. First class, airmail, student, and emeritus rates on request. Canadian rates with GST available upon request, GST #1254 88122. Publications Mail Agreement Number 1069624. **Printed in the U.S.A.**

Change of address: Allow 4 weeks, giving old and new addresses and 8-digit account number. **Postmaster:** Send change of address to *Science*, P.O. Box 1811, Danbury, CT 06813–1811. **Single-copy sales:** $10.00 per issue prepaid includes surface postage; bulk rates on request. **Authorization to photocopy** material for internal or personal use under circumstances not falling within the fair use provisions of the Copyright Act is granted by AAAS to libraries and other users registered with the Copyright Clearance Center (CCC) Transactional Reporting Service, provided that $18.00 per article is paid directly to CCC, 222 Rosewood Drive, Danvers, MA 01923. The identification code for *Science* is 0036-8075/83 $18.00. *Science* is indexed in the *Reader's Guide to Periodical Literature* and in several specialized indexes.

CONTENTS continued **>>**

Criterion™ Precast Gel System

Criterion — the real king of protein electrophoresis.

Often imitated, never equaled, Bio-Rad's Criterion precast gel system is the right choice for those who demand genuine quality and convenience.

Outstanding Performance
Criterion is famous for straight bands, excellent resolution, and gel-to-gel reproducibility.

Stellar Composition*
The integrated upper buffer chamber ensures leak-free runs every time. Its patented design enables quick, safe opening of cassettes without any additional tools.

Fantastic Footwork*
The patented J-foot design allows easy removal of the gel from its cassette without ripping or tearing. No tools required!

For a closer look, visit us on the Web at **criterion.bio-rad.com**

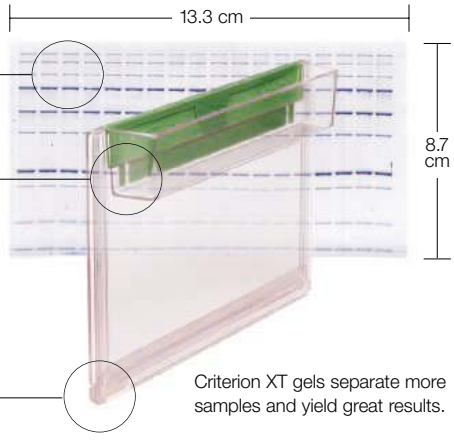

Criterion XT gels separate more samples and yield great results.

* US patents 6,093,301 and 5,073,246.

Visit us on the Web at **discover.bio-rad.com**
Call toll free at 1-800-4BIORAD (1-800-424-6723);
outside the US, contact your local sales office.

BIO-RAD

Investigating the neuromuscular junction.

SCIENCE'S **STKE**

www.stke.org SIGNAL TRANSDUCTION KNOWLEDGE ENVIRONMENT

TEACHING RESOURCE: The Sherlock Holmes Lab—Investigations in Neurophysiology
E. M. Adler and P. J. Schwartz
This exercise can be used to assess student understanding of basic electrophysiology and synaptic transmission.

TEACHING RESOURCE: Cell Culture as a Model System for Teaching—Using PC12 Cells
E. M. Adler
This exercise allows undergraduate neuroscience students to investigate signaling related to neuronal differentiation.

Lamin A and aging.

SCIENCE'S **SAGE KE**

www.sageke.org SCIENCE OF AGING KNOWLEDGE ENVIRONMENT

NEWS FOCUS: A Shared Splice Site?
M. Leslie
Defect behind "premature aging" disorder might foster normal aging.

GENES/INTERVENTIONS DATABASE: LMNA
Mutations that affect lamin A, a component of the nuclear lamina, cause Hutchinson-Gilford progeria syndrome.

SCIENCE**NOW**

www.sciencenow.org DAILY NEWS COVERAGE

Mineral Time Capsules on Mars?
Organic compounds trapped in sulfate minerals may reveal traces of life.

Evolution Gets Hot and Steamy
The pace of molecular evolution picks up in the tropics.

The Body's Alternative Energy Source
Study provides further evidence that lactic acid is an important muscle backup fuel.

Inspecting nuclear programs.

SCIENCE **CAREERS**

www.sciencecareers.org CAREER RESOURCES FOR SCIENTISTS

EUROPE: A Career in Nuclear Inspection
J. Bohannon
Paulus Nangonya is the youngest nuclear inspector ever at the United Nations International Atomic Energy Agency.

US: A Novel Look at Postdocs
B. Benderly
Researchers in Allegra Goodman's fictional lab put postdoc life under the microscope.
>> Book Review p. 698

MISCINET: The Surprising Effect of Diversity on Groups
A. Sasso
A recent study indicates that juries with a mix of ethnicities perform better than all-white juries.

US: Surf's Up
A. Fazekas
The passion of a lifeguard and surfer carried him to a career in ocean science.

GRANTSNET: May 2006 Funding News
J. Fernandez
Get the latest index of research funding, scholarships, fellowships, and internships.

Separate individual or institutional subscriptions to these products may be required for full-text access.

All truths are easy to understand once they are discovered; the point is to discover them.

Galileo Galilei

Italian physicist, astronomer, philosopher (1564-1642)

Shimadzu is a participant in
the 54th ASMS Conference on Mass Spectrometry
in Seattle, Washington from May 28 to June 1, 2006.

Please visit us at
Booth # 115 or in Hospitality Suite Grand III-FGH
in the Westin Hotel

Shimadzu transcends modern assumptions and limits to shine a beam of light on yet undiscovered scientific truths. Shimadzu believes in the value of science to transform society for the better. For more than a century, we have led the way in the development of cutting-edge technology to help measure, analyze, diagnose and solve problems. The solutions we develop find applications in areas ranging from life sciences and medicine to flat-panel displays. We have learned much in the past hundred years. Expect a lot more.

www.shimadzu.com

SHIMADZU

EDITED BY STELLA HURTLEY AND PHIL SZUROMI

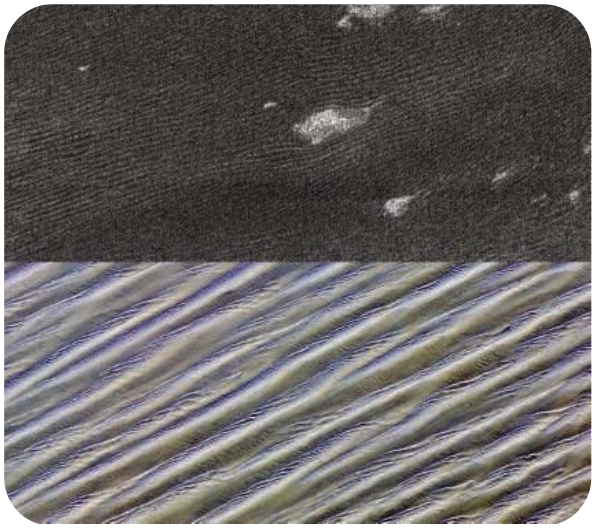

Titan's Dunes

Cassini radar observations of Titan by **Lorenz *et al.*** (p. 724; see the Perspective by **Lancaster**) show that large regions of its surface contain parallel or 'seif,' dune fields, similar to those in the Sahara Desert on Earth. The height of the dunes is about 150 meters, and they occur in regions up to 1500 by 200 kilometers in extent, especially near the equator. The east-west alignment of the dunes and other flow features suggest that they form from the actions of easterly surface winds. The presence of dunes indicates that processes create sand-sized particles, and that Titan's equatorial surface lacks persistent liquids that would otherwise trap the sand.

Shuttle Service for Polymer Synthesis

In a "living" polymerization, each polymer chain grows at a steady rate from a single catalyst site. The successive removal and addition of different monomers to the reactor yields block copolymers with structurally distinct chain segments. **Arriola *et al.*** (p. 714; see the Perspective by **Gibson**) present an alternative strategy for building block copolymers in which diverse monomers are all present at once and a molecular shuttle transfers growing polymer chains back and forth between catalysts with differing selectivities. The shuttling technique tolerates high temperatures (to maintain polymer solubility) and is amenable to economically efficient continuous flow conditions. Screening of a wide range of catalyst and shuttle combinations revealed useful elastomeric copolymers in which polyethylene blocks alternate with high and low levels of a higher olefin, 1-octene, with a high degree of block intermixing.

Turbulent Route to Extreme Magnetic Fields

Short gamma-ray bursts are thought to result when two compact neutron stars merge to form a black hole. Strong magnetism has been thought to produce the gamma rays, but the mechanism is not clear. **Price and Rosswog** (p. 719, published online 30 March; see the cover) have modeled the death throes of a binary pair of neutron stars and included the effects of magnetism as well as hydrodynamics and gravity. In their simulations, a strong shear layer develops at the interface between the two stars during the first few milliseconds of the merger. Turbulent eddies within this layer amplify the magnetic fields to greater than 10^{15} Gauss, which is even stronger than those in known magnetic stars. This process occurs very quickly, so that the gamma-ray bursts may be emitted before the black hole is actually formed.

CREDITS (TOP TO BOTTOM): LORENZ *ET AL.*; BUSEMANN *ET AL.*

Primitive Organics

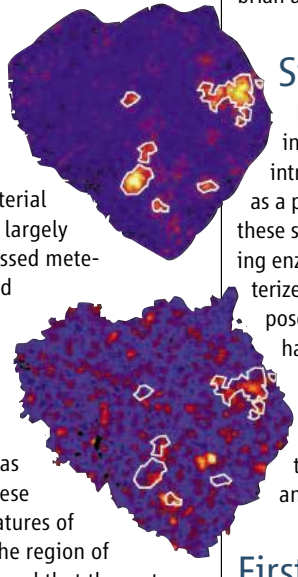

Interplanetary dust particles are particularly carbon rich, and are thought to have their origins outside the solar system in interstellar material and comets. This primitive material was thought to have been largely lost in more heavily processed meteorites. Using hydrogen and nitrogen isotopes, **Busemann *et al.*** (p. 727; see the Perspective by **Marty**) show that the organic matter in carbonaceous meteorites is as primitive as that in the dust grains. These results imply that temperatures of the protosolar nebula in the region of the asteroid belt were low and that the meteoritic material has suffered little alteration since then.

Holding On into the Cambrian

Vendobionts are one of several enigmatic animals from the Ediacaran, the time before the Cambrian radiation of animals, and represent some of Earth's earliest animals. Details of their relation to later animals have been unclear; indeed, most Ediacaran animals seem to have no later or extant relatives. **Shu *et al.*** (p. 731) now describe a vendobiont from the Lower Cambrian of China in which the preservation is sufficient to see internal soft tissues. The fossil suggests that they lived attached to the sea floor by a stalk. These animals not only survived the Ediacaran but also show some similarity to younger Cambrian animals.

Starved for Energy

During times of food deprivation or increased energy demand, mammals use intracellular triglycerides stored in fat tissue as a primary energy source. Mobilization of these stores requires activation of lipid-degrading enzymes. **Haemmerle *et al.*** (p. 734) characterized mice deficient in one such enzyme, adipose triglyceride lipase (ATGL). Its absence had major metabolic consequences, including alterations in glucose tolerance and insulin sensitivity, defective thermogenesis, and massive accumulation of lipids in the heart that resulted in cardiomyopathy and premature death.

First, Collect Antigens

Antibodies are produced by B cells after antigens stimulate receptors on their surface and other appropriate signals have been received. If antigens are bound to the surface of another cell, activation signals can be particularly strong and allow B cells to discriminate among a wide range of antigen affinities. **Fleire *et al.*** (p. 738; see the Perspective by **Harnett**) show that B cells can actually focus antigen into aggregates that resemble the well-characterized immune synapses of T cells. After initial

Continued on page 655

Cool Products for Stem Cell Research

Chemicon offers a wide range of reagents for stem cell culture through our subsidiary Specialty Media, a trusted name in cell culture products and services. New products include reagents for mouse embryo and ES Cell culture, specialized cell culture, cell dissociation and molecular biology.

- **Embryonic Stem Cells & Feeder Cells**
- **Liquid Cell Culture Media & Reagents**
- **Mouse Embryo Media & Reagents**
- **ES Cell Qualified Products**
- **Cell Dissociation Reagents**
- **Gene Transfer & Expression Products**

Together with Chemicon's existing product portfolio that includes ESGRO®, Leukemia Inhibitory Factor (LIF), stem cell marker antibodies & kits, Chemicon offers a complete solution for your stem cell research needs.

CHEMICON® INTERNATIONAL
a Serologicals® Company

Europe
Austria 01 585 4116
France 0805 300 576
Germany 0800 759 8965
Sweden 040 22 42 00
UK 0800 0190 333

USA
800 437 7500

Australia
03 9839 2000

To find your local distributor, please call +44 (0) 23 8026 2233 or visit our website

www.chemicon.com

CHEMICON® INTERNATIONAL upstate® cell signaling solutions Celliance®

the Serologicals® Group

1589-0206

Continued from page 653

contact, B cells spread themselves over the other cell and then contract, gathering up antigens in the process. This response depended on both antigen affinity and ligand occupancy, suggesting how both parameters might be used to optimize an evolving antibody response.

Who Let the Drugs Out?

Bacteria achieve multidrug resistance partly through families of integral membrane transporters that efflux drugs. Transporters in one such family, the Major Facilitator Superfamily (MFS), export a broad spectrum of hydrophobic compounds. Now **Yin *et al.*** (p. 741) have determined a 3.5 angstrom resolution structure for EmrD, a proton-dependent MFS transporter in the inner membrane of *Escherichia coli*. Two long loops extend into the inner leaflet of the membrane bilayer where they likely recognize and bind substrate.

Makings of a Modified Histone Binding Module

To understand how histone modifications affect processes such as transcriptional regulation and epigenetic inheritance, we must understand how these modifications are recognized and deciphered. **Huang *et al.*** (p. 748; published online 6 April) determined crystal structures of the double tudor domain of the histone demethylase JMJD2A alone and in complex with its substrate, a methylated histone peptide. The two domains form an interdigitated structure that is required for binding to the methylated histone peptide. This reveals the potential for forming new histone binding modules from familiar effector domains.

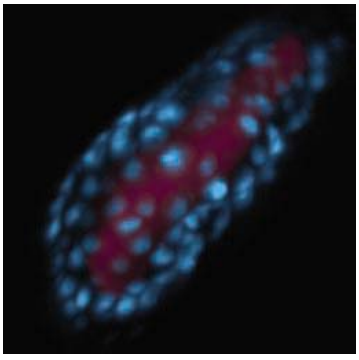

A Small, But Not So Simple, Heart

Vertebrates hearts begin as a valveless tube that has generally been described as a peristaltic pump. Using confocal laser scanning microscopy and time-resolved three-dimensional visualization methods, **Forouhar *et al.*** (p. 751) followed the heart wall and blood cells in the zebrafish embryo. The embryonic heart tube did not show the properties expected of a peristaltic pump. Instead, elastic wave propagation and reflection in the heart tube produced an action that is more consistent with a hydroimpedance pump influenced by mechanical features of the heart tube, such as its diameter, length, and elasticity.

Defining the Neural Basis of Dread

Deciding between two choices can be difficult, particularly when they are separated in time. Economic theory accommodates the calculation by discounting the future outcome by the amount of time, most simply via a hyperbolic function. An additional factor is the cost of waiting, which can be represented clearly when the outcomes are unpleasant (electric shocks to one's foot), and the choice is between a stronger shock in a few seconds versus a weaker shock a half minute later. Many people will opt to "get it over with," primarily, one assumes, to avoid the anticipation of future pain, which is used as an operational definition by **Berns *et al.*** (p. 754) in examining the neural basis of dread. Areas within the cortical pain matrix respond in a fashion that can be associated with the extent of dread expressed across individuals.

The Grid in the Brain

Spatial navigation depends on several brain regions that interface with the medial entorhinal cortex (MEC), whose layer II cells express an environment-independent, gridlike coordinate system. The interaction of these grid cells with other cell types in the enthorhinal cortex is not well understood. **Sargolini *et al.*** (p. 758; see the Perspective by **Loewenstein**) analyzed the firing properties of neurons from different layers in the most posterior portion of the medial entorhinal cortex in rats that explored a square arena. The neurons of layer II were predominately grid cells, but in deeper layers, the grid cells commingled with head-direction cells. Some cells in the deep layers signal a conjunction of both head direction and spatial grid information. Cell activity in all layers was modulated by running speed.

CREDIT: FOROUHAR *ET AL.*

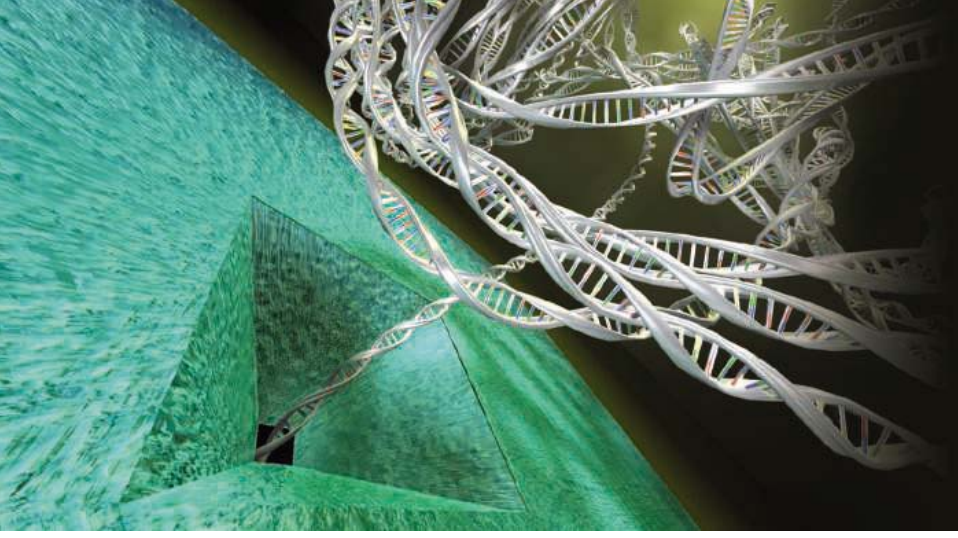

Manuscript submission to acceptance: 5 weeks

Manuscript submission to published on the web: 8 weeks

Faster Publication of Your High-Impact Research in *Nano Letters*

Nano Letters offers authors extremely rapid time to publication — one of the fastest in the industry — with manuscript submission to acceptance in **5 weeks** and manuscript submission to published on the web in **8 weeks**.

The #1 most-accessed article in 2005 out of all ACS journal articles published in 2005 appeared in *Nano Letters*. The article, "**Directional Control in Thermally Driven Single-Molecule Nanocars**", is available for free access for a limited time at **http://pubs.acs.org/mostaccessed**

For rapid communication of nanoscale research, *Nano Letters* is the leading forum.

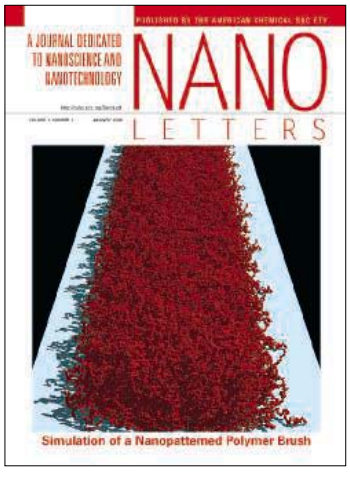

ISI impact factor 8.449

2006 SUBSCRIPTION INFORMATION
Volume: 6, 12 Issues
Print Edition ISSN: 1530-6984; Web Edition ISSN: 1530-6992
Institutional Subscription Rate: $1,356; (Outside North America: $1,436)
For more information, call Member & Subscriber Services:
1-888-338-0012 in U.S. and Canada, or
(614) 447-3674 outside North America

Co-Editor
A. Paul Alivisatos
University of California, Berkeley

Co-Editor
Charles M. Lieber
Harvard University

To submit your manuscript, register for RSS feeds or e-mail Alerts, and view a free sample issue, go to http://pubs.acs.org/NanoLett

ACS PUBLICATIONS
HIGH QUALITY. HIGH IMPACT.

Al Teich is director of Science and Policy Programs at the American Association for the Advancement of Science.

Wendy D. White is director of the Board on International Scientific Organizations at the National Academies.

The High Cost of Coming to America

IMAGINE THAT YOU ARE A RECENTLY RETIRED PROFESSOR FROM A UNIVERSITY IN THE UNITED STATES. A democratic country friendly to the United States has invited you to give a lecture at a major scientific event. You are a life-long academic with an international reputation who has traveled often to that country. Aware of new visa regulations, you schedule an interview at one of four consulates in the United States. The average waiting time for the interview is 4 months, but you are successful, through the intercession of your hosts, in getting an earlier date. You fly to the nearest consulate, stand in line for several hours, and finally see an officer. You pay the $100 application fee and your photograph and fingerprints are taken. You're asked to explain your research, starting with your Ph.D. thesis, completed over 40 years ago. You do this but to no avail, as the officer lacks scientific training and does not understand. Your application is refused and will be reconsidered only after you provide additional written information, the review of which will somehow ensure that you are not a security threat. This will take at least 2 more weeks. You return home without your visa and cancel your trip, because even if your responses pass scrutiny, your visa would be issued only after the date on which you have been invited to lecture.

An absurd scenario? Perhaps—but barriers like these face many scientists who apply for a visa to visit the United States. That most are willing to put up with them testifies to the importance of the United States in world science. But to some, the transaction costs are simply too high, and as we saw recently in the case of Goverdhan Mehta, more and more scientists are simply saying "no." Like Mehta, a distinguished chemist from India who serves as president of the International Council for Science (ICSU), they find the process humiliating and unjustified. If other countries treated U.S. scientists like this, we would certainly protest.

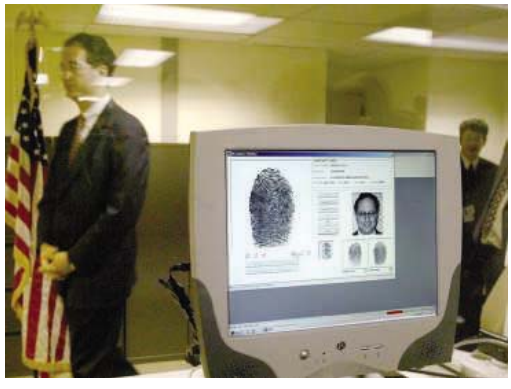

After the attacks of September 11, 2001, the federal government enacted new security policies, but it quickly became apparent that they would cause serious problems for international collaboration in science and education. The number of visa applicants subject to review under Visas Mantis, a program used since 1998 to provide extra scrutiny for visitors with backgrounds in certain sensitive areas of science and technology, grew from about 1000 in 2000 to about 20,000 in 2003. The massive backlogs led to delays in visa issuance of 2 months and longer. The need to appear in person at a consulate to undergo an interview and submit biometric information has been a financial hardship for many. And dignity is an issue; many applicants have reported rude, insensitive treatment.

The research and higher education communities recommended improvements, and the State Department responded with efforts to address some of the problems. Compared to 2003, U.S. consulates today are better staffed and officers are better trained. There are more efficient clearance procedures in place, resulting in average processing times for Visas Mantis reviews of 14 days, once the applicant completes the interview process. There is more transparency in the system, as consulate Web sites provide information about appointments for interviews and average wait times.

But when, in 2006, the president of ICSU can still experience what he did, one has to question whether these incremental improvements are sufficient. Patching holes in the visa system is no longer enough. The scientific community needs to join with the Department of State to examine the fundamental assumptions that underlie current visa policies, especially as they apply to foreign scientists, engineers, and students. A joint working group could peel back the layers of policies and procedures to determine if, for example, the interviews and the Visas Mantis reviews are achieving their intended purpose; if a "trusted traveler" program would avoid subjecting frequent visitors to repetitive, irritating, and time-consuming screening; and if consular officers have the tools and training they need to do their jobs effectively. In short, the working group could help ensure that the benefits of the current system offset the monetary costs, damage to our nation's reputation, and harm to our scientific and educational enterprise. Our security, the strength of our nation's science, and our international technological competitiveness depend on getting the system right and on finding comprehensive solutions to the visa problem.

Al Teich and Wendy D. White

10.1126/science.1127775

CREDIT (RIGHT): SERGEY PONOMAREV/AP

More Modes

INSTRUMENTS

SOFTWARE

VALIDATION

Molecular Devices is the leading supplier of benchtop microplate readers. Now we're giving you more modes in one compact instrument by introducing SpectraMax® M5^e, a tunable benchtop reader that gives you superior results in five modes.

- Widest spectrum of absorbance and fluorescence applications in microplates or cuvettes
- Sensitive luminescence at one or multiple wavelengths
- FP performance that is unparalleled by any monochromator-based instrument
- TRF, HTRF®, IMAP® TR-FRET, and other TR-FRET assay capabilities
- Complete hardware and software validation tools

Whether you're screening at high throughput or developing assays in cuvettes or 6- to 384-well microplates, SpectraMax M5^e is the only reader you'll need.

Expect more. We'll do our very best to exceed your expectations.

Molecular Devices

tel. +1-800-635-5577 | www.moleculardevices.com

Members of the species-rich families Geometridae (above) and Carabidae (right).

ECOLOGY/EVOLUTION

Think Globally, Conserve Locally

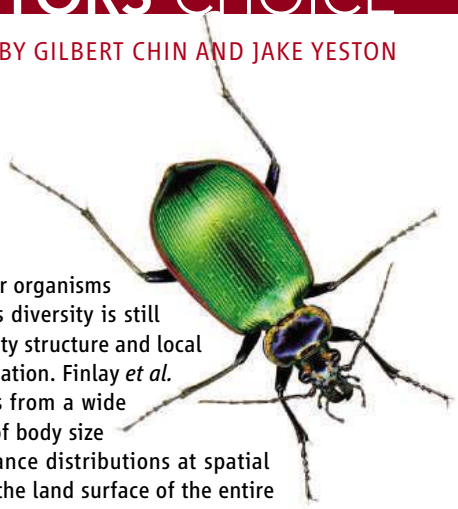

Insects are undoubtedly the most diverse multicellular organisms on Earth, yet our understanding of the extent of this diversity is still patchy, and to be able to predict patterns of community structure and local diversity would be important in the context of conservation. Finlay *et al.* analyzed data for more than 600,000 insect species from a wide variety of localities, and report self-similar patterns of body size distribution, species-area relationships, and abundance distributions at spatial scales ranging from a few hectares (Hilbre Island) to the land surface of the entire planet. The similarity of the observed patterns presents a useful tool for monitoring the status of insect communities in the face of human disturbance (including climate change); deviations from the general patterns, such as an unusual distribution of body sizes in an insect community, could provide useful indicators of local extinctions. — AMS

Proc. R. Soc. London Ser. B **273**, 10.1098/rspb.2006.3525 (2006).

CHEMISTRY

A Higher Power

Nearly 80 years ago, Born and Oppenheimer showed that during a typical molecular transformation, electronic and nuclear motions can be treated independently of each other. The validity of this Born-Oppenheimer (BO) approximation arises from the nearly 2000-fold mass difference between electrons and protons, which results in the electrons completing their rearrangement before the slower, heavier nuclei begin to move. The approximation provides a mathematically tractable framework for accurate modeling of many chemical reactions (for example, see Nieto *et al.,* Reports, 7 April 2006, p. 86). Although there are a number of well-established cases in which the approximation breaks down, these systems generally involve coupling between electronic and vibrational coordinates, rather than mass variations.

Takahashi and Takatsuka explore the breakdown of the BO approximation in unusual molecules, of interest in fusion research, which host more massive negatively charged particles in place of electrons. Specifically, they model H_2^+ analogs in which two protons bind either an antiproton or a muon (a product of nuclear decay ~200 times heavier than an electron). Using semiclassical trajectory calculations, they find that the error in the approximation scales with the 3/2 power of the light-to-heavy particle mass ratio. This result implies that the BO approximation is valid over a wider mass range than is commonly assumed from a 1/4 power mass dependence that appears in the theory's derivation. The authors further confirm this error-scaling relation by carrying out an analysis of the system's energy based on the same perturbational approach used by Born and Oppenheimer. — JSY

J. Chem. Phys. **124**, 144101 (2006).

GEOCHEMISTRY

Wrinkles of Life

A variety of geochemical evidence implies that life evolved on Earth roughly 3.5 billion years ago, yet more direct evidence—specifically, fossils or fossil-derived structures such as stromatolites or alteration pits—is still sparse or disputed in rocks dating several hundred million years closer to the present. Most of the evidence has been found in siliceous oozes or sediments, carbonate rocks, or altered basalt from deep oceanic or hydrothermal settings.

Noffke *et al.* have discovered fossil microbial mats in another environment, South African tidal sandstones, dated to ~3.2 billion years ago. These rocks display wrinkles, layered roll-up structures, and carbon-rich laminations that resemble features seen in modern intertidal sandstones and commonly preserved in much younger rocks. Such structures form as ductile microbial mats are buried. Analysis of the carbon isotope compositions of the laminations further supports their bacterial origin. Concentration of these features at the top of sedimentary sequences formed in shallow water environments suggests that the microbes in the mats may have derived their energy through photosynthesis. — BH

Sandstone patterned by ancient microbes.

Geology **34**, 253 (2006).

MOLECULAR BIOLOGY

An Internal Iron Sensor

To a cyanobacterium, photosynthesis is a very important activity. One of the components of the photosystem I (PSI) complex is iron, which can be a limiting nutrient in a marine environment. Consequently, when iron levels are low, *Synechocystis* makes the iron stress–induced protein A (IsiA) and deploys it in circumferential formation around the valuable PSI centers, where it serves both to enhance the absorption of light and to dissipate excess photoenergy. Dühring *et al.* describe how, in times of plenty, the expression of *isiA* is controlled by a 177-nucleotide (nt) RNA, which is called IsrR and is transcribed from the complementary or noncoding strand of *isiA*. They propose that when iron is abundant, the IsrR RNA binds to the *isiA* mRNA and targets it for degradation. Because artificially decreasing IsrR levels does not produce an increase in

Continued on page 661

CREDITS (TOP TO BOTTOM): PETER ARNOLD/JAMES LASSWELL/TEXAS AGRICULTURAL EXPERIMENT STATION; NOFFKE *ET AL.*, *GEOLOGY* **34**, 253 (2006)

Vinton G. Cerf
Vice President and Chief Internet Evangelist
Google

Amy Wu
Computer Science Student
Stanford University

Benjamin Mako Hill
Research Assistant
MIT Media Laboratory

Maria Klawe
Dean of Engineering
Princeton University

Continued from page 659

isiA mRNA if enough iron is available, the authors suggest that another control element, such as an attenuator, must exist. In *Salmonella*, expression of the magnesium transporter MgtA is turned on when internal Mg^{2+} levels drop, and a critical regulatory element resides in the 5′ untranslated region (UTR) of the *mgtA* gene. Cromie *et al.* show that the 200-nt 5′ UTR of *mgtA* consists of a riboswitch (see also Thore *et al.*, *Science* Express, 4 May 2006) that adopts a transcription-attenuating, two stem-loop structure when Mg^{2+} is bound. The 160-nt 5′ UTR region of *isiA* may harbor an ion- (or iron-) sensor. — GJC

Proc. Natl. Acad. Sci. U.S.A. **103**, 7054 (2006); *Cell* **125**, 71 (2006).

PHYSICS

Exciting the Nucleus

Modern laser sources can generate sufficient intensity to induce nuclear reactions. However, the excitation mechanism is indirect: optical laser photons deliver energy to electrons, creating a plasma, and the electrons in turn heat the nuclei sufficiently to overcome the barrier to fission or fusion.

Calculations by Bürvenich *et al.* suggest a plausible approach for direct nuclear excitation, using current and future generations of high-power laser systems emitting at x-ray frequencies. If the nuclei are accelerated to high velocities, the resulting Doppler shift of the laser light in the nuclear reference frame brings the nuclear transitions into resonance with the photon frequencies. This technique would enable nuclear quantum optics studies—analogous to the richly developed field of coherent electronic excitation—and could afford higher precision in measurements of nuclear properties, as well as control and detection. — DV

Phys. Rev. Lett. **96**, 142501 (2006).

IMMUNOLOGY

Rendered Powerless by Heme

Malaria represents one of the greatest threats to human health in tropical and subtropical regions. Aside from its direct effects, the *Plasmodium* parasite causes a general suppression of the immune system.

Millington *et al.* observed that mice infected with the rodent-specific strain *P. chabaudi* were less able to produce antibodies to a third-party antigen. Both in culture and in vivo, parasite-infected erythrocytes inhibited the maturation of dendritic cells, as shown by a reduction in the expression of activation markers. Hemozoin (the product of hemoglobin degradation) was found to impede dendritic cell maturation and, in turn, to reduce the ability to activate naïve T cell responses. During an infection with *P. chabaudi,* these effects on dendritic cells manifest themselves as a reduction in $CD4^+$ T cell proliferation and migration into B cell–rich regions of the lymph node. The subsequent deficit in T cell–assisted B cell expansion thereby offers an explanation for the reduced antibody production seen in infected mice. — SJS

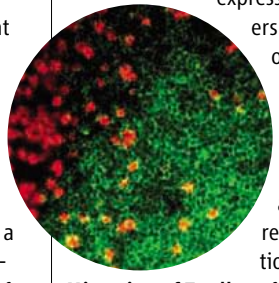

Migration of T cells (red) into a population of B cells (green).

CREDIT: MILLINGTON *ET AL.*, *J. BIOL.* **5**, 5 (2006)

J. Biol. **5**, 5 (2006).

Science stke AAAS

www.stke.org

<< FSH Increases Bone Resorption

Osteoporosis, a decrease in bone mass, is a common condition affecting postmenopausal women and is due at least in part to decreased estrogen. Sun *et al*. show that follicle-stimulating hormone (FSH), a pituitary hormone that regulates estrogen production, has a direct effect on bone mass by stimulating the differentiation and resorptive activity of osteoclasts. The cells that degrade and resorb bone are osteoclasts, whereas osteoblasts are the bone-depositing cells. Mice deficient for FSHβ or the FSH receptor were hypogonadal and exhibited many symptoms of estrogen deficiency, yet had normal bone mass. Heterozygous mice ($FSH\beta^{+/-}$) had a 50% reduction in circulating FSHβ and showed decreased bone resorption, decreased abundance of circulating tartrate-resistant acid phosphatase (a marker of osteoclast activity), and decreased expression of osteoclast markers in bone marrow, all of which are consistent with the observed increase in bone density. In cultured cells, FSH stimulated osteoclastogenesis by stimulating differentiation, but not proliferation, and enhanced the resorptive activity of individual osteoclasts. These results point to a direct estrogen-independent effect of FSH on bone density and a crucial role for this hormone in postmenopausal osteoporosis. — NRG

Cell **125**, 247 (2006).

www.sciencemag.org

Science

1200 New York Avenue, NW
Washington, DC 20005
Editorial: 202-326-6550, FAX 202-289-7562
News: 202-326-6500, FAX 202-371-9227

Bateman House, 82-88 Hills Road
Cambridge, UK CB2 1LQ
+44 (0) 1223 326500, FAX +44 (0) 1223 326501

Subscription Services For change of address, missing issues, new orders and renewals, and payment questions: 800-731-4939 or 202-326-6417, FAX 202-842-1065. Mailing addresses: AAAS, P.O. Box 1811, Danbury, CT 06813 or AAAS Member Services, 1200 New York Avenue, NW, Washington, DC 20005

Institutional Site Licenses please call 202-326-6755 for any questions or information

Reprints: Author Inquiries 800-635-7181
Commercial Inquiries 803-359-4578
Corrections 202-326-6501

Permissions 202-326-7074, FAX 202-682-0816

Member Benefits Bookstore: AAAS/BarnesandNoble.com bookstore www.aaas.org/bn; Car purchase discount: Subaru VIP Program 202-326-6417; Credit Card: MBNA 800-847-7378; Car Rentals: Hertz 800-654-2200 CDP#343457, Dollar 800-800-4000 #AA1115; AAAS Travels: Betchart Expeditions 800-252-4910; Life Insurance: Seabury & Smith 800-424-9883; Other Benefits: AAAS Member Services 202-326-6417 or www.aaasmember.org.

science_editors@aaas.org	(for general editorial queries)
science_letters@aaas.org	(for queries about letters)
science_reviews@aaas.org	(for returning manuscript reviews)
science_bookrevs@aaas.org	(for book review queries)

Published by the American Association for the Advancement of Science (AAAS), *Science* serves its readers as a forum for the presentation and discussion of important issues related to the advancement of science, including the presentation of minority or conflicting points of view, rather than by publishing only material on which a consensus has been reached. Accordingly, all articles published in *Science*—including editorials, news and comment, and book reviews—are signed and reflect the individual views of the authors and not official points of view adopted by the AAAS or the institutions with which the authors are affiliated.

AAAS was founded in 1848 and incorporated in 1874. Its mission is to advance science and innovation throughout the world for the benefit of all people. The goals of the association are to: foster communication among scientists, engineers and the public; enhance international cooperation in science and its applications; promote the responsible conduct and use of science and technology; foster education in science and technology for everyone; enhance the science and technology workforce and infrastructure; increase public understanding and appreciation of science and technology; and strengthen support for the science and technology enterprise.

Information for Contributors

See pages 102 and 103 of the 6 January 2006 issue or access www.sciencemag.org/feature/contribinfo/home.shtml

EDITOR-IN-CHIEF **Donald Kennedy**
EXECUTIVE EDITOR **Monica M. Bradford**
DEPUTY EDITORS **R. Brooks Hanson, Katrina L. Kelner**
NEWS EDITOR **Colin Norman**

Editorial supervisory senior editors Barbara Jasny, Phillip D. Szuromi; **senior editor/perspectives** Lisa D. Chong; **senior editors** Gilbert J. Chin, Pamela J. Hines, Paula A. Kiberstis (Boston), Marc S. Lavine (Toronto), Beverly A. Purnell, L. Bryan Ray, Guy Riddihough (Manila), H. Jesse Smith, Valda Vinson, David Voss; **associate editors** Jake S. Yeston, Laura M. Zahn; **online editor** Stewart Wills; **associate online editor** Tara S. Marathe; **book review editor** Sherman J. Suter; **associate letters editor** Etta Kavanagh; **information specialist** Janet Kegg; **editorial manager** Cara Tate; **senior copy editors** Jeffrey E. Cook, Cynthia Howe, Harry Jach, Barbara P. Ordway, Jennifer Sills, Trista Wagoner; **copy editors** Alexis Wynne Mogul, Peter Mooreside; **editorial coordinators** Carolyn Kyle, Beverly Shields; **publication assistants** Ramatoulaye Diop, Chris Filiatreau, Joi S. Granger, Jeffrey Hearn, Lisa Johnson, Scott Miller, Jerry Richardson, Brian White, Anita Wynn; **editorial assistants** Lauren Kmec, Patricia M. Moore, Brendan Nardozzi, Michael Rodewald; **executive assistant** Sylvia S. Kihara

News senior correspondent Jean Marx; **deputy news editors** Robert Coontz, Jeffrey Mervis, Leslie Roberts, John Travis; **contributing editors** Elizabeth Culotta, Polly Shulman; **news writers** Yudhijit Bhattacharjee, Adrian Cho, Jennifer Couzin, David Grimm, Constance Holden, Jocelyn Kaiser, Richard A. Kerr, Eli Kintisch, Andrew Lawler (New England), Greg Miller, Elizabeth Pennisi, Robert F. Service (Pacific NW), Erik Stokstad; Katherine Unger (intern); **contributing correspondents** Barry A. Cipra, Jon Cohen (San Diego, CA), Daniel Ferber, Ann Gibbons, Robert Irion, Mitch Leslie (NetWatch), Charles C. Mann, Evelyn Strauss, Gary Taubes, Ingrid Wickelgren; **copy editors** Linda B. Felaco, Rachel Curran, Sean Richardson; **administrative support** Scherraine Mack, Fannie Groom **bureaus:** Berkeley, CA: 510-652-0302, FAX 510-652-1867, New England: 207-549-7755, San Diego, CA: 760-942-3252, FAX 760-942-4979, Pacific Northwest: 503-963-1940

Production director James Landry; **senior manager** Wendy K. Shank; **assistant manager** Rebecca Doshi; **senior specialists** Jay Covert, Chris Redwood; **specialist** Steve Forrester **Preflight director** David M. Tompkins; **manager** Marcus Spiegler; **specialist** Jessie Mudjitaba

Art director Joshua Moglia; **associate art director** Kelly Buckheit; **illustrators** Chris Bickel, Katharine Sutliff; **senior art associates** Holly Bishop, Laura Creveling, Preston Huey; **associate** Nayomi Kevitiyagala; **photo editor** Leslie Blizard

***Science* International**

Europe (science@science-int.co.uk) **editorial: international managing editor** Andrew M. Sugden; **senior editor/perspectives** Julia Fahrenkamp-Uppenbrink; **senior editors** Caroline Ash (Geneva: +41 (0) 222 346 3106), Stella M. Hurtley, Ian S. Osborne, Stephen J. Simpson, Peter Stern; **associate editor** Joanne Baker **editorial support** Alice Whaley; Deborah Dennison **administrative support** Janet Clements, Phil Marlow, Jill White; **news: international news editor** Eliot Marshall **deputy news editor** Daniel Clery; **correspondent** Gretchen Vogel (Berlin: +49 (0) 30 2809 3902, FAX +49 (0) 30 2809 8365); **contributing correspondents** Michael Balter (Paris), Martin Enserink (Amsterdam and Paris), John Bohannon (Berlin); **intern** Laura Blackburn

Asia Japan Office: Asca Corporation, Eiko Ishioka, Fusako Tamura, 1-8-13, Hirano-cho, Chuo-ku, Osaka-shi, Osaka, 541-0046 Japan; +81 (0) 6 6202 6272, FAX +81 (0) 6 6202 6271; asca@os.gulf.or.jp; **asia news editor** Richard Stone +66 2 662 5818 (rstone@aaas.org) **japan news bureau** Dennis Normile (contributing correspondent, +81 (0) 3 3391 0630, FAX 81 (0) 3 5936 3531; dnormile@gol.com); **china representative** Hao Xin, + 86 (0) 10 6307 4439 or 6307 3676, FAX +86 (0) 10 6307 4358; haoxin@earthlink.net; **south asia** Pallava Bagla (contributing correspondent +91 (0) 11 2271 2896; pbagla@vsnl.com)

EXECUTIVE PUBLISHER **Alan I. Leshner**
PUBLISHER **Beth Rosner**

Fulfillment & Membership Services (membership@aaas.org) **director** Marlene Zendell; **manager** Waylon Butler; **systems specialist** Andrew Vargo; **specialists** Pat Butler, Laurie Baker, Tamara Alfson, Karena Smith, Vicki Linton; **circulation associate** Christopher Refice

Business Operations and Administration director Deborah Rivera-Wienhold; **business manager** Randy Yi; **senior business analyst** Lisa Donovan; **business analyst** Jessica Tierney; **financial analyst** Michael LoBue, Farida Yeasmin; **rights and permissions: administrator** Emilie David; **associate** Elizabeth Sandler; **marketing: director** John Meyers; **marketing managers** Darryl Walter, Allison Pritchard; **marketing associates** Julianne Wielga, Mary Ellen Crowley, Catherine Featherston, Alison Chandler; **director of international marketing and recruitment advertising** Deborah Harris; **international marketing manager** Wendy Sturley; **marketing/member services executive:** Linda Rusk; **japan sales** Jason Hannaford; **site license sales: director** Tom Ryan; **sales and customer service** Mehan Dossani, Kiki Forsythe, Catherine Holland, Wendy Wise; **electronic media: manager** Lizabeth Harman; **production associates** Sheila Mackall, Amanda K. Skelton, Lisa Stanford, Nichele Johnston; **applications developer** Carl Saffell

Advertising director worldwide ad sales Bill Moran

Product (science_advertising@aaas.org); **midwest/west coast/w. canada** Rick Bongiovanni: 330-405-7080, FAX 330-405-7081 • **east coast/e. canada** Christopher Breslin: 443-512-0330, FAX 443-512-0331 • **uk/europe/asia** Tracey Peers (Associate Director): +44 (0) 1782 752530, FAX +44 (0) 1782 752531 **japan** Mashy Yoshikawa: +81 (0) 33235 5961, FAX +81 (0) 33235 5852 **traffic manager** Carol Maddox; **sales coordinator** Deiandra Simms

Classified (advertise@sciencecareers.org); **u.s.: sales director** Gabrielle Boguslawski: 718-491-1607, FAX 202-289-6742; **inside sales manager** Daryl Anderson: 202-326-6543; **west coast/midwest** Kristine von Zedlitz: 415-956-2531; **east coast** Jill Downing: 631-580-2445; **canada, meetings and announcements** Kathleen Clark: 510-271-8349; **line ad sales** Emnet Tesfaye: 202-326-6740; **sales coordinators** Erika Bryant; Rohan Edmonson Christopher Normile, Joyce Scott, Shirley Young; **international: sales manager** Tracy Holmes: +44 (0) 1223 326525, FAX +44 (0) 1223 326532; **sales** Christina Harrison, Svitlana Barnes; **sales assistant** Helen Moroney; **japan:** Jason Hannaford: +81 (0) 52 789 1860, FAX +81 (0) 52 789 1861; **production: manager** Jennifer Rankin; **assistant manager** Deborah Tompkins; **associates** Christine Hall; Amy Hardcastle; **publications assistants** Robert Buck; Mary Lagnaoui

AAAS Board of Directors retiring president, chair Gilbert S. Omenn; **president** John P. Holdren; **president-elect** David Baltimore; **treasurer** David E. Shaw; **chief executive officer** Alan I. Leshner; **board** Rosina M. Bierbaum; John E. Dowling; Lynn W. Enquist; Susan M. Fitzpatrick; Alice Gast; Thomas Pollard; Peter J. Stang; Kathryn D. Sullivan

AAAS
ADVANCING SCIENCE, SERVING SOCIETY

val´i·da´tion

It's a synonym for TaqMan® Gene Expression Assays.

Your single easiest solution
TaqMan® Gene Expression Assays deliver accurate real-time PCR results to validate your microarray discoveries. TaqMan® Assays are designed to run under universal thermal cycling conditions and are formulated into a single 20X solution—less pipetting means less chance of error.

NOW AVAILABLE
Arabidopsis and Drosophila Assays!

>600,000 assays, and all very affordable
Virtually every gene and every transcript for human, mouse, rat, Arabidopsis and Drosophila is covered—with no time, reagents or effort spent on design and optimization, you save money on every experiment.

The gold standard in quantitative gene expression analysis
TaqMan Assays provide unmatched sensitivity, specificity and reliability for true gene expression validation—you can publish your data with confidence.

To learn more about TaqMan Gene Expression Assays and how they can help you validate your research, visit **www.allgenes.com**.

Applied Biosystems

25 YEARS
ADVANCING SCIENCE

INTRODUCING...

THE DR. PAUL JANSSEN AWARD FOR BIOMEDICAL RESEARCH

To honor the work of an active scientist in academia, industry or a scientific institute who exhibits the standards of innovation, insight and leadership that Dr. Paul Janssen showed while moving the boundaries of medical science and touching the lives of patients.

INNOVATIVE

INSPIRING

GIFTED

PASSIONATE

REVOLUTIONARY

BRILLIANT

EXCEPTIONAL

PROMINENT

SUCCESSFUL

LEADER

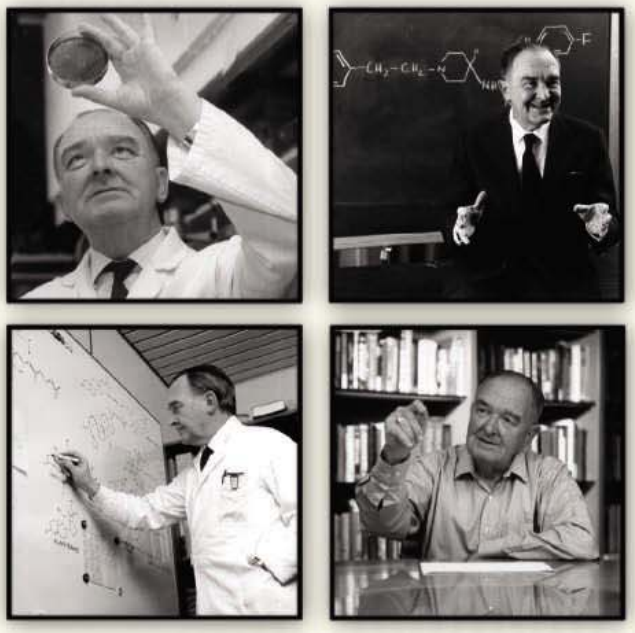

To be awarded September 2006
at The Dr. Paul Janssen Biomedical
Research Symposium in Beerse, Belgium.

Visit **www.pauljanssenaward.com** for more information.

Johnson & Johnson

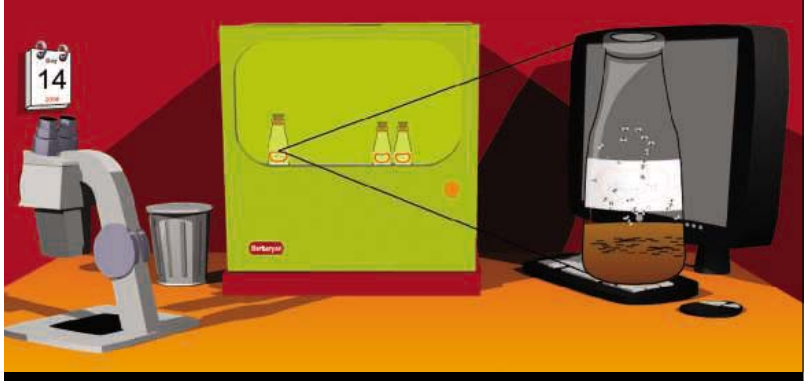

EDUCATION

VIRTUAL FRUIT FLY LAB

Introductory genetics can be more interesting than laboriously working through crosses and filling in Punnett squares. At this online *Drosophila* lab, high school and beginning college students get the chance to run virtual experiments and test hypotheses about the inheritance of fly traits. The latest offering from the Virtual Courseware project at California State University, Los Angeles (NetWatch, 1 April 2005, p. 29), the site lets users pair up e-flies that vary in characteristics such as wing shape, eye color, and type of bristles on the thorax. After incubating and sorting the offspring, students statistically analyze the results of the crosses. >> www.sciencecourseware.org/vcise/drosophila/Drosophila.php

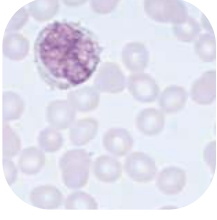

WEB TEXT

Blood Basics

Looking for a synopsis of the genes that control early development of the thymus, the gland in the neck where T cells grow up? Need a rundown on the different kinds of anemia? Page through Molecular Hematology from M.D. researcher Daniele Focosi of the University of Pisa in Italy. The outline-style primer teems with information on the layout of the circulatory system and the workings of its cells. You can bore into a lymph node, for example, or browse a chart summarizing the major blood enzymes. Or read up on leukemia and other diseases in which blood cells go awry. >> www.blood.interhealth.info

TOOLS

Bodily Functions >>

Don't fret if you can't get your simulation of aortic blood flow to work. Download one of the models available at SimTK. The site, hosted by researchers at Stanford University, is part of a project to devise and share "physics-based" models and software that emulate how force and motion affect a range of biological processes. Visitors can take home code that mimics RNA folding, blood dynamics, and ions jostling a large molecule. Plenty more projects are under way, including a model of the colon lining and SimBody, a dynamics program that can help researchers studying everything from molecular shape to walking. The site also offers modules that you can plug into your own creations to perform tasks such as rapidly solving linear equations. Researchers can contribute their models and algorithms to the site. At right, a simulation to gauge blood pressure and velocity in coarctation of the aorta, a congenital narrowing of the vessel. >> simtk.org

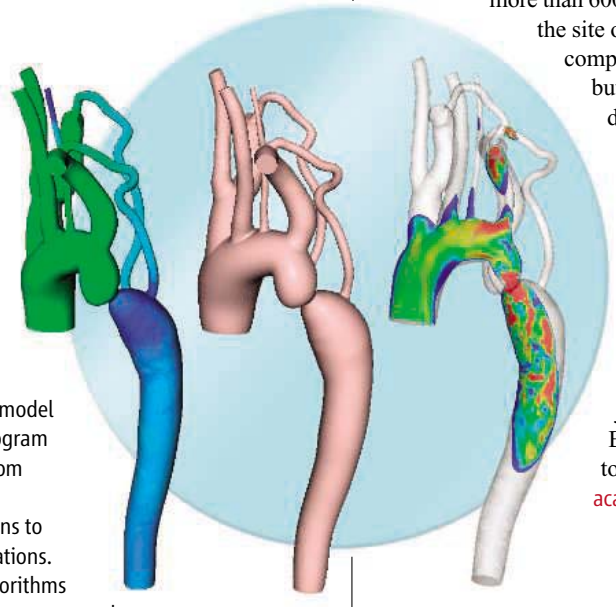

DATABASE

Pinning Down RNA

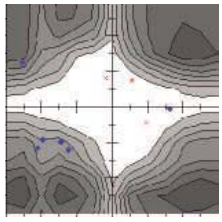

RNA is a slippery character that can trick software that deduces molecular architecture from crystallography and nuclear magnetic resonance data. As a result, RNA structures in public databases often contain errors. RNABase can help researchers identify these mistakes and find more likely conformations. Developed and curated by molecular biophysicist Venkatesh Murthy of Washington University School of Medicine in St. Louis, Missouri, the site automatically collects and analyzes every RNA structure in the Protein Data Bank and the Nucleic Acid Database—more than 800 molecules so far. Entries in RNABase include a list of "outliers," or errors in the published structure, along with contour maps (above) that indicate which positions are possible and impossible for each nucleotide in the molecule. >> www.rnabase.org

TOOLS

Google Scholar, Look Out

Microsoft has debuted its answer to the literature search engine Google Scholar (NetWatch, 3 December 2004, p. 1661). Released last month as a beta version, Windows Live Academic ferrets out articles and abstracts from more than 6000 journals and conferences. So far, the site only covers electrical engineering, computer science, and physics, but Microsoft plans to add more disciplines. Unlike Google Scholar, Windows Live Academic doesn't factor the number of citations into its rankings of articles, relying instead on each paper's quality and how closely it matches your search criteria. Microsoft's engine also offers more options for displaying the results, which you can sort by date, journal, author, or conference. But you'll still need subscriptions to access many of the articles. >> academic.live.com

Send site suggestions to >>
netwatch@aaas.org
Archive: www.sciencemag.org/netwatch

CREDITS (TOP TO BOTTOM): VIRTUAL COURSEWARE PROJECT; VENKATESH MURTHY; DANIELE FOCOSI/UNIVERSITY OF PISA; CHARLES TAYLOR/STANFORD UNIVERSITY

Cambridge Healthtech Institute's

Top Ten Opportunities in the Post Genome Era

June 19-21, 2006 • Fairmont Hotel • San Francisco, California

Featuring 10 Programs for 2006

15th Annual Bioinformatics
Biomarker Data Analysis

10th Annual Proteomics
Unraveling the Human Proteome

4th Annual
RNA Interference

8th Annual Systems Biology
Pathway and Disease Modeling

2nd Annual
Genomic Biomarkers

2nd Annual
Translational Research

Inaugural West Coast
Target Validation

Inaugural
Cancer Genomics and Proteomics

Inaugural
Personalized Medicine

Executive Summit:
Developing Novel Therapeutic Classes

New for Beyond Genome 2006

- New Theme: Top Ten Opportunities in the Post-Genome Era
- Expanded and flexible program: choose from ten different themes and pre-conference events to customize your 3-day Beyond Genome experience
- Projected 1200+ delegates, 120+ speakers, 100+ posters, 34 exhibits, 30+ technology presentations
- New Focus for 15th Annual Bioinformatics: Biomarker Data Analysis
- New Focus for 10th Annual Proteomics: Unraveling the Human Proteome
- New Focus for 8th Annual Systems Biology: Pathway and Disease Modeling
- Now part of Beyond Genome 2006: 2nd Annual Genomic Biomarkers and 2nd Annual Translational Research
- New Additions to Beyond Genome 2006: Target Validation; Cancer Genomics and Proteomics; and Personalized Medicine
- New Executive Summit: Developing Novel Therapeutic Classes
- SAME 15-year track-record of delivering consistent quality of thescientific program, net working with top delegates, and exhibit/sponsor ship experience.

Reference Keycode L35 when registering online

www.BeyondGenome.com

EDITED BY YUDHIJIT BHATTACHARJEE

HOW CHILDREN SHOULD GROW

The World Health Organization (WHO) last week issued new standards for child growth that are more globally applicable than existing ones.

Based on measurements of 8440 children in six countries including their weight, length/height, and body mass index, the new standards provide an international measure of how children should grow until age 5, given optimal nutrition and health. The old standards were not necessarily internationally applicable, as they described the growth of children from one area of the United States in the 1970s. They also made no distinction between how the children were fed, which affects growth rates; formula-fed babies grow faster. The new standards may prove to be controversial in countries such as the United States where many children are fed formula, because 20% to 30% more children may be categorized as overweight on the new charts.

The children measured for the new standards were breastfed, received suitable additional nutrition after 6 months, and had mothers who were also healthy, well-nourished, and did not smoke. "For the first time, we have a world standard to see how children are doing," says Cutberto Garza of Boston College, chair of the Multicentre Growth Reference Study that was responsible for measuring the children. The new standards will enable doctors and researchers to better predict whether a child is becoming overweight or underweight, explains project coordinator Mercedes de Onis of WHO, and should also help them develop better strategies for dealing with malnutrition.

<<Space Kimchi

Scientists at the Korea Atomic Energy Research Institute in Daejeon say they have cooked up a special kimchi for space travel, which they hope to launch in 2008 when Korea's first astronaut boards the Russian spaceship Soyuz.

Kimchi is a traditional Korean dish consisting of fermented chili peppers and cabbage or other vegetables. Working with researchers at the Institute of Biomedical Problems, a state facility in Russia that conducts biomedical support of space flights, the Korean scientists, led by Myung Woo Byun, used gamma- and electro-irradiation to sterilize fully fermented kimchi. They then froze it to a half-dried state and packed it in a vacuum-sealed pouch.

Byun says the development of kimchi was symbolic, but also that the food is not without merits. "Space food is now entirely Western food, so we thought it would be meaningful to have a Korean food on the menu. Also, astronauts suffer failing digestive and intestinal functions from lack of fiber in space-food diet. Kimchi is abundant in fiber."

The group plans to present the kimchi later this year to Russian space authorities, who must approve it as an official food for astronauts. Such approvals are not automatic. In the United States, NASA takes months to analyze potential new space foods, checking nutritional value, conducting a sensory evaluation, and ultimately performing a zero-gravity test on an airplane.

CREDITS (TOP TO BOTTOM): SOURCE: THOMPSON SCIENTIFIC'S *SCIENCEWATCH*; KAERI; JESSICA ROTHMAN

Top of the U.K. Heap

The familiar names of Oxford and Cambridge still dominate research in the United Kingdom, but lesser-known universities have proved themselves to be big players in several fields, according to rankings reported in the May/June issue of Thompson Scientific's *ScienceWatch*.

Examining 21 fields within the life, physical, and social sciences, the survey used two measures of scientific heft to evaluate universities: citation impact, or the number of citations per paper, and the total number of citations. Based on the first measure, Oxford and Cambridge ranked among the top three institutions in 10 fields, with Oxford taking top honors in four disciplines, including immunology and psychology/psychiatry, and Cambridge winning first place in one, neurosciences. Based on the number of citations, Cambridge was the top-ranked institution in 10 fields, whereas Oxford was ranked first in only two.

U.K. University Olympics*

	Gold†	Silver	Bronze	Total
Oxford	4	4	2	10
Southampton	2		1	3
Sussex	2			2
Dundee	2			2
East Anglia	2			2
Cambridge	1	6	3	10

* *Based on scientific impact measured by average citations per paper.*
† *Number of disciplines in which an institution ranked first.*

The current survey analyzed papers published between 2001 and 2005, but the basic trend of "Oxbridge" dominating several disciplines and other universities distinguishing themselves in certain fields is similar to what was found in the last survey, conducted in 1997.

SODIUM SOURCE

Mountain gorillas love to munch on rotting wood, and now we know why: The food is a source of sodium. Researchers from Cornell University reported in a study published online in *Biology Letters* on 25 April that gorillas in Uganda get more than 95% of their sodium requirements from decaying wood, which makes up only 4% of their diet. They also found that the apes avoided timber with low sodium content. The researchers plan to see if this taste for salty wood is common in other primate species.

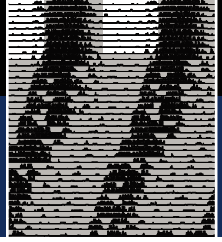

Timekeeping without CLOCK 673

Energy efficiency under threat 675

VETERANS ADMINISTRATION

Texas Earmark Allots Millions to Disputed Theory of Gulf War Illness

Scientists usually bristle when U.S. legislators mandate a project that benefits their constituents. But Gulf War illness researchers are especially troubled by such a funding provision inserted by Senator Kay Bailey Hutchison (R–TX) in this year's budget for the Department of Veterans Affairs (VA). The $15 million earmark to the University of Texas (UT) Southwestern Medical Center in Dallas not only avoids the traditional peer-review process, but it also marks the rare—and possibly first ever—VA funding of a program outside its research network, and to a researcher whose theory of the debilitating illness hasn't won much scientific support.

"The particular avenue of research being pursued is not one that has found much favor with the scientific community," says Simon Wessely, director of the King's Centre for Military Health Research at King's College London. Adds John Feussner, a former head of VA research now at the Medical University of South Carolina in Charleston, "This takes money directly out of the VA research portfolio. … I can't think of any advantage" from the new Gulf War research program.

The money will fund a new center at UT Southwestern, unveiled on 21 April. It exists thanks to Hutchison, who chairs the spending panel that sets the VA's budget and has long urged more government-funded research into Gulf War illness. Her priority "is getting the money to the person who can best help battle this illness," says spokesperson Chris Paulitz. In her mind, that individual is epidemiologist Robert Haley, who for years has reported a strong link between exposure to neurotoxins, such as nerve gas and pesticides, and the puzzling cluster of symptoms that struck thousands of veterans after the 1990–'91 Gulf War.

Haley was initially funded by former presidential candidate and businessman Ross Perot and later by the Department of Defense. He believes that Gulf War illness is "an encephalopathy" marked by abnormalities in brain structures and in the nervous system. Many troops, he believes, were exposed to low levels of nerve gas during the first Gulf War.

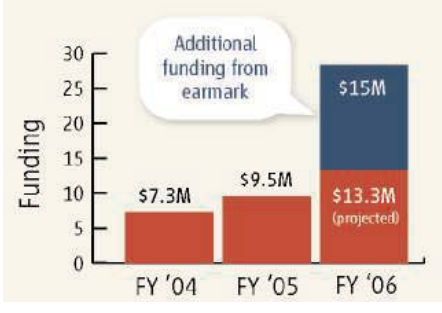

Setting priorities. Senator Kay Bailey Hutchison (R–TX) (*standing, right*) and epidemiologist Robert Haley (*standing, far left*) help launch a new Gulf War illness research center. Hutchison's $15 million earmark more than doubles the Veteran Administration's spending in this area.

Now, Haley expects to pin down how these toxins affect the brain, and how to ease their effects, once and for all. Certainly, there's no shortage of funds: Hutchison expects the center—which Haley says will be called the Gulf War Illness and Chemical Exposure Research Center—will receive $75 million from VA over 5 years. Haley says it will initially focus on brain imaging, a survey of veterans from the first Gulf War, animal studies, and a Gulf War illness research and treatment clinic at the Dallas VA Medical Center.

But "this is not a grant to Robert Haley," he says. The dean of UT Southwestern's medical school, Alfred Gilman, will convene a merit review committee, and "all of our projects will go through" it, says Haley, adding that the committee's precise function hasn't been set. Traditional peer review as practiced by agencies such as VA and the National Institutes of Health, says Haley, has helped scientists take small steps forward. But it has failed to solve the enigma of Gulf War illness. "If we continue at this rate," he says, "it's going to be 50 years before we help these people."

Haley's Gulf War theories, however, put him in the minority. Animal studies disagree on whether low-dose neurotoxin exposure is deleterious in the long term, and the neurotoxin theory has come up short in expert reviews. In 2004, the Institute of Medicine (IOM) in Washington, D.C., concluded that "there is inadequate/ insufficient evidence" to forge a link between exposure to low levels of sarin gas and the memory loss, muscle and joint pain, and other symptoms that characterize Gulf War illness. Wessely argues that British troops, which have the same rates of Gulf War illness as seen in Americans, were nowhere near the Khamisayah weapons depot in Iraq, the most cited example of suspected nerve gas exposure during the war. The IOM report notes that an attempt to replicate Haley's findings of genetic susceptibility to nerve gas proved unsuccessful.

A VA committee that included Haley came to a different conclusion. It reported in 2004 that neurotoxin exposure was a "probable" explanation for Gulf War illness and recommended that VA spend at least $60 million over 4 years on Gulf War illness research. The neurotoxin arena "is the most promising area for research at the present time," says James Binns, a Vietnam veteran and Arizona businessman, who chaired the committee that wrote the report. VA agreed (*Science*, 19 November 2004, p. 1275) but never put up the money—until Hutchison's amendment compelled it to do so. Initial funding will be limited to UT Southwestern and other schools, generally in Dallas, with which Haley collaborates, he says.

Joel Kupersmith, VA's chief research and development officer, calls the plan "an opportunity to move ahead on Gulf War research" and expressed "confidence" in UT Southwestern. But then again, VA had little choice but to move forward. "We follow what the laws and regulations are," says Kupersmith. **–JENNIFER COUZIN**

CREDITS: (PHOTO) UNIVERSITY OF TEXAS SOUTHWESTERN MEDICAL CENTER; (SOURCE) U.S. DEPARTMENT OF VETERANS AFFAIRS

BIOMEDICINE

Genes and Chronic Fatigue: How Strong Is the Evidence?

The U.S. Centers for Disease Control and Prevention (CDC) in Atlanta, Georgia, announced last month that it has cracked a medical mystery: Chronic fatigue syndrome (CFS) has a biological and genetic basis. CDC Director Julie Gerberding called the study "groundbreaking" and also hailed its novel methodology. These claims have attracted widespread media attention. But, like most aspects of CFS, the study and its findings are controversial. Some scientists think the agency is overstating the case for a link between the syndrome and genetic mutations. "Most complex-trait geneticists would interpret [these] findings more cautiously than the authors have," says Patrick Sullivan, a psychiatric geneticist at the University of North Carolina, Chapel Hill.

CFS is defined as severe fatigue lasting more than 6 months, accompanied by symptoms such as muscle pain and memory problems. It is thought to afflict at least 1 million Americans, mostly women. The lack of specific diagnostic criteria since CFS was first defined 20 years ago has led to debate over whether the cause could be an infectious agent, psychiatric, or something else—and made research funding for the disorder highly political. In 2000, a CDC division director lost his job after the agency diverted $12.9 million that Congress had instructed CDC to spend on CFS research to other infectious disease studies (*Science*, 7 January 2000, p. 22). The agency agreed to restore the money over 4 years and launch a major study.

The new project, led by William Reeves, CDC's lead CFS researcher (who had blown the whistle on the diverted funds), took an unusual approach. Instead of recruiting patients already diagnosed with CFS, CDC surveyed one-quarter of the population of Wichita, Kansas, by phone to find people suffering from severe fatigue. Several thousand then underwent screening at a clinic for CFS. The population-based aspect is "a big plus" because it avoids the possible bias in tapping a pool of patients seeking treatment for their problems, says Simon Wessely, who studies CFS and a similar disorder, Gulf War illness, at King's College London.

Out of this survey, 172 people, most of them white middle-aged women, were deemed to fit the criteria for CFS (58) or CFS-like illness (114). A total of 227 people, including 55 controls, then underwent an extensive 2-day battery of clinical measurements, including sleep studies, cognitive tests, biochemical analyses, and gene-expression studies on blood cells. This part of the study alone cost upward of $2 million, says Reeves.

In another unusual step, CDC's Suzanne Vernon then handed this massive data set to four teams of outside epidemiologists, mathematicians, physicists, and other experts. They spent 6 months examining statistical patterns in the data. For instance, one group analyzed patient characteristics such as obesity, sleep disturbance, and depression and grouped them into four to six distinct subtypes; they also looked for different gene-expression patterns in these categories. Some groups also looked for associations between CFS and 43 common mutations in 11 genes involved in the hypothalamic-pituitary-adrenal axis, which controls the body's reaction to stress. The 14 papers were published last month in the journal *Pharmacogenomics*.

The results, which include the finding that the patterns of expression of about two dozen genes involved in immune function, cell signaling, and other roles are different in CFS patients, provide what Harvard University CFS researcher Anthony Komaroff calls "solid evidence" for a biological basis of CFS. They dispel the notion that "this is a bunch of hysterical upper-class professional white women," says Reeves.

Other scientists are much more cautious. The gene-expression results, says Jonathan Kerr of Imperial College London, are "meaningless" because they don't demonstrate conclusively, using the polymerase chain reaction, that the genes' RNA is indeed expressed. After this step, says Kerr, 30% to 40% of genes could drop out.

The most controversial assertion, however, is that the Wichita study has tied CFS to particular mutations in three genes, including the glucocorticoid receptor and one affecting serotonin levels. Genetic epidemiologists are skeptical for two reasons. First, the team looked for associations with just 43 gene variants; some other set of genes might have correlated just as closely, notes Nancy Cox of the University of Chicago in Illinois. Second, the researchers studied no more than 100 or so individuals with fatigue. The results, although they meet the threshold for statistical significance, are "very likely not robust," says Sullivan. (Sullivan himself has co-authored twin studies finding a "modest" genetic component for CFS, although without pointing to a particular gene.)

Reeves doesn't disagree: "One of our caveats is that it is a small study," he says. CDC researchers are now planning to repeat the study with 100 CFS patients. Vernon ▶

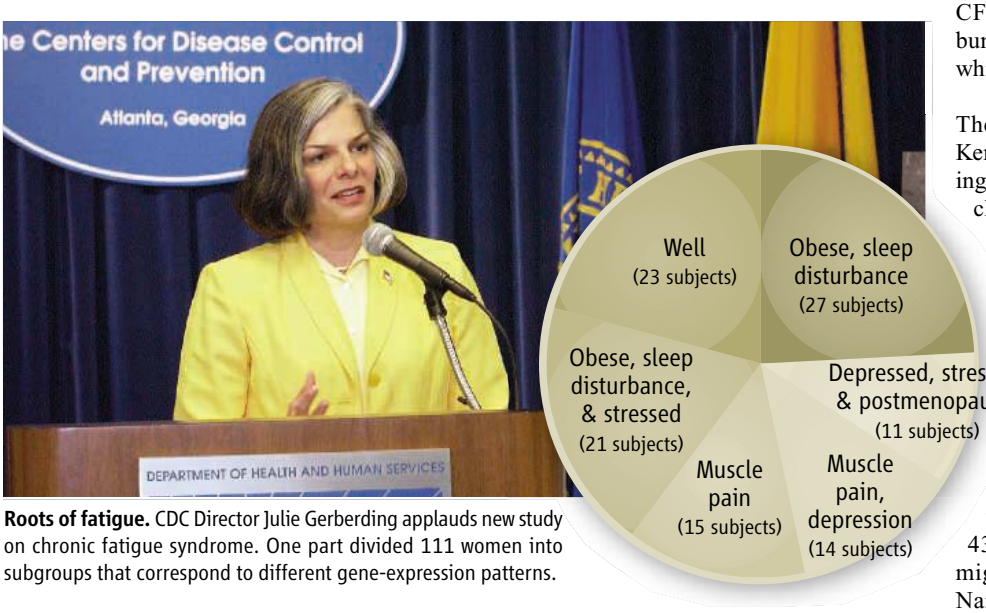

Roots of fatigue. CDC Director Julie Gerberding applauds new study on chronic fatigue syndrome. One part divided 111 women into subgroups that correspond to different gene-expression patterns.

CREDITS: (PHOTO) CDC; (SOURCE) ADAPTED FROM L. CARMEL *ET AL.*, *PHARMACOGENOMICS* **7**, 375-386 (2006)

SPECIAL INTRODUCTORY OFFER
See our website for details.

NEW ENGLAND BIOLABS

Competent Cells from New England Biolabs

SUPERIOR COMPETENT *E.COLI* STRAINS FOR CLONING AND PROTEIN EXPRESSION

For many years staff scientists at New England Biolabs have been using their own line of optimized chemically competent *E.coli* cells for cloning and protein expression. These strains have made all the difference to a highly demanding research and production program. Now when you are looking for a versatile cloning strain, rapid colony growth, or tight control of protein expression, you can benefit from the superior performance and high quality of these strains.

- **NEB Turbo Competent *E.coli*** **C2984H**
  Ligate, transform, plate and pick colonies in one day
- **NEB 5-alpha Competent *E.coli*** **C2991H**
  Versatile cloning strain
- **T7 Express Competent *E.coli*** **C2566H**
  High efficiency transformation and protein expression
- **T7 Express *I*^{q} Competent *E.coli*** **C2833H**
  Tight control of protein expression
- **dam^{-}/dcm^{-} Competent *E.coli*** **C2925H**
  Grow plasmids free of dam and dcm methylation

Advantages:

- Ready to transform – packaged in single-use transformation tubes (20 x 0.05 ml)
- Free of animal products
- 5 minute transformation protocols
- Supplied with outgrowth media and control DNA

	NEB Turbo	NEB 5-alpha	T7 Express	T7 Express *I*^{q}	dam^{-}/dcm^{-}
Transformation Efficiency (cfu/µg)	>10^{9}	1-3 x 10^{9}	2-6 x 10^{8}	2-6 x 10^{8}	>2 x 10^{6}
Strain	K12	K12	B	B	K12
T1 Phage Resistant	✓	✓	✓	✓	✓
Blue/White Screening	✓	✓	–	–	–
lac *I*^{q}	✓	✓	–	✓	–
Colonies Visible after 8 hours	✓	–	–	–	–
Endonuclease I Deficient	✓	✓	✓	✓	✓
Protease Deficient	–	–	✓	✓	–
Restriction Deficient	✓	✓	✓	✓	✓
M13 Phage Capable (F^{+})	✓	✓	–	✓	–
RecA Deficient	–	✓	–	–	–

Chemically Competent *E.coli* Strain Characteristics

For more information and international distribution network, please visit www.neb.com

- **New England Biolabs Inc.** 240 County Road, Ipswich, MA 01938 USA 1-800-NEB-LABS Tel. (978) 927-5054 Fax (978) 921-1350 info@neb.com
- **Canada** Tel. (800) 387-1095 info@ca.neb.com
- **Germany** Tel. 0800/246 5227 info@de.neb.com
- **UK** Tel. (0800) 318486 info@uk.neb.com
- **China** Tel. 010-82378266 beijing@neb-china.com

NEW ENGLAND BioLabs® Inc.
the leader in enzyme technology

says her group is also validating the gene-expression results and will hold another computational exercise next month at Duke University in Durham, North Carolina, with a larger data set.

Meanwhile, Gerberding has suggested that the same multipronged approach could be applied to seek genetic links to other complex diseases such as autism. That's already being done for many other diseases, from cancer to schizophrenia, notes Sullivan, although the studies use much larger samples and search the entire genome for disease markers. That scale may never be possible for relatively uncommon diseases such as CFS, he says. And he and other human geneticists warn that it's unclear whether any conclusions can be drawn from gene hunts carried out on such very small sample sizes.

–JOCELYN KAISER

U.S. RESEARCH FUNDING

Industry Shrinks Academic Support

After 2 decades of steady increases, industrial funding for U.S. academic research is on the skids, according to a new report* from the National Science Foundation (NSF). University and industry officials say the 5% cumulative decline from 2002 to 2004—the first-ever 3-year slide for a funding source since NSF began compiling such data in the 1950s—reflects a slowing economy and shrinking company research budgets. But some fear the trend might continue even as the economy picks up unless companies and universities figure out how to share the fruits of industry-sponsored research.

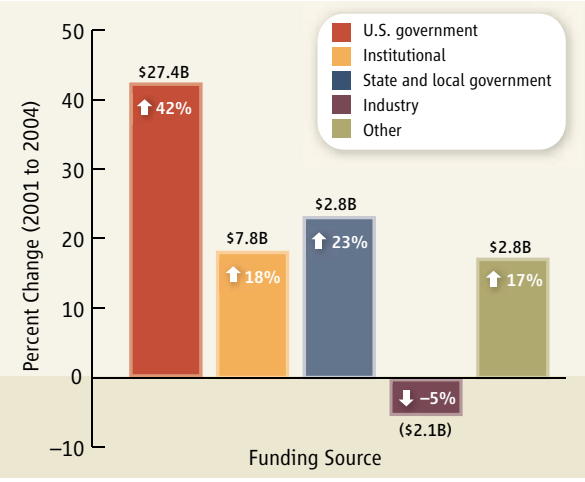

Company flight? Disagreements over the ownership of intellectual property may be limiting industrial support to U.S. universities as other sources increase their contributions.

University officials see collaborations with the private sector as an increasingly important revenue source. But they also want to maximize income from technologies developed on campus. Institutions have become so aggressive in protecting intellectual property arising out of industry-funded projects, some industry representatives say, that negotiating research contracts is becoming more difficult and time-consuming.

"Even if we come in with the ideas and the money, we are expected to pay a licensing fee for the product of research that we already paid for," says Stanley Williams, a computer scientist at Hewlett-Packard Laboratories in Palo Alto, California. "Then we get into a negotiating dance that can take 2 years, by which time the idea is no longer viable."

That hard-nosed attitude could hurt universities in the long run by damaging their relationship with industry, says Susan Butts, director of external technology at Dow Chemical Co. and co-founder of a national university-industry group that is working to improve partnerships between the two sectors. "Most universities receive more industry funding for research than total revenue from licensing inventions," she says. (The ratio is 3 to 1 according to the 2004 survey of the Association of Technology Managers.) "It doesn't make sense to jeopardize funding to try to increase licensing income."

Michael Pratt, director of corporate business development at Boston University, says most companies have fewer dollars available for outside research when times are tough. Susan Gaud, chair of the Industrial Research Institute, adds that "funding research doesn't fit into" the increasing emphasis on short-term corporate productivity. But like Butts, she sees protracted negotiations as a contributing factor behind the current decline and a stumbling block for the future.

Williams says he wouldn't be surprised if the trend continues, fueled in part by a receptive audience among academics in France, Russia, and China. "We call it research by purchase order. You get on the phone, you talk to a professor, and the professor says it'll cost this much," he says. "The research can start the next day. And we own everything that comes out of it."

–YUDHIJIT BHATTACHARJEE

SOURCE: NSF

* www.nsf.gov/statistics/infbrief/nsf06315

Academy to Probe Minority Programs

Are federal programs to attract minorities into biomedical research working? The National Institutes of Health (NIH) doesn't know, and moreover, it doesn't know how to find out. So it's asked the U.S. National Academies to sponsor a workshop this summer on the best way to assess the dozens of programs NIH offers to attract minorities into biomedical research.

"We want to test some of the underlying assumptions for these sorts of interventions," says Clifton Poodry, head of the Minority Opportunities in Research division at NIH's National Institute of General Medical Sciences, which is funding the project. "We're looking for evidence-based interventions, not somebody's best guess."

The workshop won't assess the programs themselves, says National Research Council program officer Adam Fagen, a task that has proven to be devilishly difficult (*Science*, 20 January, p. 328). Fagen's first step is assembling a team to plan the July event, which will include 40 or so experts in evaluation science.

–JEFFREY MERVIS

Whale Stranding: Sonar Cited

Submarine sonar was "a plausible, if not likely" cause of the harm suffered by whales during a 2004 incident that stranded more than 150 melon-headed whales off the shore of Kaua'i, Hawai'i, an investigation by the National Oceanic and Atmospheric Administration (NOAA) has concluded. The U.S. Navy says it's unknown what caused the incident, but they reject NOAA's interpretation. One calf died in the episode, despite local canoeists' efforts to herd the whales away from the beach.

Using time-stamped maps of joint U.S. and Japanese submarine exercises under way during the nearby Rim of the Pacific Exercises (RIMPAC), NOAA determined that the whales could have been within hearing range, and the report ruled out algal blooms or other natural causes. Now NOAA is considering a Navy request to authorize this year's RIMPAC; NOAA official Brandon Southall said that the incident will be part of the "range of information" that the agency uses to make its decision. The Navy has promised new mitigation measures during the event, but activists want NOAA to force it to turn its sonar volume down, avoid islands, and switch sonar off while traveling between exercise sites.

–ELI KINTISCH

QUANTUM OPTICS

A New Way to Beat the Limits on Shrinking Transistors?

A new lithography scheme could sidestep a fundamental limit of classical optics and open the way to drawing ultraprecise patterns with simple lasers, a team of electrical engineers and physicists predicts. If it works, the scheme would allow chipmakers to continue to shrink the transistors on microchips using standard technologies.

"It seems quite cool, and it could be an advance in the field," say Jonathan Dowling, a mathematical physicist at Louisiana State University in Baton Rouge. Still, he says, researchers have a long way to go before they can put the plan into practice.

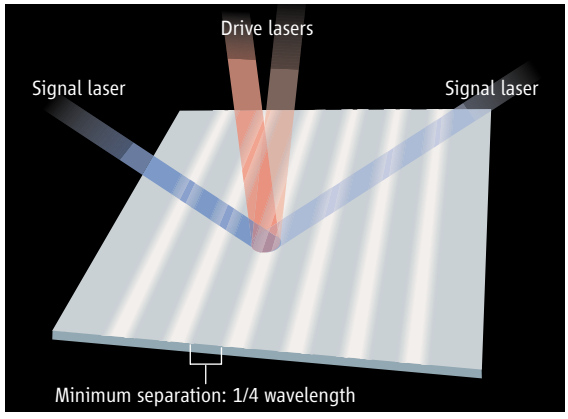

A fine line. A photoresist that absorbs two photons from one signal laser or the other would produce stripes half as wide as the diffraction limit.

Chipmakers "write" the pattern of transistors and circuits on a microchip by shining laser light onto a film called a photoresist that lies atop a silicon wafer. According to classical optics, the light cannot create a pattern with details smaller than half its wavelength—the so-called diffraction limit. So to shrink transistors, chipmakers must use light of shorter wavelengths, such as ultraviolet light and soft x-rays. The problem is, ordinary lenses don't work at such short wavelengths.

Physicists know that, in theory, they can beat the diffraction limit through quantum weirdness. They split a beam of light, send the two halves on paths of different lengths, and bring them back together at the surface of the target. The recombining beams can interfere with one another to make a pattern of bright and dark regions. The trick is to create a quantum connection called "entanglement" between a pair of photons traveling the two paths so that the duo acts like a single photon of twice the energy and half the wavelength. The interfering beams can then write details onto the photoresist that are half the size of the diffraction limit. Entangling more photons produces smaller features still.

Such "quantum lithography" has yet to find its way into production lines, however, largely because it's hard to produce the entangled photons. Now, electrical engineer Philip Hemmer and physicist Suhail Zubairy of Texas A&M University in College Station and colleagues have concocted a scheme that they say can produce the same result with ordinary unentangled laser light.

Instead of splitting a beam, the researchers propose shining two "signal" lasers of slightly different wavelengths onto a surface coated with photoresist. They would also shine two "drive" lasers onto the same spot. In their scheme, the molecules of the photoresist can absorb only a very specific amount of energy—less than twice the energy of either signal beam. If the drive beams are tuned just right, a molecule would simultaneously absorb two photons from one signal beam or the other—but not one from each—while spitting a single photon into one of the drive beams. The photoresist would effectively be patterned by beams of twice the energy and half the wavelength of each signal beam, yielding details half as small as the diffraction limit would allow, the researchers report in the 28 April *Physical Review Letters*.

The challenge will be to find just the right absorbing material for the photoresist, says Dowling, one of the inventors of the entanglement approach. "I call this conservation of magic," he says. "Either you have to have a magic state of light, or you need a magic absorber." Yanhua Shih of the University of Maryland, Baltimore County, adds that the researchers have shown only that they can make a tight pattern of parallel lines. In principle, the new technique may not be able to make more elaborate patterns, Shih says. Others say that, in theory, any pattern can be fashioned from an appropriate superposition of stripes.

Hemmer says he's working on an experimental realization of the scheme. Time will tell whether it's one giant half-step for technologists.

–ADRIAN CHO

IMMUNOLOGY

Differences in Immune Cell "Brakes" May Explain Chimp-Human Split on AIDS

A new study that compares the immune responses of chimps and humans offers yet more compelling evidence that subtle differences in gene activity can result in big distinctions between the two species. The researchers, led by hematologist Ajit Varki of the University of California, San Diego (UCSD), suggest that their findings may explain why chimps and other great apes do not typically develop AIDS when infected with HIV, cirrhosis after infection with hepatitis B or C viruses, or any of several other diseases common in humans. Pathologist Kurt Benirschke, who also is at UCSD but did not participate in this study, calls the new work "terrific" and "really great science."

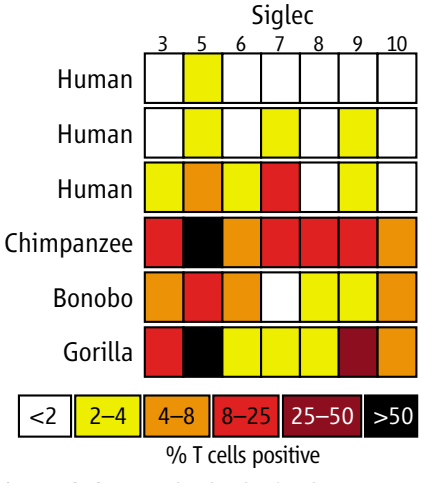

Disease dodger? Higher levels of Siglecs expressed by ape T cells may explain why they do not suffer many common ailments that plague humans.

As they report in the 1 May *Proceedings of the National Academy of Sciences*, Varki and co-workers studied proteins called Siglecs that his lab co-discovered in the 1990s. Many immune cells express Siglecs (which stands for sialic acid–recognizing Ig-superfamily lectins), and some of them appear to calm the immune response by preventing a process of immune cell expansion known as activation. Humans and apes share the same Siglec genes, but Varki's group explored whether they were turned on to the same degree in T lymphocytes taken from humans, chimps, gorillas, and bonobos.

Using monoclonal antibodies to various Siglecs, the researchers found that although the T cells of people from many different geographic and ethnic backgrounds sported low levels of the Siglecs or none at all, the ape T cells produced clearly detectable amounts ▶

CREDITS (TOP TO BOTTOM): P. HUEY/*SCIENCE*; ADAPTED FROM D. H. NGUYEN *ET AL.*, *PNAS*

of the molecules. When they genetically engineered the human cells to express high levels of one key Siglec, they found that, as predicted, T cell activation was inhibited. Conversely, they cranked up activation of chimp cells by using an antibody to block that same Siglec on them. "I think what's happening is that Siglecs are providing a brake in ape T cells," says Varki. "Human T cells seem to have lost these brakes." Varki and his co-authors speculate that early humans faced novel pathogens as they migrated into new areas, which may have created pressure for hyperactivated T cells to evolve.

Varki's team notes that AIDS, chronic hepatitis B and C, rheumatoid arthritis, bronchial asthma, and type 1 diabetes are all T cell–mediated diseases that are linked to overactivation of the immune cells—and none appear to afflict apes. Varki says it may ultimately be possible to develop a therapy that turns up expression of Siglecs in humans with these diseases, dampening activation and preventing symptoms. But he emphasizes that this study only hints at that possibility. "At the moment it's all in vitro," stresses Varki. "But it is all internally consistent with what we know about the biology."

The new insights on Siglecs may also help avoid tragedies like the one that recently occurred in a U.K. drug trial (*Science*, 24 March, p. 1688). The study involved a monoclonal antibody that stimulates T cell activation and proved safe in monkeys. But when given at much lower doses to six humans, it quickly caused serious illness. "When it comes to the immune system, be careful about predicting whether a primate model will predict human responses, especially for T cells," cautions Varki, noting that an in vitro comparison of rhesus and human cells similar to his study might have revealed the stark differences between the species.

AIDS researchers are taking note of the new work as well. In AIDS, T cell activation appears to play a central role in the destruction of the immune system as it signals the expansion of lymphocytes bearing CD4 receptors, the key cells that HIV targets and destroys. Anthony Fauci, director of the National Institute of Allergy and Infectious Diseases in Bethesda, Maryland, points out that such activation in people creates more targets for HIV. "If you didn't have that robust activation, you wouldn't provide a fertile environment for HIV to replicate," he says. "Varki makes an interesting story."

Immunologist Gene Shearer of the National Cancer Institute in Bethesda, Maryland, who studies how HIV causes immune destruction by activating CD4 cells that then commit suicide, agrees that the lower Siglec expression in human T cells could be an important new factor to study in AIDS. Varki's results have already prompted him to "do some rethinking."

–JON COHEN

NEUROBIOLOGY

Despite Mutated Gene, Mouse Circadian Clock Keeps on Ticking

If you opened up a clock and took out the most important-looking cog in its works, how well do you suppose the clock would work? A team of neurobiologists recently tried an analogous experiment with the biological clocks of mice, knocking out a gene thought to encode a crucial part of the molecular machinery that generates circadian rhythms. To their great surprise, the clock didn't stop.

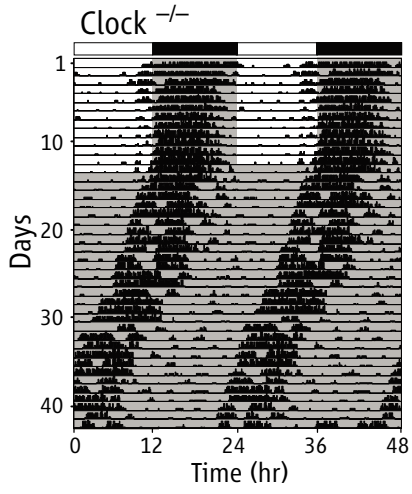

Running on time. CLOCK-deficient mice maintain a daily schedule of wheel running (black) even in constant darkness (gray areas).

The mutant mice had nearly normal daily cycles of activity, even in total darkness, and the activity levels of other clock genes continued to wax and wane. "It was pretty heretical," says Steven Reppert, who reports the findings in the 4 May issue of *Neuron* along with David Weaver and Jason DeBruyne of the University of Massachusetts Medical School in Worcester and other colleagues. "On first reading, this is a striking finding," says Steve Kay, a clock researcher at the Scripps Research Institute in San Diego, California. Still, Kay and others aren't quite ready to toss out everything they know about molecular clocks. "There's a distinct possibility that this result has a simple explanation," Kay says.

The current model of the mammalian circadian clock has at its heart two transcription factors, CLOCK and BMAL1, that drive a 24-hour cycle of gene expression. The details are complicated, but the general idea is that CLOCK and BMAL1, bound together, kick off each cycle by spurring transcription of several other genes, whose protein products accumulate and interact in the ensuing hours, ultimately switching off CLOCK-BMAL1 to bring the cycle to an end. Researchers already knew that knocking out the *Bmal1* gene abolishes circadian rhythms, and they have long assumed that knocking out *Clock* would do the same.

Joseph Takahashi and colleagues at Northwestern University in Evanston, Illinois, first identified *Clock* in 1994 and reported that mice with a mutated version of the gene that produces an altered CLOCK protein have extraordinarily long circadian cycles, up to 28 hours (*Science*, 29 April 1994, p. 719). Such mice also have disrupted molecular rhythms in the suprachiasmatic nucleus, the site of the master body clock in the brain. But creating mice with a completely disabled *Clock* gene has proven tricky, Takahashi says: "My lab has been working on it all this time."

Now Reppert's team has succeeded. "To our surprise and shock, the animals ended up having almost no change in circadian behavior," he says. The standard way to test a mouse's circadian clock is to put it in a cage with a running wheel and repeatedly turn the lights on for 12 hours, then off for 12 hours. The nocturnal animals normally spend far more time on the wheel during the dark periods, and thanks to the internal clock, they maintain this activity pattern even when the lights are off for weeks at a time. CLOCK-deficient mice did the same, for up to 6 weeks of solid darkness, Reppert and colleagues found.

Further investigations revealed that the cyclical activity of other clock-related genes continued in the brains and livers of the CLOCK-deficient mice, although with some abnormalities. "In general, it looked like the molecular clock still moved forward in the brain," Reppert says. The circadian clock in the liver appeared to be more substantially altered.

"The work is very good, and the result is somewhat unexpected," says Takahashi. However, he adds, "I don't think it says CLOCK is not playing an important role normally." In Takahashi's view, the new work simply shows that when CLOCK isn't there, something else can take its place. The reason for the severe disruption in the original *Clock* mutants may be that the altered CLOCK protein kept this substitute from interacting with BMAL1, he says.

Reppert and colleagues suspect that the substitute is a related transcription factor called NPAS2; they report in *Neuron* that it binds with BMAL1 in the brains of CLOCK-deficient mice. Now the researchers are working to create mice missing both CLOCK and NPAS2. That's a crucial experiment, says Kay: "If the mice are rhythmic, then our field will need a paradigm shift."

–GREG MILLER

CREDIT: J. P. DEBRUYNE *ET AL.*, *NEURON* **50**, 465-477 (4 MAY 2006)

You could be next

Yes, it *can* happen to you:
If you're making inroads in neurobiology research and you've received your M.D. or Ph.D. within the last 10 years, the Eppendorf & *Science* Prize for Neurobiology has been created for YOU!

$25,000 Prize

This annual research prize recognizes accomplishments in neurobiology research based on methods of molecular and cell biology. The winner and finalists are selected by a committee of independent scientists, chaired by the Editor-in-Chief of *Science*. Past winners include post-doctoral scholars and assistant professors.

If you're selected as next year's winner, you will receive $25,000, have your work published in the prestigious journal *Science* and be invited to visit Eppendorf in Hamburg, Germany.

What are you waiting for? Enter your research for consideration!

Deadline for entries:

June 15, 2006

For more information:
www.eppendorf.com/prize
www.eppendorfscienceprize.org

"It was a great honor to be the first recipient of the Prize. This prize highlights the valuable role that the scientific community can play in fostering the promise of developing researchers."

Anjen Chenn, M.D., Ph.D.
Assistant Professor
Northwestern University
2002 Winner

eppendorf & Science
PRIZE FOR NEUROBIOLOGY

ENERGY RESEARCH

Industry Conservation Programs Face White House Cuts

Mechanical engineer Christophe Beckermann has developed software to help the U.S. metal-casting industry reduce waste and save energy by modeling how cracks form as the metal cools. At a time when politicians are demanding that the country become more energy efficient, the research by his 10-person team at the University of Iowa, Iowa City, seems like a sure-fire winner.

Think again. Last week, representatives of energy-intensive industries from steel to chemicals came to Washington, D.C., to lobby against a 15% cut proposed by the Bush Administration in the program Industries of the Future (IOF) that funds Beckermann and other researchers on projects including papermaking studies and combustion research. The cut is part of an $87 million bite the White House wants to take out of the $606 million program for efficiency research and technology at the Department of Energy (DOE), the latest twist in what supporters call a "death spiral" for a program that was once much larger.

Either ore. The Department of Energy says it needs to cut industrial efficiency studies of basic industries such as steel casting to fund more promising research.

A report last year by the National Academies' National Research Council found "significant cumulative energy and cost savings" in the seven energy-intensive industries covered by IOF, a sector that together consumes three-quarters of the energy used by U.S. industry. And last week, a report from the American Council for an Energy-Efficient Economy described improvements developed by efficiency researchers such as Beckermann, who benefit from matching funds from industry on each grant, as "low-hanging fruit." But DOE officials argue that private companies should pick up the tab for that harvest. "With high energy prices, there's incentive for industry to take on some of these programs," says Jacques Beaudry-Losique, DOE's industrial technology manager.

Toni Grobstein Marechaux, a former director of the academies' manufacturing and engineering design board, says the IOF program conducts research that industry wouldn't do on its own. Corporate leaders are reluctant to wait for the payoff from most efficiency research, she says, even with energy prices rising. The government also helps companies avoid potential antitrust issues when they work collaboratively with competitors. In addition, the program subsidizes work that some heavy industries simply lack the funds to carry out. Most metal-casting firms are small and employ few if any engineers, says Beckermann, citing as proof the crude modeling software that now exists.

IOF's supporters also worry about the next generation of energy-focused industrial engineers in the wake of the Administration's proposed 35% cut in the related $6.4 million Industrial Assessment Centers program that allows undergraduates to be energy-saving consultants to manufacturing plants. Patrick Johnson, a manager at the glass giant Corning, appreciates the value of the energy audits that the students perform. "Sometimes Corning employees have blinders on," he says.

DOE officials say the cuts are a necessary consequence of limited resources. Those budget pressures place a higher priority on new, long-term research into fuel sources such as cellulosic ethanol or nuclear power (*Science*, 10 March, p. 1369). On the other end of the spectrum, they note that 72 teams have completed assessments of energy-intensive manufacturing sites under the department's current "Save Energy Now" campaign. Despite the proposed cuts, they add, the IOF program will still support work with industry in fields including nanomaterials and catalysis.

Congressional staffers say that DOE's proposed cuts are penny-wise and pound-foolish. "Congress will have to restore funding to some of these accounts," says a House appropriations staffer. Beckermann hopes they do, calling the program "a model for industry-government collaboration." **–ELI KINTISCH**

CREDIT: PHOTOS.COM

Clouds Part for NASA

It took seven tries over 7 days, but two new Earth-observing satellites are finally exploring clouds and how they form. The successful launch on 28 April from California was a relief to scientists who face long-term budget cuts at NASA and who have endured a year of delays due to strikes, technical issues, and finally, bad weather.

Cloudsat and CALIPSO—short for Cloud-Aerosol Lidar and Infrared Pathfinder Satellite Observations—will provide insights from 750 kilometers above Earth into the complex interaction between clouds and climate.

–ANDREW LAWLER

Tennessee Scientists Beaming

After 7 years of construction and a few final, tense hours tweaking the machine, engineers at the new $1.41 billion Spallation Neutron Source (SNS) at Oak Ridge National Laboratory (ORNL) in Tennessee churned out their first few blasts of neutrons last week. "Everyone cheered and jumped up and down" as they watched the results from the SNS control center, says SNS project director Thom Mason.

SNS engineers will spend the next 1 to 2 years working out the machine's glitches to create the world's most powerful source of neutrons, which are prized for condensed matter physics and materials science research. But ORNL scientists should be able to start using the neutrons for experiments as early as this summer. Five beamlines are under construction, and the Department of Energy has asked for money next year to begin construction of 15 more. **–ROBERT F. SERVICE**

Weaponeers Seek Models

Modeling the behavior of nuclear bombs is getting tougher as stockpiled weapons age, so the National Nuclear Security Administration (NNSA) is refocusing toward prediction an existing program that funds academic computer scientists. Five universities currently run NNSA-sponsored modeling centers that do nonclassified work in areas including rocket behavior and exploding stars. Program head Dimitri Kusnezov says the academics have helped root NNSA in good science as well as top computing. But old bomb tests are becoming less and less relevant to aging weapons, he says, making prediction more important. Now he wants to recompete the contracts, emphasizing prediction of complex systems. "We can ask much more complex questions today," he says.

–ELI KINTISCH

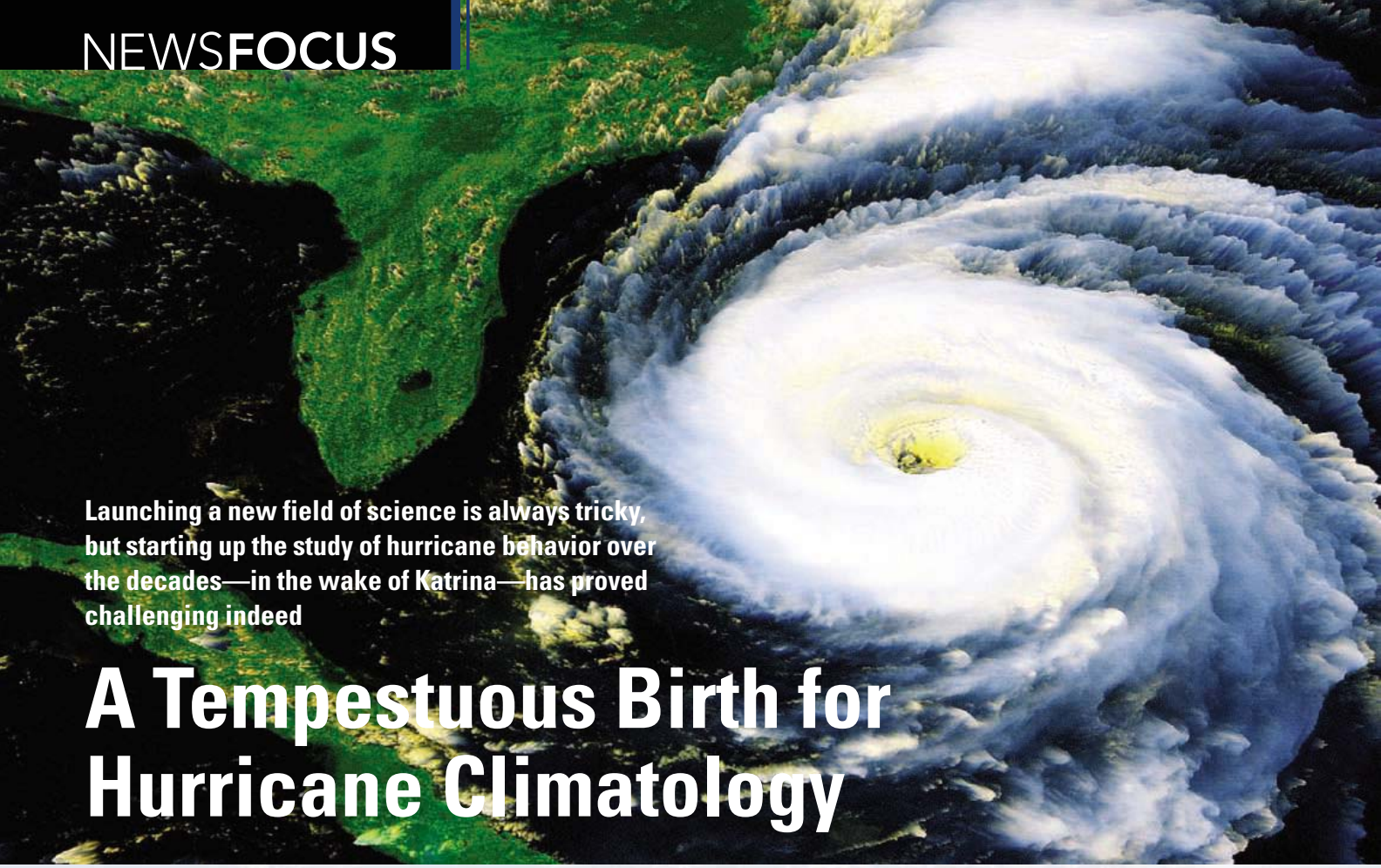

Launching a new field of science is always tricky, but starting up the study of hurricane behavior over the decades—in the wake of Katrina—has proved challenging indeed

A Tempestuous Birth for Hurricane Climatology

MONTEREY, CALIFORNIA—It's not every day one can witness the inception of a new field. Researchers attending the 27th Conference on Hurricanes and Tropical Meteorology late last month* got their usual diet of potential vorticity analyses and Madden-Julian oscillations. But they also debated a newborn science created to assess whether tropical cyclones—variously called hurricanes, typhoons, or cyclones—have strengthened under global warming.

Until *Science* and *Nature* published two papers last year contending that tropical cyclones around the world had strengthened, few scientists paid much attention to long-term variations in such storms. In those papers, a couple of academic meteorologists took the long view of tropical cyclone records compiled day-by-day by weather forecasters. From those weather records, the meteorologists extracted storm climatologies, statistical histories of storm behavior that could be searched for any change over the decades. Unexpectedly, they found a surge in tropical cyclone intensity—and if it continued under global warming, they concluded, it would noticeably amplify the destruction in coming decades. In the wake of Hurricane Katrina, those analyses were enough to spark a highly public and sometimes raucous new field: hurricane climatology.

Blown away. Tropical storm power and destruction go up with the cube of wind speed.

CREDITS (TOP TO BOTTOM): ROBERT MUNTEFERING/GETTY IMAGES; ANNIE GRIFFITHS BELT/NATIONAL GEOGRAPHIC/GETTY IMAGES

For some, a turnabout

In theory, tropical cyclones aren't supposed to be noticeably stronger after a few decades of warming, which explains why no one had been searching for a trend in the ups and downs of the storm record. Then, at an October 2004 press conference, meteorologist Kevin Trenberth of the National Center for Atmospheric Research (NCAR) in Boulder, Colorado, reacted to claims that the particularly active 2004 season in the Atlantic Ocean was just part of a natural cycle that pumps up Atlantic storms every few decades. He and the others on the panel "didn't think that was right," says Trenberth. "We thought global warming was playing a role." The burst of hurricane activity since 1995 just seemed too strong to be entirely natural.

Others thought Trenberth was the one getting it wrong. "We were rather skeptical" of Trenberth's remarks, says Peter Webster, who specializes in monsoons and other tropical phenomena. "We thought Kevin was sounding his trumpet a little bit." So Webster, a meteorologist at the Georgia Institute of Technology in Atlanta, and his colleagues looked at records of maximum wind speed of storms around the world as gauged from satellite images.

In the 16 September 2005 issue of *Science* (p. 1844), less than 3 weeks

* 27th Conference on Hurricanes and Tropical Meteorology, 24–28 April, Monterey, California (sponsored by the American Meteorological Society).

Rising threat? The number of Atlantic hurricanes (*left*) jumped in 1995, but globally the number of tropical cyclones is steady. The debate is over whether storms have been getting stronger as the world warms.

after Hurricane Katrina ravaged New Orleans, Webster and colleagues reported that in fact the abundance of tropical cyclones had not increased between 1970 and 2004. But the number of the strongest storms—those in categories 4 and 5—had jumped 57% from the first half of the period to the second. That reinforced findings by meteorologist and hurricane specialist Kerry Emanuel of the Massachusetts Institute of Technology in Cambridge. He had reported in the 4 August 2005 issue of *Nature* that the total power released during the lives of Atlantic and western North Pacific storms had risen between 40% and 50% from the first half of a 45-year record to the last half.

Both Webster and Emanuel were taken aback by their own findings. "I changed my mind in a big way" about how much the warming could be intensifying storms, says Emanuel. But it wasn't just because of the apparent upward trend of storm intensity. When Emanuel looked at how storm power and ocean temperature had varied, "what I found startled me," he told the conference. In the area just north of the equator in the Atlantic Ocean, where most hurricanes get their start, the power released during the lifetimes of storms is "spectacularly well correlated with sea surface temperature," says Emanuel. Hurricane intensity had risen along with temperature over the past half-century, even matching ups and downs along the way.

The region where Atlantic hurricanes develop has in turn warmed in step with the Northern Hemisphere for the past half-century, Emanuel noted. And that warming is widely held to be driven at least in part by rising greenhouse gases. Two studies may not be enough to prove that Trenberth is right about greenhouse warming driving storm activity, but both Emanuel and Webster now believe they see a strengthening of tropical cyclones suspiciously in synchrony with global warming.

Stormier models

Newly minted hurricane climatologists at the conference got some support from climate modelers. Kazuyoshi Oouchi of the Advanced Earth Science and Technology Organization in Yokohama, Japan, and his colleagues presented results from highly detailed climate simulations run on Japan's Earth Simulator, the world's most powerful supercomputer devoted to earth sciences. Global climate models typically calculate climate at points 200 kilometers or more apart. The resulting pictures of climate are too fuzzy to pick up anything as small as a tropical cyclone. But the Japanese group simulated the present climate and the greenhouse-warmed climate near the end of the century at a resolution of just 20 kilometers, thanks to the Earth Simulator's power. That was detailed enough for tropical cyclones to appear in the model, allowing the researchers to roughly gauge their intensities. In the warmer world, the total number of storms over the globe had actually decreased by 30%. But the number of the rarer category 3 and 4 storms had increased substantially, not unlike Webster's observational results.

Additional support for intensification also came from a new, independent analysis of wind data, mentioned in passing at the conference.

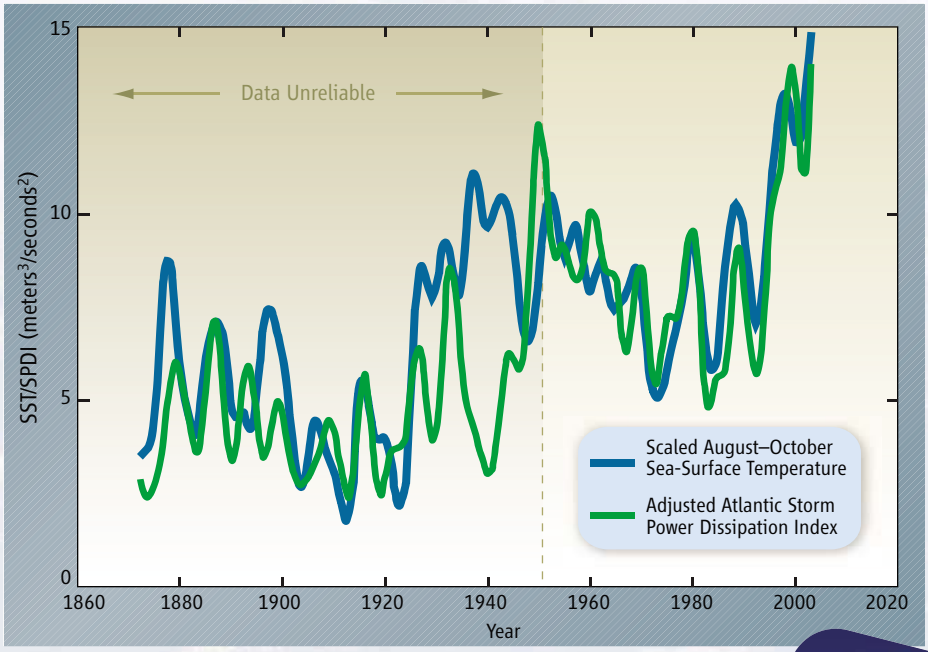

Cause and effect? As late-summer water temperatures rose in the tropical Atlantic, where hurricanes get started, the power released by Atlantic hurricanes rose too.

Climate researchers Ryan Sriver and Matthew Huber of Purdue University in West Lafayette, Indiana, will soon report in *Geophysical Research Letters* on how they measured the power released by storms by using a compilation of the world's weather data developed at the European Centre for Medium-Range Weather Forecasting in Reading, U.K. They found a 25% increase in storm power between the first half of the 45-year record and the second, consistent with Emanuel's analyses.

Even stormier objections

Intensifying tropical cyclones possibly driven by the greenhouse might sound like one more chapter in the familiar global warming story—melting glaciers, rising seas, searing heat waves—but some read it differently. The U.S. National Oceanic and Atmospheric Administration (NOAA) stated last year in press releases that "longer-term climate change appears to be a minor factor" in "the most devastating hurricane season the country has experienced in modern times." The surge in Atlantic hurricane activity since 1995 is the latest upswing in a natural cycle, the releases said. As the Atlantic Ocean warms and wind patterns shift, hurricanes increase for a decade or two until a lull sets in again.

NOAA's seemingly official pronouncements sounded moderate next to that of William Gray of Colorado State University (CSU) in Fort Collins, an elder statesman of the hurricane community. Well known for his forecasts of the coming hurricane season, Gray pushes natural cycles with a vengeance. "There's definitely a big multidecadal cycle going on," he said in his conference talk, not just in the Atlantic Ocean but around the world. "This isn't global-warming induced; this is natural. We may go for a few years, and then it's going to cool." And with the cooling, hurricanes will calm down again, he said, just as they have before.

The warming of recent decades and the jump in hurricanes are being driven by a surging ocean current that brings warm water northward into the Atlantic Ocean, Gray insisted. Climate models in which mounting greenhouse gases drive global warming have simply got it wrong, he said; greenhouse gases are feeble agents of warming. "I'm a great believer in computer models," he said. The audience laughed skeptically. No, he assured them, "I am—out to 10 or

CREDITS: (SOURCE) K. EMANUEL/MIT; (RIGHT) ALAN SCHEIN PHOTOGRAPHY/CORBIS; (BACKGROUND) NASA

Storm central. Planes were able to penetrate Katrina's eye wall (*left*) and drop probes through the storm (*lower left*), greatly improving storm-intensity measurements.

12 days. But when you get to the climate scale, you get into a can of worms. Any climate person who believes in a model should have their head examined. They all stink."

"This was highly entertaining," observed meteorologist Gregory Holland of NCAR from the audience, "but unfortunately you obfuscate the real issue." Holland, a graduate student of Gray's at CSU in the early 1980s, is second author on Webster's *Science* paper. He went on to staunchly defend climate models. "Right now, they're providing a very good, rational picture of the situation," he concluded. Supportive applause rose from the audience.

Later, during a panel discussion, Emanuel questioned even the existence of a natural cycle of Atlantic warming and cooling, at least one that influences the development of hurricanes. He believes a misstep in a classic analysis—a 2001 *Science* paper on which Gray was an author—tended to create a cycle where none exists. By subtracting a linear trend from a record of rising temperature that actually contained the nonlinear, upward-curved trend of global warming, the analysis created an oscillation, he said. In the end, Emanuel finds "no evidence for natural cycles in late summer tropical Atlantic sea surface on these time scales," which for him leaves global warming as the leading candidate for a driver.

A haphazard record

Emanuel's line of argument caught critics by surprise, and his challenge to a purely natural driver for hurricane activity went largely unanswered at the conference. NOAA scientists such as meteorologist Christopher Landsea of the National Hurricane Center in Miami, Florida—another former Gray student—claimed that NOAA public affairs staff members writing the press releases had overstated the case for a natural cycle. And the warming may well be largely human-induced, said Landsea. The question, he argued, is not what's causing tropical warming, but how much of an impact does that warming have on hurricane intensity? Not much, he suspects. According to theory and computer modeling, by now the intensification should be only a sixth of what Webster and Emanuel have reported, he noted. Rather than a real strengthening, Landsea said, Emanuel and Webster may well be seeing a fictitious one created by a deeply flawed hurricane record.

Emanuel disagrees. "They tend to count [the anomalous strengthening] against the observations," he says. "I count it against the theory, although I helped develop the theory."

That moved the debate to the observational record of tropical cyclone intensity, where attendees found considerable grounds for agreement: The record is far, far from perfect. Hurricane climate researchers have the same problem as climate researchers had when they began searching for signs of global warming. Weather forecasters created the surface temperature record as they went about their business predicting the next day's weather. They never planned to string their twice-daily measurements into a century-long record, so they had no qualms about moving their thermometers from place to place, and they paid no mind when heat-retaining cities grew up around them.

Likewise, forecasters' observations of tropical cyclones "weren't designed to be climate records," notes Landsea. And to make matters even worse for hurricane climatologists, hurricane forecasters almost never directly measure storm intensity—the maximum wind speed 10 meters above the surface averaged over 1 minute. Instead, they usually gauge maximum wind speed indirectly.

Indirect measurements of storm intensity haven't always been done well or frequently, either. By the time Hurricane Carol hit in 1954, Landsea noted, forecasters were flying into storms—if they weren't too strong—and judging wind speed by looking down at waves on the ocean. Sometimes they would estimate maximum winds by making their best guess of how winds would change from their aircraft's altitude to the near-surface. Such sampling wouldn't have caught Hurricane Wilma's 1-day leap last fall from minimal hurricane to category 5, he said. That took eight types of measurements made 280 times over 12 days, and some of those measurements required air-dropped instrumentation and satellites. Even today, says Landsea, "there are big discrepancies about how strong a storm was." The U.S. and Japanese typhoon warning centers for the Pacific Ocean—where no aircraft reconnaissance is done now—at times differ in their estimates by as much as two categories.

At the conference, a half-dozen speakers documented the sad state of tropical cyclone intensity measurements. Two groups—led by John Knaff of CSU and by Bruce Harper of Systems Engineering Australia Proprietary Limited in Brisbane—attempted to correct intensity records from parts of the Pacific Ocean for now-obvious errors. Both reanalyses reduced the upward trend of storm intensity. Knaff's work, in particular, suggests that Emanuel's and Webster's studies "may have been premature," says Landsea. "The database wasn't up to it."

On the other hand, the reanalyses did not eliminate the trend. "The data's not very good," agreed Webster. "However, to say it's all artificial is an exaggeration. We would have had to have misidentified 160 to 180 category 4's and 5's." He doubts they were off by that much.

The discussions at the conference, although informative, did not change many minds. "There are persuasive arguments on both sides," says Hugh Willoughby of Florida International University in Miami and former director of NOAA's Hurricane Research Division. "Honestly, we don't know" who's right, he says. "That's the real story." Tropical cyclones probably intensify under warmer climates, he says, but most likely not as much as Webster and Emanuel believe. "We don't know where we are in the middle." That's what the new field of hurricane climatology hopes to find out.

–RICHARD A. KERR

CREDITS (TOP TO BOTTOM): LCDR SILAH/NOAA AIRCRAFT OPERATIONS CENTER (AOC); NOAA AOC

NUCLEAR PHYSICS

Indian Angst Over Atomic Pact

Facing new restrictions on where and with whom they work, some Indian nuclear scientists assert that a historic agreement will narrow their research horizons

MUMBAI—Over the years, physicists at two scientific powerhouses here—the Tata Institute of Fundamental Research (TIFR) and the Bhabha Atomic Research Centre (BARC)—have enjoyed a tight-knit collaboration in superconductivity research, producing two dozen papers and a handful of patents. But their days of working side by side may be numbered. Under a controversial nuclear deal with the United States, India has agreed to separate its vast nuclear establishment into civilian and military programs—and BARC is on the military list. If the pact is finalized, BARC scientists may no longer be allowed to work with their civilian counterparts. If TIFR were forced to sever all linkages with BARC, says TIFR director Sabyasachi "Shobo" Bhattacharya, a condensed matter physicist, "it would be a real tragedy, but the worst-case scenario may not unfold." Others are not so optimistic.

In March, India and the United States unveiled a landmark agreement that would end India's status as a pariah for having snubbed the Nuclear Nonproliferation Treaty and acquired a nuclear arsenal. Under the agreement, India would be allowed to import civilian nuclear technology in exchange for submitting key facilities to international inspections. Even before the ink was dry, however, some U.S. nonproliferation analysts assailed the pact as a bad deal that would not make the world safer. Indian scientists and officials, meanwhile, hailed it as a triumph (*Science*, 10 March, p. 1356).

Now many Indian nuclear scientists are having second thoughts. They fear that a key provision—cordoning off military facilities—will end scores of collaborations and maroon thousands of physicists in military labs. Civilian labs would suffer as well, they claim, under the scrutiny and paperwork demands of inspectors. Some fear that their research environment, already hampered by U.S. sanctions and prohibitions on nuclear imports, will deteriorate further. "The India–United States deal will destroy nuclear research in India," fumes Padmanabha Krishnagopala Iyengar, a nuclear physicist and former chair of the Indian Atomic Energy Commission. "How can one subject any scientific creativity to safeguards and inspections?"

These concerns could undermine negotiations aimed at tweaking the agreement to make it more palatable to the U.S. Congress, which must amend laws for the deal to go through. A Senate hearing on 26 April challenged the deal; Democrat Joseph Biden of Delaware demanded "a full list of India's civilian facilities." Already, India has spurned a U.S. request to forswear nuclear tests. Indian negotiators, contacted by *Science*, say they will raise the possibility of continued scientific collaborations between BARC and TIFR—possibly in negotiations with the International Atomic Energy Agency (IAEA) in Vienna, Austria, and during upcoming talks with the United States on a special Indian inspection regime.

Inspections "are extremely intrusive, immensely disruptive, and are often conducted in an atmosphere vitiated by suspicion," contends Iyengar, who served on IAEA's board of governors. India has listed nine of the Department of Atomic Energy's two dozen or so research facilities as civilian (see table, below). "Any or all research [at these labs] may come under scrutiny," Iyengar says. IAEA declined to comment on the ongoing negotiations.

Nuclear researchers also object to U.S. demands that India erect firewalls to prevent skilled scientists from serving in both civilian and military labs. Annaswamy Narayana Prasad, a mechanical engineer and former BARC director, says that "effective separation of the two components is a near impossibility." The proposal would require the Department of Atomic Energy to label each of its 65,000 staff members as civilian or military personnel, possibly freeze movement between the sectors by 2014, and perhaps end collaborations. Says Avinash Khare, a theoretical physicist at the Institute of Physics in Bhubaneswar, this "would be a real calamity."

India also may have to speed up work on new training and research facilities. Already, India has agreed to decommission two of three research reactors at BARC by 2010. The remaining reactor, the 100-megawatt Dhruva, would be overwhelmed by current users.

The bottleneck could be solved if a new reactor is built on a civilian site—but Indian officials say they may choose to build it at BARC, a military center. According to Anil Kakodkar, a mechanical engineer and chair of the Atomic Energy Commission, the government has not yet decided whether to site the proposed $100 million, 30-megawatt multipurpose reactor on BARC's main campus or at a satellite facility in Vizag, which might enable classification as a civilian reactor. It could come online as early as 2014. Srikumar Banerjee, a materials scientist and director of BARC, says plans are under way to ensure that a small research reactor at BARC, Apsara, is not shut down but refurbished using Indian nuclear fuel.

With the nuclear deal under fire in both India and the United States, its fate for now seems uncertain. To a growing number of Indian scientists, that would not be the end of the world.

–PALLAVA BAGLA

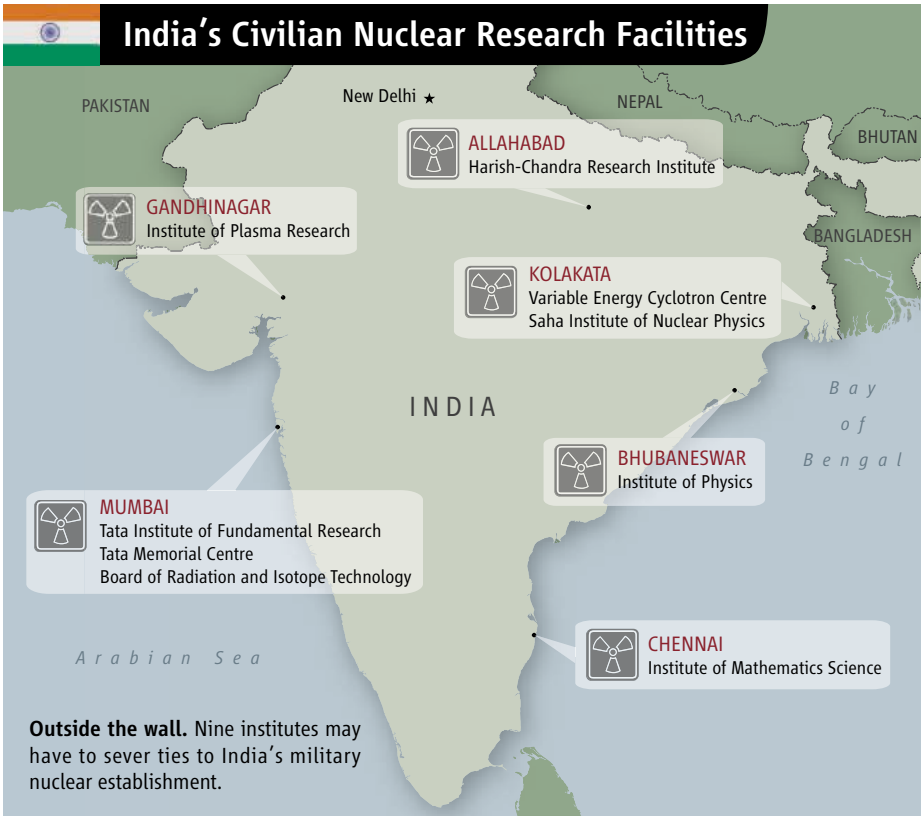

Outside the wall. Nine institutes may have to sever ties to India's military nuclear establishment.

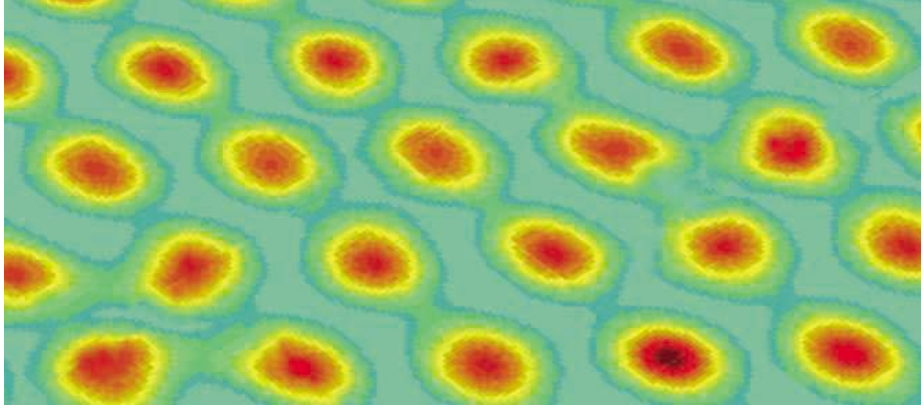

On the grid. As rodents explore an environment, neurons called grid cells fire in a regular geometric pattern such as this one.

NEUROSCIENCE

The Map in the Brain: Grid Cells May Help Us Navigate

A newfound class of neurons enables the brain to perform complex spatial navigation—and may even help form memories

If you're in an unfamiliar city and trying to locate the convention center for yet another conference, a map prepared by the local Visitor's Bureau can come in handy. It's likely to incorporate a navigational aid: an overlaid square grid, often with rows labeled with letters of the alphabet and columns labeled with numbers. An index might tell you that your hotel is in the A2 square, and the convention center can be found in Q22.

Last November, scientists who successfully reached the new Washington, D.C., convention center heard Norwegian neuroscientist Edvard Moser address the Society for Neuroscience's annual meeting. In an invited talk, he told the audience that rodents, and presumably people, have their own versions of such navigational grids embedded in their brains. "I swear my jaw just dropped," recalls computational neuroscientist David Redish of the University of Minnesota, Minneapolis. "It's amazing to see the interaction between theory and experiment that has come together in the Mosers' work." James Knierim, a neuroscientist at the University of Texas Medical School in Houston, was equally impressed by the talk, declaring, "Moser's work is the most important discovery in our field in over 20 years."

The jaw-dropping discovery, announced 3 months earlier in a paper in *Nature*, centers on a brain region called the entorhinal cortex. Moser and his colleagues, including his wife May-Britt Moser and postdoctoral researchers Torkel Hafting and Marianne Fyhn, let rats roam freely in large enclosures while recording the firing of individual neurons from this cortical region. The neurons fired at distinct places: If plotted on a map of the enclosure, the firing locations of each neuron formed a triangular grid. "It's a lattice that's repeated over and over again," says Edvard Moser. Consequently, he and his team at the Norwegian University of Science and Technology in Trondheim have dubbed these previously unknown neurons "grid cells."

Notably, the grid is self-generated. The cells fire almost as if there were invisible, overlapping grids painted on the enclosure's floor, with each individual neuron laying out its own "virtual" grid—and the scale of the grids can vary in size from neuron to neuron. "Somehow the system, in this totally abstract way, is saying it's time for this cell to fire," explains Patricia Sharp of Bowling Green State University in Ohio. "You just can't explain it through external input; … there's no such pattern in the animal's world." Indeed, the rat doesn't need visual cues once it has been in an enclosure; a grid cell still fires in the same pattern if the animal roams in the dark.

Even Moser and his team doubted their results at first. "We didn't really believe it," he says. "We had to do some additional analysis to make sure this was biological." On page 758, the Mosers and their colleagues add to the unfolding story, describing neurons in the entorhinal cortex that encode not only where a rat is, but also how fast it is moving and in what direction. Theoreticians believe that grid cells and their connections to other neurons may finally clarify ideas about how the brain performs spatial navigation. "We're over the moon about this discovery," says John O'Keefe of University College London (UCL).

Fired up. Edvard and May-Britt Moser analyze the neuronal activity of brain regions involved in spatial navigation.

Everything in its place

In the 1970s, O'Keefe and his UCL colleagues discovered "place cells" in the hippocampus of the rat. On the simplest level, these neurons fire in response to where an animal is in space. Similar to the Mosers' new work, place cell experiments often feature a rat, with multiple electrodes implanted in its hippocampus, freely moving within an experimental environment; a given place cell only fires when the rat walks in a particular area, dubbed the cell's "place field." Transfer the rodent to a different environment, and some of the same place cells are used to create a new map of the surroundings, a process called "hippocampal remapping." This allows place cells to store representations of many different environments.

After O'Keefe's initial discovery, he and colleague Lynn Nadel felt that place cells must form the basis of a "cognitive map" in the hippocampus, but they realized it would take more than just place cells for an animal to navigate its world. Says O'Keefe, "We predicted right from the beginning that there would have to be information about directions and distances to tie together the place cells into something like a map formation."

In the 1980s, James Ranck of the State University of New York Downstate Medical Center in Brooklyn identified another key group of navigational neurons: head direction cells, which have connections projecting into the entorhinal cortex. Depending on which way the animal is pointing its head, different groups of these cells fire, letting the animal know which way it faces.

Still, the brain needs more to navigate through a complex world. "You have information about place cells—it tells you where you are located—and you have information from head direction cells that tells you what direction you're facing, but how do you then use all that information to update over time your path through an environment?" asks Jeffrey Taube, who was a postdoc with Ranck and continues to study head direction cells at Dartmouth College.

That process of real-time updating is known as "dead reckoning" or "path integration," and it is now thought that grid cells might be the key to how it works. These neurons' discovery came about through follow-up experiments on place cells. As scientists probed more deeply into the

CREDITS (TOP TO BOTTOM): BJARNE RØSJØ/FAKTOTUM INFORMASJON, NORWAY; F. SARGOLINI *ET AL.*, *SCIENCE*

hippocampus, they found place cells with larger and larger place fields. But it's hard to gauge the extent of a large place field, because one can't track neuronal activity in rats running in the wild. In the standard, small experimental enclosure, "the cells either don't fire, because you're not in the place field, or they fire everywhere, because the place field is huge," explains the Mosers' collaborator Bruce McNaughton of the University of Arizona, Tucson.

In order to better understand larger place fields in the hippocampus, the Mosers had built an enclosure about twice the standard size. After they published a paper in *Science* in 2004 that reported regularly structured peaks in the firing patterns of entorhinal cortical cells, they conducted follow-up experiments in the larger enclosure. "It seemed almost silly not to do it," says Edvard Moser. Once they were able to analyze more entorhinal neurons firing over a larger territory, the group realized they were looking at grids.

How do grid cells help rats, and presumably people, find their way? "The fundamental duty of the grid cells is to provide the coordinate system, with which the place cells can then do their association of objects," says Redish.

Consider the find-the-college-library problem. For most schools, you can get a map that lays the campus out on a grid. At Princeton, the Gothic Firestone Library is at grid square F1. At the University of California, San Diego, the spaceship-like Geisel Library is at grid square E7. The underlying map grid is the same; only the identity and position of individual buildings differ. The hippocampus notes the landmarks (Gothic buildings = Princeton) and maps them onto the entorhinal grid. "The grid cells in the entorhinal cortex provide a coordinate system, but the hippocampus must use those inputs to create a map of the environment," says Terry Sejnowski of the Salk Institute in San Diego, California.

What lies beneath

That still begs the question of how the brain generates its grids. The leading theories, proposed by several groups, among them McNaughton and his collaborators, and David Touretzky and Mark Fuhs of Carnegie Mellon University in Pittsburgh, Pennsylvania, have to do with "attractor networks," which can be conceptualized as a sheet of neurons packed closely together like marbles on the surface of a table. In the grid cell attractor network, each neuron in the sheet is a different grid cell. Grid cells adjacent to one another in this sheet are not necessarily next to each other in the brain, but they represent locations that are next to each other in the real world. Thus, if one grid cell fires at a certain location, then the neurons surrounding it in the sheet will fire at nearby locations.

When the rat stands at one location, the grid cell that represents that position will be very active along with neighboring cells in the network. All this activity forms a "bump" on the sheet. Excitatory connections between each cell and itself, and between it and its nearest neighbors, make the bump self-sustaining. The activated neurons also excite a bunch of inhibitory cells that prevent distant neurons from firing, thus the surrounding flatness. As the rat walks through space, the bump moves along the grid to keep track of its location, like Bugs Bunny burrowing in an old cartoon.

"In order for this network to work, the bump has to move with the rat exactly, so if the rat moves 3 feet in real space, the bump has to move however many cells in the brain correspond to 3 feet in real space—and that's not a trivial problem," says Hugh Blair of the University of California, Los Angeles. "You would need neurons in the attractor network that would encode the speed and direction in which the rat is moving."

And that is what the Mosers, postdoc Francesca Sargolini, and their collaborators report finding in the new *Science* paper. The work reveals "conjunctive cells," a class of grid cells that give exactly the path integration information—speed of movement and direction—needed to move the bump.

The entorhinal cortex is "a complicated network consisting of four layers of principal cells … with different morphologies and different interconnections," notes Edvard Moser. As they probed deeper into these layers with electrodes, they found cells with the properties of both head direction cells and grid cells. Additionally, they found other cells whose firing rate expressed the speed of the animal. "You have cells that express position, direction, and speed," says Moser. "That's what you need to really tell you where you are at any given time as you're walking around. It's the conjunction of those properties that I believe—and I say 'believe' because we haven't shown it—could be fed up to the attractor network of the pure grid cells."

Mapping the future

Because of the connections between the entorhinal cortex and the hippocampus, O'Keefe, UCL's Neil Burgess, and others have begun to explore whether grid cells have something to do with the mysterious oscillatory firing of groups of hippocampal cells. The role of these 6-to-10-Hz "theta" oscillations has fascinated O'Keefe for years. He and Burgess have recently suggested that interference patterns formed by theta waves with slightly differing frequencies guide the firing of grid cells and thus the creation of the grid.

Grid cells could have an even more fundamental purpose than navigation, according to Blair. "Grid cells may be giving us our first real glimpse of the building blocks of hippocampal-dependent memories," he suggests. In collaboration with Kechen Zhang of Johns Hopkins University in Baltimore, Maryland, Blair's lab is exploring whether grid cells can be used as fundamental components for assembling representations of two-dimensional objects. Blair suggests that grid cells could also construct mental representations of more complex objects, such as visual images of faces and scenes.

"The really remarkable thing is that when you build a two-dimensional memory representation out of grid fields, there is a simple trick you can do to make the memory 'scale-invariant,' " says Blair. "For example, when you meet a new person, you don't have to store a separate memory of what they look like from close up versus far away. Our work suggests that if you build your memory representation of the person's face out of grid fields, then you can easily represent their face at all possible sizes." If he's right, grid cells may underlie both how you can find the convention center and how you can find a colleague in the crowd there.

–KAREN HEYMAN

Karen Heyman is a writer in Santa Monica, California.

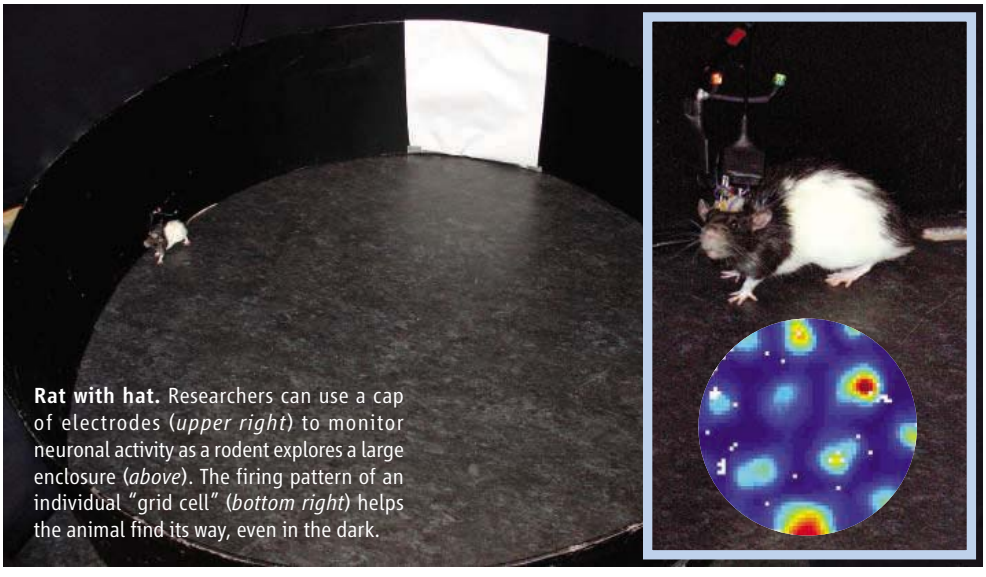

Rat with hat. Researchers can use a cap of electrodes (*upper right*) to monitor neuronal activity as a rodent explores a large enclosure (*above*). The firing pattern of an individual "grid cell" (*bottom right*) helps the animal find its way, even in the dark.

CREDITS: EDVARD MOSER/CENTRE FOR THE BIOLOGY OF MEMORY, NORWEGIAN UNIVERSITY OF SCIENCE AND TECHNOLOGY

GE & Science Prize for Young Life Scientists

Your essay may be the winner this year

GE & Science Prize for Young Life Scientists was established in 1995, and is presented by *Science*/AAAS and GE Healthcare. The prize was established to help bring science to life by recognizing outstanding PhDs from around the world and rewarding their research in the field of molecular biology.

This is your chance to gain international acclaim and recognition for yourself and your faculty, as well as to turn your scientific ideas into reality. If you were awarded your PhD in molecular biology* during 2005, describe your work in a 1,000-word essay. Then submit it for the 2006 GE & Science Prize for Young Life Scientists. Your essay will be reviewed by a panel of distinguished scientists who will select one grand prizewinner and four regional winners.

The grand prizewinner will get his or her essay published in *Science*, receive US$25,000, and be flown to the awards ceremony in Stockholm, Sweden. Entries should be received by **July 15, 2006**.

GE & Science Prize for Young Scientists: Life Science Re-imagined.

For more information on how to enter, go to www.gehealthcare.com/science

Established and presented by:

Science AAAS

* For the purpose of this prize, molecular biology is defined as "that part of biology which attempts to interpret biological events in terms of the physico-chemical properties of molecules in a cell" (McGraw-Hill Dictionary of Scientific and Technical Terms, 4th Edition).

PHYSICS

Tipping the Scales—Just Barely

Researchers are making big strides in a race to build nano-sized devices capable of weighing a single proton

Next to Kate Moss, Michael Roukes may be the most obsessive weight watcher on Earth. Roukes, a physicist at the California Institute of Technology (Caltech) in Pasadena, isn't particularly worried about putting on or shedding a kilogram. He's thinking much lighter than that. In the 4 April issue of *Nano Letters*, Roukes and colleagues report making the most sensitive mechanical scale ever, capable of registering 0.00000000000000000007 grams, or 7 zeptograms.

Even that achievement—weighing the equivalent of 30 xenon atoms—isn't enough to satisfy him, however. Within 2 years, Roukes and colleagues hope to register the weight of individual hydrogen atoms, a mere 1.66 yoctograms ($1.66 \cdot 10^{-24}$ grams). For perspective, a yoctogram is to a gram as a gram is to the mass of the continental crust under Europe. Top that, Kate.

Roukes's team isn't alone in its effort. Numerous groups around the globe are pushing the boundaries of ultrasensitive mechanical mass detectors. Most researchers, including Roukes, are seeking practical applications such as nanoscale versions of mass spectrometers, large and ubiquitous machines used for weighing molecules. A few, such as the Caltech group, are also hoping that their scales are sensitive enough to pick up individual protons. "It's within reach," says Rashid Bashir, a ultrasensitive mass detection expert at Purdue University in West Lafayette, Indiana. "But it won't be easy."

The race to zeptogram sensitivity began heating up in 2003, when a pair of researchers at Oak Ridge National Laboratory in Tennessee reported that they had created nanoscale devices capable of registering organic compounds with a mass of 5.5 femtograms (10^{-15} grams). Harold Craighead and colleagues at Cornell University leaped past that figure in April 2004 with a report that they could detect mass changes down to the attogram level (10^{-18}). Kamil Ekinci, a former postdoc of Roukes who now runs his own lab at Boston University, patented an attogram detector with his mentor back in 2001, although their results didn't hit the scientific literature until May 2004. Now, with their *Nano Letters* paper, Roukes and Ekinci have taken the sensitivity to nearly the single-zeptogram scale.

There are many ways to measure mass. Most mechanical scales are made from tiny wires of silicon or other sturdy materials suspended over a surface. The scales are anchored either on one end, like a diving board, or at both ends, like a bridge. Researchers trigger oscillations in the wires and track how the frequency of those oscillations changes when a tiny speck of mass is added.

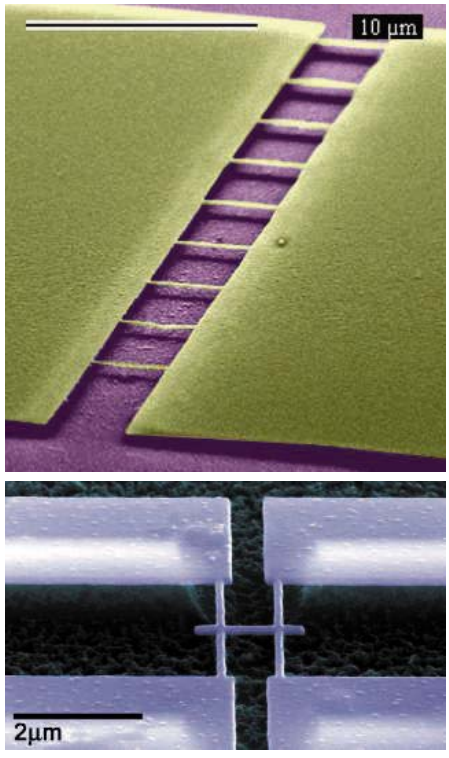

Lightweights. Nanoscale sensors made by teams at Caltech (*above*) and Boston University (*top*) register tiny weights by creating oscillations in wirelike slivers of material and then gauging how those oscillations change when a tiny collection of atoms or molecules is sprayed on top.

In their paper, Roukes, Ekinci, and Caltech colleagues describe how they constructed tiny bridges from silicon carbide and connected a wire to each end of the bridge. They then placed their device in a vacuum chamber and within a large magnetic field, passing a current through the silicon carbide bridge from one wire to the other. The motion of the electrical charges in the magnetic field exerted a sideways force on the bridge, essentially plucking it like a guitar string and causing it to oscillate up and down.

The team then used a specially designed electrical feedback loop to make it vibrate at a steady frequency of either 133 or 190 megahertz. This motion created a steady pattern of voltage changes between the wires at either end of the bridge. The researchers then sprayed xenon atoms or nitrogen molecules through a specially designed shutter in the vacuum chamber. When the extra atoms landed on the bridge, the added mass slowed the bridge's vibrations, causing a change in the pattern of voltage readouts.

Ekinci says that since 2002 the team has improved the sensitivity of its apparatus 1000-fold. But he says it will take another such jump to detect individual hydrogen atoms. "This approach has very good potential to go to higher sensitivity," Ekinci says. To succeed, however, Ekinci and Roukes will need to make slightly smaller, more responsive bridges, get them to oscillate at a slightly higher frequency, and tweak the feedback circuitry to improve detection. Each advance has already been demonstrated independently; now Roukes's current team is working on putting them all together.

Other groups are also hard at work. One, led by Andrew Cleland at the University of California, Santa Barbara, for example, is using thermal energy to push an oscillating beam right up to a critical point, at which a tiny amount of added mass will push it over the threshold and cause the beam to oscillate at a markedly different frequency. But Cleland concedes that Roukes's team is the current leader.

The ability to weigh individual hydrogen atoms is expected to stimulate interest in nanomechanical mass sensors. Much of the payoff will likely come in differentiating the weights of different biomolecules, such as proteins. Such an advance could lead to nanoscale mass spectrometers capable of weighing individual molecules.

Current mass spectrometers, by contrast, start with millions of molecules and compute their average weight. By looking at single molecules, researchers could detect minute changes, such as proteins with a very slight sequence change or ones labeled with different isotopes. They could also track the weights of neutrally charged molecules, a feat mass spectrometers cannot perform because they use the charge of different molecules to propel them through the mass detector. By using the lithographic tools of the electronics industry, researchers also could make huge arrays of nanoscale mass spectrometers that look at vast numbers of biomolecules simultaneously.

Efforts to use nanomechanical sensors to weigh biomolecules are well under way. Craighead's group at Cornell, for example, reported in 2001 that it was able to detect single cells with attogram-scale masses. More recently, researchers have tracked individual viruses and DNA molecules. "But it will take a bit more time" to make practical devices, Ekinci says.

One challenge is that biomolecules exist in watery environments rather than in vacuums. But operating nanoelectromechanical systems devices in water causes the molecules to stick to their cantilevers and change their motion. Numerous teams are working on specialized coatings to fend off nontarget molecules or latch onto targeted ones. Their success promises to open new windows into the biochemistry of individual cells.

–ROBERT F. SERVICE

CREDITS (TOP TO BOTTOM): K. EKINCI/BOSTON UNIVERSITY; X. L. FENG AND M. L. ROUKES/CALTECH

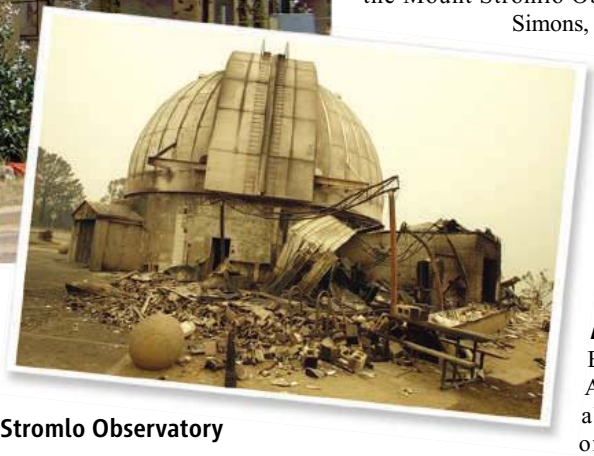

ASTRONOMY

Rising From the Ashes

Three years after a devastating fire, Australia's Mount Stromlo Observatory is well on the road to a Phoenix-like recovery

MOUNT STROMLO, CANBERRA—The loss didn't sink in until Rachel Campbell saw the charred remains for herself. Then a Ph.D. candidate at the Research School of Astronomy and Astrophysics (RSAA) of Australia National University (ANU), Campbell had been wrapping up a search for large objects beyond Neptune that, she hoped, would challenge conventional notions of planet formation. When wildfires swept over Mount Stromlo on 18 January 2003, she heard that RSAA's mountaintop observatory had been "damaged." Only when the staff was allowed to visit several days later did Campbell discover that the 50-inch Great Melbourne Telescope she had been using, along with her computer with 3 years' worth of analyzed data, had been "totally destroyed."

"I felt a lot of confusion," she recalls. "I knew that the project was ended but didn't know what would happen to me or my thesis."

Confusion quickly turned to gritty resolve. Three weeks after the fire, Campbell was ensconced in a lab at the University of Pennsylvania, reconstructing her unique software and preparing to process backup copies of raw image data. Finishing her degree took a year longer than expected. "But I got to reanalyze the data and did a better job the second time around," she says. She found three new candidate objects and confirmed several others. Besides a Ph.D., her findings led to several invited talks and a research position at Macquarie University in Sydney. The fire was a shock, she says, "but more positives than negatives came out of it."

Campbell was not alone in her determination to turn adversity into advantage. Using salvaged computers, temporary offices, and borrowed observing time, RSAA researchers have been so productive over the last 3 years you might never suspect that a fire had gutted some of their key facilities. They have described the oldest star yet found, finished releasing data from the largest-ever galaxy survey, and published on topics including gamma ray bursts and the universe's expansion. Even with their workshops reduced to cinders, RSAA's instrument team delivered a major device to the Gemini North 8-meter telescope on Mauna Kea, Hawaii, last fall and will ship another to the Gemini South telescope in Chile by June. Charles Alcock, head of the Harvard-Smithsonian Center for Astrophysics in Cambridge, Massachusetts, says the group's resilience "is revealing of how strong they are intellectually."

Fortunately, RSAA did not lose all of the Mount Stromlo Observatory, a leading astronomy center that over its 82-year history has been known for achievements such as deciphering the nature of the solar corona and gathering some of the first clues to the chemical makeup of the universe beyond the Milky Way. Most staff offices and computing facilities survived, as did newer telescopes at Siding Spring Observatory, about 450 kilometers north of Mount Stromlo. The surviving facilities helped the astronomers get right back to research, and "they were immediately talking about what to rebuild, what to let go of, and what to do better," says John Tonry, an astronomer at the University of Hawaii, Manoa. As a result, RSAA is now completing the first phase of facility reconstruction, with larger and better equipped workshops opening this summer and a new, advanced telescope set to see first light in late 2006 or early 2007.

"The staff were determined that this was just going to have as little impact as possible," says Penny Sackett, director of RSAA and the Mount Stromlo Observatory. Douglas Simons, director of the Gemini Observatory in Hilo, Hawaii, who visited Canberra days after the fire, says he is "incredibly impressed" with how Sackett's group "pulled through that gigantic mess."

Annihilation

Bushfires regularly set Australia's dry interior ablaze. But the fires of January 2003 were unusually intense. Touched off by lightning strikes in the grasslands west of Canberra, the flames advanced slowly toward Mount Stromlo over 2 weeks. On Friday, 17 January, fire modelers assured RSAA officials that Mount Stromlo was safe for the time being. But the next morning, the fires surged, gaining 10 kilometers in 15 minutes, by one estimate. By noon, authorities ordered people off the mountain. By dusk, Mount Stromlo lay in ruins.

Sackett made it to the top of Mount Stromlo on Sunday afternoon, 19 January. There, she says, she found "a scene of total devastation." The losses included:

- A 74-inch telescope fitted with an advanced spectrometer. It was being used to search for ancient stars and to determine the chemical compositions of stars, both essential to developing models of the early universe.
- The 50-inch Great Melbourne Telescope, once the world's largest. Built in 1868, it had been extensively upgraded and had been a key facility in the hunt for dark matter as part of the Massive Compact Halo Objects (MACHO) project.
- The instrument workshops, where the Near-Infrared Integral-Field Spectrograph (NIFS), a tool for studying black holes, was undergoing final testing before shipment to the Gemini North telescope.
- The historic 1924 Commonwealth Solar Observatory building, which housed the library, including irreplaceable monographs.
- Three smaller telescopes used for public viewing and a half-dozen observatory houses.

Fortunately, an administration complex and the bulk of Mount Stromlo's computing facilities were spared.

CREDITS: D. NORMILE; (INSET) PHOTO BY DANIEL BEREHULAK/GETTY IMAGES

Reeking of smoke, Sackett drove straight from the mountain to the ANU campus in Canberra, where vice chancellor Ian Chubb had marshaled two dozen university officials to start planning Mount Stromlo's recovery.

Although Mount Stromlo's offices were intact, all utilities were down. Within 3 days, ANU's computing staff had a copy of the Mount Stromlo server running on campus; 80 astronomers and grad students occupied a computer center for 3 weeks. That gave ANU technicians time to set up generators and a microwave link on the mountain. The staff felt "we can do without toilets, we can bring our own water, but we have to have Internet," says Sackett.

The return to Mount Stromlo was not so pleasant. "It was pretty stinky" from the smoke, says Ph.D. candidate Anna Frebel. Graduate students say they felt under particular pressure to get their research back on track. Offers of observing time, access to specialized computers, and support to attend conferences poured in from around the world. "It really was wonderful how the astronomical community helped us out," says Campbell.

Back on track. While Stromlo director Penny Sackett (*above*) solved institutional issues, grad students such as Anna Frebel (*inset*) took care of the science.

Another student grateful for the community's generosity is Gayandhi de Silva, who had been using the high-resolution spectrograph on the 74-inch Mount Stromlo telescope to chemically fingerprint stars. Stars with similar compositions are thought to have formed in the same galactic region; tracking their positions can give clues to how a particular galaxy has evolved. With several observatories offering observing time, de Silva says, "I was able to choose the one with the best capabilities for my work." That was Princeton University's Apache Point Observatory in Sunspot, New Mexico. De Silva is now finishing her dissertation and is headed for a postdoc at the European Southern Observatory in Santiago, Chile.

Frebel was lucky. Part of a team trawling for very old stars, which reflect conditions in the early universe, she was not using Mount Stromlo's telescopes before the fire. All she needed to resume work was a computer and Internet access. Still, she says, "I wanted to do my bit to get [Stromlo research] back on track." Shortly after the fire, she spotted a candidate old star among survey data from a collaborating telescope. Her team took high-resolution spectra using the National Astronomical Observatory of Japan's 8-meter Subaru Telescope on Mauna Kea, Hawaii. It turned out to be the oldest star yet observed. Frebel was first author on the team's *Nature* paper and was featured in dozens of newspaper and magazine stories. She is also completing her thesis and has accepted a postdoc position at the University of Texas, Austin.

As the grad students were showing their mettle, senior staff tackled institutional questions. "One of the big tragedies was losing NIFS," says RSAA astronomer Brian Schmidt. Designed to provide the most detailed views ever of black holes and address questions about star formation, NIFS was an important instrument for the Gemini consortium. With other large telescopes bringing similar instruments on line in the coming years, there were worries that a delay would close NIFS's window of opportunity for making discoveries, says Simons, who was then Gemini's facilities director. RSAA had also just won a competition to build an Adaptive Optics Imager for Gemini South, an 8-meter telescope on Cerro Pachón in Chile.

At the postinferno meeting in Chubb's office, Sackett recalls telling the vice chancellor that "we should rebuild NIFS, because it's a symbol, because people need something to do, and because it's science that we care about."

It was easier said than done. They didn't have a workshop. They would need to find about $3.5 million. And the Gemini consortium would have to agree. Still, just 3 weeks after the fire, when Simons arrived in Canberra, RSAA had a plan: Mount Stromlo staff would oversee work on a NIFS replacement using the facilities and staff of Auspace, a defense and aerospace contractor in Canberra. The university promised to fund the work immediately and settle with insurers later. With that can-do spirit and university support, Simons says, "it was a no-brainer" to let RSAA go forward with both NIFS and the Adaptive Optics Imager.

Resurrection

Sackett and her senior staff also had to contemplate Mount Stromlo's long-term future. The 50-inch Great Melbourne Telescope had been scheduled for another major upgrade. Instead, it was redesigned from the ground up, keeping the same size reflector but with a vastly enlarged field of view and a snazzy 300-million-pixel digital camera. Schmidt says the new scope, called SkyMapper, will be capable of surveying the entire southern sky in two nights, something that would "take a lifetime" with current telescopes. A primary target will be keeping an eye out for extremely rare nearby supernovas. "SkyMapper is really going to be quite revolutionary for [studying] supernovas," predicts the University of Hawaii's Tonry.

SkyMapper, expected to see first light in December or January, is being built at Siding Spring. A high-bandwidth optical fiber cable connection will allow control of the instrument from Mount Stromlo, where increasing light pollution from Canberra is degrading observing conditions.

Inevitably, there have been stumbling blocks. Demolition and construction were delayed by the need to develop a master plan that considered the historical and ecological aspects of development, as Mount Stromlo is an Australian Heritage Site. And ANU has sued its insurers, alleging that they have so far paid only a fraction of what the university says it is entitled to. A shortage of funds is delaying restoration of the Commonwealth Solar Observatory and the replacement of the 74-inch telescope. "That has left a big hole in our observing program," says Schmidt.

But 3 years after the fire, RSAA has passed or is reaching a number of milestones. NIFS was delivered to Gemini North last fall, and the Adaptive Optics Imager for Gemini South is nearing completion. Once SkyMapper comes on line, it will largely be business as usual again for Mount Stromlo's astronomers. But their remarkable recovery suggests that the fire of 2003, if anything, has broadened their horizons.

–DENNIS NORMILE

CREDITS: D. NORMILE

AIDS 2006

Time to Deliver

Join us in Toronto to be part of the world's premier gathering of scientists and other stakeholders involved in the global response to HIV/AIDS. With a record 12,000-plus abstracts submitted, the AIDS 2006 programme will offer research findings unparalleled in scope.

XVI International AIDS Conference

Toronto Canada
13 - 18 August 2006

www.aids2006.org

Register by 15 May and Avoid the Last-Minute Surcharge

CONFIRMED PLENARY SPEAKERS AND TOPICS*

Françoise Barre-Sinoussi
France
Vaccines

Christopher Beyrer, USA
Epidemiology Update and Transmission Factors

Agnes Binagwaho, Rwanda
Universal Access – Country Perspective

Louise Binder, Canada
Women and Girls

Kevin De Cock, UK
Treatment Access

Anand Grover, India
Human Rights and Social Vulnerabilities

Mark Heywood, South Africa
The Price of Inaction

Musimbi Kanyoro, Kenya
Religion, Politics and Civil Society

Kerrel McKay, Jamaica
Youth and the Future

Julio Montaner, Canada
State-of-the-Art Treatment and New Drugs

Ruth Nduati, Kenya
Children and AIDS

Julie Overbaugh, USA
Pathogenesis

Cristina Pimenta, Brazil
Prevention Response

Gita Ramjee, South Africa
New Prevention Technologies

Aleksandra Volgina, Russia
Poverty and Development

Alex Wodak, Australia
Harm Reduction

*subject to change

EDITED BY YUDHIJIT BHATTACHARJEE

Behind the Scenes

FUEL FOR A CAUSE. Penny by penny, a central California gas station has raised $177,000 for research into a rare and devastating bone disease that afflicts two local teenagers. Last month, Clark Crandall, 54, owner of the Main Street Shell Station in Santa Maria, learned that 6 years of donating a penny for every gallon of gas sold had paid off: Researchers had identified the gene defect behind fibrodysplasia ossificans progressiva (FOP), which immobilizes patients by forcing muscle and connective tissue to turn to bone.

"I was just ecstatic," says Crandall of the discovery, reported online last week in *Nature Genetics* (*Science*, 28 April, p. 514). He's been passing the news on to delighted customers. (The campaign also tripled business, Crandall says, although that was never the goal.) Pictures of the two girls with FOP grace the station, and a billboard displays a tally of money raised.

Crandall's campaign and others like it have raised more than two-thirds of the money spent in recent years on FOP research, says Fred Kaplan, an orthopedic surgeon at the University of Pennsylvania. (This 2001 photo shows him with Crandall [right] and one of the girls.) He spearheaded the 15-year hunt to find the gene with help from scientists worldwide. The money has funded "just about everything," he notes, from a steady stream of postdocs to DNA sequencing.

Pioneers >>

WOMEN ASCENDANT. As a child, Marta Tienda spent two summers as a migrant laborer picking tomatoes with her family. Now a sociologist at Princeton University, Tienda draws upon that experience to explore why some ethnic and racial groups have a harder time than others in moving up the economic ladder.

Tienda's rise from poverty is one of 10 stories in a new book series from the National Academies about female scientists. The series, *Women's Adventures in Science*, is intended to whet the appetites of middle and high school students for scientific careers. The stories convey the glamour and excitement of science and engineering, making it clear how scientists can make a difference.

Along with the series, the academies have unveiled a Web site (www.iwaswondering.org) with a number of interactive features, including a comic strip dedicated to each scientist. The cartoon above describes the work of Mimi Koehl, a biomechanist at the University of California, Berkeley, who studies how animals move.

CREDITS (TOP TO BOTTOM): FRED KAPLAN; FABLEVISION/JOSEPH HENRY PRESS; CALTECH; OFFICE OF PUBLIC AFFAIRS/UNIVERSITY OF TEXAS, AUSTIN

DEATHS

TOUGH AS NAILS. Israeli physicist Yuval Ne'eman, who helped develop the Eightfold Way classification of elementary particles and went on to become a major political figure in his country, died on 27 April at the age of 80.

Born in Tel Aviv and trained as an engineer, Ne'eman fought in Israel's 1948 War of Independence. He worked in military intelligence—he is the Ne'eman in Fredrick Forsyth's spy thriller *The Odessa File*—while studying physics under Abdus Salam at Imperial College London before becoming scientific director of the Nahal Soreq Nuclear Research Center, where he forged Israel's first research group in particle physics and helped develop its nuclear arsenal.

He also established the physics department at Tel Aviv University and served as its president before founding a far-right political party that opposed returning the Sinai to Egypt. He died of complications from a fall.

AWARDS

ALBANY PRIZE. Seymour Benzer, a neuroscientist at the California Institute of Technology in Pasadena, has won the $500,000 Albany Medical Center Prize in Medicine and Biomedical Research for his work linking genes to behavior in fruit flies. The research paved the way for the use of fruit flies as a model for studying human neurological diseases.

In the 1960s, Benzer and his colleagues showed that mutations in single genes could radically alter behavior in the fruit fly. The findings overturned the prevailing idea that behavior was primarily shaped by the environment. Over the next few decades, Benzer and other researchers identified the genetic bases for differences in courtship, learning, and memory in fruit flies, which launched the field of neurogenetics. Researchers now use fruit fly models to study human illnesses such as Alzheimer's, Huntington's, and Parkinson's.

Benzer, 84, was honored last week in a ceremony that also paid tribute to the founder of the award, businessman Morris "Marty" Silverman, who died in January at the age of 93.

NEW NAS FELLOWS. The U.S. National Academy of Sciences has named 72 new members and 18 foreign associates, bringing its domestic membership to 2013. The list is at www.nas.edu/morenews/20060425.html.

Got a tip for this page? E-mail people@aaas.org

SCIENCE & ENGINEERING

VISUALIZATION CHALLENGE

CALL FOR ENTRIES

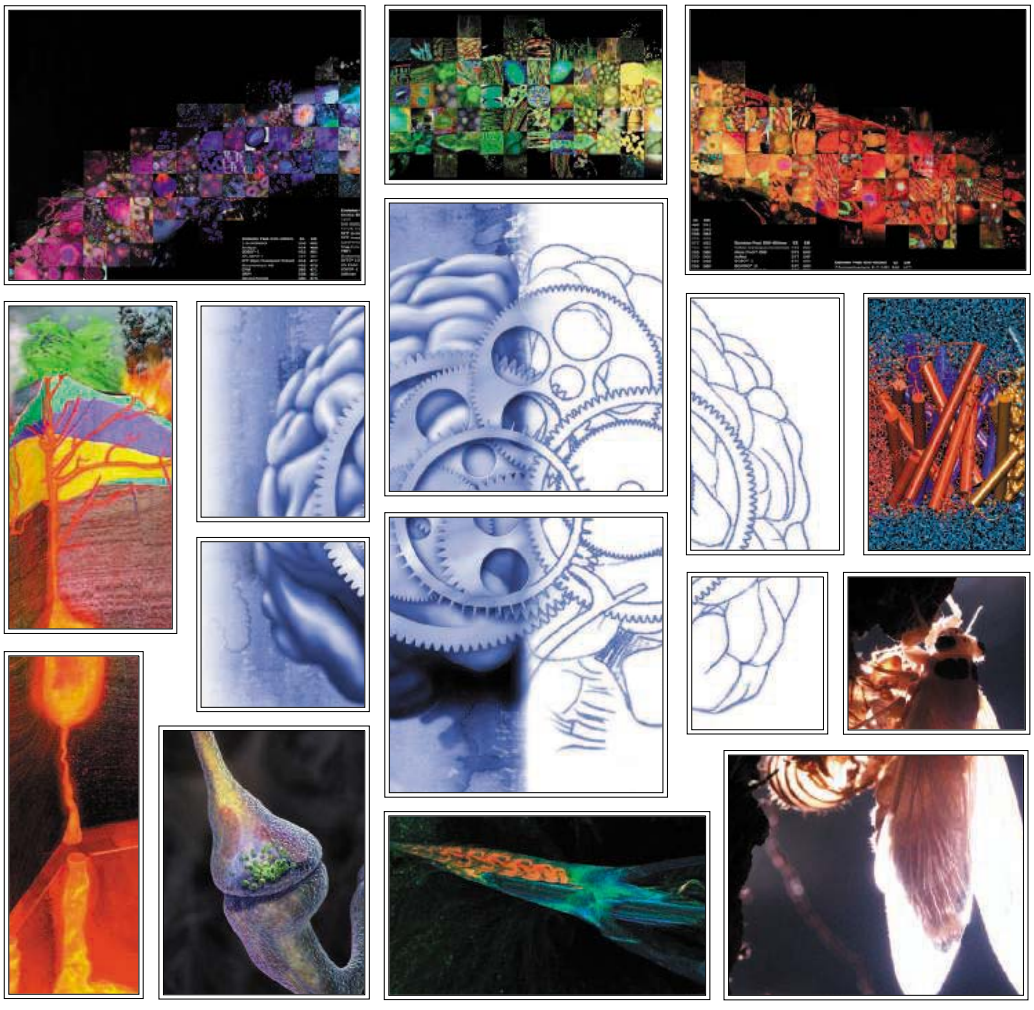

SCIENCE AND ENGINEERING'S MOST POWERFUL STATEMENTS ARE NOT MADE FROM WORDS ALONE

When the left brain collaborates with the right brain, science emerges with art to enhance communication and understanding of research results—illustrating concepts, depicting phenomena and drawing conclusions.

The National Science Foundation (NSF) and the journal *Science*, published by the American Association for the Advancement of Science, invite you to participate in the fourth annual Science and Engineering Visualization Challenge. The competition recognizes scientists, engineers, visualization specialists and artists for producing or commissioning innovative work in visual communication.

ENTRY DEADLINE: MAY 31, 2006

Award categories: Photographs, Illustrations, Interactive Media, Non-Interactive Media and Informational Graphics. Winners in each category will be published in the Sept. 22, 2006 issue of *Science* and *Science* Online, and will be displayed on the NSF Web site.

Complete Entry Information: www.nsf.gov/news/special-reports/scivis/index AND www.sciencemag.org/prizes/

LETTERS

edited by Etta Kavanagh

Debating Sexual Selection and Mating Strategies

J. ROUGHGARDEN *ET AL*. (REVIEWS, 17 FEB., P. 965) CLAIM THAT COOPERATIVE GAME THEORY IS an ideal replacement for sexual selection theory. However, their description of cooperative and noncooperative games is misleading. Roughgarden *et al*. state that "in competitive [noncooperative] games, the players do not communicate" (text in brackets added) and that "in cooperative games, players make threats, promises, and side payments to each other; play together as teams; and form and dissolve coalitions." This contrasts with the textbook definitions: "A game is cooperative if commitments—agreements, promises, threats—are fully binding and enforcing. It is non-cooperative if commitments are not enforceable (note that pre-play communication between players does not imply that any agreements that may have been reached are enforceable)" (*1*). Thus, contrary to Roughgarden *et al*., the distinction between cooperative and noncooperative games lies in the assumption of a priori, binding "contracts" between players, and communication between individuals does not necessitate a cooperative game. In fact, signaling theory, a branch of evolutionary game theory [which is fundamentally noncooperative (*2*)], is devoted to animal communication (*3*). Furthermore, sexually interacting individuals are unlikely to be bound to any contracts they form without enforcement that is external to the interaction, which is unlikely for the vast majority of sexual (or indeed any biological) interactions; if commitments are not implicitly enforceable, then games are by definition noncooperative. Roughgarden *et al*. are correct that actions chosen while individuals interact need not be in Nash competitive equilibrium, but this does not mean we need to abandon the Nash competitive equilibrium concept, just apply it at a different level (*4*). When interactions are possible, it is the negotiation rules that are inherited and subject to selection, rather than the unconditional choice of action. There is no logical reason to apply cooperative game theory to interactions, just the old-fashioned Nash competitive equilibrium concept at the correct level (*5*).

SASHA R. X. DALL,[1]* JOHN M. MCNAMARA,[2] NINA WEDELL,[1] DAVID J. HOSKEN[1]

[1]Centre for Ecology and Conservation, University of Exeter, Cornwall Campus, Tremough, Penryn TR10 9EZ, UK. [2]School of Mathematics, University of Bristol, University Walk, Clifton, Bristol BS8 1TW, UK.

*To whom correspondence should be addressed. E-mail: sashadall@iname.com

References and Notes

1. R. J. Aumann, S. Hart, *Handbook of Game Theory with Economic Applications* (Elsevier Science Publishers, Amsterdam, North Holland, 1992), vol. 1.
2. P. Hammerstein, in *Game Theory and Animal Behavior*, L. A. Dugatkin, H. K. Reeve, Eds. (Oxford Univ. Press, New York, 1998), pp. 3–15.
3. J. Maynard Smith, D. Harper, *Animal Signals* (Oxford Univ. Press, Oxford, 2003).
4. At evolutionary stability, negotiation rules are the best responses to each other, but this does not mean that the actions that result from using such a pair of negotiation rules are the best responses to each other. Roughgarden *et al*. are correct to emphasize that the process by which actions are chosen is important to the outcome (choice of action), but this point has been made before (*6*, *7*). Furthermore, under some modeling assumptions, the outcomes are more cooperative than with no interaction, while with other assumptions they are less cooperative (*7*–*9*).
5. For a detailed discussion of the points raised in this letter, see www.sciencemag.org/cgi/eletters/311/5763/965.
6. J. M. McNamara, C. E. Gasson, A. I. Houston, *Nature* **401**, 368 (1999).
7. J. M. McNamara, A. I. Houston, T. Szekely, J. N. Webb, *Animal Behav.* **64**, 147 (2002).
8. T. Killingback, M. Doebeli, *Am. Naturalist* **160**, 421 (2002).
9. T. N. Sherratt, G. Roberts, *J. Theoret. Biol*. **215**, 47 (2002).

IN THEIR REVIEW "REPRODUCTIVE SOCIAL behavior: cooperative games to replace sexual selection" (17 Feb., p. 965), J. Roughgarden *et al*. propose what superficially appears to be a radically novel explanation for reproductive social behavior. They argue (i) that sexual selection, which has been a cornerstone of the evolutionary explanation of sexual behavior since Darwin (*1*), "is always mistaken" and "needs to be replaced," and (ii) that "social selection," "expressed mathematically in a branch of game theory," is the necessary alternative. We believe that their Review is profoundly misleading. In particular, we argue that "social selection" does not represent a novel view of reproductive behavior and that, far from being an alternative to sexual selection, their models are themselves models of sexual selection.

The use of game theory models to study reproductive behavior, including the kinds of situations considered by Roughgarden *et al*., is not new in evolutionary biology. Even threats and side payments, which they specifically highlight, have been included in models for more than 10 years, and it has been recognized for still longer that a lack of alternative reproductive opportunities—which they implicitly assume—selects for cooperation between reproductive partners. They present their models as functioning "in developmental time," but the only rationale for expecting behavioral strategies to maximize payoffs within a generation is that they have been built in by selection over many generations: The correct currency to use for the payoffs in their models must therefore be fitness, as in existing game theory models.

If payoffs are in units of fitness, then the variation in payoffs in Roughgarden *et al*.'s models is by definition selection. Since sexual selection is, also by definition, due to variation in the number or phenotype of mates, the selection in the models, which arises during interactions in which mates use

different strategies, is sexual selection. We conclude that Roughgarden *et al*.'s models, rather than being alternatives to sexual selection, are in fact themselves models of sexual selection (*2*).

C. (KATE) M. LESSELLS,[1]* ANDREW T. D. BENNETT,[2] TIM R. BIRKHEAD,[3] NICK COLEGRAVE,[4] SASHA R. X. DALL,[5] PAUL H. HARVEY,[6] BEN HATCHWELL,[3] DAVE J. HOSKEN,[5] JOHN HUNT,[5] ALLEN J. MOORE,[5] GEOFF A. PARKER,[7] SCOTT PITNICK,[8] TOMMASO PIZZARI,[6] JACEK RADWAN,[9] MIKE RITCHIE,[10] BEN C. SHELDON,[6] DAVID M. SHUKER,[4] LEIGH W. SIMMONS,[11] PAULA STOCKLEY,[12] TOM TREGENZA,[5] MARLENE ZUK[13]

[1]NIOO-KNAW, Post Office Box 40, 6666 ZG Heteren, The Netherlands. [2]University of Bristol, Bristol BS8 1UG, UK. [3]Department of Animal and Plant Sciences, University of Sheffield, Sheffield S10 2TN, UK. [4]IEB, School of Biological Sciences, University of Edinburgh, Edinburgh EH9 3JT, UK. [5]Centre for Ecology and Conservation, School of Biosciences, University of Exeter, Cornwall Campus, Tremough, Penryn TR10 9EZ, UK. [6]Department of Zoology, University of Oxford, Oxford OX1 3PS, UK. [7]School of Biological Sciences, Biosciences Building, Crown Street, University of Liverpool, Liverpool L69 7ZB, UK. [8]Department of Biology, University of Syracuse, 108 College Place, Syracuse, NY 13244, USA. [9]Institute of Environmental Sciences, Jagiellonian University, ul. Gronostajowa 3, 30-387 Krakow, Poland. [10]Department of Environmental and Evolutionary Biology, Dyers Brae House, University of St. Andrews, St. Andrews, Fife KY16 9TH, UK. [11]School of Animal Biology (M092), University of Western Australia, Crawley, WA 6009, Australia. [12]Faculty of Veterinary Science, University of Liverpool, Chester High Road, Neston, South Wirral CH64 7TE, UK. [13]Department of Biology, University of California, Riverside, Riverside, CA 92521, USA.

*To whom correspondence should be addressed. E-mail: k.lessells@nioo.knaw.nl

References and Notes

1. C. R.Darwin, *The Descent of Man and Selection in Relation to Sex* (Murray, London, 1871).
2. For a detailed discussion of the points raised in this letter, see www.sciencemag.org/cgi/eletters/311/5763/965.

ANY TRAIT CONFERRING A COMPETITIVE ADVANTAGE for access to copulation partners or in fertilization is, by definition, under sexual selection. Since Darwin's (*1*) original proposal of sexual selection, a unitary theoretical framework has been developed that successfully explains much of the bewildering variation in sex differences, reproductive strategies, and mating systems among taxa. Sexual selection is now widely recognized as one of the most powerful agents of evolutionary change, a vital component of modern evolutionary theory and among the most intellectually dynamic areas in evolutionary biology over the past three decades.

J. Roughgarden *et al.* ("Reproductive social behavior: cooperative games to replace sexual selection," Review, 17 Feb., p. 965) propose that sexual selection theory "needs to be replaced" because it "is always mistaken" and suggest an approach based on social selection that appears to be a drastic paradigm shift. However, their Review is based on unsupported opinion, misconceptions, failure to acknowledge contrary evidence, and attempts to claim novelty and a new perspective where none in fact exists.

The problems in the Review are numerous and profound. For example, all 17 points in the Supporting Online Material contain major errors of omission and interpretation. Roughgarden *et al.* fail to provide either a scholarly review of sexual selection research or a genuine alternative to sexual selection theory. In particular, unlike models of sexual selection, those proposed by Roughgarden *et al.* cannot apply to most sexually reproducing organisms and crucially are not at all novel, being instead entirely consistent with current sexual selection theory.

Eurasian oystercatcher, a sexually monomorphic wading bird.

As with every rapidly developing field, the study of sexual selection generates debate. None of the currently unresolved issues, however, has implications that would call into question the theory of sexual selection itself. Indeed, the theoretical framework of sexual selection has proven extremely robust. It remains the best functional explanation for the evolution of the sex differences that initially puzzled Darwin and for a tremendous variety of other remarkable characters discovered as a consequence of intense research in this field during the last decades (*2*).

TOMMASO PIZZARI,[1]* TIM R. BIRKHEAD,[2] MARK W. BLOWS,[3] ROB BROOKS,[4] KATHERINE L. BUCHANAN,[5] TIM H. CLUTTON-BROCK,[6] PAUL H. HARVEY,[1] DAVE J. HOSKEN,[7] MICHAEL D. JENNIONS,[8] HANNA KOKKO,[9] JANNE S. KOTIAHO,[10] C. (KATE) M. LESSELLS,[11] CONSTANTINO MACIAS-GARCÍA,[12] ALLEN J. MOORE,[7] GEOFF A. PARKER,[13] LINDA PARTRIDGE,[14] SCOTT PITNICK,[15] JACEK RADWAN,[16] MIKE RITCHIE,[17] BEN C. SHELDON,[1] LEIGH W. SIMMONS,[18] RHONDA R. SNOOK,[2] PAULA STOCKLEY,[19] MARLENE ZUK[20]

[1]Edward Grey Institute, Department of Zoology, University of Oxford, Oxford OX1 3PS, UK. [2]Department of Animal and Plant Sciences, University of Sheffield, Sheffield S10 2TN UK. [3]School of Integrative Biology, University of Queensland, St. Lucia 4072, QLD, Australia. [4]School of Biological, Earth and Environmental Sciences, The University of New South Wales, Kensington, Sydney 2052, NSW, Australia. [5]Cardiff School of Biosciences, Cardiff University, Main Building, Park Place, Cardiff CF10 3TL, UK. [6]Department of Zoology, University of Cambridge, Downing Street, Cambridge CB2 3EJ, UK. [7]Centre for Ecology and Conservation, University of Exeter in Cornwall, Tremough Campus, Penryn, TR10 9EZ, UK. [8]School of Botany and Zoology, The Australian National University, Canberra, ACT 0200, Australia. [9]Laboratory of Ecological and Evolutionary Dynamics, Department of Biological and Environmental Sciences, Post Office Box 65, University of Helsinki, 00014, Helsinki Finland. [10]Department of Biological and Environmental Science, University of Jyväskylä, Post Office Box 35, 40014 Jyväskylä, Finland. [11]NIOO-KNAW, Centre for Terrestrial Ecology, Post Office Box 40, 6666 ZG Heteren, The Netherlands. [12]Universidad Nacional Autonoma de Mexico, Instituto de Ecología, Departamento de Ecología Evolutiva, AP 70-275, Mexico City, DF 07510, México. [13]School of Biological Sciences, Biosciences Building, Crown Street, University of Liverpool, Liverpool L69 7ZB, UK. [14]Department of Biology, University College London, Gower Street, London WC1E 6BT. [15]Department of Biology, Syracuse University, 108 College Place, Syracuse, NY 13244, USA. [16]Institute of Environmental Sciences, Jagiellonian University, ul. Gronostajowa 3, 30-387 Krakow, Poland. [17]Department of Environmental and Evolutionary Biology, Dyers Brae House, University of St. Andrews, St. Andrews, Fife KY16 9TH, UK. [18]Zoology Building, School of Animal Biology (M092), University of Western Australia, Nedlands, WA 6009, Australia. [19]Faculty of Veterinary Science, University of Liverpool, Chester High Road, Neston, South Wirral, CH64 7TE, UK. [20]Department of Biology, University of California, Riverside, Riverside, CA 92521 USA.

*To whom correspondence should be addressed. E-mail: tommaso.pizzari@zoo.ox.ac.uk

References and Notes

1. C. R. Darwin, *The Descent of Man and Selection in Relation to Sex* (Appleton, New York, 1871).
2. For a more detailed discussion of the points raised in this letter, see www.sciencemag.org/cgi/eletters/311/5763/965.

IN THEIR REVIEW "REPRODUCTIVE SOCIAL behavior: cooperative games to replace sexual selection" (17 Feb., p. 965), J. Roughgarden *et al*. mischaracterize theory and research on human mating strategies. Although they provide one decontextualized quote from Buss (*1*), the characterization that men pursue a singular strategy of promiscuous mating while women pursue low-quantity monogamous mating is factually incorrect.

Evolutionary psychologists have long theorized and empirically verified that humans possess a menu of mating strategies: Both women and men pursue long-term committed mating, short-term mating, serial mating, polygynous mating, polyandrous mating, and mixed mating strategies (including extra-pair copulations) (*1*, *2*). A particular individual's mating strategy is predictably contingent on sex ratio, mate value, influence from kin, and cultural norms (*1*–*3*).

Contrary to Roughgarden's statement that it is "axiomatic" in evolutionary psychology that only males pursue promiscuity, much

CREDIT: B. DE LANGE/VIREO

theoretical and empirical research documents the adaptive benefits to females of short-term mating (*1*). These include access to resources, advantageous mate switching, and possibly beneficial genes. Men typically benefit from long-term committed mating (e.g., increased offspring survival) and incur costs when pursuing promiscuous mating (e.g., violence from other men and decrement in mate value) (*2*).

These findings do not negate the importance of the differential parental investment in driving the intrasexual and intersexual components of sexual selection (*4*). Nor do they contravene well-documented sex differences in these components, which follow logically from parental investment theory (*2*, *3*). It is precisely because both sexes invest so heavily parentally when pursuing long-term mating that evolutionary psychologists stress that both sexes fully engage in mutual mate choice and intrasexual competition for desirable mates. Reducing the well-documented diversity of human mating strategies to outmoded clichés about male promiscuity and female monogamy does a gross disservice to the current scientific understanding of human mating.

DAVID M. BUSS

Department of Psychology, University of Texas, Austin, TX 78712, USA.

References

1. D. M. Buss, *The Evolution of Desire* (Basic, New York, 1994/2003).
2. D. M. Buss, *Evolutionary Psychology* (Allyn & Bacon, Boston, 2004).
3. S. W. Gangestad *et al.*, *Proc. R. Soc. London B* **272**, 2023 (2005).
4. R. Trivers, in *Sexual Selection and the Descent of Man: 1871–1971* (Aldine, Chicago, 1972), pp. 136–179.

IN THEIR REVIEW (17 FEB., P. 965), J. ROUGHgarden *et al*. assert that the theory of sexual selection is a wholesale failure and advocate an approach based on cooperative game theory. They introduce a standard "tragedy of the commons" type game between two players and suggest that communication between players might promote the evolution of larger payoffs through cooperation. This negotiation was introduced into evolutionary game theory long ago (*1*), and similar types of behavioral flexibility have been incorporated into models of sexual conflict between parents (*2*). It is clear from these more rigorous analyses that neither communication through repeated interactions, nor selection for behavior that sometimes favors the common good, undermines the basic premises of sexual selection theory. On the contrary, the model developed by Roughgarden *et al.* for the dynamics of individual versus team play is a case in point. This is nothing more than a restatement of the well-known idea that an individual's evolutionary interests can sometimes conflict and sometimes coincide with those of its partner. (*3*). It is precisely this idea that underlies the widespread understanding that the form of a species' mating system greatly influences the extent to which sexual conflict versus sexual cooperation predominates (*4*).

TROY DAY,[1] DAVID HOULE,[2] LOCKE ROWE[3]

[1]Departments of Mathematics and Biology, Jeffery Hall, Queen's University, Kingston, ON K7L 3N6, Canada. [2]Department of Biological Science, Florida State University, Tallahassee, FL 32306–1100, USA. [3]Department of Zoology, University of Toronto, Toronto, ON M5S 3G5, Canada.

References

1. R. Axelrod, W. D. Hamilton, *Science* **211**, 1390 (1981).
2. J. M. McNamara *et al.*, *Nature* **401**, 368 (1999).
3. L. Keller, *Levels of Selection in Evolution* (Princeton Univ. Press, Princeton, NJ, 1999).
4. G. A. Parker, in *Sexual Selection and Reproductive Competition in Insects*, M. S. Blum, N. A. Blum, Eds. (Academic Press, New York, 1979), pp. 123–166.

IN THEIR REVIEW "REPRODUCTIVE SOCIAL behavior: cooperative games to replace sexual selection" (17 Feb., p. 965), J. Roughgarden *et al.* make claims that have already been rebutted and debated (*1*–*4*). Darwin's views have been misrepresented again. A quotation

asserts that Darwin attributed secondary sexual characters to "females choosing mates who are 'vigorous and well-armed … just as man can improve the breed of his game-cocks by the selection of those birds which are victorious in the cock-pit.'" The words before the ellipsis are taken from page 229 of the second edition of *The Descent of Man*, whereas those to the right are from page 226. The ones on the left are part of a discussion on a difficulty in the theory of female choice. Those on the right are concerned with male combat and do not refer to female choice.

It is generally accepted practice in all branches of learning that quotations will accurately reflect what the author has asserted. Readers of a scientific journal also expect authors to follow the rules of logic and common sense. Irrespective of whether the innovations proposed by Roughgarden *et al.* are meritorious or not, the conclusion that Darwin's theory is wrong does not follow from the premises. That a theory may need to be supplemented does not mean that it has to be replaced. That there are cases to which a theory does not apply does not mean that it is false.

MICHAEL T. GHISELIN

Center for the History and Philosophy of Science, California Academy of Sciences, 875 Howard Street, San Francisco, CA 94103, USA. E-mail: mghiselin@calacademy.org

References

1. J. Roughgarden, *Calif. Wild* **58** (no. 3), 18 (2005).
2. M. T. Ghiselin, *Calif. Wild* **59** (no. 1), 13 (2006).
3. J. Roughgarden, *Calif. Wild* **59** (no. 2), in press.
4. M. T. Ghiselin, *Calif. Wild* **59** (no. 2), in press.

THE NASH BARGAINING GAME (*1*), FIRST APPLIED to intramarital negotiations more than 25 years ago, is the standard model for resource allocation within marriages (*2*, *3*). It also forms the core of the model proposed by J. Roughgarden *et al*. ("Reproductive social behavior: cooperative games to replace sexual selection," Reviews, 17 Feb., p. 965) as an alternative to sexual selection models.

Unlike virtually all of the game theoretical models used in biology (which are noncooperative games), the Nash bargaining game is a cooperative game-theory model. Cooperative and noncooperative games form two distinct branches of game theory, with fundamentally different assumptions. Roughgarden *et al*. assume players choose strategically which one to apply, but it is impossible to choose environmental constraints. If the circumstances meet the assumptions of cooperative game theory, then cooperative game theory is the only correct model; if the situation meets the assumptions of noncooperative game theory, then noncooperative game theory's predictions will follow.

One critical assumption that differs between the two branches of game theory is that cooperative game theory requires that threats

always be enforced, even though "in general, to execute the threat will not be something [the player] would want to do, just of itself" (*1*). If we agree with Roughgarden *et al*. that "a sense of friendship resides in animal bonding, a joy or synergy in the spirit of cooperation that allows animals to sense and experience the product, not merely the sum, of their individual well-beings," then we may also allow that the pair-bond relationship includes the vengeful hatred and spite required to fulfill the assumptions. Evolution does not provide an explanation for why such behavior should be expected, nor do Roughgarden *et al*. A sensible alternative to spite would be for players to revert to playing the evolutionarily stable strategy (ESS), which returns us completely to the realm of noncooperative game theory.

PETER L. HURD

Department of Psychology, University of Alberta, Edmonton, AB T6G 2E9, Canada.

References

1. J. F. Nash, *Econometrica* **21**, 128 (1953).
2. S. Lundberg, R. A. Pollak, *J. Econ. Perspect.* **10**, 139 (1996).
3. T. C. Bergstrom, *J. Econ. Lit.* **34**, 903 (1996).

IN THEIR REVIEW ARTICLE "REPRODUCTIVE social behavior: cooperative games to replace sexual selection" (17 Feb., p. 965), J. Roughgarden *et al*. propose replacing Darwinian sexual selection theory with a vague new model of cooperative "team-play dynamics." Game theorists have developed dozens of "equilibrium refinement" theories and "replicator dynamic" models (*1*) that can solve the same problems as team-play dynamics without relying on Roughgarden's mystical "joy or synergy in the spirit of cooperation."

Roughgarden's cooperation theory also cannot explain the dozens of recent papers documenting ovulatory cycle shifts in female human mate preferences (*2*). Resource benefits from sexual relationships are stable across the ovulatory cycle, but potential good-genes benefits from mating are only relevant in the high-fertility period a few days before ovulation. Thus, women have evolved to focus more during this high-fertility period on male good-genes indicators such as facial masculinity (*3*, *4*), pheromones (*5*), behavioral dominance (*6*), and artistic creativity (*7*). These cycle shifts are stronger among women in long-term relationships with men who lack these characteristics (*8*). The Roughgarden *et al*. model cannot explain these good-genes preferences, because it focuses on the direct ecological benefits of efficient coordination in mating games.

GEOFFREY MILLER

Psychology Department, University of New Mexico, Albuquerque, NM 87131, USA. E-mail: gfmiller@unm.edu

References

1. K. Binmore, L. Samuelson, *Rev. Econ. Stud.* **66**, 363 (1999).
2. S. W. Gangestad *et al.*, *Curr. Dir. Psych. Sci.* **14**, 312 (2005).
3. I. S. Penton-Voak *et al*., *Nature* **399**, 741 (1999).
4. C. N. Macrae *et al*., *Psych. Sci.* **13**, 532 (2002).
5. S. W. Gangestad *et al*., *Proc. R. Soc. London Ser. B* **265**, 927 (1998).
6. S. W. Gangestad *et al*., *Psych. Sci.* **15,** 203 (2004).
7. M. G. Haselton, G. F. Miller, *Hum. Nature* **17**, 50 (2006).
8. E. G. Pillsworth *et al*., *J. Sex Res.*, **41**, 55 (2004).

IN 1977, *SCIENCE* PUBLISHED A LANDMARK paper bringing together ecology and sexual selection to explain the diversity of mating systems (*1*). This framework has survived largely intact, with only changes in emphasis arising through insights into the importance of conflicts of interest between mating partners, and the near ubiquity of multiple mating by females (*2*). In their Review "Reproductive social behavior: cooperative games to replace sexual selection" (17 Feb., p. 965), J. Roughgarden *et al*. dismiss this framework in its entirety by stating that sexual selection is fatally flawed.

Sexual selection arises from the differential reproductive success of individuals, regardless of gender, that results from competition for mates (*3*). The caricature of the sexes (aggressive or showy males, coy or choosy females) that Roughgarden *et al*. deride is merely that—a caricature. It is not a basis for dismissing sexual selection any more than a rubber sheet and a football are a basis for a detailed discussion of the action of gravity. The crucial point is that sexual reproduction requires two individuals to pool their resources to produce offspring. Any heritable variation that leads to some individuals being more successful at finding mates than others will drive evolution by sexual selection, as will the existence of genes that allow individuals to invest less than their partner in a given mating and to use these resources for future reproduction. Roughgarden *et al*. need to show that such variation rarely occurs if they are to refute sexual selection. The empirical data are against them, however (*2*–*4*).

The competition and conflict fundamental to sexual reproduction cannot be dismissed, even if it may pay individuals to cooperate in some circumstances. The existence of benefits to cooperation does not remove conflict, as is apparent from animal and human societies (*5*). Sexual selection happens, however fervently some people may wish that it did not.

DAVID M. SHUKER[1]* AND TOM TREGENZA[2]

[1]Institute of Evolutionary Biology, School of Biological Sciences, University of Edinburgh, West Mains Road, Edinburgh, EH9 3JT, UK. [2]Centre for Ecology and Conservation, School of Biosciences, University of Exeter, Cornwall Campus, Penryn TR10 9EZ, UK.

*To whom correspondence should be addressed. E-mail: david.shuker@ed.ac.uk

References

1. S. T. Emlen, L. W. Oring, *Science* **197**, 215 (1977).
2. G. Arnqvist, L. Rowe, *Sexual Conflict* (Princeton Univ.

Press, Princeton, NJ, 2005).
3. M. Andersson, *Sexual Selection* (Princeton Univ. Press, Princeton, NJ, 1994).
4. S. M. Shuster, M. J. Wade, *Mating Systems and Strategies* (Princeton Univ. Press, Princeton, NJ, 2003).
5. F. L. W. Ratnieks, K. R. Foster, T. Wenseleers, *Annu. Rev. Entomol.* **51**, 581 (2006).

IN THEIR REVIEW, "REPRODUCTIVE SOCIAL behavior: cooperative games to replace sexual selection" (17 Feb., p. 965), J. Roughgarden *et al*. propose the use of game theory to describe reproductive behavior. The logic is well-argued, but the theory depends on individuals making choices through the use of reasoning, and there is little evidence that animals use reasoning to make choices. In the scenarios that the authors describe, the benefits are to the species, not to the individual animal. In many cases, as they point out, breeding leads to a decreased fitness and survivability of the individual.

An alternate to the assumption that individuals make choices on the basis of reasoned judgments about what constitutes a benefit to the species is that they make choices as a result of pushes from internal chemical signals. For instance, a male leopard roaming his territory picks up a scent of a female in heat; this stimulates a number of biochemical pathways that result in an urge for him to find the female and eventually mate with her. No reasoned thought at all is required.

Choices could also be made by females in this manner: for example, a chemical push evolved in female lions that causes them to prefer male lions with darker manes. Whether this push results in better genetics for lions is irrelevant. Once females mate and have a litter, another set of chemical signals takes over that pushes her to take care of her offspring rather than abandon them. In other species, there is no chemical push, so females abandon their offspring to survive on their own.

In summary, the game theory idea might be better argued with chemical pushes as "rewards" and lack of pushes as "penalties" in the authors' line of reasoning. Nevertheless, the use of game theory and the associated mathematics of reproductive behavior research could prove extremely useful in this field.

JEFFREY STEWART

Aeri Park Institute of Molecular Biology and its Applications, 3000 Kent Avenue, West Lafayette, IN 47906, USA.

Response

WE THANK THE MANY PEOPLE WHO HAVE RESponded to our Review. We offer specific replies before raising general themes.

We agree with Dall *et al.* that social behavior should be viewed in two tiers: one tier in evolutionary time for which the "old-fashioned" evolutionary stable strategy (ESS) is appropriate, and the other in behavioral/developmental time. The strategies developed in behavioral time may represent an ESS too, provided the players play as individuals, or may represent a Nash bargaining solution (NBS) if players play as a team. We introduce the terminology of competitive game versus cooperative game following Axelrod (*1*), who refers to the "fundamental form" of the prisoner's dilemma as a game in which "the players can communicate with each other only through the sequence of their own behavior" (p. 12), and who discusses the tit-for-tat strategy as a way to obtain "cooperation without friendship or foresight" (chapter heading, p. 71). In contrast, the games we envision employ friendship as the mechanism for attaining coordinated team play and for discerning team welfare (*2*).

We agree with Lessells *et al.* that "the only rationale for expecting behavioral strategies to maximize payoffs within a generation is that they have been built in by selection over many generations." We understand the evolutionary tier as producing the capabilities for developing social behavior through bargaining, threats, communication, and team play, and not directly producing the social behaviors themselves. The selection coefficients induced on

genetic variation for such developmental capabilities are computed from the generation-long integral of the fitness accumulation rates realized by the strategies that these capabilities produce. We do not "implicitly assume" that a "lack of alternative reproductive opportunities … selects for cooperation between reproductive partners." We hypothesize that cooperation is beneficial on its own merits to increase the number of offspring successfully reared, regardless of the availability of alternative mates. Our theory is not about selection resulting from "variation in the number or phenotype of mates" but is about variation in the number of offspring successfully reared and is not an extension of sexual selection theory (*2*).

In response to Pizzari *et al.*, we acknowledge that sexual selection theory has become "a unitary theoretical framework" and a "vital component of modern evolutionary theory." We appreciate that workers in this subject feel that "none of the currently unresolved issues … has implications that would call into question the theory of sexual selection itself." We beg to differ (*2*).

Emphasizing human mating as a "menu" of strategies not limited to the male-promiscuity-female-monogamy template, as Buss does in his Letter, is helpful. Still, the Letter confirms the axiomatic status of sexual selection in evolutionary psychology because various items in the mating-strategy menu are explained as circumstantial deviations from normal templates said to "follow logically from parental investment theory."

We agree with Day *et al.* that "neither communication through repeated interactions, nor selection for behavior that sometimes favors the common good, undermines the basic premises of sexual selection theory." Sexual selection theory is being challenged in its assumption that the male-female relationship begins with sexual conflict from which cooperation may be derived, whereas we hypothesize that the male-female relationship begins with shared investment that may devolve into conflict. Cooperative game theory implements this alternative to sexual selection theory—it does not by itself contradict sexual selection theory.

Ghiselin's fastidious pagination obscures the clear Darwinian vision that female choice breeds males to be both well armed and ornamented, like a fighting cock (*3*). We quote the phrase, "vigorous and well-armed," from p. 222 of the second edition of *The Descent of Man*, and the phrase referring to breeding game-cocks from p. 218. If one prefers a less succinct but equivalent quotation drawn completely from a single paragraph residing on a single page, consider instead: "the more vigorous females, which are the first to breed, will have the choice of many males … this apparently has sufficed during a long course of generations to add not only to the strength and fighting powers of the males, but likewise to their various ornaments or other attractions." (p. 222). Ghiselin's rebuttal was itself rebutted (*4*).

We agree with Hurd "that the pair-bond relationship includes … vengeful hatred and spite," which offer one way for threats to be enforceable. To this list we would add the grief that attends the breakdown of a relationship. These capabilities, as well as those for communicating and for forming friendships, result from dynamics in the evolutionary tier. We agree too that reverting to competitive play leads to an ESS within the behavioral tier that might itself constitute a sufficient threat to motivate seeking the NBS without the need to further postulate hatred, spite, or grief.

In reference to Miller's Letter, the joy of friendship is not "mystical" and can be confirmed with assays of pleasure-producing hormones or neurons if need be. Preference for the "male good-genes indicators" that women are said to have may instead indicate preference for direct benefits that men may provide. These preferences may be especially pronounced at times during the ovulatory cycle when the need for direct benefits is high because of the immi-

nent possibility of conceiving children. Goodgene explanations from evolutionary psychology remain unconvincing because (i) a stable polymorphism among good and bad genes cannot be maintained in the face of sustained directional selection from female choice against bad genes every generation, and (ii) large direct ecological benefits mask minuscule indirect genetic benefits.

Shuker and Tregenza write that "sexual selection… results from competition for mates." Instead, our theory focuses on selection resulting from how to maximize number of young successfully reared, not from mate competition. We hypothesize that the social dynamics within reproductive groups normally revolve around this objective, not mate competition. Sexual selection theory states that "the existence of genes that allow individuals to invest less than their partner in a given mating" will evolve. Instead, we propose that mating partners are not playing to make the other do most of the work, but to do whatever is necessary to raise the largest number of young together. We disagree that sexual conflict is "fundamental to sexual reproduction." Instead, we envision that mating begins with shared investment, and that conflict may appear secondarily if the partners cannot agree on a distribution of work and control. By our theory, cooperation is logically and causally prior to conflict, and by sexual selection theory, conflict is logically and causally prior to cooperation. Asserting that "sexual selection happens, however fervently some people may wish that it did not" assumes the conclusion before the alternative has been investigated.

We do not assume "the benefits are to the species, not to the individual animal," as Stewart states. In our theory, the animals that work as a team accrue individual benefits. We agree that mechanisms of cooperation that yield cooperative outcomes without requiring the players to "use reasoning to make choices" need further research.

The spectacular acceptance of natural selection theory contrasts with sexual selection theory. When evolutionary change is attributed to natural selection, alternative hypotheses of genetic drift and/or recurrent mutation are tested as well, and for some molecular traits, these alternatives are preferred. In contrast, sexual selection theory has lacked alternatives. We suggest that if sexual selection theory is correct, its credibility will be enhanced once it is successfully tested against alternative hypotheses.

The alternative of social selection that we propose views heterosexual mating as similar to funding a joint investment. A new narrative to explain reproductive social behavior then unfolds focused on the control of this investment. For example, we do not take the promiscuous-male–monogamous-female template as a norm, but as a derived case (*5*). Male

promiscuity is likely when the initial control and feeding of young resides solely with the female, as in mammals. In this situation, to have a part in controlling or feeding the young, the male must also control and feed the female, or alternatively, he may cede control of his reproductive destiny in hopes of finding enough other mates to yield sufficient offspring who are successfully reared without his help. In birds, however, the monogamy percentage is reversed relative to mammals because male birds have a part in controlling, feeding, and protecting eggs in the shared nest from the moment the eggs are laid. Male promiscuity is thus a strategy of last resort—a response to exclusion from parental involvement, not a norm.

JOAN ROUGHGARDEN,[1] EROL AKÇAY,[1] MEEKO OISHI[2]

[1]Department of Biological Sciences, Stanford University, Stanford, CA 94305–5020, USA. [2]Sandia National Laboratory, Post Office Box 5800, Albuquerque, NM 87185–1137, USA.

References and Notes

1. R. Axelrod, *The Evolution of Cooperation* (Basic Books, New York, 1984).
2. Our reply to the expanded versions of the Letters by Dall *et al.*, Lessells *et al.*, and Pizzari *et al.* can be found at www.sciencemag.org/cgi/eletters/311/5763/965.
3. C. Darwin, *The Descent of Man* (Prometheus Books, New York, ed. 2, 1874).
4. J. Roughgarden, *Calif. Wild* **59** (no. 2), 5 (2006).
5. J. Roughgarden, *Evolution's Rainbow* (University of California Press, Berkeley, CA, 2004), p. 57.

CORRECTIONS AND CLARIFICATIONS

News Focus: "Life in silico: a different kind of intelligent design" by K. Krieger (14 Apr., p. 189). The article should have noted that Aneil Mallavarapu of the Virtual Cell Program at Harvard Medical School is the inventor and author of the "Little b" program and is leading the project.

Reports: "Toward automatic reconstruction of a highly resolved tree of life" by F. D. Ciccarelli *et al.* (3 Mar., p. 1283). The authors wish to acknowledge the valuable sources for some unpublished data that were accidentally omitted. Five of the 191 genomes used were preliminary. Sequence data of 52 genes from *Fibrobacter succinogenes* (U.S. Department of Agriculture-CSREES grant 2000-52100-9618), *Gemmata obscuriglobus* (Department of Energy grant DEFC0295ER61962), and *Acidobacterium capsulatum* (NSF grant MCB0237365) were obtained from The Institute of Genomic Research (TIGR) through its Web site, www.tigr.org. The sequencing was undertaken at TIGR with support from the respective sequencing consortia. *Giardia lamblia* data were taken from the Web site www.mbl.edu/Giardia [A. G. McArthur, *FEMS Microbiol. Lett.* **189**, 271 (2000)], and for *Solibacter usitatus*, open reading frames were extracted by homology searches against the NCBI GenBank database (this genome was sequenced by the Joint Genomics Institute and funded by the Department of Energy).

Reports: "The spatial extent of 20th-century warmth in the context of the past 1200 years" by T. J. Osborn and K. R. Briffa (10 Feb., p. 841). Data used in the analysis are available at www.ncdc.noaa.gov/paleo/pubs/osborn2006/osborn2006.html. The URL for these data was not included in the paper because it was assigned only on the day of publication of the manuscript.

News Focus: "Development out of sync" by E. Pennisi (18 Nov. 2005, p. 1109). Christopher Rose's affiliation was incorrect. He is at James Madison University.

Reports: "Gigantic photoresponse in 1/4-filled-band organic salt $(EDO\text{-}TTF)_2PF_6$" by M. Chollet *et al.* (7 Jan., 2005, p.86). There was an error in temperature reported in the inset of Fig. 3A. The correct temperature is 30 K. The corrected caption should be "(Inset) Raman spectrum in the low-energy region for the I phase observed at 30 K." The sentence on p. 88, third column, second full paragraph, line 3 should read "The 84 cm^{-1} band observed at 30 K (red) softened as the sample temperature was increased (Fig. 3B, inset, red circles)."

Letters to the Editor

Letters (~300 words) discuss material published in *Science* in the previous 6 months or issues of general interest. They can be submitted through the Web (www.submit2science.org) or by regular mail (1200 New York Ave., NW, Washington, DC 20005, USA). Letters are not acknowledged upon receipt, nor are authors generally consulted before publication. Whether published in full or in part, letters are subject to editing for clarity and space.

BIOMEDICINE

Lipids, Genes, and Health

James M. Ntambi

Obesity and diabetes are currently among the world's most important health problems. Studies have shown that individuals who ingest diets high in fat, particularly saturated fat, suffer an increased risk of developing these conditions. There is also evidence that low-fat, high-carbohydrate diets can contribute to disease. Therefore, whether it is the fat per se that causes disease is still not well understood.

Although researchers, particularly those working in the area of fat metabolism, can attest to the progress made in the field over the last several years, people in other disciplines often lack information about fat and how it may relate to health. In *How Fat Works*, Philip Wood offers both professional and lay readers an excellent, nontechnical introduction to both the normal and the pathological physiology of fat metabolism. In his own research, Wood (a geneticist at the University of Alabama at Birmingham) uses gene knockout mouse models to investigate the regulation of fat metabolism. As one might expect, the book stresses that approach, but the author has also incorporated a good deal of information from the primary literature on fat and obesity.

Animal models, which retain the complex interactions among genes and nutrients, offer a productive means of uncovering the roles of diet in human diseases. More important, such models allow researchers access to key tissues involved in fat metabolism that are inaccessible in humans. Thus the largest benefits from animal studies are likely to be in understanding and predicting how genetic variability determines responsiveness to changes in nutrient supply, exercise, and other environmental factors.

Wood captures the reader's interest by developing topics in a logical and stepwise manner. Along the way, he takes every opportunity to point out the connections that make the processes he is discussing relevant to human nutrition. Expanding the original biological models of fat metabolism, the author integrates social, cultural, and environmental effects with the biological factors that determine how fat is made available in and processed by the body. Two themes brought forward in the book are worth emphasizing: the emerging science of nutrigenomics (which offers great potential to extend our understanding of diet-gene interactions) and our current knowledge about the effects of nutritional and physical-activity interventions in obese and diabetic individuals.

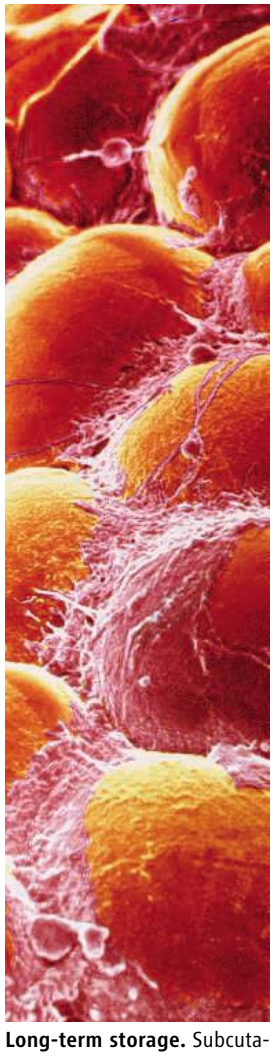

Long-term storage. Subcutaneous fat (here in a colored scanning electron micrograph) is metabolically "safer" than visceral adipose tissue deposits, but difficult to get out.

We have reached the state where nutritional recommendations are largely based on experimental evidence. The challenge now is to develop strategies that will facilitate the implementation of the recommendations—particularly for those individuals who are at risk of becoming overweight or developing diabetes, individuals for whom we want to minimize the possibility of developing the full-blown conditions. For people who are already obese or have already developed diabetes, the interventions provide a means of reducing the risks of associated complications.

The health professions and the media have already spread the message that excess dietary fat is a serious risk factor for the development of obesity and diabetes. Wood makes the additional point that some fat-regulated genes are likely to play major roles in the onset, incidence, progression, and/or severity of these conditions. The book also reminds readers that the degree to which fat influences the development of obesity depends on the individual's genetic makeup and that dietary interventions based on genotype and nutritional requirements and status may help prevent or manage obesity. Because human health is influenced by many different factors (ranging from genetic susceptibility to the effects of dietary intake and the environment), effective health management—of both individuals and populations (on all scales up to global)—requires a systems approach. The pressure for personalized nutrition guidelines is building, and we need to establish criteria that must be satisfied before incorporating specific effects in individualized dietary advice.

Amidst the ongoing debates over weight-loss regimes and how to formulate healthy diets for individuals, *How Fat Works* appears at an ideal moment. Wood writes in a clear and concise style, and he has produced an easy-to-understand overview of fat metabolism and its connections to human health. His account successfully blends results from genetic, physiologic, social, and environmental approaches to the topic. The book will help readers from any of those fields and the general public better appreciate the connections among high-fat diets, obesity, and diabetes.

The reviewer is at the Department of Biochemistry, University of Wisconsin–Madison, 433 Babcock Drive, Madison, WI 53706, USA. E-mail: ntambi@biochem.wisc.edu

How Fat Works

by Philip A. Wood

Harvard University Press, Cambridge, MA, 2006. 263 pp. $35, £21.95, €32.30. ISBN 0-674-01947-4.

10.1126/science.1127012

RESEARCH CONDUCT

Under Suspicion

Derek T. Scholes

Bookstore shelves are filled with literature that brings the thrill of science to the general public. Scientists' day-to-day work, however, for most people remains very much a mystery. Books that accurately portray bench research's combination of breakthroughs and setbacks are rare. In her novel *Intuition*, Allegra Goodman submerges the reader in the world of the laboratory, the animal facility, and the conference room to watch scientists experimenting and debating—and to observe what happens when those debates reach ears beyond the laboratory walls.

It is 1985. Sandy Glass and Marion Mendelssohn are anxious co-directors of a cancer research laboratory at the fictional Philpott Institute in Cambridge, Massachusetts. Money is tight, the lab is not publishing, and they have little preliminary data for the looming renewal of their National Institutes of Health grant.

Their latest frustrations are with postdoctoral fellow Cliff Bannaker, whom they accuse of wasting valuable resources on repeatedly

The reviewer is a National Human Genome Research Institute/American Society of Human Genetics policy fellow in the office of Senator Edward M. Kennedy. E-mail: derek_scholes@help.senate.gov

unsuccessful attempts to develop a revolutionary new technique for reversing tumor growth in mice. Although a talented researcher, Cliff has invested years on the project without success. As Goodman observes, postdocs "might be prepared and bright and diligent, and fail and fail and fail."

But ultimately Cliff doesn't fail. When tumors shrink in three of his nude mice, the mood of the lab is lifted and Cliff becomes the darling of Glass and Mendelssohn. All but Robin Decker, Cliff's fellow postdoc in the lab and girlfriend, are elated. Robin has spent five unproductive years on her own project and finds all the excitement about Cliff's breakthough hard to tolerate. Her feelings of abandonment while Cliff spends more and more evenings in the lab turn to suspicion when her intuition tells her that Cliff's latest results are just a bit too good to be true. The stage is set for a battle between Robin and the lab when she finds a discrepancy between data in the resulting landmark *Nature* paper and Cliff's notes and openly accuses Cliff of fraud. What begins as the seeds of doubt of one postdoc grows into a national scandal.

Science-crime scene?

Intuition
A Novel
by Allegra Goodman
Dial (Random House), New York, 2006. 351 pp. $25, C$35. ISBN 0-385-33612-8.

In *Intuition*, her third novel [after (*1*, *2*)] and the first with a scientific theme, Goodman captures many aspects of life in a biomedical research laboratory. She paints a lab scene of too little bench space, shelves filled with media, old cartoons taped to the walls, and postcards stuck on the refrigerator. She accurately conveys the pressure on scientists to maintain the production line of data and publications that is required to sustain funding. And she fills the lab with characters all scientists would recognize, describing the passion they feel for their research, the long hours they endure in pursuit of the next discovery, and the fear they have of being beaten to a discovery by their competitors.

Yet, as a thriller, the novel disappoints. While the plot develops, it does not thicken. As the media and government investigate the Mendelssohn-Glass lab, we learn little new that indicates whether Cliff is falsifying his data. When other labs fail to reproduce Cliff's results, we cannot tell whether this indicates that Cliff's results are fraudulent or if there is a legitimate scientific explanation. When a follow-up paper is written, we are not told to what extent the results confirm the original findings. We learn that Robin tracks down a bitter former member of the Glass-Mendelssohn lab, but we do not discover whether his grievances are legitimate or not.

What keeps the book engaging as the scandal unfolds, however, are the decisions, reactions, and changing perspectives of the well-developed cast of characters. Glass launches into a full-blown publicity campaign to uphold the public reputation of the lab. Mendelssohn despairs as the investigations delay the very experiments that would vindicate Cliff's findings. Self-doubt creeps into Robin's mind as she begins to realize the full consequences of voicing her suspicions. And the story is given depth by subplots and a supporting cast of family, friends, and ex-colleagues that Goodman skillfully weaves into the narrative.

Ultimately, more than a scientific thriller, *Intuition* is a story about how co-workers and their families respond to career-threatening accusations and public scrutiny. It will appeal to fans of drama and to members of the public curious about life in the lab. Scientists, however, may close the book still wanting answers—wishing that they could compare Cliff's notes with the *Nature* paper for themselves.

References

1. A. Goodman, *Kaaterskill Falls: A Novel* (Dial, New York, 1998).
2. A. Goodman, *Paradise Park: A Novel* (Dial, New York, 2001).

10.1126/science.1127564

BROWSINGS

Sustainable Fossil Fuels. The Unusual Suspect in the Quest for Clean and Enduring Energy. Mark Jaccard. Cambridge University Press, Cambridge, 2006. 397 pp. $70, £40. ISBN 0-521-86179-9. Paper, $24.99, £14.99. ISBN 0-521-67979-6.
Many believe that our continued reliance on fossil fuels—coal, oil, and natural gas—must lead to environmental catastrophe, wars over energy supplies, and economic collapse. Jaccard takes a contrary position. He argues that carbon dioxide emissions can be curbed by using gasification to convert these fuels to cleaner forms of energy (e.g., electricity, hydrogen, and synthetic fuels) while capturing and storing the carbon. He estimates that shifting to zero-emission processes would involve increases in real energy prices of well under 1% per year. The author predicts that even as the global energy system expands to support the economic and social development of the world's poorer countries, it can be shaped to minimize environmental impacts without harming economic growth. Even less-optimistic readers or those unconvinced by the arguments will find Jaccard's case worth careful consideration.

Moments of Truth in Genetic Medicine. Susan Lindee. Johns Hopkins University Press, Baltimore, MD, 2005. 282 pp. $40, £26.50. ISBN 0-8018-8175-7.
In the two decades after 1955, medical genetics grew from an obscure specialty to a core area of biomedicine. Lindee discusses five episodes from this period: phenylketonuria and the first neonatal testing program; Victor McKusick's studies of an inbred population, the Old Order Amish in Pennsylvania; the standardization of human chromosomes; the study of twins to determine genetic components of human behavior; and the efforts to find genes for familial dysautonomia, a rare disease that afflicts Ashkenazi Jews. She uses these to illustrate different aspects of the technical and social contexts of genetic disease. Lindee also highlights how patients, family members, research subjects, and lay organizations have contributed to the "patchwork quilt" of the science. This history will reward anyone interested in the paths from gene discoveries to cures or the potential for genomic medicine.

CREDIT: CAMERON SLAYDON

ANIMAL RESEARCH

Harmonization of Animal Care and Use Guidance

International guidance for animal care and use is important to facilitate conduct of appropriate animal-based science on a global level and to protect the welfare of animals used in science.

Gilles Demers,[1]* Gilly Griffin,[2] Guy De Vroey,[3] Joseph R. Haywood,[4] Joanne Zurlo,[5] Marie Bédard[2]

Societal expectations for improvements in the health of humans and animals require scientific studies involving the use of animals. At the same time, the public is concerned about the welfare of animals used in science. Animal welfare is also of importance because of the link between healthy, well-cared-for animals and sound science.

Enhanced online at www.sciencemag.org/cgi/content/full/312/5774/700

Most national oversight mechanisms emphasize basic principles of humane science, in particular the "three R's" tenet of replacement, reduction, and refinement of animal use (*1*). However, the oversight of animal care and use occurs through a wide variety of local, national, and international mechanisms, some based on legislation [the European Union (EU); (*2*)], others on peer review or other forms of nonlegislated oversight (Canada) and yet others on a combination of legislated and nonlegislated oversight (United States). This patchwork of mechanisms can cause problems, given the global nature of science.

Different standards for animal care and use can complicate the comparison of results from animal-based studies and the reproducibility of such results and can also slow international scientific collaboration. For example, CO_2 euthanasia is more commonly used for rodents in the United States than in the EU, and T-61 (a combination of three drugs—a local anesthetic, a general anesthetic, and a curariform drug) is available to animal users in Europe but not the United States. There are also international trade implications: multinational companies face the challenge of having to work with research and testing sites operating within very different regulatory structures. Specific standards of animal care and use required by scientific journals can also present a barrier to publication. The patchwork of mechanisms can be especially daunting for developing countries, in elaborating their own mechanisms and in international collaboration. Finally, there is concern that differences in animal care and use requirements may lead to the transfer of animal-based studies to countries with weaker requirements. As far back as 1985, the Committee of International Organizations of Medical Science (CIOMS), which works closely with the World Health Organization, said "The varying approaches in different countries to the use of animals for biomedical purposes, and the lack of relevant legislation or of formal self regulatory mechanisms in some, point to the need for international guiding principles elaborated as a result of international and interdisciplinary consultations" (*3*).

> "Whenever an animal's life is to be taken, **it should be treated with the highest respect.**"

There are international efforts to use guidance that is based on performance standards [i.e., standards that define an outcome and provide criteria for assessing that outcome, but do not limit the methods by which that outcome may be achieved (*4*)], and to work on filling gaps in the science needed for sound animal welfare guidance. Examples of international collaboration include the CIOMS Principles, the Mutual Acceptance of Data Program of the Organisation for Economic Cooperation and Development (OECD), and the International Conference on Harmonization of Technical Requirements for Registration of Pharmaceuticals for Human Use (ICH). These instances of collaboration have reduced unnecessary duplication of studies involving animals by developing internationally accepted common methods for chemical testing and drug development.

Guidance on the recognition of clinical signs as humane end points is now being implemented by member nations of the OECD, in conjunction with the OECD test guidelines for safety evaluation, which means that regulatory agencies in these countries should no longer require death in extremis as an end point for safety tests (*5*). In countries that are not OECD members, death may still be commonly accepted as an end point.

The International Council for Laboratory Animal Science [ICLAS (*6*)] has brought members of the

Principles for Establishment of Humane End Points

1. There is strong evidence that animals experience pain and distress in situations comparable to those that cause pain and distress for humans.
2. Death or severe pain and distress should be avoided as end points.
3. The earliest possible end point should be used that is consistent with the scientific objectives.
4. Studies should be designed to minimize any pain or distress likely to be experienced by the animals, while meeting the scientific objectives.
5. The duration of studies involving pain and distress should be kept to a minimum.
6. Pilot studies should be encouraged as a means of determining morbidity, time course of effects, and frequency of observations required to set an earlier end point.
7. Before commencing the experiment, agreement should be reached on (i) appropriate end points for the study and (ii) the person or persons to be responsible for making the judgment that the end point has been reached.
8. A team approach should be used, employing the professional judgment of the scientist, veterinarian, animal care staff, and ethics committee to agree on the appropriate end point for the study.
9. Research and animal care staff must be adequately trained and competent in recognition of species-specific behavior and, in particular, species-specific signs of pain, distress, and moribundity.
10. Animals should be monitored by means of behavioral, physiological, and/or clinical signs at an appropriate frequency to permit timely termination of the experiment once the end point has been reached.

All of the authors are members of the Working Group on Harmonization of Guidelines for ICLAS. G. Demers is the President of ICLAS, and G. De Vroey and J. R. Haywood are members of the ICLAS Governing Board; J. R. Haywood represents the International Union of Basic and Clinical Pharmacology. In addition, G. De Vroey was the chair of the subcommittee (of the ICLAS Working Group on Harmonization) on euthanasia and J. R. Haywood the chair of the subcommittee on endpoints. [1]ICLAS, St-Hilaire, Quebec, QC, Canada J3H 4W1. [2]Canadian Council on Animal Care, Ottawa, ON, Canada K1P 5G4. [3]Johnson & Johnson, B-2340 Beerse, Belgium. [4]Department of Pharmacology and Toxicology, Michigan State University, East Lansing, MI 48824, USA. [5]Institute for Laboratory Animal Research, National Academy of Science, Washington, DC 20001, USA.

*To whom correspondence should be addressed. E-mail: gdemers@ccac.ca

international community together to identify and to recommend acceptance of guidance documents. ICLAS believes in the harmonization of animal care and use guidance as a reflection of the globalization of research. However, harmonization must be distinguished from standardization (one worldwide set of regulations); ICLAS believes that each country should be able to maintain an oversight mechanism for animals used in science that reflects its cultures, traditions, religions, laws, and regulations.

ICLAS first worked with the Canadian Council on Animal Care (CCAC) on best practices to minimize pain and distress for animals used in regulatory testing; these were agreed upon and published (*7*). Two guidance documents on humane end points were recognized as effective refinement tools (*5*, *8*).

In November 2003, the Institute for Laboratory Animal Research (ILAR) organized an international workshop (*9*) to discuss harmonization. During this workshop, many experts from around the world independently reported about a desire for and worldwide pressures to have international benchmarks for animal welfare. However, many participants pointed out that there are strong attachments to existing national guidance and gaps in the science needed as a basis for some of the regulations, standards, and guidelines.

ICLAS held its First International Meeting for the Harmonization of Guidelines on the Use of Animals in Science in Nantes, France, on 13 and 14 June 2004 (*10*). An ICLAS Working Group on Harmonization of Guidelines, composed of representatives from major organizations producing and/or using guidelines for the use of animals in science, was created at the meeting (*11*). The working group agreed on general principles for the establishment of humane end points that are based on the earlier documents from the OECD and CCAC (*5*, *8*, *12*). The working group encourages consultation of the extensive literature available on end points and recognizes the need for research to support performance-based standards. The current general principles for humane end points defined by the working group are described in the table above.

The working group also agreed on general principles for euthanasia and recommended two documents (*13*, *14*) as international references (*15*). Both documents provide general principles and guidance on ways to ensure that euthanasia methods meet the goal of assuring the humane death of animals. There are some areas of inconsistency between the two references. This is partly because the American Veterinary Medical Association document is designed for a more general audience (i.e., not only for animal use in science) and because of differing practices and traditions in the United States and Europe, but mostly it is due to insufficient knowledge about the best methods of euthanasia for various species at different life stages. The areas in which further research will be needed were identified as mass animal euthanasia, euthanasia of fetuses and neonates, euthanasia of cold-blooded animals, proper use of CO_2 for various species, decapitation with or without prior anesthesia, cervical dislocation, and the use of N_2 and/or argon gas. With more research in these areas, the working group felt that the discrepancies between the documents could be addressed and better guidance incorporated into future versions of the guidelines. The general principles for euthanasia defined by the working group are shown in the table above.

Principles for Animal Euthanasia

1. Whenever an animal's life is to be taken, it should be treated with the highest respect.

2. Euthanasia should place emphasis on making the animal's death painless and distress-free. The method likely to cause the least pain and distress to the animals should be used whenever possible.

3. Euthanasia techniques should result in rapid loss of consciousness, followed by cardiac or respiratory arrest and ultimate loss of brain function.

4. Techniques should require minimum restraint of the animal and should minimize distress and anxiety experienced by the animal, before loss of consciousness.

5. Techniques used should be appropriate for the species, age, and health of the animal.

6. Death must be verified following euthanasia and before disposal of the animal.

7. Personnel responsible for carrying out the euthanasia techniques should be trained: (i) to carry out euthanasia in the most effective and humane manner; (ii) to recognize signs of pain, fear, and distress in relevant species; and (iii) to recognize and confirm death in relevant species.

8. Human psychological responses to euthanasia should be taken into account when selecting the method of euthanasia, but should not take precedence over animal welfare considerations.

9. Ethics committees should be responsible for approval of the method of euthanasia (in line with any relevant legislation). This should include euthanasia as part of the experimental protocol, as well as euthanasia for animals experiencing unanticipated pain and distress.

10. A veterinarian experienced with the species in question should be consulted when selecting the method of euthanasia, particularly when little species-specific euthanasia research has been done.

ICLAS will continue to work with its many partners around the world to identify solid, practical guidance that can easily be used by the international community to promote good animal welfare while conducting sound animal-based science.

References and Notes

1. W. M. S. Russell, R. L. Burch, *The Principles of Humane Experimental Technique* (Methuen, London, 1959; reprinted, Universities Federation for Animal Welfare, Wheathampstead, UK, 1992).
2. European Science Foundation (ESF) Policy Briefing, "Use of Animals in Research" (ESF, Strasbourg, France, August 2001); (www.esf.org/publication/115/ESPB15.pdf).
3. Z. Bankowski, N. Howard-Jones, Eds., *International Guiding Principles for Biomedical Research Involving Animals* [Committee of International Organizations of Medical Science (CIOMS), Geneva, 1986].
4. National Research Council, *Guide for the Care and Use of Laboratory Animals* (National Academies Press, Washington, DC, ed.7, 1996).
5. Organisation for Economic Cooperation and Development (OECD), "Guidance document on the recognition, assessment, and use of clinical signs as humane endpoints for experimental animals used in safety evaluation" (OECD, Paris, 2000); [www.olis.oecd.org/olis/2000doc.nsf/LinkTo/env-jm-mono(2000)7].
6. International Council for Laboratory Animal Science (ICLAS) (www.iclas.org/).
7. G. Griffin, W. Stokes, Eds., Regulatory Testing and Animal Welfare: Proceedings of the ICLAS/CCAC International Symposium, Quebec City, Canada, 21 to 23 June 2001. *ILAR J.* **43** (suppl.), 140 pp. (2002).
8. Canadian Council on Animal Care (CCAC), "[CCAC] guidelines on: choosing an appropriate endpoint in experiments using animals for research, teaching, and testing" (CCAC, Ottawa, 1998); (www.ccac.ca/en/CCAC_Programs/Guidelines_Policies/GDLINES/ENDPTS/APPOPEN.HTM).
9. National Research Council, "*The Development of Science-based Guidelines for Laboratory Animal Care*, *Proceedings of the November 2003 International Workshop*, Washington, DC, 18 and 19 November 2003 (National Academies Press, Washington, DC, 2004).
10. Federation of European Laboratory Animal Science Associations (FELASA), "First ICLAS meeting for the harmonization of guidelines on the use of animals in science" in *Proceedings of the Ninth FELASA Symposium, Section 2, International Harmonisation of Care and Use Issues*, Nantes, France, 13 and 14 June 2004 (FELASA, London, 2005); (www.lal.org.uk/pdffiles/FELASA/Section2.pdf), p. 40.
11. List of participants available on *Science* Online.
12. ICLAS, "International harmonization of guidelines on humane endpoints" (ICLAS, Nantes, France, 2004), approved in Athens, Greece, May 2005, available on *Science* Online.
13. "2000 Report of the American Veterinary Medical Association (AVMA) Panel on Euthanasia" (www.avma.org/issues/animal_welfare/euthanasia.pdf).
14. "1996/1997 EC recommendations for euthanasia of experimental animals," parts 1 and 2 (www.lal.org.uk/workp.html).
15. ICLAS, "International harmonization of guidelines on euthanasia" (ICLAS, Nantes, France, 2004), approved in Buenos Aires, Argentina, November 2004, available on *Science* Online.

16. ICLAS thanks all those who have volunteered their time and expertise for its work, in particular those working on international harmonization.

10.1126/science.1124036

Supporting Online Material

www.sciencemag.org/cgi/content/full/312/5774/700/DC1

PLANETARY SCIENCE

Linear Dunes on Titan

Nicholas Lancaster

Extensive dunes, produced by wind transport of sand-sized particles, are common on Earth and are also seen on Mars and Venus. Saturn's moon Titan is now shown to have similar dunes.

Landforms and deposits created by the dynamic interactions between granular material and airflow occur on several planetary bodies, including Earth, Mars, and Venus. Recent orbital image data indicate that such aeolian (wind-produced) landforms and deposits also occur on Titan, as originally predicted by Greeley (*1*). As reported on page 724 of this issue, Lorenz and colleagues have analyzed high-resolution radar image data of Titan and conclude that extensive areas of dark linear features are directly comparable to large linear desert dune fields on Earth (*2*). This interpretation provides intriguing new information on the nature of surface processes on one of Saturn's moons, one of the few in the solar system known to possess an atmosphere.

The recognition of landforms on other planetary bodies involves comparison of orbiter and lander images with terrestrial analogs (see the figure). Because morphologically similar landforms are assumed to be formed in essentially the same manner on different planetary surfaces, this approach can indicate the types of surface processes and environments that occur on an unfamiliar landscape, provided that the fundamentals of the landforms and processes are well understood on Earth (*3*). Such an approach has been applied most successfully on Mars, where studies of terrestrial analogs of landforms and deposits go back to the recognition of dunes on Mariner 9 images in the early 1970s (*4*). It has also been used to understand airflow and aeolian processes on Venus (*5*). In many instances, the need to understand the physics of surface processes on other planetary bodies has generated fundamental studies of such processes on Earth. The report by Lorenz *et al.* is an excellent example of the application of well-chosen Earth analogs to understand geomorphic processes and wind patterns on Titan.

The dunes on Titan are very similar in geometry (width, crest-to-crest spacing, and length) to linear dunes in Namibia and the Rub al Khali of Arabia and show patterns and interactions with preexisting topography that have direct parallels in terrestrial desert regions. On Earth, existence of linear dunes indicates a moderate supply of sand and seasonally varying winds from two directions oblique to the dune and separated by less than 180°. Such winds tend to promote extension of the dune in the direction of the mean transport vector with some lateral migration of the form (*6*, *7*).

Occurrence of aeolian features on any planetary body indicates the existence of a sufficient supply of sand-sized sediment, winds to transport that sediment, surface conditions (such as lack of vegetation and low surface moisture) that make it possible for the wind to transport sediment (sediment availability), and topographic and/or meteorological conditions that promote deposition of the transported sediment (*8*). Production of sand-sized sediment can be achieved by a number of processes, including explosive volcanism that produces ash and tephra, cratering and meteorite impacts, and weathering and erosion by water and/or ice. On Titan, Lorenz *et al.* suggest that sand-sized material could be produced by fluvial processes, based on the existence of channel systems. Alternatively, atmospheric deposition could produce agglomeration of hydrocarbon solids of sand size.

Assuming that material of sand size is available, existence of aeolian landforms indicates that wind is currently capable of transporting such material, or has been capable of trans-

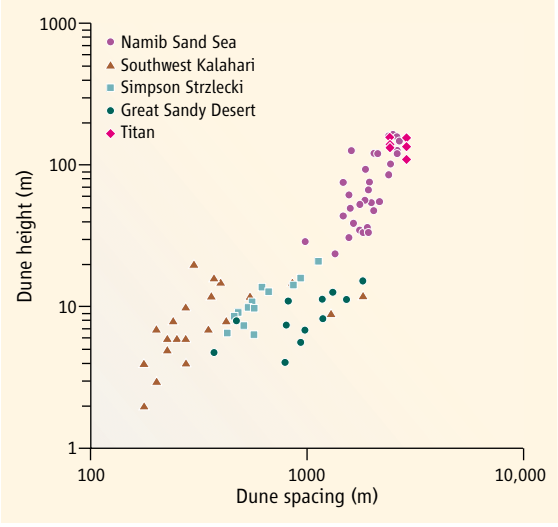

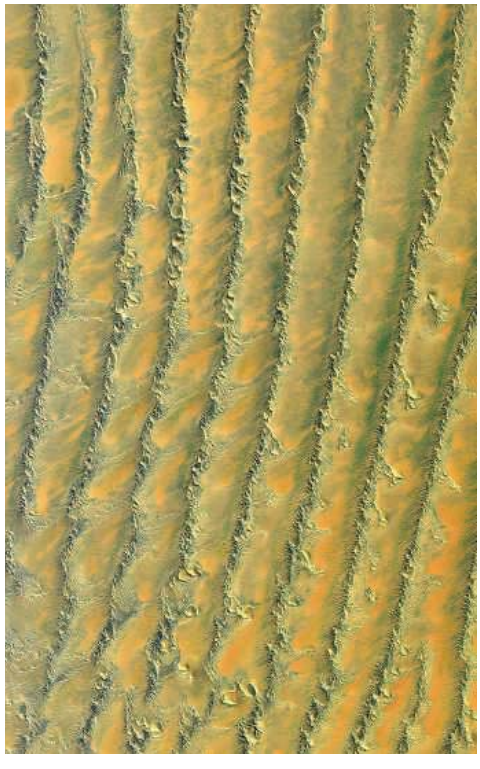

Patterns in a sea of sand. (**Top**) Plot of height versus crest-to-crest spacing of linear dunes in Namibia, Kalahari, and Australia, compared to Titan dunes. Data for terrestrial dunes are from field measurements and aerial photographs (*6*). Titan data are interpreted from figure 1 of (*2*). Note that Titan dunes are directly comparable in size and spacing to Namibian examples. (**Left**) Landsat 7 image of linear dunes in the central Namib Sand Sea. Dune crests are spaced ~2.5 km apart; dunes are 100 to 150 m high. (**Right**) Ground photograph of linear dunes in Namib Sand Sea. Dunes shown are ~100 m high.

CREDIT: LANDSAT IMAGE FROM USGS/EROS, SIOUX FALLS, SD; GROUND PHOTO BY N. LANCASTER

The author is at the Desert Research Institute, Reno, NV 89512, USA. E-mail: nick@dri.edu

porting sand-sized material in the geologic past. On Titan, the low gravity and high atmospheric density combine to produce conditions in which material of sand size can be transported by winds with a velocity as low as 0.1 m s^{-1}. Atmospheric models and limited observations by landers indicate that these conditions are currently met on Titan. This is in contrast to Mars, where winds capable of transporting the materials found in aeolian landforms appear to be very rare in modern atmospheric conditions (*9*). Movement of large volumes of sediments across the surface of Titan to form sand seas also indicates generally dry surface conditions.

The accumulation of sand-size material in certain areas to form sand seas or dune fields implies spatially varying wind and sediment-transport patterns in which the influx of material into an area exceeds the outflux, resulting in deposition of sediment. Such spatial variations in wind energy are likely the product of global and regional circulation patterns, with topography playing a local role, as in terrestrial deserts.

Recognition of extensive linear dune fields on Titan provides further evidence of the variety of processes on planetary surfaces and the wonders of our solar system. The existence of such dunes constrains the nature of surface and atmospheric processes in the exotic environment of this moon of Saturn by providing evidence for the existence of granular material and its large-scale transport by wind.

References

1. R. Greeley, *Mem. Soc. Astron. Ital.* **52**, 409 (1981).
2. R. D. Lorenz *et al.*, *Science* **312**, 724 (2006).
3. R. Greeley, J. D. Iversen, *Wind as a Geological Process* (Cambridge Univ. Press, Cambridge, 1985).
4. J. F. McCauley, *J. Geophys. Res.* **78**, 4123 (1973).
5. R. Greeley *et al.*, *J. Geophys. Res.* **97**, 13319 (1992).
6. N. Lancaster, *Geomorphology of Desert Dunes* (Routledge, London, 1995).
7. C. S. Bristow, S. D. Bailey, N. Lancaster, *Nature* **406**, 56 (2000).
8. G. Kocurek, N. Lancaster, *Sedimentology* **46**, 505 (1999).
9. R. Sullivan *et al.*, *Nature* **436** (2005).

10.1126/science.1126292

CHEMISTRY

Shuttling Polyolefins to a New Materials Dimension

A combination of two catalysts with a chemical species that shuttles a growing polymeric chain between them will allow the fabrication of tailored polymers on a commercial scale.

Vernon C. Gibson

The past 20 years have seen unparalleled developments in the design and development of single-site catalysts for the production of polyolefins (*1*, *2*), plastic materials that are presently generated on a scale approaching 100 million tons per year. These new catalyst systems display comparable activities to classical catalysts but also have the potential to control the molecular weight, molecular weight distribution, and microstructure of the polymer, thus providing access to new materials without major penalties on productivity.

However, catalysts are not the "be all and end all" in the quest for new materials. Arriola *et al.* (*3*) report on page 714 of this issue, an ingenious use of chain shuttling reagents to transfer growing polymer chains from one active catalyst site to another, allowing microblock polyolefin materials to be produced on a commercially viable scale.

Tailored block copolymers (in which each molecule consists of sequences of one unit followed by long sequences of another) often perform better than homopolymer blends or random copolymers, but their large-scale preparation has been thwarted by the fact that living polymerization catalysts are usually required to assemble polymers block by block. (A living polymerization is a chain growth process that is not accompanied by any chain termination or chain-transfer processes; that is, the catalyst "lives" on the end of the polymer chain until deliberately destroyed or removed.)

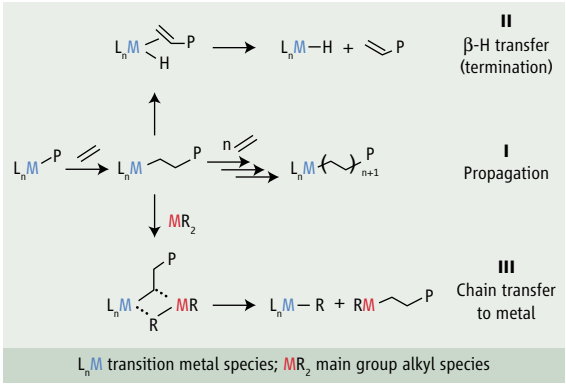

Living polymerization. Propagation (I) is not accompanied by β-H transfer (II) or chain transfer to metal (III). M. metal; L, ligand; P, polymer chain; R, alkyl group; H, hydrogen.

Living single-site olefin polymerization catalysts do exist (*4*, *5*). However, they have a serious downside. Normally, catalysts terminate one chain and restart growth of another chain, and they can do this for several hundred chains, such that very little catalyst is required to make a lot of polymer. In a living polymerization system, there is no termination, which—while having the advantage of allowing a second block to be added—means that only one chain can be grown per metal center. Multigram quantities of quite expensive catalyst would therefore be required for a relatively small batch of polymer, placing practical limits on their exploitation.

In a living polymerization system, chain propagation (see the first figure, middle) must not be accompanied by chain termination processes such as β-H transfer (see the first figure, top). Although potentially reversible, the latter process usually leads to the formation a new initiating species that catalyzes the growth of a new polyethylene chain. Another type of chain-transfer process that has been long-known to accompany chain growth is chain transfer to metal (see the first figure, bottom). In this case, the growing polymer chain is transferred to a main-group metal center (usually present as an additive) in a reversible reaction. The main-group alkyls are stable to decomposition under the polymerization conditions, and the polymer chain eventually transfers back to the propagating transition-metal center. If chain transfer to metal is efficient and reversible, and is the only process to accompany propagation, then the polymerization can take on some of the attractive features of a living process (*6*).

Arriola *et al.* (*3*) now take the concept of transferring a growing polymer chain from a metal catalyst center to a main-group metal species and extend it to a dual-catalyst system. In their system, the main-group alkyl species is used to shuttle a polymer chain back and forth from one active site to another. This process gives rise to polymers that contain block segments with the microstructural signature of each catalyst and allows microblock polyolefin materials to be produced on a large scale for the first time.

The concept of a polymer chain being transferred from a polymerization-active transition-

The author is in the Department of Chemistry, Imperial College, Exhibition Road, London SW7 2AZ, UK. E-mail: v.gibson@imperial.com.uk

metal center to a dormant main-group metal species has been known since the early days of polyolefin catalysis. Its origin can be traced back to Karl Ziegler (*7*), who, in the early 1950s, discovered that a mixture of $TiCl_4$ and trialkylaluminums could catalyze the formation of polyethylene (hence founding metal-catalyzed polyolefin production). Ziegler postulated that the transition metal could be acting as a catalyst for the insertion of ethylene into the Al–C bond, a reaction which he termed a metal-catalyzed Aufbau reaction.

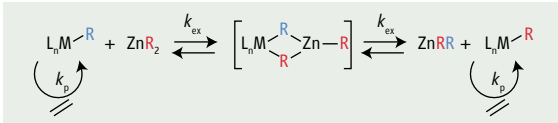

Chain shuttling. Reversible alkyl-group exchange between dormant zinc and polymerization-active transition-metal centers can be used to tune the properties of the resulting polymers.

Ziegler soon realized that the titanium centers were responsible for catalyzing C–C bond formation, whereas the function of the Al species was to deliver an alkyl-initiating group to the transition metal. However, analyses of polyethylene samples generated by a variety of catalysts have revealed that aluminum alkyls readily engage in an exchange reaction with their transition-metal catalyst partners (*6*). Some have been found to do this very efficiently, to the extent that chain transfer to aluminum is actually faster than ethylene insertion into a metal-carbon bond. This regime, known as catalyzed chain growth (*8*) or degenerative group transfer (see the second figure), leads to chains with a remarkably narrow (< 1.1) and symmetrical distribution of chain lengths. The narrow molecular weight distributions can be used as an indicator of suitable chain-transfer behavior for the chain shuttling reaction.

Other main-group alkyls, including those of Mg (*9*), and more recently Zn (*5*, *10*, *11*), have also been shown to facilitate highly efficient chain transfer to and from transition-metal centers. Zn is among the most efficient chain-transfer reagents for single-site catalysts across the transition series, because the metal-carbon bond energies of the zinc alkyl closely match those of transition-metal alkyl species, the polarities of the Zn–C and M–C bonds are similar, and the mononuclear dicoordinated Zn centers are uncrowded.

To form microblock materials, two catalysts are used within a common pool of chain-transfer reagent (*3*); propagation must be faster than chain transfer to the main-group metal center, and the relative rates of chain transfer will dictate the average block lengths. Because the degree of chain transfer is affected by several factors—including the concentration of chain-transfer reagent, the concentration of monomer, and the temperature of the polymerization—it should be possible to find a set of conditions to allow the formation of the desired microblock structures.

However, the identification of catalysts that yield differentiated microstructures at appropriate rates of chain transfer presented a substantial challenge. By combining advances in single-site polymerization catalysis with powerful high-throughput screening methodologies, Arriola *et al.* have been able to home in on catalysts that enable both microstructural control and efficient chain shuttling. Moreover, they show that the catalysts can be used in a continuous process, which has the advantageous effect (from a polymer processing viewpoint) of broadening the molecular weight distribution; a broad molecular weight distribution allows the polymer to be extruded (pushed) through a narrow aperture. The shorter chains present in the broad distribution effectively lubricate the material.

Arriola *et al.* elegantly demonstrate the advantages of combining two catalysts and a single type of monomer with a shuttle reagent, but the plethora of materials that might prove accessible by using multiple catalysts and monomers can only be imagined at this point. Combining catalysts would add many additional and attractive possibilities. Because the polymer chains end up attached to a main-group species, the intrinsic reactivity of the main-group alkyl may potentially be harnessed to access end-functionalized products. For example, Zn alkyls react readily with gases such as oxygen to give Zn alkoxides, which can then be hydrolyzed to alcohols, or with CO_2 to form carboxylic acids; these may have applications as surfactants (for low–molecular-weight products) or as functionalized polyolefins with enhanced surface energies. This catalyst shuttle technology provides the long-sought platform for producing microblock polyolefin materials on a commercial scale.

References

1. V. C. Gibson, S. K. Spitzmesser, *Chem. Rev.* **103**, 283 (2003).
2. S. D. Ittel, L. K. Johnson, M. Brookhart, *Chem. Rev.* **100,** 1169 (2000).
3. D. J. Arriola, E. M. Carnahan, P. D. Hustad, R. L. Kuhlman, T. T. Wenzel, *Science* **312**, 714 (2006).
4. J. Tian, P. D. Hustad, G. W. Coates, *J. Am. Chem. Soc.* **123**, 5134 (2001).
5. J. Saito *et al.*, *Angew. Chem. Int. Ed.* **40**, 2918 (2001).
6. G. J. P. Britovsek, S. A. Cohen, V. C. Gibson, M. Van Meurs, *J. Am. Chem. Soc.* **126**, 10701 (2004).
7. K. Ziegler, E. Holzkamp, H. Breil, H. Martin, *Angew. Chem.* **67**, 541 (1955).
8. E. G. Samsel, D. C. Eisenberg, European patent 0574854 (1993).
9. J.-F. Pelletier, A. Mortreux, X. Olonde, K. Bujadoux, *Angew. Chem. Int. Ed.* **35**, 1854 (1996).
10. M. Van Meurs, G. J. P. Britovsek, V. C. Gibson, S. A.Cohen, *J. Am. Chem. Soc.* **127**, 9913 (2005).
11. G. J. P. Britovsek, S. A. Cohen, V. C. Gibson (BP Chemicals Limited, UK), WO 03/14046 (2003).

10.1126/science.1127258

SOCIAL SCIENCE

The Pleasures and Pains of Information

George Loewenstein

Information serves not only as an input into decision-making, but is a source of pleasure and pain in its own right. This has diverse consequences for human decision-making.

In 1961, economist and Nobel Laureate George Stigler (*1*) initiated the "economics of information" when he relaxed an assumption that had dominated economics until that point. Rather than assume that people are fully knowledgeable of relevant information when it comes to making a decision, he allowed for the possibility that people might lack information and be motivated to acquire it. As Stigler noted when he accepted the 1982 Nobel Prize, "The proposal to study the economics of information was promptly and widely accepted, and without even a respectable minimum of controversy. Within a decade and a half, the literature had become so extensive and the theorists working in the field so prominent, that the subject was given a separate classification in the *Index of Economic Articles*." Stigler acknowledged that "The absence of controversy certainly was no tribute to the definitiveness of my exposition." Rather, "All I had done was to open a door to a room that contained many fascinating and important problems" (*2*).

Relaxing the assumption of perfect information did, indeed, open new doors for econo-

The author is in the Department of Social and Decision Sciences, Carnegie Mellon University, Pittsburgh, PA 15213, USA. E-mail: gl20@andrew.cmu.edu

mists. Yet the economics of information that emerged from Stigler's seminal contribution embraced its own set of strong assumptions about how people deal with the information they acquire. Although these assumptions have proven their value, forming the basis for tractable models that generate testable, often valid, predictions of decision-making and market outcomes, several of the new assumptions are as patently unrealistic as the original assumption of perfect information. Much as the allowance for imperfect information initiated a rich vein of new work, relaxing some of the assumptions that took its place has the potential to help resolve important puzzles for economics. These include inconsistencies in the apparent degree to which people take account of the future, and the human tendency to avoid information in certain situations or fail to draw seemingly obvious conclusions from the information one receives.

One tenet of the economics of information that may be ripe for modification is the assumption that information is not valued in its own right, but only insofar as it informs decision making and enables decision-makers to secure desired outcomes. On page 754 in this issue, Berns *et al*. (*3*) challenge this assumption by showing that people not only dislike experiencing unpleasant outcomes, but also dislike waiting for them. Confronting human subjects with the prospect of an impending electric shock, the authors find that regions of the pain matrix (a cluster of brain regions that are activated during the experience of pain) are also activated in anticipation of shock. This activation intensifies as the shock becomes imminent. The information that one is going to receive an electric shock, like the shock itself, is a source of misery.

The idea that people derive pleasure and pain directly from information, rather than from any material benefits that the information procures, has diverse implications for decision-making. As highlighted by Berns *et al*., utility derived from anticipating future outcomes can have a major impact on intertemporal choices—decisions involving costs and benefits that extend over time. The standard economic account of intertemporal choice predicts that people will generally want to expedite pleasant outcomes and delay unpleasant ones (*4*). If, however, people derive pleasure or pain from the information that an outcome will occur in the future, they may prefer to defer desired outcomes so as to prolong the pleasure of anticipation or to expedite unpleasant outcomes so as to shorten the period of dread. In the Berns *et al*. study, 84% of subjects preferred to get electric shocks over with quickly. Ignoring the utility of information, the standard account would predict instead that subjects would prefer to defer the shocks.

Earlier studies posited a causal link between anticipatory utility and the desire to get unpleasant outcomes over with quickly (*5*). However, Berns *et al*. actually observe a correlate of dread in the brain activity of human subjects and a significant relationship between individual differences in this measure and individual differences in intertemporal choice behavior (*6*). In tandem with other recent work that highlights the role of emotions in intertemporal choice (*7*), and consistent with historical accounts of intertemporal choice behavior (*8*), these findings support the idea that the decision to delay or expedite an outcome depends critically on how a person feels while waiting. When waiting is pleasurable, people will often prefer to defer. When it is unpleasant, however, because waiting for an unpleasant outcome produces dread or waiting for a pleasant outcome generates frustration, people will prefer to expedite outcomes—even, sometimes, at the cost of experiencing worse ones.

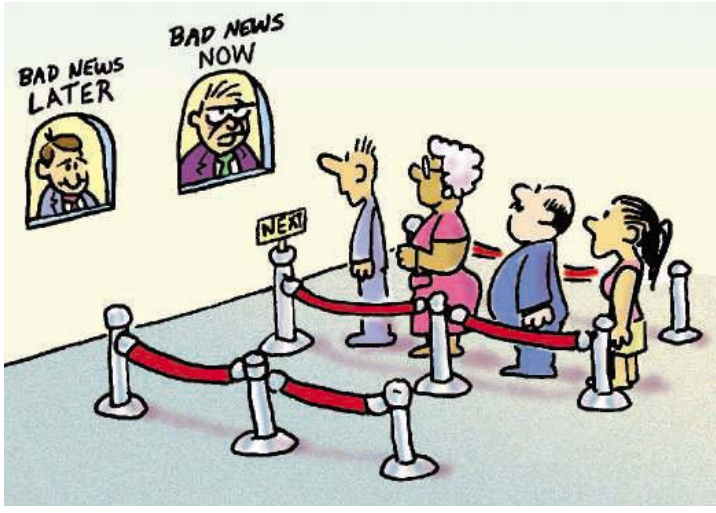

Bring it on. People generally choose to get unpleasant things over with quickly.

CREDIT: JOE SUTLIFF

The idea that people derive utility directly from information has a variety of consequences that go well beyond the domain of intertemporal choice. Emotions, such as fear and excitement, can dramatically change people's willingness to take risks (*9*–*11*). And utility derived from self-image—that is, from information about one's value as a person—can have diverse ramifications, including encouraging prosocial behavior (*12*, *13*).

Utility from information can also affect the demand for information. Conventional economics predicts that people should prefer more information to less. If people derive utility directly from information, however, they may sometimes be motivated to avoid information, even if it is free and useful for decision-making (*14*). Indeed, people often avoid getting tested for medical conditions because they are afraid of getting bad news (*15*), and investors are more likely to look up the value of their portfolios when the stock market is up (and the news about one's own portfolio promises to be favorable) than when the market is down (*16*).

Beyond sometimes motivating the avoidance of information, the utility associated with information also provides people with an incentive to process information in a biased fashion—to form "motivated" beliefs that feel good in the short run but can distort decision-making (*17*). People are remarkably adept at finding reasons to believe what they wish were true and not believe what they wish were not true (*18*). For example, someone who is worried about the health of a loved one is often the last to view the situation in objective terms. Instead, he or she grasps at remedies—however far-fetched—that promise hope. Or consider the many people who fall prey to pyramid and Ponzi financial investment schemes. Although economists argue that there is no such thing as a free lunch, this behavior suggests that many people are quite willing to be persuaded otherwise.

These examples just scratch the surface of promising directions for research on the utility of information. For example, neither economists nor psychologists have advanced a theory that can explain when and why waiting for a desired outcome is pleasurable or, instead, frustrating, even though the emotional response to anticipation may be the single most important determinant of people's willingness to delay gratification. As another example, theories of investor behavior assume unrealistically that paper gains and losses (changes in the value of owned assets) provide the same utility as realized gains and losses (those that result from actually selling assets). Relaxing this assumption may help to explain a wide range of perplexing investor behaviors, such as the tendency to hold on to losing stocks (by holding such stocks, investors limit themselves to paper losses as opposed to actual losses). We also lack a convincing theory to account for and predict the market bubbles and busts that wreak havoc on economies. Such a theory will almost inevitably incorporate interactions between expectations and emotions such as the paradigmatic "fear and greed."

As the first of its kind, the study by Berns *et al*.

has limitations. Given the constraints of brain imaging, for example, the time intervals over which the study's subjects make decisions (about 30 s) are shorter than the decision intervals of greatest interest to economics. Moreover, the authors observed the connection between dread and intertemporal choice across subjects in two separate tasks. It would provide stronger evidence that dread is playing a causal role if activation in a single task was correlated with decisions made in the same task. The authors assume, finally, that dread is better represented by the summed total of anticipatory activation over the duration of the waiting period. But it might make more sense to represent dread as the level of activation at a particular time. These are, obviously, minor limitations given the novelty and importance of the research.

The Berns *et al*. study is a superb new addition to the nascent field of neuroeconomics (*19*, *20*). It also contributes to a new wave of research in behavioral economics that, following Stigler's lead, examines the consequences of relaxing economists' stylized assumptions about how people deal with information (*21*). Both of these new lines of research have generated more controversy than Stigler's initial insight, but will likely prove similarly rich in yielding theoretical results.

References and Notes

1. G. Stigler, *J. Pol. Econ.* **69**, 213 (1961).
2. http://nobelprize.org/economics/laureates/1982/stigler-lecture.html
3. G. S. Berns *et al*., *Science* **312**, 754 (2006).
4. S. Frederick, G. Loewenstein, T. O'Donoghue, *J. Econ. Lit*. **40**, 351 (2002).
5. G. Loewenstein, *Econ J*. **97**, 666 (1987).
6. Also providing evidence of a relationship, across persons, between dread and intertemporal choice behavior, Hare (22) found that, whereas normal people showed physiological signs of fear well before receiving an anticipated electric shock, psychopaths, whose behavior is characterized not only by indifference to the well-being of others but also impulsivity, only exhibited symptoms of fear moments before shock onset.
7. S. M. McClure, D. I. Laibson, G. Loewenstein, J. D. Cohen, *Science* **306**, 503 (2004).
8. G. Loewenstein, in *Choice Over Time*, G. Loewenstein, J. Elster, Eds. (Russell Sage, New York, 1992), pp. 3–34.
9. A. Caplin, J. Leahy, *Q. J. Econ.* **116**, 55 (2001).
10. G. Loewenstein, E. Weber, C. Hsee, N. Welch, *Psychol. Bull*. **127**, 267 (2001).
11. B. Shiv, G. Loewenstein, A. Bechara, H. Damasio, A. R. Damasio, *Psych. Sci*. **16**, 435 (2005).
12. R. Benabou, J. Tirole, *J. Am. Econ. Rev*., in press.
13. R. Bodner, D. Prelec, in *Collected Essays in Psychology and Economics*, I. Brocas, J. Carillo, Eds. (Oxford Univ. Press, Oxford, 2002).
14. Conversely, people often seek out information even when they know it will make them miserable. Such curiosity is such a powerful, and often self-destructive, motivator of human behavior that many psychologists advocate classifying curiosity as a drive, like hunger and thirst (*20*).
15. A. Caplin, in *Time and Decision*, G. Loewenstein, D. Read, R. Baumeister, Eds. (Russell Sage, New York, 2003), pp. 441–458.
16. N. Karlsson, G. Loewenstein, D. J. Seppi, Social Science Research Network (http://ssrn.com/abstract=772125).
17. M. K. Brunnermeier, J. A. Parker, *Am. Econ. Rev.* **95**, 1092 (2005).
18. P. H. Ditto, D. F. Lopez, *J. Pers. Soc. Psychol*. **63**, 568 (1992).
19. C. Camerer, G. Loewenstein, D. Prelec, *J. Econ. Lit.* **43**, 9 (2005).
20. A. Sanfey, G. Loewenstein, S. M. McClure, J. D. Cohen, *Trends Cognit. Sci.* **10**, 108 (2006).
21. M. Rabin, J. Schrag, *Q. J. Econ.* **114**, 37 (1999).
22. R. D. Hare, *J. Abnorm. Soc. Psychol*. **70**, 442 (1966).

23. I thank R. Benabou, A. Caplin, J. Cohen, S. Frederick, T. O'Donoghue, D. Prelec, D. Read, and E. Angner for helpful comments.

10.1126/science.1128388

PLANETARY SCIENCE

The Primordial Porridge

Interplanetary dust particles contain organic matter thought to have formed either before our solar system or early in its history. Similar matter appears in the oldest meteorites.

Bernard Marty

The solar system formed from the collapse of a cloud of gas and dust called the solar nebula, through a series of energetic events that have left few traces. Studies of planetary bodies including meteorites have demonstrated that matter was efficiently mixed at an atomic scale before solids were formed. The isotopic compositions of some of the light elements such as hydrogen and nitrogen, however, vary dramatically across the solar system. Mass balance considerations indicate that these isotope heterogeneities are not inherited from previous nucleosynthesic processes in stars. Instead, these isotope variations are likely to have formed in the solar nebula or in interstellar space. Until now, the largest hydrogen and nitrogen isotopic variations have been found in interplanetary dust particles (IDPs), which are micrometer-sized particles flowing in interplanetary space that have been collected in the high atmosphere by NASA stratospheric planes. IDPs have deuterium (D) and nitrogen isotope anomalies found in organic matter, which suggests that IDPs are among the most primitive type of matter in the solar system and could be, in some cases, cometary in origin (*1*). Carbonaceous chondrites, which are volatile-rich meteorites originating from planetary bodies that never melted and differentiated, also exhibit enrichments in deuterium and ^{15}N associated with organic matter, but to a much lesser extent (*2*). These differences are in line with the more "primitive" character of IDPs compared with carbonaceous chondrites. Now, observations by Busemann *et al*. reported on page 727 of this issue (*3*) shed a different light on this view.

By using a new imagery technique that allows the spatial distribution of isotope enrichments to be mapped on a micrometer scale, Busemann *et al*. have discovered tiny "hot spots," where D and ^{15}N are highly enriched in the organic matter of several carbonaceous chondrites. Remarkably, these enrichments even exceed those found in IDPs. Busemann *et al*. propose that carbonaceous chondrites, which are thought to originate from the asteroid belt at 2 to 4 AU (astronomical units equal to the Earth-Sun reference distance), and IDPs, some of which are thought to represent cometary material originating at several tens to hundreds of AU, have both sampled a similar reservoir of exotic material (see the figure). They further propose that the host of these components is a particular resistant form of organic matter that has been equally preserved in carbonaceous chondrites and in IDPs, despite secondary processing that often affected the former or their parent bodies. The discovery made by Busemann *et al*. suggests that comets contain material that shares similarities with carbonaceous chondrites, a possibility in line with the occurrence of refractory silicates and calcium-aluminum–rich inclusions in cometary grains recovered by the Stardust mission and presented in March 2006 at the Lunar and Planetary Science Conference in Houston, Texas (*4*). Thus it appears that large-scale turbulence occurred in the nascent solar system that transferred refractory phases from the inner, hot regions toward the outer solar system and, conversely, disseminated matter that was presumably synthesized outside the solar nebula or in its colder regions up to inner solar regions.

How and where did these isotope anomalies develop? Hydrogen and nitrogen isotope hot spots observed by Busemann *et al*. in meteoritic organics do not coincide spatially. On a larger scale, such isotope variations among different solar system objects do not define a single relationship, suggesting that different paths or processes may

The author is at the Centre de Recherches Pétrographiques et Géochimiques, Vandoeuvre-lès-Nancy Cedex, 54501 France. E-mail: bmarty@crpg.cnrs-nancy.fr

have occurred. Selective isotopic enrichment during gas-gas or solid-gas reactions at low temperature is a strong possibility for the following reasons: (i) hydrogen and nitrogen are among the most abundant gaseous species in the interstellar medium and nascent stellar systems, and (ii) the magnitude of isotopic fractionation increases with decreasing temperature. Large D/H ratios observed in the cold interstellar medium are indeed attributed to ion-molecule reactions and have led to the consensual view of an exotic (relative to the solar nebula) origin for D enrichments observed in solar system matter. However, recent findings suggest that such isotopic enrichment instead might have occurred in cold regions of the nascent solar system. From the analysis of the D/H ratios of molecular fragments extracted from meteoritic organics, Remusat *et al.* (*5*) found that the extent of deuterium enrichment increases with decreasing C-H dissociation energy of the molecular fragments they analyzed. An opposite trend would be expected in the case of an exotic origin of deuterium-rich molecules, because the survival of exotic hydrogen-isotope anomalies acquired before the formation of the solar system should have been seen mainly in the most robust molecular fragments, contrary to the observation. Rather, this tendency is consistent with isotopic exchange between "normal" organic matter and a deuterium-rich solar system reservoir.

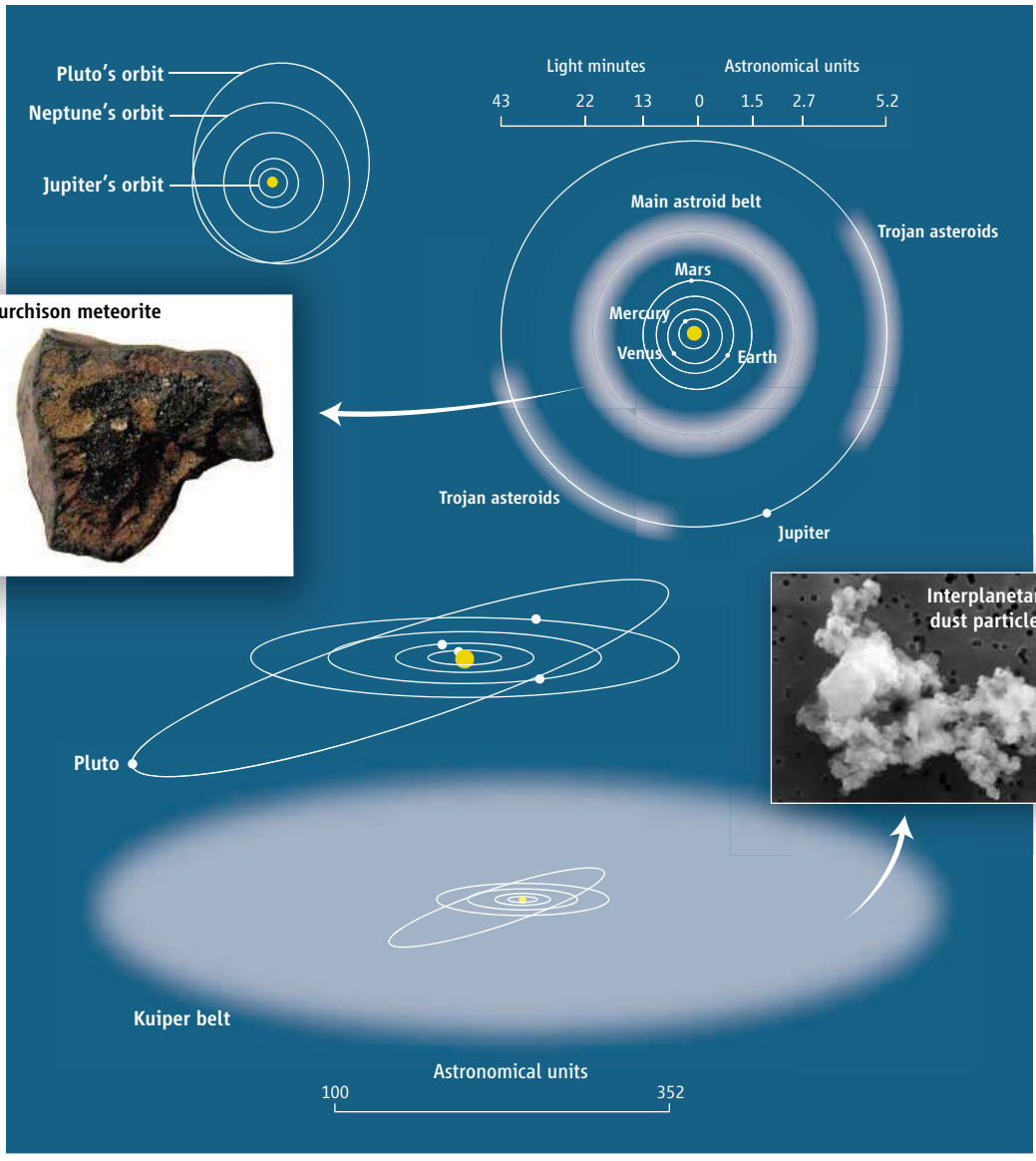

Early matter. Primitive meteorites, such as the Murchison meteorite analyzed by Busemann *et al.*, have hydrogen and nitrogen isotope anomalies even more pronounced than those of IDPs. Meteorites originate from the asteroid belt between the orbits of Mars and Jupiter, whereas IDPs, at least some of them, may come from comets that originate beyond the orbit of Neptune, in the Kuiper belt. IDPs were thought to be the most primitive solar system material matter available on Earth for analysis, and the results of Busemann *et al.* suggest large-scale mixing in the nascent solar system.

In contrast to the case of hydrogen, ion-molecule reactions in the interstellar molecular clouds are apparently unable to produce the nitrogen isotope enrichments observed in IDPs and meteoritic organics (*6*). Recent models of early solar evolution advocate intense irradiation of matter situated within the inner solar system, opening the possibility that ^{15}N enrichments found in organics could have happened by solar ultraviolet (UV)-triggered dissociation of N_2 gas and by the incorporation of newly formed N ions into organics. UV photons that have the right wavelength to dissociate the abundant ^{14}N-^{14}N molecules could have been consumed at a faster rate than those dissociating the rare ^{15}N-^{14}N or ^{15}N-^{15}N molecules, a process called self-shielding recently advocated for fractionating oxygen isotopes (*7*). However, it is unclear why this would have produced ≥300% ^{15}N enrichments (as suggested by Busemann *et al.*) and only about 5% for oxygen. Alternatively, Aléon *et al.* (*8*) have recently found extreme oxygen isotope anomalies up to 6000% in tiny silicate particles embedded in meteoritic organic matter. The characteristics of this oxygen isotope enrichment are consistent with an irradiation origin during highly energetic solar flare events that happened when the solar system formed, and independent evidence for such high-energy irradiation long ago also stems from the study of other isotope systems. We still don't know much about the infancy of our solar system, and there is little doubt that tremendous advances in our understanding of this period will arise from the combination of high-precision microanalysis of extraterrestrial matter and of missions returning samples to Earth.

CREDIT: P. HUEY/*SCIENCE*; MURCHISON IMAGE, TOMK/CRYSTAL WORLD; IDP IMAGE/NASA.

References

1. S. Messenger, F. J. Stadermann, C. Floss, L. R. Nittler, S. Mukhopadhyay, *Space Sci. Rev.* **106**, 155 (2003).
2. F. Robert, S. Epstein, *Geochim. Cosmochim. Acta* **46**, 81 (1982).
3. H. Busemann *et al.*, *Science* **312**, 727 (2006).
4. D. E. Brownlee *et al.*, paper 2286 presented at the 37th Lunar and Planetary Science Conference, 13 to 17 March 2006, Houston, TX.
5. L. Remusat *et al.*, *Earth Planet. Sci. Lett.* **243**, 15 (2006).
6. R. Terzieva, E. Herbst, *Mon. Not. R. Astron. Soc.* **317**, 563 (2000).
7. R. N. Clayton, *Nature* **415**, 860 (2002).
8. J. Aléon, F. Robert, J. Duprat, S. Derenne, *Nature* **437**, 385 (2005).

10.1126/science.1125967

GEOCHEMISTRY

Follow the Nitrogen

On Mars, the jovian satellites, and other planetary bodies, nitrogen species may provide important clues to the presence of life.

Douglas G. Capone, Radu Popa, Beverly Flood, Kenneth H. Nealson

"Follow the water" is the mantra used by NASA in the search for life in the universe. It is hard to imagine life without a fluid, or to imagine that the fluid could be anything other than water. From our Earth-centric point of view, it is equally difficult to imagine life without carbon and nitrogen. These two elements, by virtue of their ability to form double bonds, allow the formation of a multitude of unsaturated and aromatic compounds that impart both structural strength and energetic versatility to earthly life. We propose here that the lack of a substantial geological reservoir of nitrogen (*1*, *2*) makes it an ideal candidate in the search for life on Mars and other planetary bodies: "follow the nitrogen."

As shown in the figure, the carbon and nitrogen cycles involve similar conversions of various redox states (from completely oxidized to completely reduced). These transformations are catalyzed at the organismal level and lead to the movement of carbon and nitrogen among the biosphere, atmosphere, geosphere, and ocean; to this extent, the two cycles seem quite similar. However, when the scale is global rather than organismal, carbon and nitrogen offer remarkable contrasts with regard to both their abundance and distribution (see the figure).

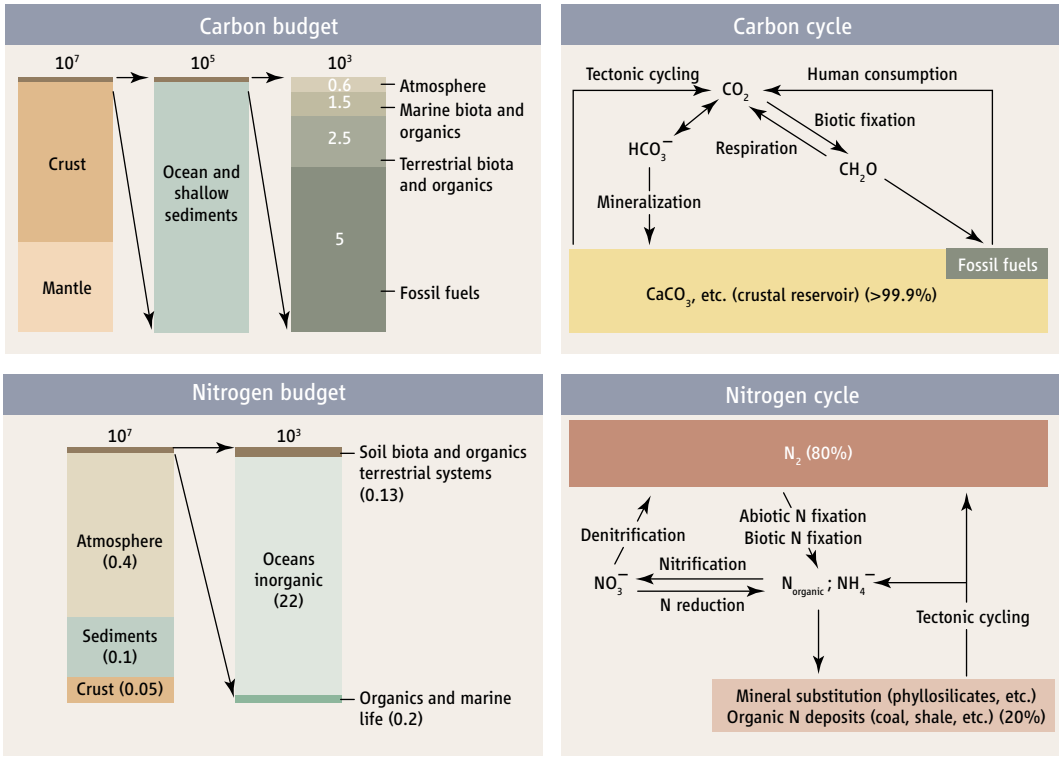

Comparative carbon and nitrogen cycles on Earth. (**Left**) Budgets of carbon and nitrogen in the major reservoirs on Earth. Values are taken from many different sources, as summarized in (*1*, *2*). (**Right**) Major changes in redox chemistry catalyzed by biota. The reactions due to anaerobic ammonium oxidation (*11*) are not included in the diagram. Budget values are in pedagrams (10^{15} g).

Carbon resides primarily in the lithosphere (mantle-derived rocks, crust, and sediments), with less than 0.05% being cycled through the biosphere, hydrosphere, and atmosphere. In contrast, nitrogen resides primarily in the atmosphere as dinitrogen (N_2) and trace amounts of N_2O (an important atmospheric biosignature) (*2*). With the exception of a few phyllosilicates that contain ammonia substituted for potassium, nitrogen has no substantial geological reservoirs. Because of this unusual distribution, the amount of nitrogen found in the biosphere (in living species and deposited as shales) is actually a few percent of the total fixed nitrogen.

Nitrogen is "fixed" from N_2 through both physical (such as nitrogen oxide formation by lightning) and biological processes. Minerals containing fixed nitrogen, such as nitrate and ammonium salts, tend to dissolve in the presence of even small amounts of liquid water. Thus, except for extremely dry sites such as the Atacama desert, nitrogen moves from the continents to the oceans as soluble nitrates in water flow (*1*, *2*) and returns to the atmosphere as N_2 via denitrification, the return pathway that keeps the nitrogen cycle going.

Nitrogen fixation—the transformation of N_2 to a reduced, biologically useful form—is often touted as the great evolutionary invention that allowed life to prosper on Earth (*3*). Although there is some truth to this with regard to organic productivity, it may well be that an important point with regard to the development of life on Earth has been missed. Nitrates are not readily converted to N_2 by abiotic processes, so that in an abiological oxidizing environment, any conversion of N_2 to soluble nitrates should result in the progressive loss of N_2 from the atmosphere and the accumulation of nitrates in the oceans. On a tectonically active planet such as Earth, some nitrogen is returned on geological time scales via volcanic emissions, but given the absence of nitrogen-rich minerals, this effect will be relatively small (*4*). Thus, if biological pathways such as denitrification (including anaerobic ammonium oxidation) (*5*) did not occur, the terrestrial nitrogen cycle (and terrestrial life as we know it) could not be sustained. Even on Earth, over the course of billions of years, abiotic processes such as lightning would substantially deplete the atmosphere of N_2, leaving an ocean of soluble nitrogen and a land mass substantially depleted in this element (*6*, *7*). Denitrification is the driving force for the return of nitrogen to the land and its equitable redistribution via nitrogen fixation. In our view, biological nitrogen fixation was needed only when the productivity of Earth exceeded the ability of existing fixed reservoirs and abiotic nitrogen fixation to supply it (*8*); in contrast, we see denitrification as essential for the maintenance of the nitrogen cycle itself.

D. G. Capone and B. Flood are in the Department of Biological Sciences, and K. H. Nealson is in the Department of Earth Sciences, University of Southern California, Los Angeles, CA 90089, USA. R. Popa is in the Department of Biology, Portland State University, Portland, OR 97207, USA. E-mail: knealson@usc.edu

On Mars, things are very different. N_2 constitutes only about 2.7% of a very thin atmosphere (*9*). Isotopic measurements of the martian atmosphere suggest that the nitrogen has been lost from the planet over geological time (*6*, *10*), and to date, no ammonia has been identified. If nitrogen-containing life ever existed on Mars, then we would expect evidence of this to exist in the form of sedimentary deposits containing substantial amounts of nitrogen (for example, fixed nitrogen in organics, such as alkyl porphyrin derivatives, and its stable isotopic signatures in shales and kerogen) (*11*). Given the lack of tectonic processing and the absence of continuing life that might recycle the evidence of the past, there might be relatively accessible and unaltered evidence for this life, perhaps visible even today in outflow channels. Alternatively, life may have never evolved, leaving perhaps only abiotic nitrate deposits, the understanding of which might reveal the workings of past planetary chemistry (*6*, *7*, *12*). For any of these scenarios, "follow the nitrogen" is a mantra that makes sense both for understanding the past planetary chemistry and for searching for life, be it extant or extinct, on Mars.

The presence of nitrogen in any form should be a signal to planetary scientists to take notice. It may well be that the form and amount of nitrogen could constitute a roadmap for understanding whether chemical or biological processes were involved in its deposition. At least on a body that has had a separation of continental and oceanic components, the existence of nitrogen on continents is not easy to explain without special life-supplied chemistry.

Does this logic extend to considerations of the jovian satellites Europa, Ganymede, and Callisto? We think so. These moons may have liquid oceans hidden under layers of ice, presenting a very different scenario with regard to their nitrogen cycles; it is easy to imagine a nitrogen cycle that does not involve N_2, perhaps instead moving from organic nitrogen to nitrate and back, or perhaps even a nonredox cycle involving organic and inorganic forms of reduced nitrogen. Saturn's moon Titan, already known to be replete with nitrogen, offers other problems and opportunities (*9*). Life at such low temperatures may be a special case with regard to nitrogen.

Is N_2 in planetary atmospheres a useful signal for life? On those bodies where N_2 should otherwise be lost by diffusional escape from the atmosphere, the presence of fixed nitrogen would be an exciting finding. Recent mass spectrometric analyses of the atmosphere of Enceladus, a moon of Saturn, revealed a peak at 28 mass units, which could be either N_2 or CO; no definitive assignment could be made (*13*–*15*). Thus, the reports are not particularly encouraging with regard to life; as the authors say, it is worthy of more study (*13*–*15*).

As noted above, there are some planetary bodies with adequate gravity and/or very low temperatures that might be expected to maintain their nitrogen gases without the help of the biota. Thus, our recommended approach might be to search for the nitrogen; characterize and quantify it; if its abundance and chemistry cannot be explained by abiotic processes, do not leave until it is explained; and when it comes to sample return—bring back anything that is enriched in nitrogen!

References and Notes

1. J. Galloway *et al.*, *Biogeochemistry* **70**, 153 (2004).
2. J. N. Galloway, in *Treatise on Geochemistry*, H. D. Holland, K. K. Turekian, Eds. (Elsevier, Amsterdam, 2004), vol. 8, pp. 557–583.
3. V. Smil, *Enriching the Earth* (MIT Press, Cambridge, MA, 2001).
4. J. F. Kasting, D. P. Whitmire, R. T. Reynolds, *Icarus* **101**, 108 (1993).
5. A. A. van de Graaf *et al.*, *Appl. Environ. Microbiol.* **61**, 1246 (1995).
6. Y. L. Yung, M. B. McElroy, *Science* **203**, 1002 (1979).
7. R. L. Mancinelli, A. Banin, *Int. J. Astrobiol.* **2**, 217 (2003).
8. J. A. Brandes *et al.*, *Nature* **395**, 365 (1998).
9. Y. L. Yung, W. B. DeMore, *Photochemistry of Planetary Atmospheres* (Oxford Univ. Press, Oxford, 1999).
10. M. B. McElroy, T. Y. Kong, Y. L. Yung, *J. Geophys. Res.* **82**, 4379 (1977).
11. M. I. Chicarelli *et al.*, *Geochim. Cosmochim. Acta* **57**, 1307 (1993).
12. R. Plumb, R. Tantayanon, M. Libby, W. W. Xu, *Nature* **338**, 633 (1989).
13. J. S. Kargel, *Science* **311**, 1389 (2006).
14. J. H. Waite Jr. *et al.*, *Science* **311**, 1419 (2006).
15. C. C. Porco *et al.*, *Science* **311**, 1393 (2006).

16. We thank NASA, the U.S. Department of Energy, and NSF for financial support. We also thank the USC students of Geobiology and Astrobiology (BISC 483, spring 2004) for some of the discussion leading to this Perspective.

10.1126/science.1111863

IMMUNOLOGY

B Cells Spread and Gather

Immune cells that produce effective antibodies against foreign proteins are selected by a synapse-like interaction with antigen-presenting cells that promotes the survival of the cells with high-affinity binding.

Margaret M. Harnett

B lymphocytes play an important role in the immune response to infection, secreting neutralizing antibodies to combat invading pathogens. They are activated to clonally proliferate and differentiate into such antibody-secreting cells after binding of their cell surface antigen receptors to specific foreign antigen that gets trapped in lymphoid tissue. This interaction with antigen also activates B cell receptor signaling, resulting in the internalization, processing, and presentation of antigen to T lymphocytes in the context of cell surface proteins of the major histocompatibility complex class II family. Recognition of such processed antigen by the T cell receptor induces the formation of a stable association, or synapse, between the two cell types (*1*), resulting in the transmission of signals required for regulating the B cell response.

The B cell receptor has often been portrayed as simply binding and internalizing soluble antigen, with the degree of receptor activation reflecting the affinity of interaction with the antigen. What has not been clear is how B cells deal with antigens that are not soluble but rather are integral to, or tethered to, cellular membranes. How do B cells recognize, discriminate by affinity, and acquire membrane-associated antigens? Indeed, given experimental findings that antigens associated with membranes are particularly effective at activating B cells and promoting consequential B cell–driven T cell activation in vitro, it is thought that such B cell receptor recognition and affinity discrimination of membrane-associated antigens is likely to be of paramount importance in vivo. For example, in the germinal centers of lymphoid tissues, B cells undergo a maturation process that selects for those cells that produce antibodies with high affinity for antigen and for those that will recognize the same antigen in the future (memory B cells). Here, follicular dendritic cells trap, retain, and present antigen to B cells in the form of immune complexes (antigen associated with antibodies) that bind to receptors at the follicular dendritic cell surface (*2*).

On page 738 of this issue (*3*), Batista and colleagues explain how, in the early stages of the selection process, B cells dynamically spread and contract over cell membranes that bear antigen (either anchored in the membrane or tethered to the membrane as an immune complex) (see the figure). This allows the B cell receptor to differentially sense antigens of widely varying affinities by the amount of anti-

The author is in the Division of Immunology, Infection and Inflammation, Glasgow Biomedical Research Centre, University of Glasgow, Glasgow G12 8TA, UK. E-mail: M.Harnett@bio.gla.ac.uk

gen acquired, as this dictates the resulting level of B cell activation.

In their initial groundbreaking studies (*4*), Batista *et al*. showed that B cell receptor recognition of antigens tethered to the membrane leads to the formation of an immunological synapse. By internalizing the B cell receptor–antigen complex, B cells acquire antigens from target cells. This process enhances the activation of B cells at low antigen concentration and affinity, thereby potentiating (by several orders of magnitude relative to soluble antigen) subsequent antigen processing and presentation to T cells. Although the precise nature of the synapse was not defined, it was reminiscent of the classic immunological synapse described for T cell interaction with an antigen-presenting cell because the B cell receptor and signaling molecules are similarly concentrated in the center of the synapse, whereas molecules that mediate inhibitory signals are excluded.

Further work (*5*) showed that the integrin LFA-1, which has been implicated in the interaction of B cells with follicular dendritic cells, forms a region called the peripheral supramolecular activation cluster (pSMAC) that surrounds the central cluster of B cell receptor–antigen (cSMAC), indicating that B cells can form mature immunological synapses. Interestingly, although B cell synapses can form in the absence of integrins, LFA-1 increases the adhesion of the B cells under conditions of limited antigen. This decreases, by at least an order of magnitude, the avidity threshold of B cells required for synapse formation, B cell activation, and subsequent presentation of antigen to T cells. Carrasco and Batista (*6*) further showed that interaction of another B cell adhesion molecule, VLA-4, cooperates with LFA-1 to provide strong adhesion after antigen recognition by the B cell receptor. Strikingly, they found that when the affinity of the B cell receptor for antigen is low, VLA-4–mediated adhesion is essential for B cell receptor–antigen recognition under flow shear stress conditions such as those encountered when lymphocytes traffic through the vasculature or germinal centers. This led the authors to postulate that such VLA-4–mediated interactions play a key role in the capture, recruitment, and activation of B cells.

Although B cells in the initial stages of the immune response are likely to use such strategies to respond to antigen via low-affinity receptors, somatic mutation in the germinal centers generates high-affinity B cell receptors that are selected by competitive binding to antigen tethered to follicular dendritic cells in the form of immune complexes. Therefore, unlike T cells that recognize antigen through low-affinity interactions, B cells sense and differentiate an extremely wide range of different affinities in vivo. In the present study, Fleire *et al.* use a combination of sophisticated imaging and mathematical modeling technologies to investigate how the B cell receptor uses an immunological synapse to discriminate among membrane-associated antigens of differing affinities. They explain, by using mutant lysozyme antigens covering a factor of 20,000 range of affinity for wild-type and signaling-deficient B cell receptors, that the B cell receptor can discriminate antigens of varying affinities by integrating the kinetics of the B cell's ability to dynamically spread and contract over antigen-bearing membranes. Such spreading and contraction induces gathering of antigen in a manner that depends on the cytoskeleton and B cell receptor signaling. This allows the B cell receptor to sense the amount of antigen acquired and, hence, to dictate the resulting level of B cell activation.

Mathematical modeling corroborates the experimental data by showing that if high-affinity interactions occur, then rapid binding and high receptor occupancy iteratively induce further cell spreading and exposure of receptors for antigen binding before contraction and collection of B cell receptor–antigen complexes. In contrast, for low-affinity antigen, spreading and binding occur more slowly, resulting in collection of fewer B cell receptor–antigen complexes. Moreover, if critical receptor occupancy is not achieved, as would be expected under conditions of insufficient antigen or avidity, the cell detaches and signaling is aborted. Thus, the affinity of the B cell receptor–antigen interaction determines the extent of spreading and ultimately the total amount of antigen accumulated, providing a mechanism for affinity discrimination by B cells.

The immunological synapse provides a mechanism for the selection and survival of higher affinity B cells within the germinal centers, not only by providing a strong signal for B cell activation, but also by increasing the efficiency by which B cells present foreign peptides to elicit cognate T cell help. Moreover, this preferential selection and presentation of membrane-associated high-affinity antigen should act to protect against promiscuous T cell activation in response to irrelevant foreign antigen, and to impede the development of autoimmune disease if autologous membrane proteins are presented by B cells to T cells. Thus, in conclusion, such discriminatory membrane antigen recognition is likely to play a key role in directing both immunity and tolerance, in vivo.

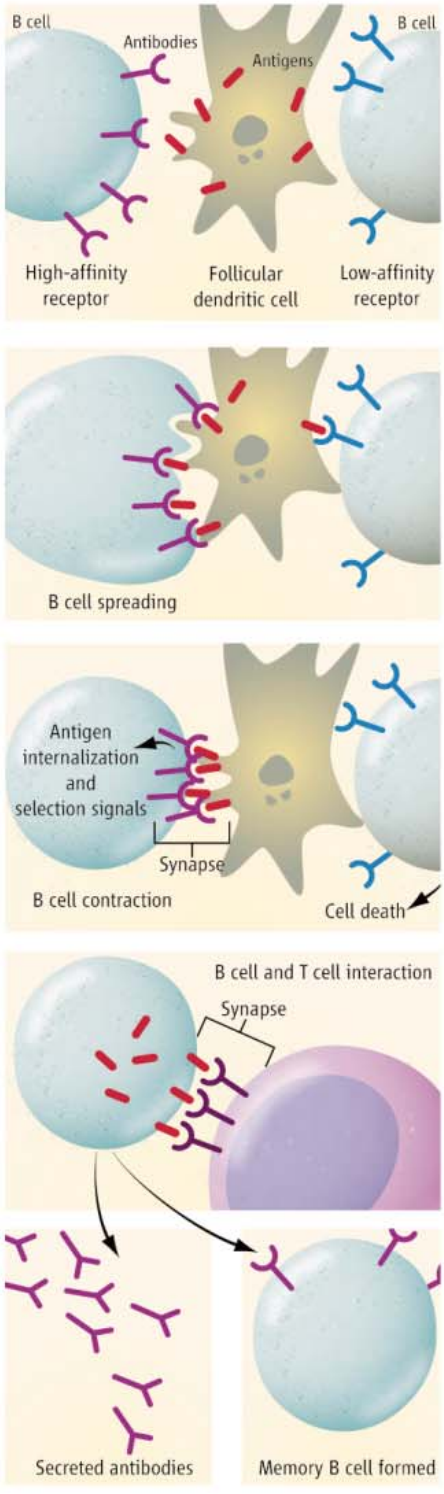

B cell discrimination of antigen affinity can dictate cell fate. Recognition of membrane-associated antigen by high-affinity B cell receptors promotes rapid and sustained spreading of a B cell over an antigen-presenting follicular dendritic cell. This allows acquisition of large amounts of antigen by high-affinity B cell receptors, resulting in strong B cell receptor signaling and subsequent interaction with helper T cells. B cells bearing low-affinity receptors undergo slower spreading and fail to gather antigen, resulting in cell death.

CREDIT: P. HUEY/*SCIENCE*

References

1. P. Friedl *et al*., *Nat. Rev. Immunol*. **5**, 532 (2005).
2. M. H. Kosco-Vilbois, *Nat. Rev. Immunol*. **3**, 764 (2003).
3. S. J. Fleire *et al*., *Science* **312**, 738 (2006).
4. F. D. Batista *et al*., *Nature* **411**, 489 (2001).
5. Y. R. Carrasco *et al*., *Immunity* **20**, 589 (2004).
6. Y. R. Carrasco, F. D. Batista, *EMBO J*. **25**, 889 (2006).

10.1126/science.1127652

RETROSPECTIVE

Nicholas J. Shackleton (1937–2006)

William F. Ruddiman

N. J. Shackleton was a scientific explorer who developed ways to extract climate data from the sea floor and found that the periodic appearance of ice sheets is governed by Earth's orbit.

With Nicholas Shackleton's death on 24 January 2006 at age 69, the field of climate science lost one of its founders and a scientist still at the forefront of research. During his four-decade career, Nick received most of the major awards in this field, along with a knighthood bestowed by Queen Elizabeth II in 1998. Nick's legacy includes a long list of major scientific contributions, a full description of which would not fit within the confines of this retrospective.

Nick was born on 23 June 1937 in London, a distant relative of the explorer Sir Ernest Shackleton. Although his father was a distinguished geologist, he credited his mother with encouraging an early scientific curiosity. As a young student, he often came home from school with some new tidbit he had learned. If his mother knew something about the subject, she would talk about it with him. If not, she and Nick would search for more information.

Nick received his B.A. in 1961 and Ph.D. in 1967 at Cambridge University, where he stayed his entire career. His first major scientific contribution was the discovery that oxygen-isotopic variations recorded in calcite shells of foraminifera are dominated by ice-volume changes, rather than by the temperature at which the shells form. This insight meant that a common ice-volume signal is present in all carbonate-bearing sediments and that oxygen-isotopic signals can be used to correlate ice-age marine records on a nearly global basis. Based on this insight, the 1970s Climate/Long Range Investigation Mappings and Predictions Project (CLIMAP) used oxygen-isotope signals to determine the level of the most recent ice-sheet maximum and to reconstruct global ocean temperatures during the last ice age (*1*).

During this time, Nick also collaborated with Jim Hays and John Imbrie to evaluate the Milankovitch hypothesis of orbital control of ice sheets (*2*). They found prominent oxygen-isotopic (ice-volume) variations at the 41,000-year and 23,000-year orbital periods, with both signals lagging several thousand years behind changes in Northern Hemisphere summer insolation. This forcing-and-response relationship confirmed predictions made decades earlier by Milankovitch. In the 1980s, John Imbrie, Nick, and the Spectral Analysis and Mapping Project (SPECMAP) created a marine time scale based on the assumption that ice sheets (oxygen-isotope values) lag systematically behind driving changes in summer insolation (*3*). That time scale is still in use.

Unexpectedly, the strongest oxygen-isotopic changes occurred in a band centered near 100,000 years. Nick and paleomagnetics expert Neil Opdyke showed that this ice-volume response first emerged some 900,000 years ago (*4*). Nick was still working on this "100k problem" in recent years, but it remains unsolved.

CREDIT: ANDRE BERGER/UNIVERSITÉ CATHOLIQUE DE LOUVAIN, BELGIUM

With the acquisition of long-undisturbed cores from deep-ocean drilling in the 1980s, Nick reconstructed the full history of Northern Hemisphere ice ages. He showed that major glaciations began near 2.5 million years ago, with dozens of ice-age cycles since that time (*5*). Textbooks of this era were still claiming that only four or five glaciations had occurred, on the basis of fragmentary evidence from land-based sequences.

In the late 1980s, Nick's attention turned to carbon isotopes, where he again made fundamental contributions. He compared ^{13}C records from planktonic foraminifera from different depths to determine the amount of "bio-pumping" of ^{12}C-rich carbon from the surface to the deep ocean; he used ^{13}C values in benthic foraminifera as an index of deep-circulation changes in the world's oceans; and he measured $\delta^{13}C$ in bulk carbonate to estimate the long-term balance between burial of organic carbon and inorganic carbonate (*6*–*8*).

Much of Nick's recent attention had focused on improving the geologic time scale by tuning isotopic (and other) marine records to astronomically dated signals of incoming solar radiation. An initial collaboration with Andre Berger and Richard Peltier in the late 1980s led to the radical-sounding suggestion that the potassium/argon ages of magnetic reversal boundaries during the last 2 million years were too young by several percent (*9*). Geochemists soon found evidence of systematic argon loss that convinced them that Nick's time scale must be correct. During the past 15 years, Nick and other groups have gradually pushed the tuning method back millions of years in time. Who could have imagined decades ago that cycles recorded in marine cores would become the definitive way to date the younger geologic record?

Several aspects of Nick's scientific style and modus operandi stand out in my mind. Once having chosen a new problem to explore, he forged well-chosen alliances to figure out which sediment core was best for his purposes. Invariably, he made the optimal decision and wrote the definitive paper. He also liked to take strong positions in his talks, often proposing that a particular factor was primary in a causal sense and that others could be ignored. Over the years, his designations of which factors were "primary" versus "secondary" sometimes varied, because he preferred stimulating debate more than holding to a strict consistency. Such was his reputation that he was rarely challenged, probably to his disappointment. Even in appearance, Nick was one of a kind. Not many men grew their hair so long and unstyled over four decades, nor did many favor muttonchops for facial hair. And no one else wore sandals at all times, even in subfreezing weather.

When Nick Shackleton began his research, the investigation of past climatic changes was an area of "academic" interest only. Four decades later, his lifetime achievements define the emergence of our understanding of the operation of Earth's natural climate system. This understanding of the past is now central to efforts to predict the future climate we have begun to create.

The author is in the Department of Environmental Sciences, University of Virginia, Charlottesville, VA 22904, USA. E-mail: wfr5c@virginia.edu

References

1. CLIMAP project members, Map Chart Series MC-36 (Geological Society of America, Boulder, CO, 1981).
2. J. D. Hays, J. Imbrie, N. J. Shackleton, *Science* **194**, 1121 (1976).
3. J. Imbrie *et al.*, in *Milankovitch and Climate*, A. L. Berger *et al.*, Eds. (Reidel, Dordrecht, Netherlands, 1984), part 1, pp. 269–305.
4. N. J. Shackleton, N. D. Opdyke, in *Investigation of Late Quaternary Paleoceanography and Paleoclimatology Memoir 145*, R. M. Cline, J. D. Hays, Eds. (Geological Society of America, Boulder, CO, 1976), pp. 449–464.
5. J. Imbrie *et al.*, *Paleoceanography* **7**, 701 (1992).
6. N. J. Shackleton, N. G. Pisias, in *The Carbon Cycle and Atmospheric CO_2: Natural Variations, Archean to Present*, E. T. Sundquist, W. S. Broecker, Eds. (American Geophysical Union, Washington, DC, 1985), pp. 303–317.
7. M. E. Raymo, W. F. Ruddiman, N. J. Shackleton, D. W. Oppo, *Earth Planet. Sci. Lett.* **97**, 353 (1990).
8. N. J. Shackleton, in *The Carbon Cycle and Atmospheric CO_2: Natural Variations, Archean to Present*, E. T. Sundquist, W. S. Broecker, Eds. (American Geophysical Union, Washington, DC, 1985), pp. 412–417.
9. N. J. Shackleton, A. Berger, W. R. Peltier, *Trans. R. Soc. Edinb. Earth Sci.* **81**, 251 (1990).

10.1126/science.1126255

Genome-Wide Association Studies: Design and Analysis
An International Colloquium

October 26-27, 2006
New Haven, CT

Genome-wide association studies are increasingly utilized but with little consensus on optimal research design and analysis strategies. These studies include large arrays of candidate genes as well as hypothesis-free strategies involving several hundred thousand polymorphisms. Critical and sometimes controversial issues in designing and analyzing both types of study will be examined. The conference also explores novel technological developments that make genome-wide studies possible and population genetics that must be considered for proper interpretation. These issues will be discussed in the context of ongoing genome-wide association studies.

Conference Chairs
Michael B. Bracken, PhD - Yale University
Hongyu Zhao, PhD - Yale University

For more information or to register for the conference, please visit our website at http://cme.yale.edu/conferences/genome
You can also contact Yale CME at cme@yale.edu or 203.785.4578

Environmental Monitoring by Wireless Communication Networks

Hagit Messer,[1]* Artem Zinevich,[2] Pinhas Alpert[3]

High-resolution, continuous, accurate monitoring of the environment is of great importance for many applications—from weather forecasting to pollution regulation. We propose to use measurements from existing wireless communication networks for environmental studies, complementing existing monitoring systems such as weather radars. Weather, atmospheric conditions, and constituents cause propagation impairments on radio links. As such, similar to global positioning systems (GPS) (*1*), cellular networks provide built-in monitoring facilities and can be considered as a widely distributed, high-resolution atmospheric observation network, operating in real time with minimum supervision and without additional cost.

Meteorological monitoring of rainfall by radar is less accurate at surface levels (*2*), whereas rain gauges, although quite accurate, are expensive and do not provide sufficient spatial resolution. We demonstrate the feasibility of environmental monitoring with wireless communication networks by estimating the surface rainfall using standard data collected from a cellular network, and show its improved accuracy compared with radar-based estimates.

There are a variety of wireless communication systems, and we focus on the digital fixed radio systems (DFRS) that have a number of useful properties: They work at up to a few tens of meters above the ground, they operate at frequencies of tens of GHz, and they are impaired mainly by near-surface precipitation. DFRS have already established themselves as the premier cellular backhaul technology in Europe and Asia, accounting for the majority of cellular base-station connections.

The years of research by telecommunication specialists (*3*) generated tools for modeling and interpretation of atmosphere-induced impairments on radio links. The rain attenuation depends on the size and distribution of the water droplets. There are several models relating the attenuation rate A (given in dB/km) with the rain intensity. The common approach is a power law model for the attenuation, $A = aR^b$, where R is the rain rate and the constants a and b are functions of frequency and polarization. Given measurements of the received signal level (RSL), we estimated the rain-induced attenuation A, and then the average rainfall rate over each time frame (*4*).

Based on the data collected every 15 min from a few DFRS cellular backhaul links during a rain event in Israel in January 2005, we have estimated local rainfall. Figure 1 compares the rainfall estimates from the cellular backhauls, from radar, and from rain gauges. The skill of our method (correlation with rain gauges) is 0.86 for a 15-min-interval rain intensity and 0.9 for an hourly interval, versus 0.81 and 0.85, respectively, for radar, when evaluated from the maximal value over a 3 × 7 km^2 area. However, the corresponding correlation values from the literature at 3-km gauge-separation distance with radar are 0.59 and 0.71, respectively (*5*).

The density of the DFRS cellular backhaul links, according to the data from one Israeli cellular provider, varies in average from 3 links per km^2 to 0.3 links per km^2 in urban areas, and is less in suburban and rural areas. That allows, for example, the creation of rainfall intensity maps at an average spatial resolution of 1 to 3 km, using tomographic reconstruction.

Our results suggest that cellular rainfall measurements have features in between those of gauges and of radar. Cellular measurement can either replace existing techniques or colaborate with them to achieve better performance. However, the potential of the cellular environmental monitoring is not limited to rainfall measurements. Solid particles, fog, snow, sleet, and hail can be detected by microwaves. In particular, the capabilities of cellular networks (measuring of the refraction index of the atmosphere) may provide valuable facilities for studying water vapor, which plays a key role in weather and the global climate system.

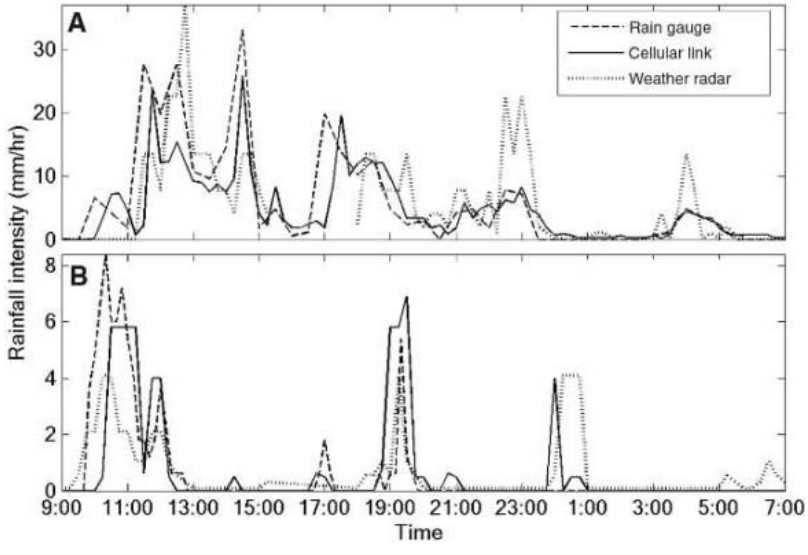

Fig. 1. Comparison of the time series of rainfall intensity measured by cellular links, rain gauges, and a weather radar, in two areas in Israel: (**A**) Tel-Aviv and (**B**) Haifa. The rainfall event was observed on 19 to 20 January 2005. The location of the radar is given in Movie S1. The rain gauges work at temporal resolutions of 30 min (A) and 10 min (B), whereas the wireless links provide measurements every 15 min. Temporal lags between the cellular data and the rain gauges are partly due to differences in locations of the links and the rain gauges (they are separated in space by about 2 km). Disparities, such as time lags, are also caused by the different nature of observations, i.e., line-integrated data in the cellular links versus point measurements in the rain gauges.

References and Notes

1. M. Bevis *et al.*, *J. Geophys. Res.* **97**, 15787 (1992).
2. S. Raghavan, *Radar Meteorology* (Kluwer, London, 2003).
3. ITU-R P. 530-7 (International Telecommunication Union Radiocommunication Bureau Propagation Recommendation).
4. Materials and methods are available as supporting material on *Science* Online.
5. E. Morin, *J. Hydrometeorology* **4**, 782 (2003).
6. We deeply thank S. Mouallem and H. Pistiner (Cellcom) for their cooperation and for providing the cellular data. We also thank Y. Levy (Shacham/Mekorot) for radar data and A. Arie (Meteo-Tech), A. Stupp (Tel-Aviv University), and H. Kutiel (Haifa University) for rain gauge data.

Supporting Online Material

www.sciencemag.org/cgi/content/full/312/5774/713/DC1
Materials and Methods
Table S1
References
Movie S1

12 September 2005; accepted 27 March 2006
10.1126/science.1120034

[1]School of Electrical Engineering, [2]The Porter School of Environmental Studies, [3]Department of Geophysics and Planetary Sciences, Tel-Aviv University, 69978 Tel-Aviv, Israel.

Catalytic Production of Olefin Block Copolymers via Chain Shuttling Polymerization

Daniel J. Arriola,[1]* Edmund M. Carnahan,[2]* Phillip D. Hustad,[2]* Roger L. Kuhlman,[2]* Timothy T. Wenzel[1]*

We report a catalytic system that produces olefin block copolymers with alternating semicrystalline and amorphous segments, achieved by varying the ratio of α-olefin to ethylene in the two types of blocks. The system uses a chain shuttling agent to transfer growing chains between two distinct catalysts with different monomer selectivities in a single polymerization reactor. The block copolymers simultaneously have high melting temperatures and low glass transition temperatures, and therefore they maintain excellent elastomeric properties at high temperatures. Furthermore, the materials are effectively produced in economically favorable, continuous polymerization processes.

During the past 50 years, polyolefins have become, by far, the highest volume commercial class of synthetic polymers. Olefin polymerization catalysts have evolved during this time from heterogeneous mixtures (*1*) to well-defined soluble molecules (*2*), allowing chemists to understand and control the effects of catalyst structure on polymer composition and microstructure. These advancements in catalysis have enabled the production of polyolefins with an exquisite degree of control over stereochemistry (*3*) and macromolecular branch architecture (*4*), leading to new classes of polymers with useful combinations of physical properties. However, the economical preparation of olefin block copolymers (*5*) having both "hard" (semicrystalline or high glass transition temperature) and "soft" (amorphous and low glass transition temperature) segments remains one of the major challenges in the field of polymerization catalysis. Here we report a method for the preparation of linear ethylene-based block copolymers with such properties by using chain shuttling polymerization.

A few strategies for preparation of stereoblock polyolefins have been reported in the recent literature (*6*–*9*). Despite the high melting temperatures exhibited by isotactic or syndiotactic polypropylenes (PPs), the relatively high glass transition temperatures of these materials ($T_g \sim 0$°C) limit their utility in elastomeric applications. More recently, olefin-based block copolymers have been made using living coordination polymerization catalysts (*10*). These catalysts, like living anionic (*11*), cationic (*12*), or radical (*13*–*15*) polymerization processes, can be used to achieve precise structural control in block copolymer synthesis through sequential monomer addition strategies. However, living polymerization processes are uneconomical because they produce only one polymer chain per catalyst molecule and operate in a batch polymerization process. In addition, the low reaction temperatures typically required to achieve living behavior with these systems inhibit the synthesis of materials containing more than one semicrystalline block because of premature precipitation of the polymer.

To circumvent the problems associated with previous strategies for the preparation of polyolefin block copolymers, we pursued the synthesis of these materials via a technique that we call "chain shuttling polymerization" (*16*). We define chain shuttling as the passing of a growing polymer chain between catalyst sites, such that portions of a single polymer molecule are synthesized by at least two different catalysts. Likewise, a chain shuttling agent (CSA) is a component such as a metal alkyl complex that facilitates this transfer. This approach can thus be used to prepare block copolymers from a common monomer environment by using a mixture of catalysts of different selectivities, namely stereoselectivity or monomer selectivity. Under the right conditions, efficient chain shuttling produces a linear multiblock copolymer that features alternating hard and soft blocks.

One key to forming differentiated block copolymers via chain shuttling is finding a monomer or combination of monomers that, on the basis of their arrangement in the polymer chain, can give rise to both hard and soft materials. Stereoblock PPs do not have the low glass transition temperatures required for most elastomeric applications. On the other hand, ethylene-based polymers that incorporate varying fractions of α-olefin fit this criterion. Polyethylenes (PE) with low co-monomer content are semicrystalline (hard) materials with melting temperatures (T_m) approaching 135°C, whereas PEs with high levels of comonomer are amorphous (soft) materials with very low glass transition temperatures ($T_g <$ –40°C). We therefore focused on ethylene-based block copolymers with both hard and soft segments, with the hypothesis that the benefits of both the high T_m and low T_g would be retained. To this end, we required a mixed catalyst system capable of producing these different types of polymer in a common reaction environment. A further important requirement is that each of the catalysts undergoes chain shuttling with a common chain shuttling agent.

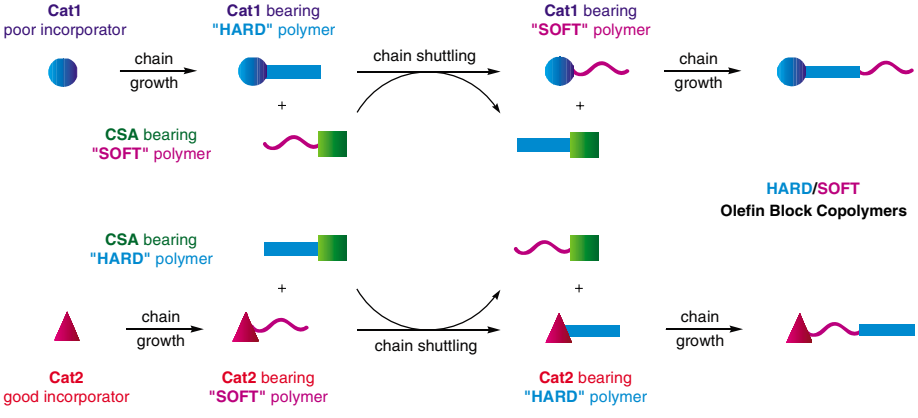

Fig. 1. Depiction of the likely chain shuttling mechanism in a single reactor, dual-catalyst approach. Cat1 (solid circles) and Cat2 (solid triangles) represent catalysts with high and low monomer selectivity, respectively, whereas the CSA (solid squares) facilitates the chain shuttling reaction. Cat1 produces a segment of hard polymer with low comonomer content. Shuttling occurs when this segment is exchanged with the CSA bearing a soft copolymer of higher comonomer content. Further chain growth at Cat1 then extends the soft copolymer chain with a hard segment, thus giving a block copolymer.

[1]The Dow Chemical Company, Building 1702, Midland, MI 48674, USA. [2]The Dow Chemical Company, 2301 Brazosport, Freeport, TX 77541, USA.

*To whom correspondence should be addressed. E-mail: djarriola@dow.com (D.J.A.); ecarnahan@dow.com (E.M.C.); pdhustad@dow.com (P.D.H.); kuhlmarl@dow.com (R.L.K.); wenzeltt@dow.com (T.T.W.)

This process (Fig. 1) requires one catalyst, Cat1, with high ethylene selectivity to form hard polymer chains. Meanwhile, a good incorporator of comonomer, Cat2, grows soft amorphous chains in the same reactor because of its dramatically different monomer selectivity. In the absence of chain shuttling, a polymer blend is produced with none of the advantageous properties of block copolymer architecture. In the presence of an effective CSA, however, polymer chains are swapped between catalysts before the chains terminate. To understand this swapping phenomenon, it is instructive to follow the lifetime of a representative polymer chain. The chain may begin growing on Cat1 as a hard polymer. The chain is then exchanged onto a CSA, where it is held for some period of time without growing. The dormant polymer chain may then return to another molecule of the same catalyst and lengthen the hard segment or it may shuttle to a molecule of Cat2, from which subsequent chain growth results in formation of a polymer chain with both soft and hard blocks. The process may be repeated any number of times during the lifetime of the chain before chain termination occurs via a usual mechanism such as hydrogenolysis. A statistical analysis of this chain shuttling phenomenon reveals multiblock copolymers with a most probable distribution of block lengths and number of blocks per chain. This microstructure is distinctly different from materials made with living polymerization techniques, which ideally have a Poisson distribution of block lengths and a precise number of blocks. Furthermore, the synthesis of these olefin block copolymers is not stoichiometrically limited by Cat1, Cat2, or CSA.

Furthermore, this approach enables precise control over polymer microstructure. Despite the differences in monomer selectivity between the two catalysts, fast rates of chain shuttling and judicious selection of process variables produce copolymers with homogeneous molecular weight and composition distributions. The overall composition, i.e., the hard-to-soft polymer ratio, can be easily controlled by the relative amount of the catalysts used. The comonomer content of the individual hard and soft blocks can be tailored by reactor feed or catalyst modifications. Finally, the average length of the blocks, which is a function of the relative rates of chain growth and shuttling, can be controlled simply by adjusting the ratio of concentrations of CSA and monomer ([CSA]/[C_2H_4]).

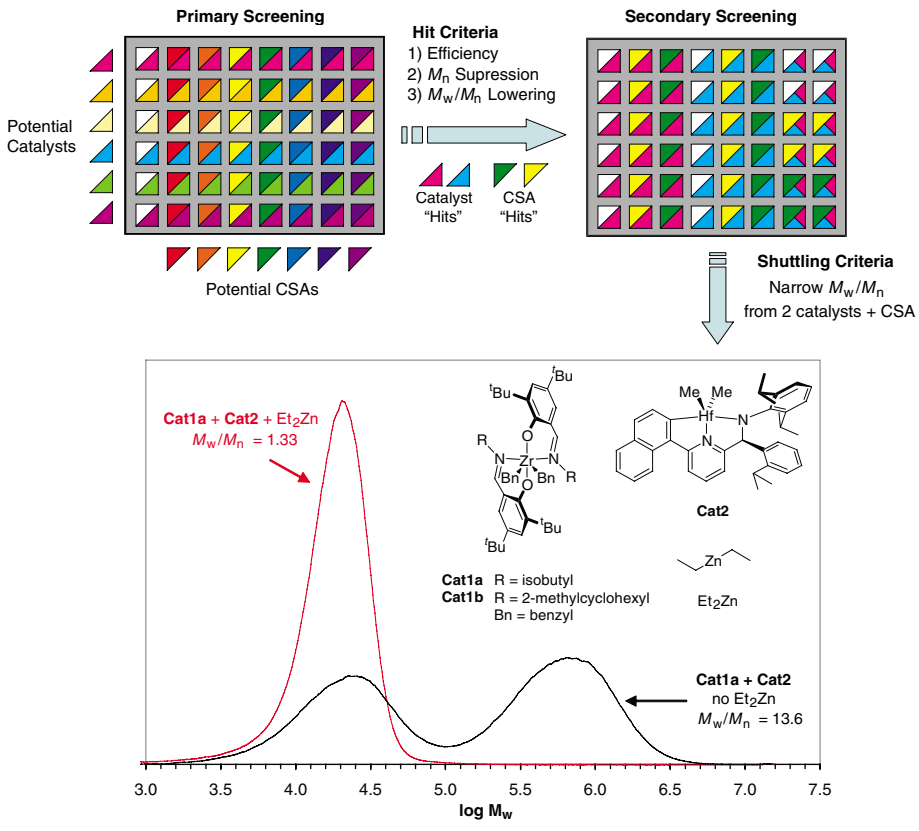

Fig. 2. High-throughput screening protocol and selected data from the chain shuttling screen. Polymerizations are conducted in a parallel grid of individual computer-controlled reactors with robotic addition of reagents and real-time monitoring, coupled with high-throughput characterization techniques. Primary screening involves a broad screen of several catalysts in combination with many potential shuttling agents. Combinations that result in good efficiency, lower molecular weight (M_n), and narrower molecular weight distribution (M_w/M_n), are considered hits. These hits are then subjected to a secondary screen, including individual catalyst and dual-catalyst/CSA combinations. Structures of **Cat1a**, **Cat1b**, **Cat2**, and the CSA are depicted. Shuttling for this trio is demonstrated by the coalescence of the bimodal molecular weight distribution by adding Et_2Zn to the dual-catalyst system.

Selection of CSA and catalysts. It is well established in olefin polymerization that growing chains can be transferred from the catalyst to an added main-group metal in exchange for an alkyl group (i.e., chain transfer to metal) (*1*, *17*). This transfer is most often irreversible, leading to the termination of the growing chain and the initiation of a new polymer chain. However, the synthesis of block copolymers via chain shuttling requires this polymer chain transfer to be reversible. The main-group centers cannot act as a final repository for "dead" polymer chains; instead, they must serve as a reservoir of "live" chains that are intermittently reattached to catalyst centers for further growth. Chien (*7*) and Brintzinger (*8*) have independently claimed preparations of stereoblock PPs using reversible chain transfer between two catalyst centers with different stereoselectivities. However, polymer fractionation revealed that the samples were largely blends of isotactic and atactic PPs, with at most a small fraction of block copolymer. For single-catalyst systems, this process has been used to prepare long-chain metal alkyls (*18*–*22*) and has more recently been described as "catalyzed chain growth" (*23*, *24*). Gibson *et al*. have discussed the effects of catalyzed chain growth on molecular weight distribution, reporting that a Poisson distribution of molecular weights (M_w/M_n = 1, where M_w is the weight-average molecular weight and M_n is the number-average molecular weight) is expected under these conditions instead of the Schulz-Flory distribution (M_w/M_n = 2), observed when chain termination occurs (*24*). This behavior provides an easy means of probing the capabilities of a catalyst system for chain shuttling polymerization.

Given the multitude of olefin polymerization catalysts, it was daunting to identify a pair of catalysts with substantially different monomer selectivities that are also capable of chain shuttling. Furthermore, the chosen system also needs to operate at a high solution-reaction temperature ($T \geq 120$°C) to prevent undesired polymer precipitation. We therefore adopted a high-throughput method to expedite this discovery process. The technique uses a parallel screen of the effects of metal alkyl reagents on the molecular weight and molecular weight distributions of polyethylenes produced by catalyst/CSA combinations. These criteria provide a simple test for finding catalyst/CSA combinations suitable for use in our dual-catalyst system (Fig. 2).

To begin the selection process, we first selected representative examples from a broad variety of catalyst structure types known to have high polymerization rates. Two examples are shown in Fig. 2. Ethylene polymerizations were then carried out with these catalysts, in combi-

nation with a number of potential CSAs using high-throughput screening techniques (*25*). By using an array of robotically manipulated individual polymerization reactors combined with rapid polymer characterization methods, we conducted and evaluated more than 1600 individual polymerizations over a three-week period, a feat that would have taken several months using conventional techniques.

Catalyst efficiency, estimated by polymer yield, eliminated several of the potential CSAs due to their inhibition of polymerization. For those combinations that produced a sufficient amount of polymer for characterization, the molecular weight and molecular weight distribution of the polyethylene were then compared with a control polymer prepared with no added CSA (*26*). A reduction in M_n in combination with a narrowing of the molecular weight distribution (M_w/M_n) indicated a "hit" for chain shuttling behavior (*27*). A zirconium bis(phenoxyimine) catalyst (*28*), **Cat1a**, and a hafnium pyridylamide (*29*), **Cat2**, displayed significant differences in monomer selectivity and also showed characteristics of chain shuttling by using diethylzinc (Et_2Zn) as the CSA. Similar bis(phenoxyimine) catalysts have also been shown to exhibit characteristics of catalyzed chain growth (*30*). Also, whereas catalyzed chain growth on aluminum and magnesium has been well-documented, only recently has this phenomenon been claimed to occur on zinc (*23*, *24*, *30*).

After this dual-catalyst/CSA combination was identified, a secondary screening process was conducted to further validate the shuttling capability of these hits. This process involved evaluation of both individual catalyst/CSA combinations, as well as mixed catalyst experiments in the high-throughput reactor. Individual catalysts were screened to evaluate the effect of different catalyst/CSA ratios on M_n and M_w/M_n. Dual-catalyst experiments provided further confirmation of the shuttling behavior of this system. A mixture of **Cat1a** and **Cat2** produced a copolymer with a 1-octene content intermediate between those afforded by the individual catalysts, indicating that both catalysts were active in the polymerization. The copolymer had a high molecular weight (M_w = 446,000 g/mol) and a broad, bimodal molecular weight distribution (M_w/M_n = 13.6), indicating a large difference in propensities of the two catalysts for chain termination or transfer (Fig. 2). Introduction of Et_2Zn as the CSA resulted in the formation of copolymers with lower molecular weight and extremely narrow molecular weight distributions. The addition of 50 equivalents of Et_2Zn to the total catalyst metal in the mixed catalyst system gave a copolymer with M_w = 20,300 g/mol and M_w/M_n = 1.33. The resulting copolymer was again of intermediate comonomer composition, indicating that both catalysts were active. This observation of a very narrow molecular weight distribution copolymer produced by a mixture of catalysts with drastically different molecular weight capability and monomer selectivity indicates fast rates of chain shuttling with this dual-catalyst CSA system.

Although the initial dual-catalyst system met all the necessary requirements for production of olefin block copolymers, we decided to screen a small library of bis(phenoxyimine) catalysts in an attempt to increase the difference in monomer selectivities in our dual-catalyst system. A similar high-throughput screening approach allowed us to quickly evaluate these new catalysts for ethylene selectivity and chain shuttling characteristics. A simple replacement of the isobutyl substituent on the ligand of **Cat1a** with a 2-methylcyclohexyl moiety resulted in a catalyst, **Cat1b**, with higher molecular weight and ethylene selectivity and much stronger chain-shuttling response in the presence of Et_2Zn (*26*). We therefore decided to conduct dual-catalyst block copolymer synthesis with the combination of **Cat1b**, **Cat2**, and Et_2Zn.

Olefin block copolymers in a continuous process. The dual-catalyst process described above can be conducted in either a batch or in a continuous-polymerization reactor (*31*), but there are marked differences between the two. First, the catalyst onset and decay profiles are not an issue in a continuous process, because catalysts are continuously supplied and removed to give steady-state concentrations. In contrast, different catalyst deactivation rates in a batch system can lead to polymer inhomogeneities. For example, if Cat2 dies faster than Cat1, the total polymer may contain whole chains of hard polyethylene.

A second, more subtle difference is that shuttling occurs more efficiently in a continuous process. Typical CSAs begin as simple metal alkyl species such as Et_2Zn. The initial chain-transfer event with Et_2Zn involves exchange of an ethyl moiety for a polymer chain, which initiates growth of a new polymer chain but does not produce any polymer blockiness. Statistically, this event predominates over chain shuttling early in the course of the reaction. Only later in the reaction is the concentration of zinc-polymeryl species sufficient to enable true chain shuttling. In a continuous process, the reactor is populated with a steady-state concentration of these zinc-polymeryl species. Because the volume of the reactor is large compared with the volume of the continuous feed, the ratio of zinc-polymeryl species to fresh Et_2Zn is very high. Thus, polymeryl interchange predominates over ethyl-for-polymeryl exchange. In addition, the zinc alkyl compounds exhibit higher thermal stability than many catalysts. At high reactor temperatures, catalyst molecules often deactivate before exiting, but the zinc species continue to participate in chain shuttling throughout their entire residence time.

Operating an efficient chain shuttling system in a continuous process also affects the molecular weight distribution of the resulting copolymer. Extremely narrow molecular weight distributions can be achieved with fast chain shuttling between two different catalysts in a batch process. However, the same chemistry in a continuous process results in a Schulz-Flory molecular weight distribution simply because there is a distribution of residence times in a continuously-fed reactor (*32*). This feature is beneficial, because copolymers with broader distributions of molecular weights are typically easier to process.

To realize the full potential of chain-shuttling polymerization for making ethylene-based block copolymers, experiments were conducted with this dual-catalyst chain shuttling system in a continuous solution polymerization reactor. A series of ethylene-octene copolymers of similar melt index (i.e., molecular weight) were produced with a composition of ~30 weight percent (wt %) hard blocks and 70 wt % soft blocks. The level of Et_2Zn, reported in Table 1 as a $[Zn]/[C_2H_4]$ molar ratio, was

Table 1. Process details and properties of ethylene-octene block copolymers from the chain shuttling system in a continuous process.

Sample	Description	Catalyst package	$[Zn]/[C_2H_4]$* ($\times 10^3$)	Density (g/cm^3)	Efficiency (kgP/gM)	M_w† (g/mol)	M_w/M_n†	Chains per Zn‡	Chains per (Hf + Zr)‡	T_m§ (°C)	ΔH_f§ (J/g)
1	Soft PE	Cat2 + Et_2Zn	1.87	0.862	95.2	110,000	1.97	2.7	230	37	32
2	Hard PE	Cat1b + Et_2Zn	2.07	0.938	127	65,000	1.95	4.6	2,200	124	184
3	Blend	Cat1b + Cat2	–	0.890	258	137,300	13.8	–	3,600	125	90
4	Low CSA	Cat1b + Cat2 + Et_2Zn	0.56	0.883	261	129,000	3.22	12	820	124	68
5	Mid CSA	Cat1b + Cat2 + Et_2Zn	1.40	0.883	244	118,500	2.23	3.6	630	121	69
6	High CSA	Cat1b + Cat2 + Et_2Zn	2.39	0.879	118	104,600	1.97	1.9	260	120	60

*The $[Zn]/[C_2H_4]$ ratio is defined as the molar ratio of CSA to ethylene in the reactor. †Determined by GPC relative to polystyrene standards. ‡Chains per Zn was calculated by using the zinc feed and polymer production rates and the number-average molecular weight of the resulting copolymer corrected for comonomer content. Similarly, chains per (Hf + Zr) was estimated by using the total catalyst metal feed. §Melting point (T_m) and heat of fusion (ΔH_f) were determined by differential scanning calorimetry (DSC).

systematically varied to study the effects of the ratio on polymer microstructure.

The set of experiments was begun with only **Cat2** to produce a copolymer with a density of 0.862 g/cm^3 by adjusting monomer feed rates and catalyst and cocatalyst flows (*26*). Molecular weight control was achieved with a mixture of Et_2Zn and hydrogen, which were adjusted to reach a M_w of 110,000 g/mol (sample 1). **Cat2** feed was then stopped, and **Cat1b** was introduced to the reactor under identical reactor conditions. The higher ethylene selectivity of this catalyst resulted in an increase in the measured polymer density to 0.936 g/cm^3. The large difference in comonomer content between these two copolymers, made under similar reaction conditions, demonstrates the substantial difference in the monomer selectivity of the two catalysts. The molecular weight of this hard comonomer–poor material was also much lower, indicative of faster chain termination (primarily by reaction with H_2) for this catalyst system. Et_2Zn feed was maintained, but some hydrogen was removed to give a polymer with M_w = 65,000 g/mol (sample 2).

These two baseline polymerizations provided an estimate of the catalyst ratio necessary to achieve the desired composition for the dual-catalyst product; an overall density of ~0.88 g/cm^3 was targeted to give the desired copolymer composed of 30% high-density material (*33*). As a control, a mixture of **Cat1b** and **Cat2** was added to the reactor under the same process conditions with no Et_2Zn, giving a reactor blend of the two component copolymers with an overall density of 0.89 g/cm^3. Hydrogen was added to give a polymer with M_w = 137,300 g/mol (sample 3), which was a simple blend of hard and soft PE made independently by the two catalysts. Et_2Zn was then added to induce chain shuttling between the two catalysts. Products were produced at three different levels of blockiness, controlled by the ratio of concentrations of Et_2Zn to ethylene ($[Zn]/[C_2H_4]$). Sample 6 was made with the highest Et_2Zn level possible, while still achieving the desired molecular weight.

Characterization of block copolymers. During this set of experiments, it was apparent by eye that this dual-catalyst chain shuttling system was producing desirable block copolymers at higher CSA levels. Physical blends of high-density and linear low-density PE are opaque because of the large high-density PE crystallites and the immiscibility of the two copolymers. However, the copolymers made at higher $[Zn]/[C_2H_4]$ ratios are surprisingly transparent, despite having essentially identical octene content (Fig. 3). This difference is a clear indication that the copolymers produced with Et_2Zn have a very different microstructure than the physical blend of sample 3. We attribute the enhanced clarity to a decrease in crystallite size of the high-density blocks when the average block length is shorter.

From gel permeation chromatography (GPC), we found that the copolymer prepared without Et_2Zn was clearly bimodal, with M_w/M_n = 13.8 (Fig. 4). The GPC trace was deconvoluted into components of M_w ~ 240,000 and ~9600 g/mol, with the high–molecular weight, low-density copolymer making up 64 wt % of the overall material. This large molecular weight split reflects the differing propensities for hydrogen-induced termination between the two catalysts. The molecular weight distribution narrows as Et_2Zn is added, as expected for an efficient chain shuttling polymerization. At the highest Et_2Zn level, a most probable molecular weight distribution (M_w/M_n = 1.97) is obtained (sample 6). This narrow molecular weight distribution is normally associated with a single catalytic species and is indicative of the multiblock nature of the copolymer, because several shuttling events are required to generate such a homogeneous molecular weight distribution.

This molecular weight response clearly indicates that chain-shuttled ethylene-octene block copolymers, rather than blends, are formed upon introduction of Et_2Zn. The M_n can also be used in conjunction with the Et_2Zn feed and polymerization rate to calculate the number of chains produced per Zn molecule. The low Et_2Zn level of sample 4 results in the production of approximately 12 chains per Zn. However, the reaction is practically stoichiometric at higher Et_2Zn (no H_2), with the production of sample 6 resulting in 1.9 chains per Zn (or ~1 chain per Zn-alkyl moiety). This result indicates that almost every polymer chain exits the reactor bound to the CSA with very little chain termination, demonstrating the efficiency of the chain shuttling reaction.

Despite the stoichiometric nature of the reaction with the CSA, a similar calculation of the number of chains per catalyst molecule reveals that the polymerization is highly catalytic in the hafnium and zirconium species. Block copolymers produced with living polymerization techniques are inherently expensive, because the living nature of the polymerization makes it necessary to use one molecule of catalyst for each chain produced. In contrast, the chain shuttling methodology is capable of generating hundreds to thousands of olefin block copolymer chains per catalyst. For example, the synthesis of sample 6 resulted in the formation of ~260 chains per total catalyst. This feature allows these olefin block copolymers to be produced far more cheaply than materials available from living polymerization techniques.

Fig. 3. Image of compression-molded samples (thickness = 0.35 mm), illustrating the effect of chain shuttling on clarity. Sample 3 is a physical blend of high- and low-density polymer and is opaque. Adding Et_2Zn during polymerization results in a block copolymer microstructure with intimately mixed interchain hard and soft segments, resulting in the increased transparency of samples 4 to 6.

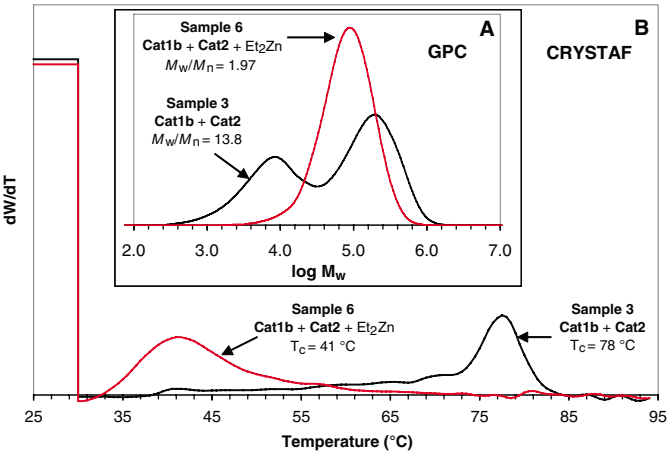

Fig. 4. Characterization of copolymers produced with the dual-catalyst chain shuttling system in a continuous process. Samples 3 (**Cat1b** + **Cat2**) and 6 (**Cat1b** + **Cat2** + CSA) are depicted. (**A**) GPC reveals a bimodal molecular weight distribution in the absence of CSA, whereas adding CSA homogenizes the copolymer to a most probable distribution (M_w/M_n = 2). (**B**) Crystallinity distributions as revealed by crystallization analysis fractionation (CRYSTAF). Sample 3, prepared in the absence of CSA, displays a bimodal composition distribution with a peak around 78°C from **Cat1b** and an amorphous soluble fraction from **Cat2**. Adding CSA gives a copolymer that crystallizes from solution at a much lower temperature, with no indication of highly crystalline material.

The comonomer distributions of these new materials, as revealed by crystallization analysis fractionation (CRYSTAF), were also indicative of their homogeneous multiblock nature. As expected, the hard polymer from **Cat1b** crystallized from solution at ~80°C, whereas the soft copolymer from **Cat2** was completely soluble at the lowest temperature studied (30°C). Sample 3, prepared with both catalysts in the absence of a CSA, displayed behavior consistent with a physical blend of these two component copolymers (Fig. 4). The characteristic peak for the high density material at 80°C was completely absent for the dual-catalyst sample made at the highest Et_2Zn level (sample 6), and a new peak appeared at 41°C. A typical ethylene-octene random copolymer (RCP) with a density near 0.88 g/cm^3 was completely soluble in 1,2,4-trichlorobenzene at room temperature and eluted in the soluble fraction. A peak at 41°C would be expected for an RCP only if it were of considerably higher density (~0.90 g/cm^3). We attribute this unique crystallization behavior to the block copolymer microstructure, in which the amorphous domains disrupt the crystallization of the semicrystalline high-density segments.

The melting temperatures of these chain-shuttled copolymers were also indicative of their unusual microstructure. In polyethylene-based materials, comonomers such as butene and octene are introduced to disrupt crystallinity and to provide elasticity to the resulting polymer products. For common RCPs, both the melting point and modulus (hardness) are direct functions of the comonomer content (Fig. 5). It should be possible to break this longstanding product-property relationship by incorporating multiple regions of crystallizable and amorphous polymer segments in single polymer chains. This phenomenon is evident in the thermal characteristics of these copolymer samples. The hard polymer from **Cat1b** (sample 1) undergoes a sharp melting transition at 124°C, whereas the soft copolymer from **Cat2** (sample 2) displays a very weak melting peak at 37°C (Fig. 5). All of the chain-shuttled copolymers have melting peaks within a few degrees of the material produced by **Cat1b** alone (Fig. 5). As $[Zn]/[C_2H_4]$ is increased, the T_m decreases slightly, dropping to 120°C at the highest CSA level examined. We hypothesize that this decrease in T_m is related to the length of the hard blocks, which become shorter as more CSA is added (*34*). More importantly, these materials display excellent elastomeric properties at temperatures far higher than those of traditional RCPs of similar density, allowing these olefin block copolymers to be used in high-temperature applications.

Outlook. The economical production of olefin block copolymers has been a goal of academic researchers and polymer manufacturers alike. Tremendous progress toward this end has been achieved in recent years with the discovery of several designer catalysts capable of living olefin polymerization. However, the stoichiometric nature of the living process, coupled with related process limitations of low polymerization temperatures and slow batch processes, have prevented these approaches from achieving widespread application. The chain shuttling system described above overcomes these challenges, providing an economical means for production of polyolefins that display advantaged combinations of physical properties. The statistical multiblock architecture afforded by the chain shuttling process, with its distribution of block lengths and number of blocks per chain, is not easily accessible by any other means. The olefin block copolymers maintain excellent elastomeric properties at temperatures far higher than traditional ethylene-based elastomers (*35*), allowing them to be used in high-performance applications long inaccessible to polyolefins.

Although this technology introduces a solution to a long-standing challenge, it also poses several new questions. We anticipate future efforts will lead to further elucidation of the kinetic and mechanistic intricacies of chain-shuttling reactions, discoveries of catalysts with improved performance, and application of this technology to other polymer systems.

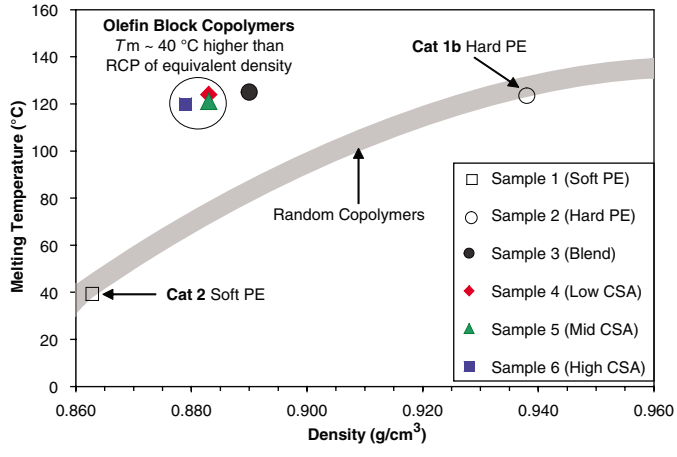

Fig. 5. Melting temperature of ethylene-octene copolymers as a function of density. Chain shuttled materials are compared to RCPs. A gray band representing ethylene-octene random copolymers and samples 1 (open squares), 2 (open circles), 3 (solid circles), 4 (solid diamonds), 5 (solid triangles), and 6 (solid squares) are displayed. Although the melting behavior of the copolymers from **Cat1b** and **Cat2** are similar to those of RCPs, the dual-catalyst chain-shuttled materials display melting temperatures >40°C higher than those of RCPs of equivalent density. The melting temperatures of the dual-catalyst samples decrease with increasing $[CSA]/[C_2H_4]$ ratio, indicative of shorter block lengths at higher CSA levels.

References and Notes

1. J. J. Boor, *Ziegler-Natta Catalysts and Polymerizations* (Academic, New York, 1979).
2. V. C. Gibson, S. K. Spitzmesser, *Chem. Rev.* **103**, 283 (2003).
3. G. W. Coates, *Chem. Rev.* **100**, 1223 (2000).
4. A. L. McKnight, R. M. Waymouth, *Chem. Rev.* **98**, 2587 (1998).
5. I. W. Hamley, *The Physics of Block Copolymers* (Oxford Univ. Press, Oxford, 1998).
6. G. W. Coates, R. M. Waymouth, *Science* **267**, 217 (1995).
7. J. C. W. Chien, Y. Iwamoto, M. D. Rausch, W. Wedler, H. H. Winter, *Macromolecules* **30**, 3447 (1997).
8. S. Lieber, H.-H. Brintzinger, *Macromolecules* **33**, 9192 (2000).
9. Y. Zhang, R. J. Keaton, L. R. Sita, *J. Am. Chem. Soc.* **125**, 9062 (2003).
10. Living or controlled olefin polymerization catalysis proceeds by rapid initiation without appreciable chain transfer or termination. For a recent review of this emerging field, see (*36*).
11. H. L. Hsieh, R. P. Quirk, Eds., *Anionic Polymerization: Principles and Practical Applications* (Marcel Dekker, New York, 1996).
12. K. Matyjaszewski, Ed., *Cationic Polymerizations: Mechanisms, Synthesis, and Applications* (Marcel Dekker, New York, 1996).
13. C. J. Hawker, A. W. Bosman, E. Harth, *Chem. Rev.* **101**, 3661 (2001).
14. M. Kamigaito, T. Ando, M. Sawamoto, *Chem. Rev.* **101**, 3689 (2001).
15. K. Matyjaszewski, J. H. Xia, *Chem. Rev.* **101**, 2921 (2001).
16. D. J. Arriola *et al.*, U.S. Patent Appl. 2005/090427 (2005).
17. G. Natta, I. Pasquon, *Advances in Catalysis and Related Subjects*, D. D. Eley, P. W. Selwood, Paul B. Weisz, Eds. (Academic Press Inc., vol. 11, issue 1, 1959).
18. E. G. Samsel, Patent EP 539876 (1993).
19. J.-F. Pelletier *et al.*, Patent EP 736536 (1996).
20. J.-F. Pelletier, A. Mortreux, X. Olonde, K. Bujadoux, *Angew. Chem. Int. Ed. Engl.* **35**, 1854 (1996).
21. S. Bogaert, T. Chenal, A. Mortreux, J.-F. Carpentier, *J. Mol. Cat. A: Chem.* **190**, 207 (2002).
22. E. G. Samsel, F. N. Brooks, U.S. Patent 6444867 (2002).
23. G. J. P. Britovsek, S. A. Cohen, V. C. Gibson, P. J. Maddox, M. Van Meurs, *Angew. Chem. Int. Ed. Engl.* **41**, 489 (2002).
24. G. J. P. Britovsek, S. A. Cohen, V. C. Gibson, M. VAN Meurs, *J. Am. Chem. Soc.* **126**, 10701 (2004).
25. V. Murphy *et al.*, *Chem. Rec.* **2**, 278 (2002).
26. Materials and methods are available as supporting material on *Science* Online.
27. We have found the molecular weight distribution of a polymer produced with a chain shuttling catalyst/CSA system to be highly dependent on reaction conditions.
28. H. Makio, N. Kashiwa, T. Fujita, *Adv. Synth. Catal.* **344**, 477 (2002).
29. K. A. Frazier, H. W. Boone, P. C. Vosejpka, J. C. Stevens, U.S. Patent Appl. 2004/0220050 A1 (2004).
30. M. Van Meurs, G. J. P. Britovsek, V. C. Gibson, S. A. Cohen, *J. Am. Chem. Soc.* **127**, 9913 (2005).
31. In a batch process, the reactor is charged with a batch of reagents and then the polymerization process is carried out. When the desired polymer is formed, it is removed and the next batch of feed is introduced. In contrast, continuous reactors process an uninterrupted feed stream. Continuous reactors are capable of handling high throughputs and are the most common reactor types in commercial polyolefin production.
32. N. A. Dotson, R. Galvan, R. L. Laurence, M. Tirrell, in *Polymerization Process Modeling, Advances in Interfacial Engineering Series.* (VCH Publishers, New York, 1996) p. 262.

33. The reciprocal density relationship $\rho = 1/(f_1/\rho_1 + f_2/\rho_2)$, where ρ is the density and f is the mass fraction, was used to estimate the resulting overall density of the desired polymer blend.
34. R. Furuyama *et al.*, *Macromolecules* **38**, 1546 (2005).
35. Preliminary studies have shown that these resins maintain some elastomeric properties at 70°C. More details of the high-temperature properties of these new copolymers with specific comparisons to similar block copolymer systems will be reported in the near future.
36. G. W. Coates, P. D. Hustad, S. Reinartz, *Angew. Chem. Int. Ed.* **41**, 2236 (2002).
37. We thank W. Cheung, D. Devore, L. Miller, B. Poon, C. Li Pi Shan, J. Stevens, P. Stirn, and J. Weinhold for helping to make this work possible.

Supporting Online Material
www.sciencemag.org/cgi/content/full/312/5774/714/DC1
Materials and Methods
Tables S1 and S2
References

23 January 2006; accepted 15 March 2006
10.1126/science.1125268

Producing Ultrastrong Magnetic Fields in Neutron Star Mergers

D. J. Price[1] and S. Rosswog[2]*

We report an extremely rapid mechanism for magnetic field amplification during the merger of a binary neutron star system. This has implications for the production of the short class of gamma-ray bursts, which recent observations suggest may originate in such mergers. In detailed magnetohydrodynamic simulations of the merger process, the fields are amplified by Kelvin-Helmholtz instabilities beyond magnetar field strength and may therefore represent the strongest magnetic fields in the universe. The amplification occurs in the shear layer that forms between the neutron stars and on a time scale of only 1 millisecond, that is, long before the remnant can collapse into a black hole.

The orbital decay of a neutron star binary system as a result of the emission of gravitational waves is one of the prime targets of gravitational wave detectors such as the Laser Interferometer Gravitational-Wave Observatory (*1*) or GEO600 (*2*). Moreover, the long-suspected connection of neutron star binaries to gamma-ray bursts (GRBs), the most luminous explosions in the universe, has received solid support from the first detections of afterglows from the short class of GRBs (*3*–*5*). Unlike their long-duration cousins (which are associated with the deaths of massive stars), short GRBs occur systematically at lower redshifts, in galaxies both with and without star formation, and are not accompanied by a supernova explosion. The millisecond variability observed in the light curves of short GRBs suggests that a compact object, either a neutron star or a stellar mass black hole, acts as the central engine.

The observed cosmological distances imply that large energies are involved; so, relativistic outflows with Lorentz factors of several hundreds are required to avoid the so-called "compactness problem" (*6*). To reach such extreme velocities, a large amount of energy has to be deposited per rest mass, for example, by the annihilation of neutrino-antineutrino pairs, $\bar{\nu}_i + \nu_i \rightarrow e + e^+$, or through magnetic mechanisms (*7*, *8*). Therefore, strong magnetic fields have been suggested as being important in producing GRBs (*9*–*13*), but the question of what field strengths can actually be reached in a merger remnant before it collapses to a black hole has so far remained unanswered. Recently, a very energetic giant flare from the magnetar SGR 1806-20 has been observed (*14*, *15*). If it had been farther away, but within 40 Mpc, its initial spike would—both on grounds of duration and spectrum—have been interpreted as a short gamma-ray burst. The lack of excess events from the direction of the Virgo cluster, however, suggests that only a small portion of previously observed short bursts could have been giant magnetar flares. Nevertheless, the similarity in physical properties may point to a common or similar mechanism behind both phenomena.

Although computer simulations of binary neutron star mergers have reached a good degree of realism (*16*–*19*), none has so far been able to take magnetic fields into account, primarily because of the numerical challenge posed by simulating even the hydrodynamics of the merger process. Here, we present global neutron star merger simulations that follow the evolution of the magnetic field. Our main result is that the existing neutron star magnetic fields (10^{12} G) become amplified by several orders of magnitude within the first millisecond after the merger, which is long before the collapse to a black hole can proceed. Our robust lower limit on the field that can be reached is 2×10^{15} G, but it is highly probable that much stronger fields are realized in nature.

Our simulations are three-dimensional computer simulations of two neutron stars that coalesce because of the emission of gravitational waves. The equations of hydrodynamics are solved with a Lagrangian particle scheme (smoothed particle hydrodynamics) [for a review see (*20*)] that is coupled to a temperature- and composition-dependent nuclear equation of state (*17*, *21*). We include the effects of cooling and the change in matter composition due to neutrino-producing weak interactions. Because the debris material covers the full range from completely opaque to completely transparent to neutrinos, we have to incorporate opacity effects. Thus, on an additional grid, we calculate for each fluid parcel the opacities for each neutrino species and take them into account in the emission process (*18*). The Newtonian self-gravity of the neutron star fluid is evaluated efficiently using a binary tree algorithm. In addition, we apply forces that emerge as a result of the emission of gravitational waves (*17*); these are the forces that drive the binary toward coalescence. The new physics employed in these simulations is the inclusion of magnetic fields. To ensure the robustness of our results, we apply two different methods: one using a recently developed algorithm for "smoothed particle magnetohydrodynamics" (*22*) and one using a method in which the magnetic field is calculated from the so-called "Euler potentials," α and β, that are advected with each fluid particle (*23*). The magnetic field is calculated from these potentials according to

$$\mathbf{B} = \nabla\alpha \times \nabla\beta \qquad (1)$$

This prescription has the advantage that the divergence constraint ("no monopoles condition") on the magnetic field is satisfied by construction. Apart from this difference, both methods yield similar results. The computational costs are dominated by the calculation of self-gravity; the costs for the magnetic fields, the equation of state, and the neutrino physics are negligible by comparison.

Our initial neutron stars are cold and have masses of 1.4 solar masses ($M_\odot$) each. The two stars are placed at an initial separation of 48 km with velocities corresponding to a circular orbit around their common center of mass. Because the inspiral dynamics only allows for a short time of tidal interaction, the neutron stars cannot be spun up substantially (*24*); therefore, we start

[1]School of Physics, University of Exeter, Stocker Road, Exeter EX4 4QL, UK. [2]School of Engineering and Science, International University Bremen, Campus Ring 1, 28759 Bremen, Germany.

*To whom correspondence should be addressed. E-mail: s.rosswog@iu-bremen.de

our calculations with nonspinning neutron stars. We choose uniform magnetic fields of the typical strength of neutron stars (10^{12} Gauss) as initial conditions (note that we are modeling the interior fields, not the exterior dipole-like fields). The field orientation is parallel to the orbital angular momentum for one star and opposite for the other. Test calculations with different orientations yield maximum field strengths that are very similar.

The global dynamical evolution is shown in Fig. 1 and Movie S1: The two stars merge into a single object within about one orbital period (~2 ms). Subsequently, excess angular momentum is transported outward in spiral arms that quickly spread into a thick accretion disk around the central object. When the stars come into contact, a shear interface forms, across which the tangential velocity exhibits a jump (Fig. 2). In such a shear layer, even infinitesimally small perturbations are unstable to the Kelvin-Helmholtz (KH) instability and will grow, in this case causing the interface to curl up into vortex rolls. An analogous effect occurs when wind blows across the surface of a lake, curling up the surface into waves. The initial growth rate, σ_λ, of the KH instability may be calculated analytically for the inviscid, incompressible case (both properties are good approximations for neutron stars). In the linear regime, the growth rate is $\sigma_\lambda = \pi v/\lambda$ (*25*), where λ is the wavelength of the growing mode and v the velocity across the jump. Because the shortest modes grow fastest, the numerical results can only be lower limits on the growth realized in nature. Inserting the smallest length that we can numerically resolve for λ and the simulation value for v into the above equation yields growth rates consistent with the simulations.

In all cases we find that the field in the vortex rolls is amplified within ~1 ms by orders of magnitude (Figs. 3 and 4). This time scale should be compared to the 50 to 100 ms that are estimated (*26*) for the newly formed, differentially rotating central object to collapse into a black hole. The high field strength material produced in the shear instability between the stars is subsequently advected with the matter to cover the surface of the central merger remnant (Fig. 1).

Because the length scales we can resolve numerically are larger than the physical lengths that will trigger the KH instability in nature, our numerical results represent robust lower limits on the true magnetic field strengths. This is demonstrated by our numerical resolution study (Fig. 4). Each time we double the numerical resolution (increase the particle number by a factor of 10), the peak field strength increases by a factor of a few. The highest numerical resolution that we can currently afford (2×10^6 fluid particles) yields a field strength beyond 2×10^{15} Gauss, i.e., larger than the largest magnetic fields that have been observed in magnetars. The growth is likely to saturate when the magnetic field becomes strong enough to feed back on the fluid or, alternatively, when the field becomes buoyant. In either case, the field strength reached will be comparable to the equipartition field strength (here 10^{16} to 10^{18} G), where the magnetic pressure becomes comparable to the gas pressure.

Although we can only speculate about the field strengths that will be actually produced in nature, it is clear that the strong magnetic fields that have been conjectured in earlier work occur naturally in the initial shear phase, even before possible dynamo mechanisms could have set in. If a fraction ε of the rotational energy of the central object of the remnant, 8×10^{52} erg, is channelled into the magnetic field, the field strength averaged over the central object will be $B = 1.2 \times 10^{17}$ G $(\varepsilon/0.1)^{1/2}(E_{kin}/8 \times 10^{52}$ erg$)^{1/2}$ (15 km/R_{co})$^{3/2}$, where R_{co} is the radius of the central object. Locally, the field strength could be even higher. Near equipartition matter blobs in high field pockets (such as the vortices seen in Fig. 3) will become buoyant, float up, and produce a relativistic blast as they break through the surface of the central object (*12*). This could be the variable, relativistic outflow that is required to produce a GRB far from the central engine. In this case the millisecond substructures would be determined by the fluid instabilities in the central object, but the overall duration would be set by the time it takes the central object to collapse or to consume its rotational energy. If

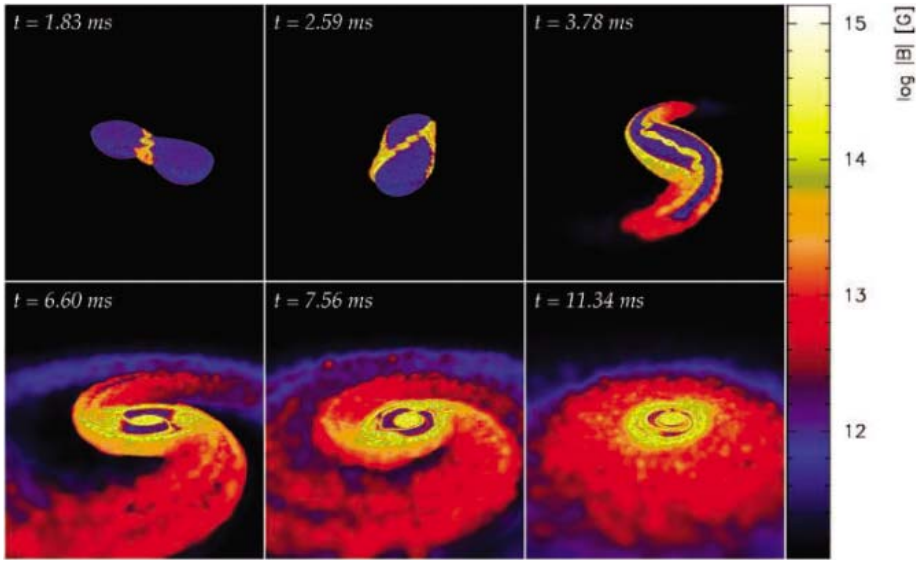

Fig. 1. Snapshots (left to right, top to bottom) of the coalescence of two magnetized neutron stars, showing magnetic field strengths in the material at and below the orbital plane. Dimensions in each panel are ~140 km from left to right. The stars move gradually toward each other and then merge in a "plunging phase" within about one orbital period (~2 ms) (first two snapshots). This object sheds mass into spiral arms that are subsequently wrapped around the central object (snapshots three to five) to form a hot torus (last snapshot). The magnetic field is amplified in the shear instability between the stars and subsequently advected with the matter to cover the surface of the central merger remnant.

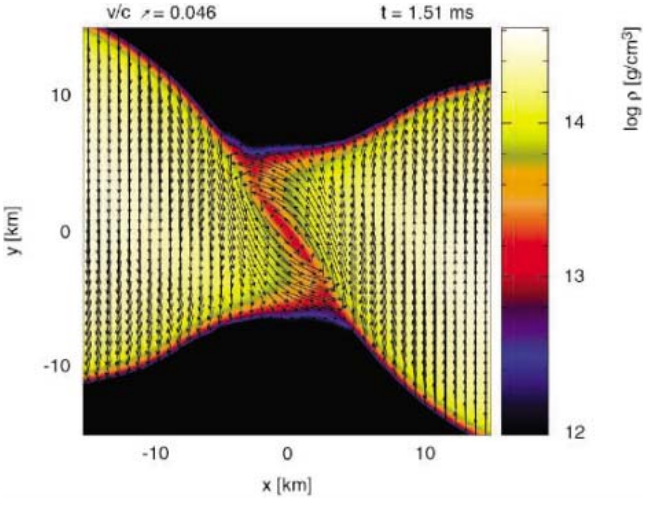

Fig. 2. Density and velocity field in the orbital plane at the moment when the stars come into contact (t = 1.51 ms). A shear interface forms between the stars, across which the tangential velocity exhibits a large jump. This interface is unstable to the Kelvin-Helmholtz instability and will curl up into vortex rolls (see Fig. 3).

we use the magnetic dipole spin-down time as an order of magnitude estimate and insert typical numbers from the simulation, we find

$$\tau = 0.14\ \mathrm{s}\left(\frac{B}{10^{17}\ \mathrm{G}}\right)^{-2}\left(\frac{P}{1.5\ \mathrm{ms}}\right)^{2} \times \left(\frac{15\ \mathrm{km}}{R_{\mathrm{CO}}}\right)^{4}\left(\frac{M_{\mathrm{CO}}}{2.5\ M_{\odot}}\right) \quad (2)$$

where P is the rotational period and M_{co} is the mass of the central object. This time scale is close to the typical duration of a short GRB. Note also that the high-field strength matter is transported by the fluid motion to the remnant surface. The sudden appearance of 10^{17}-G material at the surface of the neutron star–like central object will very plausibly launch magnetized blasts similar to those described in (*27*). Similar processes involving buoyant magnetic fields, although at lower field strengths ($\sim 10^{14}$ to 10^{16} G), may also be at work in the accretion torus. It is also worth pointing out the somewhat speculative possibility that such a merger could produce magnetars.

Recent calculations (*28*, *29*) in the GRB context have shown that the deposition of thermal energy above accretion disks, for example, from neutrino annihilation, can drive relativistic outflows. Such outflows can be narrowly collimated, but in general a large spread in energies and opening angles depending on the specifics of the merging system is expected. In the light of the above-presented results, it is hard to see how a signal from the strong magnetic fields—on top of the neutrino-annihilation driven outflows—can be avoided.

At the neutrino luminosities produced in the merger ($>10^{52}$ erg/s), neutrinos will, as in the case of newborn neutron stars, drive a strong baryonic wind (*30*). This material poses a potential threat to the emergence of the required ultrarelativistic outflow. The central object is rather hot (20 to 25 MeV, where 1 MeV = $1.16 \times 10^{11}\ K$) but very opaque to neutrinos. It therefore only contributes moderately to the total neutrino luminosity, which is dominated by the inner shock-heated torus regions from which we expect most of the wind material to come. Directly after the merger, the environment is of very low density and rising magnetic bubbles will, through magnetic pressure, help to keep the region above the central object relatively clean of baryons. However, as the neutrino luminosity rises and the continuously braked central object takes longer and longer to reach buoyancy field strength, it will become increasingly difficult to launch relativistic outflows. The interaction between such magnetic bubbles and a baryonic wind will be very complicated, and whether relativistic outflow develops may depend on the details of the merging system. The estimated double neutron star merger rate ranges from about 4 to 220×10^{-6} per year and galaxy (*31*) and is thus comfortably two orders of magnitude larger than the rate required to explain short GRBs. Thus, even allowing for beaming and for a fraction of systems that could possibly fail to provide the right conditions (instead producing baryon-loaded x-ray or ultraviolet flashes), the merger rate is still large enough to explain the observed short GRBs.

The two mechanisms—neutrino annihilation and magnetic processes—will show a different temporal evolution, and they will also differ in the energies they can provide to the burst. The torus that dominates the neutrino emission takes a few dynamical time scales to form (in our simulations, the neutrino luminosity peaks about 30 ms after the stars have come in contact). The initial amplification of the magnetic field occurs on a much shorter time scale. Therefore, we expect the very early prompt emission to come from the magnetic field alone. The outflows driven by neutrino annihilation contain typically 10^{48} ergs (*19*); magnetic mechanisms could easily provide 10^{51} ergs or more (*8*, *19*). Very energetic short bursts would therefore have to be attributed to magnetic mechanisms. In any case, short GRBs that arise from the merger of magnetized neutron stars will exhibit a large intrinsic diversity and a very complex temporal behavior, and their observed properties will drastically depend on their orientation relative to the line of sight.

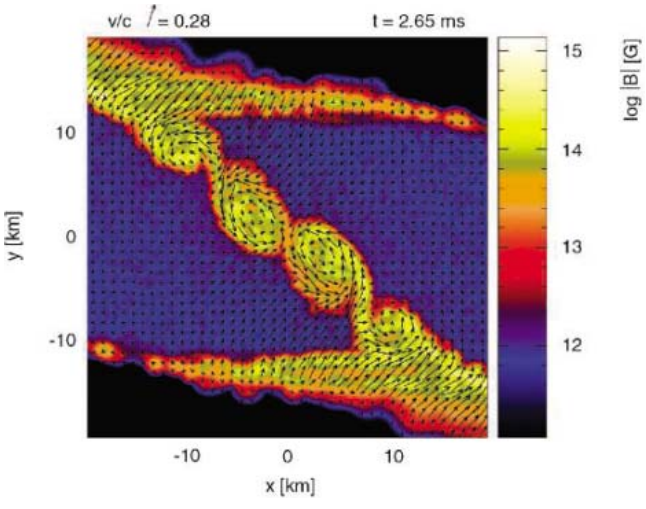

Fig. 3. Close-up of the central regions at $t = 2.65$ ms. The color coding shows strength of the magnetic field, and the arrows show the fluid velocity in the corotating frame (that is, with the dominant orbital velocity component removed). The shear interface shown in Fig. 2 can be seen to have curled up into vortex rolls. In these vortices, the field is strongly amplified to strengths exceeding 10^{15} G. High-field material that has passed through these vortex rolls is subsequently spread across the surface of the central merger remnant (see first three panels of Fig. 1).

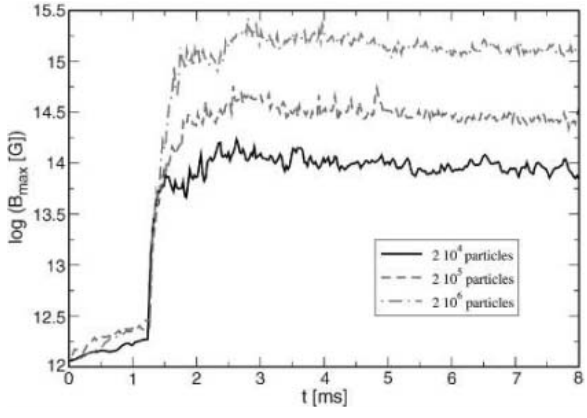

Fig. 4. Maximum magnetic field strength as a function of the number of fluid particles. All three runs are identical apart from the numerical resolution. The maximum field strength of the best resolved run, 2×10^{15} G, is a strict lower limit on the magnetic field that can be reached in a neutron star merger.

References and Notes

1. A. Abramovici *et al.*, *Science* **256**, 325 (1992).
2. H. Grote *et al.*, *Classical and Quantum Gravity* **22**, S193 (2005).
3. J. S. Bloom *et al.*, *Astrophys. J.* **638**, 354 (2006).
4. E. Berger *et al.*, *Nature* **438**, 988 (2005).
5. S. D. Barthelmy *et al.*, *Nature* **438**, 994 (2005).
6. T. Piran, *Rev. Mod. Phys.* **76**, 1143 (2005).
7. D. Eichler, M. Livio, T. Piran, D. N. Schramm, *Nature* **340**, 126 (1989).
8. R. Narayan, B. Paczynski, T. Piran, *Astrophys. J.* **395**, L83 (1992).
9. V. V. Usov, *Nature* **357**, 472 (1992).
10. R. C. Duncan, C. Thompson, *Astrophys. J.* **392**, L9 (1992).
11. P. Meszaros, M. J. Rees, *Astrophys. J.* **482**, L29 (1997).
12. W. Kluzniak, M. Ruderman, *Astrophys. J.* **505**, L113 (1998).
13. M. Lyutikov, V. I. Pariev, R. D. Blandford, *Astrophys. J.* **597**, 998 (2003).
14. K. Hurley *et al.*, *Nature* **434**, 1098 (2005).
15. D. M. Palmer *et al.*, *Nature* **434**, 1107 (2005).
16. M. Ruffert, H.-T. Janka, *Astron. Astrophys.* **380**, 544 (2001).
17. S. Rosswog, M. B. Davies, *Mon. Not. R. Astron. Soc.* **334**, 481 (2002).
18. S. Rosswog, M. Liebendörfer, *Mon. Not. R. Astron. Soc.* **342**, 673 (2003).
19. S. Rosswog, E. Ramirez-Ruiz, M. B. Davies, *Mon. Not. R. Astron. Soc.* **345**, 1077 (2003).

20. J. J. Monaghan, *Rep. Prog. Phys.* **68**, 1703 (2005).
21. H. Shen, H. Toki, K. Oyamatsu, K. Sumiyoshi, *Nucl. Phys. A.* **637**, 435 (1998).
22. D. J. Price, J. J. Monaghan, *Mon. Not. R. Astron. Soc.* **364**, 384 (2005).
23. D. P. Stern, *Am. J. Phys.* **38**, 494 (1970).
24. L. Bildsten, C. Cutler, *Astrophys. J.* **400**, 175 (1992).
25. L. D. Landau, E. M. Lifshitz, *Fluid Mechanics* (Pergamon, Oxford, 1959).
26. M. Shibata, K. Taniguchi, K. Uryu, *Phys. Rev. D* **71**, 084021 (2005).
27. M. Lyutikov, *Mon. Not. R. Astron. Soc.* **346**, 540 (2003).
28. S. Rosswog, E. Ramirez-Ruiz, *Mon. Not. R. Astron. Soc.* **343**, L36 (2003).
29. M. A. Aloy, H.-T. Janka, E. Müller, *Astron. Astrophys.* **436**, 273 (2005).
30. R. C. Duncan, S. L. Shapiro, I. Wasserman, *Astrophys. J.* **309**, 141 (1986).
31. V. Kalogera *et al.*, *Astrophys. J.* **614**, L137 (2004).
32. We thank M. Brüggen, M. Höft, J. Vogt, R. West, and M. Bate for helpful discussions and comments. D.J.P. is supported by a U.K. Particle Physics and Astronomy Research Council postdoctoral research fellowship. We thank the referees for their insightful comments.

Supporting Online Material
www.sciencemag.org/cgi/content/full/1125201/DC1
Movie S1

20 January 2006; accepted 23 March 2006
Published online 30 March 2006;
10.1126/science.1125201
Include this information when citing this paper.

Cyclopropenylidenes: From Interstellar Space to an Isolated Derivative in the Laboratory

Vincent Lavallo,[1] Yves Canac,[1] Bruno Donnadieu,[1] Wolfgang W. Schoeller,[2] Guy Bertrand[1]*

Like many of the molecular species that have been detected in the interstellar medium, the singlet carbene cyclopropenylidene (C_3H_2) has been presumed to be too unstable to isolate in the laboratory. However, by appending π-electron–donating amino groups to the triangular skeleton, we prepared a cyclopropenylidene derivative that is stable at room temperature. In contrast to previously isolated carbenes, this compound does not require a heteroatom adjacent to the electron-deficient carbon to confer stability. Despite the presence of amino groups, the geometric parameters of the cyclic skeleton, revealed by x-ray crystallography, are only slightly perturbed relative to those of the calculated structure of unsubstituted cyclopropenylidene. Stable cyclopropenylidene derivatives might thus serve as models for a better understanding of the formation of carbon-bearing molecules in the interstellar medium.

Carbenes are compounds with a neutral dicoordinate carbon atom, which features either two singly occupied nonbonding orbitals (a triplet state) or a lone pair and an accessible vacant orbital (a singlet state). With only six electrons in its valence shell, the carbene center defies the octet rule, and for a long time carbenes have been considered as prototypical reactive intermediates (*1*, *2*). During the past two decades, carbene chemistry has undergone a profound revolution. Persistent triplet carbenes have been observed (*3*), and singlet carbenes have been isolated (*4*–*6*) and even become powerful tools for synthetic chemists (*7*, *8*). However, it is generally believed that singlet carbenes can be isolated only if their electron deficiency is reduced by the presence of at least one π-donor heteroatom directly bonded to the carbene center (*9*).

Cyclopropenylidene (C_3H_2) **1a** is a cyclic singlet carbene (Fig. 1). Since its first radio astronomical detection in 1985 (*10*), it has been inferred to be the most abundant cyclic hydrocarbon observed in interstellar space (*11*). It is detectable in molecular clouds, circumstellar shells, and at least one external galaxy. Cyclopropenylidene **1a** and its linear isomers **2a** and **3a** have also been observed in several hydrocarbon-rich flames and may be involved in the chemistry of soot formation (*12*). Although carbenes are very reactive, they are not necessarily prone to self-rearrangement, which accounts for their stability in the near-vacuum of deep space and in the low-density medium of flame. However, cyclopropenylidene **1a** appears to be highly unstable in condensed phases. Reisenauer *et al*. were able to detect the molecule by infrared spectroscopy in a solid argon matrix, but it survives for only a few hours at 35 to 40 K and then polymerizes (*13*). The quest for cyclopropenylidenes in the laboratory has not been restricted to the parent compound **1a**. Because amino groups are known to stabilize the corresponding cyclopropenium salts (**4**) (*14*), bis(dialkylamino)cyclopropenylidenes such as **1c** have been among the most frequently targeted derivatives (*15*–*17*). The transient existence of **1c** has been postulated based on chemical trapping experiments, but it has been described as a highly unstable molecule, defying isolation or even observation in the free state (*15*–*21*).

Calculations predict that the rearrangement of **1a** into other C_3H_2 isomers, propadienylidene **2a** and propynylidene **3a**, is quite unlikely, because the latter are higher in energy by 42 to 58 and 54 to 92 kJ/mol, respectively (*12*, *22*, *23*). Moreover, cyclopropenylidenes (**1**) feature a large singlet-triplet energy gap: 191 kJ/mol for **1a** and 249 kJ/mol for the simplest amino-substituted derivative **1b** (*24*), which should prevent the dimerization (*25*–*27*) and subsequent polymerization. Although the gap value calculated for **1b** is smaller than for Arduengo's carbenes **A** (*28*) and **B** (*29*) (Fig. 2) [351 and 288 kJ/mol (*30*), respectively], it is comparable to that of the very stable Alder's carbene **C** (*31*) [242 kJ/mol (*30*)] and much larger than that of the first isolated carbene **D** (*32*) [113 kJ/mol (*33*)].

These calculations suggest that cyclopropenylidenes might be isolable in the laboratory and have prompted us to challenge the discouraging

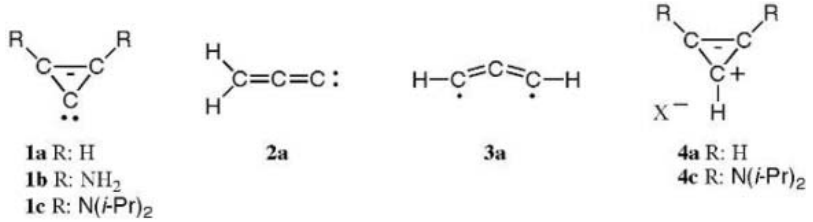

Fig. 1. Cyclopropenylidenes **1a** to **1c**, propadienylidene **2a**, propynylidene **3a**, and cyclopropenium salts **4a** and **4c**.

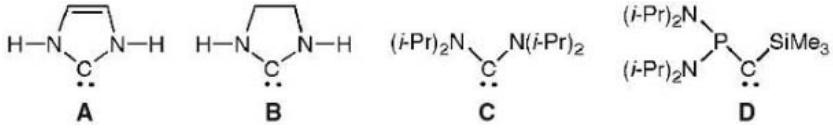

Fig. 2. Representative singlet carbenes.

[1]University of California, Riverside–CNRS Joint Research Chemistry Laboratory (Unité Mixte Internationale 2957), Department of Chemistry, University of California, Riverside, CA 92521–0403, USA. [2]Fakultät für Chemie der Universität, Postfach 10 01 31, D-33615 Bielefeld, Germany.

*To whom correspondence should be addressed. E-mail: gbertran@mail.ucr.edu

experimental results described so far. Here we report the preparation and single-crystal x-ray diffraction study of bis(diisopropylamino)cyclopropenylidene **1c**. This compound is stable at room temperature even without stabilization of the carbene center by adjacent π-donor heteroatoms, a necessary criterion for previously isolated carbenes.

Besides the photolysis and thermolysis of diazo derivatives, deprotonation of the conjugate acid of carbenes is by far the most popular method to generate singlet carbenes (*4*–*9*). A major advantage of deprotonation is its rapidity, even at low temperatures, so that carbenes that are only moderately stable can still be characterized. Moreover, for cyclopropenylidenes, the conjugate acids, namely the cyclopropenium salts (**4**) (Fig. 1), are available in large quantities, thermally very stable, and easy to handle (*14*). The bis(diisopropylamino) derivative **4c** is even insensitive to water (*34*). In order to monitor the possible formation of the desired cyclopropenylidene **1c**, we calculated its ^{13}C nuclear magnetic resonance (NMR) spectrum (*24*). The carbene carbon and the two other ring carbons were predicted to give signals at 189 and 157 parts per million (ppm), respectively, distinct from the resonances of other compounds in the reaction mixture.

Dry diethyl ether was slowly added at –78°C to an equimolar mixture of cyclopropenium tetraphenylborate **4c** (X = BPh_4) and potassium bis(trimethylsilyl)amide (*35*). After the mixture was stirred for half an hour at –78°C, the ^{13}C NMR signals at 99 and 133 ppm corresponding to the ring carbons of the starting cyclopropenium salt **4c** were absent, whereas new signals appeared at 185 and 159 ppm, in the range predicted for **1c**. These signals persisted when the solution was warmed to room temperature. After evaporation of diethyl ether under vacuum, dry hexane was added and the resulting suspension was stirred for 10 min. After filtration to remove potassium tetraphenylborate, the bright yellow solution was stored overnight at –20°C under an argon atmosphere, affording **1c** as yellow crystals in 20% yield.

In solution, dynamic ^1H and ^{13}C NMR behavior was observed for **1c**, corresponding to the exchange of isopropyl group environments. The CH resonances are broad at room temperature, but split to reveal two types of *i*-Pr groups at –30°C. The CH peaks coalesce at about –20°C and +10°C, in the ^1H (500 MHz) and ^{13}C (125 MHz) NMR spectra, respectively, corresponding to a free energy of activation for site exchange of about 53 kJ/mol. A major part of this exchange process must involve rotation about the N-C_{ring} bonds, which suggests, as expected, a π donation from the amino groups to the electron-deficient ring. However, this donation is weaker than in the starting material **4c**, for which the coalescence temperature in ^1H NMR is about 85°C, which corresponds to a free energy of activation of about of 75 kJ/mol.

In the solid state, the ring and the amino groups of both the cyclopropenylidene **1c** and cationic precursor **4c** are nearly coplanar (Fig. 3), confirming the interaction of the nitrogen lone pairs with the π system of the ring. However, it is again apparent that this interaction is less intense for carbene **1c** than for the cationic precursor **4c**. Compared to **4c**, the CN bond distances (**1c**, 1.334; **4c**, 1.305 Å), as well as the bonds flanking the carbene center, are longer (**1c**, 1.404; **4c**, 1.359 Å), whereas the formally CC double bond is shorter (**1c**, 1.344; **4c**, 1.406 Å). The geometric parameters of the ring in the isolated cyclopropenylidene derivative **1c** are very close to those calculated for the parent compound **1a** (Fig. 4).

Although **1c** is sensitive to air, it is thermally very stable. Heating a toluene solution of **1c** at 80°C for 2 hours resulted in only ~10% decomposition. Compound **1c** has a melting point of 107° to 109°C, and the NMR spectra of the melt indicate little if any decomposition.

Almost 50 years after the seminal discovery by Breslow (*36*) that cyclopropenium salts were stable at room temperature, cyclopropenylidene **1c** is a neutral analog of these classical 2 π-Huckel aromatic compounds. Stable cyclopropenylidenes might serve as models for a better understanding of the formation of carbon-bearing molecules in the interstellar medium. Moreover, the isolation of this molecule paves the way for the discovery of stable versions of other interstellar species previously thought to be unisolable under normal laboratory conditions.

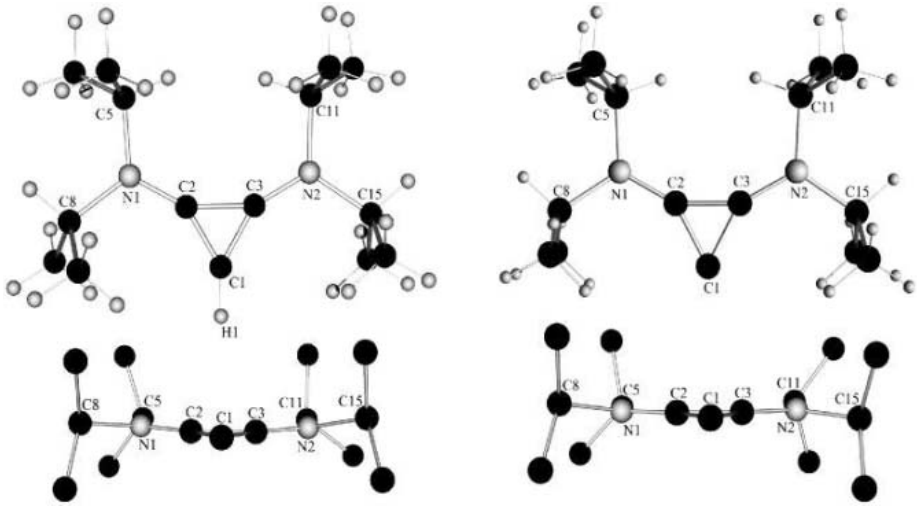

Fig. 3. Molecular (ORTEP) views of cyclopropenium tetraphenylborate **4c** (left) and cyclopropenylidene **1c** (right) in the solid state (for clarity, tetraphenylborate anion and H atoms are omitted in the left and bottom images, respectively). **4c**: C1-C2, 1.360 ± 3 Å; C1-C3, 1.358 ± 3 Å; C2-C3, 1.406 ± 3 Å; C2-N1, 1.305 ± 3 Å; C3-N2, 1.308 ± 3 Å; C2-C1-C3, 62.31° ± 17°; C1-C2-C3, 58.79° ± 16°; C1-C3-C2, 58.90° ± 16°; C1-C2-N1, 148.9° ± 2°; C3-C2-N1, 152.2° ± 2°; C1-C3-N2, 149.5° ± 2°; C2-C3-N2, 151.5° ± 2°; C2-N1-C8, 118.2° ± 2°; C8-N1-C5, 119.9° ± 2°; C2-N1-C5, 121.8° ± 2°; C3-N2-C11, 119.6° ± 2°; C3-N2-C15, 117.9° ± 2°; C11-N2-C15, 121.4° ± 2°. **1c**: C1-C2, 1.404 ± 3 Å; C1-C3, 1.405 ± 3 Å; C2-C3, 1.344 ± 3 Å; C2-N1, 1.332 ± 3 Å; C3-N2, 1.336 ± 3 Å; C2-C1-C3, 57.19° ± 16°; C1-C2-C3, 61.45° ± 18°; C1-C3-C2, 61.36° ± 17°; C1-C2-N1, 146.7° ± 2°; C3-C2-N1, 151.8° ± 2°; C1-C3-N2, 146.2° ± 2°; C2-C3-N2, 152.4° ± 2°; C2-N1-C8, 119.91° ± 19°; C8-N1-C5, 119.0° ± 2°; C2-N1-C5, 120.66° ± 19°; C3-N2-C11, 120.9° ± 2°; C3-N2-C15, 119.10° ± 19°; C11-N2-C15, 119.94° ± 19°.

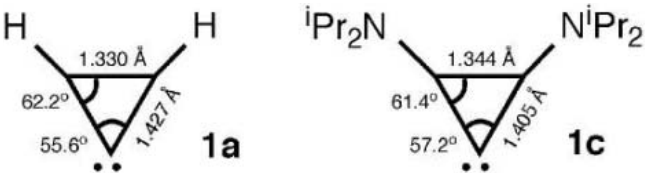

Fig. 4. Geometric parameters for the cyclic skeleton of the parent compound **1a** (calculated) and derivative **1c** (observed).

References and Notes

1. R. A. Moss, M. S. Platz, M. Jones Jr., Eds., *Reactive Intermediate Chemistry* (Wiley, New York, 2004).
2. U. H. Brinker, Ed., *Advances in Carbene Chemistry* (JAI, Greenwich, CT, 2001).
3. T. Itoh, Y. Nakata, K. Hirai, H. Tomioka, *J. Am. Chem. Soc.* **128**, 957 (2006).
4. F. E. Hahn, *Angew. Chem. Int. Ed. Engl.* **45**, 1348 (2006).
5. R. W. Alder *et al.*, *Angew. Chem. Int. Ed. Engl.* **43**, 5896 (2004).
6. D. Bourissou, O. Guerret, F. P. Gabbaï, G. Bertrand, *Chem. Rev.* **100**, 39 (2000).
7. E. Peris, R. H. Crabtree, *Coord. Chem. Rev.* **248**, 2239 (2004).
8. N. M. Scott, S. P. Nolan, *Eur. J. Inorg. Chem.* **2005**, 1815 (2005).
9. W. Kirmse, *Angew. Chem. Int. Ed. Engl.* **43**, 1767 (2004).
10. P. Thaddeus, J. M. Vrtilek, C. A. Gottlieb, *Astrophys. J.* **299**, L63 (1985).

11. R. I. Kaiser, *Chem. Rev.* **102**, 1309 (2002).
12. C. A. Taatjes *et al.*, *Phys. Chem. Chem. Phys.* **7**, 806 (2005).
13. H. P. Reisenauer, G. Maier, A. Riemann, R. W. Hoffmann, *Angew. Chem. Int. Ed. Engl.* **23**, 641 (1984).
14. K. Komatsu, K. Kitagawa, *Chem. Rev.* **103**, 1371 (2003).
15. Z. Yoshida, *Pure Appl. Chem.* **54**, 1059 (1982).
16. R. Weiss, C. Priesner, H. Wolf, *Angew. Chem. Int. Ed. Engl.* **17**, 446 (1978).
17. R. Weiss, M. Hertel, H. Wolf, *Angew. Chem. Int. Ed. Engl.* **18**, 473 (1979).
18. M. Tamm, A. Grzegorzewski, F. E. Hahn, *J. Organomet. Chem.* **501**, 309 (1995).
19. H. Schumann *et al.*, *Angew. Chem. Int. Ed. Engl.* **36**, 2232 (1997).
20. Cyclopropenylidene transition metal complexes have been known since 1968 (*21*), and main group adducts were recently reported (*19*).
21. K. Öfele, *Angew. Chem. Int. Ed. Engl.* **7**, 950 (1968).
22. E. V. Patterson, J. F. Stanton, R. J. McMahon, *J. Am. Chem. Soc.* **119**, 5847 (1997).
23. G. Maier, T. Preiss, H. P. Reisenauer, B. A. Hess Jr., L. J. Schaad, *J. Am. Chem. Soc.* **116**, 2014 (1994).
24. The singlet-triplet energy gap and the ^{13}C NMR chemical shifts have been calculated at the RI-BP86/TZVP + ZPE correction level, and RI-BP86/TZVPP//RI-BP86/TZVP level, respectively, using Turbomole 5.7 (see www.ipc.uni-karlsruhe.de/tch/tch1/turbomole/index.en.html and references cited therein).
25. For discussions on carbene dimerization, see (*5*) and (*26*); cyclopropenylidene dimers, namely triafulvalenes, remain unknown (*27*).
26. M. Driess, H. Grutzmacher, *Angew. Chem. Int. Ed. Engl.* **35**, 828 (1996).
27. B. Halton, *Eur. J. Org. Chem.* **2005**, 3391 (2005).
28. A. J. Arduengo III, R. L. Harlow, M. Kline, *J. Am. Chem. Soc.* **113**, 361 (1991).
29. A. J. Arduengo III, J. Goerlich, W. Marshall, *J. Am. Chem. Soc.* **117**, 11027 (1995).
30. C. Heinemann, W. Thiel, *Chem. Phys. Lett.* **217**, 11 (1994).
31. R. W. Alder, P. R. Allen, M. Murray, A. G. Orpen, *Angew. Chem. Int. Ed. Engl.* **35**, 1121 (1996).
32. A. Igau, H. Grützmacher, A. Baceiredo, G. Bertrand, *J. Am. Chem. Soc.* **110**, 6463 (1988).
33. L. Nyulaszi, D. Szieberth, J. Reffy, T. Veszpremi, *Theochemistry* **453**, 91 (1998).
34. R. Weiss, C. Priesner, *Angew. Chem. Int. Ed. Engl.* **17**, 445 (1978).
35. Preparation methods and spectroscopic data for compounds **1c** and **4c** are available as supporting material on *Science* Online.
36. R. Breslow, *J. Am. Chem. Soc.* **79**, 5318 (1957).

37. We are grateful to NIH (grant R01 GM 68825) and RHODIA for financial support of this work. Metrical data for the solid-state structures of **1c** and **4c** are available free of charge from the Cambridge Crystallographic Data Centre under reference numbers CCDC-602795 and CCDC-602794, respectively.

Supporting Online Material

www.sciencemag.org/cgi/content/full/1126675/DC1
SOM Text
Tables S1 and S2
References

24 February 2006; accepted 31 March 2006
Published online 13 April 2006;
10.1126/science.1126675
Include this information when citing this paper.

The Sand Seas of Titan: Cassini RADAR Observations of Longitudinal Dunes

R. D. Lorenz,[1]* S. Wall,[2] J. Radebaugh,[1] G. Boubin,[1] E. Reffet,[1] M. Janssen,[2] E. Stofan,[3] R. Lopes,[2] R. Kirk,[4] C. Elachi,[2,5] J. Lunine,[1,2] K. Mitchell,[2] F. Paganelli,[2] L. Soderblom,[4] C. Wood,[6] L. Wye,[7] H. Zebker,[7] Y. Anderson,[2] S. Ostro,[2] M. Allison,[8] R. Boehmer,[2] P. Callahan,[2] P. Encrenaz,[9] G. G. Ori,[10] G. Francescetti,[11] Y. Gim,[2] G. Hamilton,[2] S. Hensley,[2] W. Johnson,[2] K. Kelleher,[2] D. Muhleman,[12] G. Picardi,[13] F. Posa,[14] L. Roth,[2] R. Seu,[13] S. Shaffer,[2] B. Stiles,[2] S. Vetrella,[11] E. Flamini,[15] R. West[2]

The most recent Cassini RADAR images of Titan show widespread regions (up to 1500 kilometers by 200 kilometers) of near-parallel radar-dark linear features that appear to be seas of longitudinal dunes similar to those seen in the Namib desert on Earth. The Ku-band (2.17-centimeter wavelength) images show ~100-meter ridges consistent with duneforms and reveal flow interactions with underlying hills. The distribution and orientation of the dunes support a model of fluctuating surface winds of ~0.5 meter per second resulting from the combination of an eastward flow with a variable tidal wind. The existence of dunes also requires geological processes that create sand-sized (100- to 300-micrometer) particulates and a lack of persistent equatorial surface liquids to act as sand traps.

The low gravity and dense atmosphere on Titan make it a favorable environment for aeolian transportation of material (*1*–*3*) in the sense that the windspeeds needed to saltate surface particles are rather low. However, until recently (*3*, *4*) it was thought that loose particles were difficult to generate and transport (erosive processes and wind, driven by the faint sunlight reaching Titan's surface, were expected to be weak) and would be susceptible to trapping by surface liquids.

Recently, numerical circulation models (*5*) incorporating the tide in Titan's atmosphere due to Saturn's gravity (*6*) (~400 times as strong as the moon's effect on Earth) show that near-surface winds may be dominated by this effect rather than solar heating, and periodically varying winds comparable with the transport threshold may result. The winds vary both in strength and direction. Data from Cassini (*7*, *8*) and from the Huygens probe (*9*) that landed on Titan in January 2005 show a very geologically varied surface, modified by a mix of processes including strong fluvial erosion, impact, and cryovolcanism. No evidence for large bodies of surface liquids has so far been found. Thus, the setting for aeolian transport now seems much more favorable.

Aeolian features appear on planetary surfaces at a wide range of scales, from cm-wide ripples to km-scale megadunes; imaging resolutions of better than 1 km are therefore required to observe them (*10*). Early large-scale near-infrared (near-IR) imaging at ~km resolution (*8*) by the Cassini Imaging Science Subsystem (ISS) indicated large-scale albedo patterns such as dark streaks and asymmetric edge contrasts (sharp westward boundaries and diffuse eastward ones) that were suggestive of net-eastward fluid transport of materials on Titan's surface, possibly by wind, but individual features could not be resolved. Radar imaging (*11*) on Cassini's T3 flyby (15 February 2005), however, with resolution down to 300 m, found many distinct radar-dark linear features (nicknamed "cat scratches") superposed on other geological units and having a spacing of 1 to 2 km and lengths of many tens of km, in a generally east-west orientation. These covered about 20% of that swath (which, like T8, covered ~1.8 million km^2, or almost 2% of Titan's surface), in patches with extents of up to 400 km.

Our most recent radar imaging (T8, 27 October 2005; see supporting online text) finds large expanses of these features, covering some 65% of that swath. Patches of these features vary from just a few km across to the width of the swath (~200 km), and one contiguous region is ~1500 km long. Furthermore, in some places in T8 the feature size, favorable geometry, and resolution of the observations allow the detection of bright topographic glints (Fig. 1). These

[1]Lunar and Planetary Laboratory, University of Arizona, Tucson, AZ 85721, USA. [2]Jet Propulsion Laboratory, California Institute of Technology, Pasadena, CA 91109, USA. [3]Proxemy Research, Bowie, MD 20715, USA. [4]U.S. Geological Survey, Flagstaff, AZ 86001, USA. [5]RADAR Team Leader, Jet Propulsion Laboratory, California Institute of Technology, Pasadena, CA 91109, USA. [6]Planetary Science Institute, Tucson, AZ 85719, USA and Wheeling Jesuit College, Wheeling, WV 26003, USA. [7]Stanford University, Stanford, CA 94305, USA. [8]Goddard Institute for Space Studies, National Aeronautics and Space Administration, New York, NY 10025, USA. [9]Observatoire de Paris, 92195 Meudon, France. [10]International Research School of Planetary Sciences, Universita' d'Annunzio, 65127 Pescara, Italy. [11]Facoltá di Ingegneria, 80125 Naples, Italy. [12]Division of Geological and Planetary Sciences, California Institute of Technology, Pasadena, CA 91125, USA. [13]Universitá La Sapienza, 00184 Rome, Italy. [14]Istituto Nazionale per la Fisica della Materia (INFM) and Dip. Interateneo di Fisica, Politecnico di Bari, 70126 Bari, Italy. [15]Agenzia Spaziale Italiana, 00131 Rome, Italy.

*To whom correspondence should be addressed. E-mail: rlorenz@lpl.arizona.edu

glints on the nearest side of the features, made visible by fortuitous geometry (the long axis of the dunes is roughly orthogonal to the radar look direction), suggest surfaces sloping toward the radar and show that the features are not merely thin streaks of material on the surface but have considerable positive topographic relief. Preliminary radarclinometric results [Titan's radar backscatter varies approximately as the cosecant (*7*) of the incidence angle; the incidence angle relative to a flat surface, typically 20° to 30°, is known from spacecraft navigation, and thus local variations of backscatter can be interpreted as a local tilt of the surface] yield slopes of 6° to 10° and heights of 100 to 150 m (Fig. 2).

Morphologically, the features resemble longitudinal dunes such as those found in the Namib and other terrestrial deserts (Fig. 2). Their height, longitudinal symmetry, superposition on other features, and the way they merge (forming "tuning fork" junctions) suggest that they are depositional. The interpretation as longitudinal dunes is supported by the way they divert and reconverge around topographic obstacles (Fig. 1). The asymmetric streamline pattern thus formed suggests that the net transport direction is generally eastward, with some regional variation (Fig. 3) and local deviations around elevated or bright topography (Figs. 1 and 4).

Dunes cover about 5% of the land surface on Earth, and longitudinal (linear, or sometimes "seif") dunes, where the material accumulates in lanes oriented along the mean transport direction, are among the most common type of dune (*12*, *13*), covering half to two-thirds of sand seas [in contrast, they are among the least-common dune type on Mars (*14*, *15*)]. Only in one place (Fig. 3) does a different duneform appear in our images so far. In flowing around an apparently large topographic rise, the dunes become transverse in form, before the longitudinal pattern resumes. Linear dunes are characteristic of a moderately variable windfield, typically one that varies around a mean or alternates between two widely spaced directions (*16*). Similarly, linear current ridges are formed on the terrestrial seabed by tidal currents (*17*). Purely unidirectional winds tend to form transverse dunes, whereas winds highly variable in direction form star dunes (*12*). On Titan, the wind regime that forms longitudinal dunes may be a natural result of the interaction of the fluctuating tidal windfield with the steady zonal (west-east) winds that prevail higher in the atmosphere (*18*). A substantial instantaneous meridional (north-south) component is implied, and the fact that dunes are not oriented exactly west-east everywhere also suggests a net meridional component over the long term. Whether or not the meridional component can be explained by other mechanisms, the presence of substantial meridional winds was not anticipated before the tidal model.

It is evident that topography has a substantial effect on near-surface winds—the dune orientation can veer by some 45° over just 10 km. Also, it may be that the bright region in Fig. 3 acts to straighten the windflow, suppressing the fluctuating component and yielding a unidirectional wind in which transverse dunes appear (see also figs. S1 and S2 for terrestrial analogs). The presence of the transverse features also, incidentally, rules out an erosional rather than depositional origin. Terrestrial dunes—the best examples being in the Namib and Sahara, with many other examples in the Australian and Arabian deserts—are typically a third as wide as their crest spacing (*13*), a geometry we also observe on Titan. This ratio indicates an ample sand supply—some terrestrial dune fields have much wider spacing.

The dunes' generally radar-dark appearance (also typical for radar images of terrestrial dunes; see supporting online text) is consistent with a smooth surface at our radar wavelength, suggesting that the dunes are made of fine

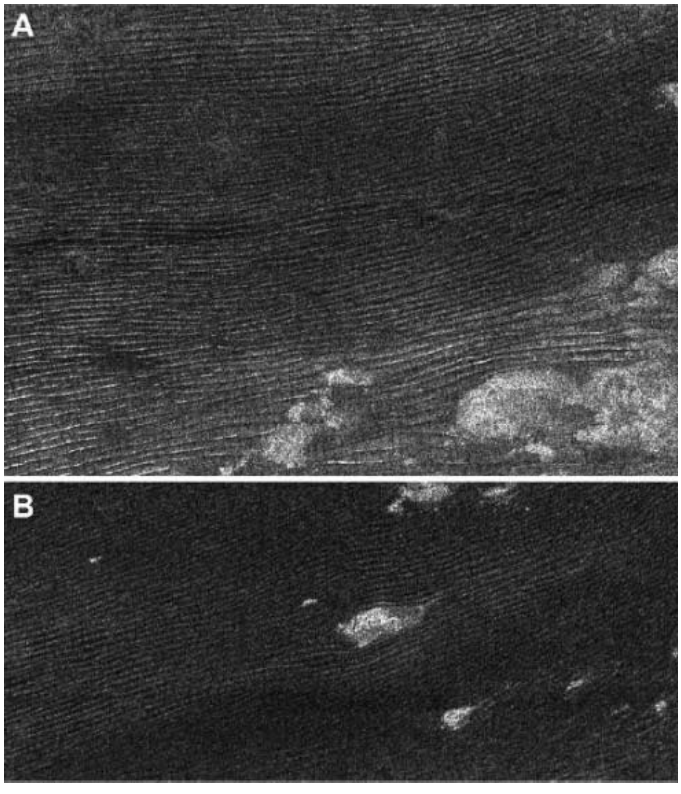

Fig. 1. (**A**) A 235 km by 175 km segment (north up) of the Belet sand sea at ~12°S, 100°W. Topographic glints are evidence of slopes facing the observer (radar illumination is from above). The subparallel orientation of the dunes and the 1:2 dune:interdune gap ratio are typical of longitudinal dunes on Earth. (**B**) Segment (235 km by 80 km) to the east of (A). Bright areas are small hills; the flow diverges around them and reconverges. A tail toward the right is evident in the lower hill, suggesting an east-northeast transport direction.

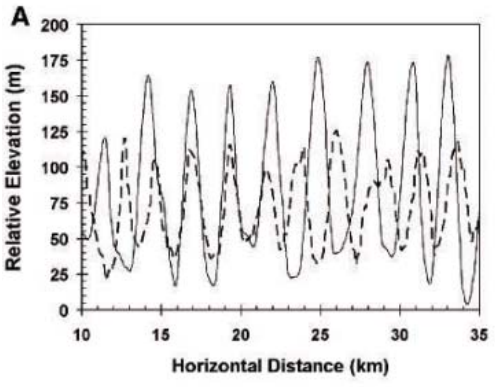

Fig. 2. (**A**) Radarclinometric profile of the Titan dunes shown in Fig. 1A (solid line). The spacing and height are typical of Namib desert dunes (B), a typical profile of which is shown by the dashed line (from Shuttle Radar Topography Mission data). (**B**) Handheld digital camera image of Namib sand sea showing undulating topography (see also fig. S2 and supporting online text.)

material with at most shallow ripples. Their composition is unknown—likely candidates are organic solids or water ice or some mixture thereof [silicates cannot be excluded but are less likely (*19*)]. At the large scale (50 km) observed by radar scatterometry, the sand seas are comparatively radar-dark too; in contrast, microwave radiometry indicates brightness temperatures 3 to 5 K above that of their surroundings, implying a high emissivity, i.e., low–dielectric constant material and little volume scattering, both consistent with a sand of ice/organic composition. It has been noted that the large low-albedo (optical and near-IR) regions on Titan appear to be concentrated around the equator (*8*, *20*). It also appears that radar sand seas and smaller dune fields correlate with low-latitude optically dark regions, notably Belet (Fig. 3) This in turn suggests that most or all of the equatorial dark regions may be covered in the dune material. One feature of the model tidal wind field is that the orbit-averaged winds at latitudes between 45°N and 45°S are directed equatorward [figure 6 of (*5*)]. An intriguing possibility is, therefore, that dark sediments may have been transported from higher latitudes to the equatorial sand seas by the tidal winds, forming this dark belt. Also, the predicted net meridional transport is weaker at 30° N (T3 region) where streaks are principally in an east-west direction, while there is a consistent east-northeast trend at 10°S (T8), where the average tidal wind has a northward flow of $\sim$0.25 ms^{-1}. Some high-latitude optically dark regions [e.g., the center of the TA swath (*7*)] have no apparent aeolian features—it may be that dark material blankets these areas, forming a sand sheet, but that it has not been swept into dunes either because winds are weaker or the ground is not dry. In this connection, our observation of dunes so far only at low latitudes is consistent with a recent model (*21*) of Titan's seasonally varying climate and methane hydrological cycle that predicts that Titan's equatorial regions should be dry, whereas higher latitudes have higher humidity and precipitation.

Fig. 3. A 515 km by 200 km segment of the T8 swath where the longitudinal dunes creeping from the left (west) encounter what appears to be a broad bright topographic rise. As the sand flows around this obstacle, it forms transverse dunes at the southwestern side before the longitudinal pattern resumes. Such a pattern confirms a depositional origin and is the only prominent example of dunes other than longitudinal ones observed so far.

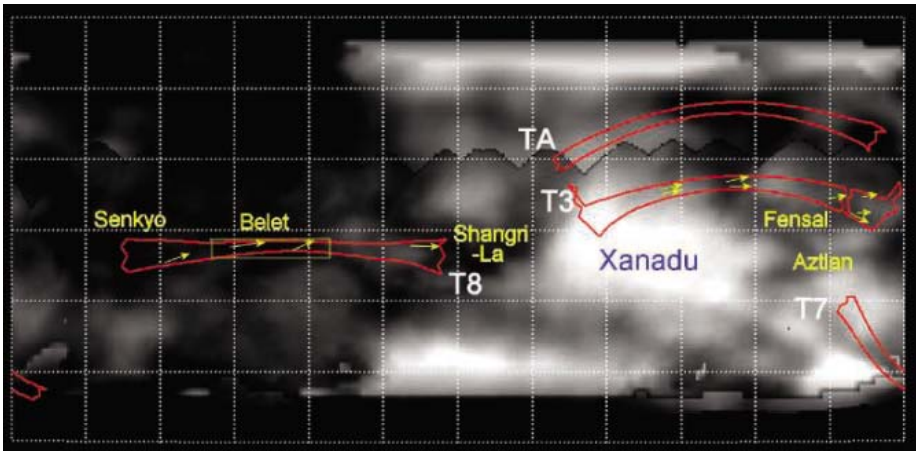

Fig. 4. Distribution and large-scale orientation of the aeolian features are indicated with yellow arrows, shown on a basemap (cylindrical projection, centered on the antisaturn point at 180°W, 30° grid spacing) derived from Hubble Space Telescope (HST) (*18*) and Cassini ISS (*8*) data. IAU names for dark albedo regions and the Xanadu bright terrain are indicated (a map with up-to-date names is maintained at http://planetarynames.wr.usgs.gov/index.html). Yellow box indicates the dunefield from which Fig. 1 is extracted. Red regions show radar imaging swaths to date (labeled TA, T3, T7, and T8); note the low-albedo regions along T7 and at the center of TA where no aeolian features were seen—all at latitudes around 45° where winds may be low. The directions indicated by the dunes appear to deviate around bright areas, suggesting that these may act as topographic obstacles to flow.

Sand transport for dune formation occurs by a wind-driven bouncing process called saltation. The optimum particle diameter (*1*–*3*) for saltation on Titan is $\sim$0.18 to 0.25 mm (larger particles have a higher weight:area ratio and are thus more difficult for wind to lift; smaller particles tend to clump together—there is thus an optimum size for which the threshold windspeed for transport by saltation is a minimum). The ease of transport in Titan's low gravity and thick atmosphere makes the optimum size somewhat larger than for Earth, Venus, and Mars (75, 75, and 115 μm, respectively), and the freestream windspeeds required for saltation are $\sim$0.1 to 0.7 ms^{-1} (*22*).

Near-surface winds predicted by the tidal model (*5*) are $\sim$0.5 ms^{-1}. Doppler tracking of the Huygens probe (*18*) indicates that winds in the lowest 5 km of descent were $\sim$1 ms^{-1}. Optical tracking by the Descent Imager and Spectral Radiometer experiment (*9*) permitted the Huygens probe's drift in the wind to be measured at $\sim$1 ms^{-1} near 2- to 3-km altitude, dropping to 0.3 ms^{-1} "close to the surface" (the last probe images from which such tracking is derived were acquired at altitudes of 200 to 300 m). Notably, in contrast to the eastward drift higher in the atmosphere, the wind near the surface blew the probe in a west-northwest direction. An analysis of the advective cooling of the Huygens probe (*23*) suggests that winds in the lowest 1 m were $\sim$0.2 ms^{-1} or less for the hour observed on the surface. It is likely that wind stress exceeds the transport threshold for only a small fraction of the time, but even the data at hand suggest winds broadly comparable with the saltation thresholds.

It is not clear how sand may be produced on Titan (*4*) because the thick atmosphere tends to inhibit explosive volcanism and many erosive processes. However, images from the Huygens probe (*9*) show clear evidence of fluvial activity at the landing site (9°S, 192°W), including rounded boulders, suggesting that particles can be generated in this way. Inspection of our radar images also indicates a number of areas where fluvial channels are present (*24*). Although channels and dunes can be within some tens of km of each other, we have so far not observed clear superposition of one on the other (*11*), nor have we so far identified obvious sand source regions anywhere. As on Earth, dunes may be formed on geologically short time scales (see supporting online text).

The existence of these dunes, their pristine appearance, and their superposition on other features tells us that in the geologically recent past, and quite probably the present, fine-grained and nonsticky (i.e., "dry") material has been moved across Titan's surface by wind. Because the net transport direction appears inclined at a small angle to eastward, it seems that if sand has migrated across large latitude ranges, the sand has circumnavigated Titan several times while doing so, apparently supporting a tidal wind model and arguing for an absence of standing liquids that would trap the sand [an absence of low-latitude lakes is also indicated by the lack of detection of specular reflections (*25*)]. The extent of the sand seas requires an origin for $\sim 10^4$ to 10^5 km^3 of sand-sized material, considerably more than would be produced by impact ejecta (*3*). It may be that fluvial erosion of ice bedrock by liquid methane is able to produce this fine material. This would then somehow have to dry out, placing constraints on Titan's meteorology. An alternative origin, perhaps supported by the optically dark appearance of the sand seas, is Titan's stratospheric methane photochemistry, which over 4.5 billion years of solar system history may have produced up to 10^6 to 10^7 km^3 of hydrocarbons and nitriles, 10% of which would be solid (*26*). At issue is how this organic material is sorted and modified to produce the equivalent (in size and material properties) of sand.

Much work remains to fully characterize the distribution, morphology, and composition of these features in data already acquired and the much larger data sets anticipated in Cassini's nominal and extended missions from RADAR and from other instruments, and to relate the features to the windfield and planetary-scale cycles of sediment generation and transport. However, the morphology of these beautiful features, familiar to us from terrestrial arid regions, is a comforting sign that even though the environment and working materials on Titan are exotic, the physical processes that shape Titan's surface (*19*) can be understood and studied here on Earth.

References and Notes

1. M. Allison, in *Proceedings Symposium on Titan, Toulouse, France, 9-12 September 1991*, B. Kaldeich, Ed. (European Space Agency SP-338, Noordwijk, Netherlands, 1992), pp. 113–118.
2. R. Greeley, J. Iverson, *Wind as a Geological Process* (Cambridge Univ. Press, Cambridge, 1985).
3. R. D. Lorenz, J. I. Lunine, J. A. Grier, M. A. Fisher, *J. Geophys. Res. (Planets)* **88**, 26377 (1995).
4. R. D. Lorenz, J. Mitton, *Lifting Titan's Veil* (Cambridge Univ. Press, Cambridge, 2002).
5. T. Tokano, F. M. Neubauer, *Icarus* **158**, 499 (2002).
6. R. D. Lorenz, in *Proceedings Symposium on Titan, Toulouse, France, 9-12 September 1991*, B. Kaldeich, Ed. (European Space Agency SP-338, Noordwijk, Netherlands, 1992), pp. 119–123.
7. C. Elachi *et al.*, *Science* **308**, 970 (2005).
8. C. C. Porco, *Nature* **434**, 159 (2005).
9. M. G. Tomasko *et al.*, *Nature* **438**, 765 (2005).
10. R. Greeley, *Planetary Landscapes* (Allen and Unwin, Boston, MA, 1987).
11. C. Elachi *et al.*, *Nature,* in press.
12. N. Lancaster, *The Geomorphology of Desert Dunes* (Routeledge, London, 1995).
13. R. Bagnold, *Physics of Wind-Blown Sand and Desert Dunes* (Methuen, London, 1941).
14. P. Lee, P. C. Thomas, *J. Geophys. Res.* **100**, 5381 (1995).
15. K. S. Edgett, M. C. Malin, *Lunar Planet. Sci.* **XXXI**, 1070 (2000).
16. D. Rubin, H. Ikeda, *Sedimentology* **37**, 673 (1990). See also (*27*).
17. J. M. Huthnance, *Estuarine Coastal Shelf Sci.* **14**, 79 (1982).
18. M. K. M. Bird, *Nature* **438**, 800 (2005).
19. R. D. Lorenz, J. I. Lunine, *Planet. Space Sci.* **53**, 557 (2005).
20. P. H. Smith *et al.*, *Icarus* **119**, 336 (1996). See also (*28*, *29*).
21. P. Rannou, F. Montmessin, F. Hourdin, S. Lebonnois, *Science* **311**, 201 (2006).
22. Transport occurs when the wind's friction speed U_* exceeds the threshold friction speed for saltation U_{*t}. U_* is a measure of wind stress that is related to the roughness-dependent drag coefficient C_d (typically 0.002 to 0.01) and the freestream windspeed U as $(U_*/U)^2 \sim C_d$; thus, the freestream threshold speed is ~10 to 25 times the friction speed. The optimum threshold speed has been estimated (*1–3*), depending on assumed density, etc., as $U_{*t} \sim 0.01$ to 0.03 ms^{-1}, and thus dune formation requires freestream windspeeds of 0.1 to 0.7 ms^{-1}. The corresponding Reynolds number range is 15 to 100.
23. R. D. Lorenz, *Icarus,* in press.
24. See http://photojournal.jpl.nasa.gov/catalog/PIA07366.
25. R. A. West, M. E. Brown, S. V. Salinas, A. H. Bouchez, H. G. Roe, *Nature* **436**, 670 (2005).
26. Y. L. Yung, M. A. Allen, J. Pinto, *Astrophys. J. Suppl.* **55**, 465 (1984).
27. S. Fryberger, G. Dean, in *A Study of Global Sand Seas*, E. D. McKee, Ed. (U.S. Geol. Surv. Prof. Pap. 1052, U.S. Government Printing Office, Washington, DC, 1979), pp. 137–169.
28. M. Hartung *et al.*, *Astron. Astrophys.* **421**, L17 (2004).
29. H. G. Roe *et al.*, *Geophys. Res. Lett.* **31**, L17S03 (2004).

30. We gratefully acknowledge those who designed, developed, and operate the Cassini/Huygens mission. The Cassini/Huygens Project is a joint endeavor of NASA, the European Space Agency (ESA), and the Italian Space Agency (ASI) and is managed by the Jet Propulsion Laboratory, California Institute of Technology, under a contract with NASA.

Supporting Online Material

www.sciencemag.org/cgi/content/full/312/5774/724/DC1
Materials and Methods
SOM Text
Figs. S1 and S2

30 November 2005; accepted 22 February 2006
10.1126/science.1123257

Interstellar Chemistry Recorded in Organic Matter from Primitive Meteorites

Henner Busemann,[1]* Andrea F. Young,[1] Conel M. O'D. Alexander,[1] Peter Hoppe,[2] Sujoy Mukhopadhyay,[1]† Larry R. Nittler[1]

Organic matter in extraterrestrial materials has isotopic anomalies in hydrogen and nitrogen that suggest an origin in the presolar molecular cloud or perhaps in the protoplanetary disk. Interplanetary dust particles are generally regarded as the most primitive solar system matter available, in part because until recently they exhibited the most extreme isotope anomalies. However, we show that hydrogen and nitrogen isotopic compositions in carbonaceous chondrite organic matter reach and even exceed those found in interplanetary dust particles. Hence, both meteorites (originating from the asteroid belt) and interplanetary dust particles (possibly from comets) preserve primitive organics that were a component of the original building blocks of the solar system.

Carbonaceous chondrites, the most primitive meteorites, and interplanetary dust particles (IDPs), primitive dust collected in Earth's stratosphere, contain up to ~2 and ~35 weight percent C in organic matter, respectively. This organic matter may represent an important source of prebiotic molecules that were essential for the origin of life on Earth (*1*). Most of the organic matter is insoluble in demineralizing acids and organic solvents, and this proportion is probably macromolecular (*1*). Isotope anomalies in H and N suggest that this insoluble organic matter (IOM) is probably interstellar material that, like other presolar materials, has survived the formation of the solar system to be incorporated into planetesimals (*2–6*), but it may also include material that formed in the cold outer regions of the solar protoplanetary disk (*7*). Heating, mixing, and chemical reactions in the collapsing protosolar cloud, in the protoplanetary disk, and during accretion of the parent bodies of meteorites and IDPs could have altered—or erased—the initial isotope signatures of interstellar IOM. Aqueous alteration and thermal metamorphism on the parent bodies of meteorites and IDPs have further modified the organic carriers of these

[1]Department of Terrestrial Magnetism, Carnegie Institution of Washington, 5241 Broad Branch Road, NW, Washington, DC 20015, USA. [2]Max-Planck-Institut für Chemie (Otto-Hahn-Institut), Becherweg 27, D-55128 Mainz, Germany.

*To whom correspondence should be addressed. E-mail: busemann@dtm.ciw.edu
†Present address: Department of Earth and Planetary Sciences, Harvard University, 20 Oxford Street, Cambridge, MA 02138, USA.

Table 1. δD and $\delta^{15}N$ in carbonaceous chondrites, as measured by SIMS and NanoSIMS (*13*) (n.m., not measured). The hotspots are manually defined regions of ≥1.3 μm (δD) and ≥500 nm ($\delta^{15}N$), respectively. "Heterogeneity" has been parameterized with the fraction of automatically created regions of interest [ROIs (*13*)] that are isotopically anomalous. We added up all ROIs with $|\delta D_{ROI} - \delta D_{average}| > 3 \times \sigma_{ROI}$ and $\sigma_{ROI} < 25\%$. Note that all hotspot values are lower limits because their sizes are comparable to the spatial resolution of the imaging techniques.

Meteorite	Class	δD				$\delta^{15}N$			
		Maximum, hotspot	Bulk IOM (*14*)	Analyzed area (μm²)	Heterogeneity (area %)	Maximum, hotspot	Bulk IOM (*14*)	Analyzed area (μm²)	Heterogeneity (area %)
				IOM					
GRO 95577	CR1	19,400 ± 4,600	2973	11,780	0.6	1510 ± 240	233.2	1440	0.04
EET 92042	CR2	16,300 ± 2,100	3004	13,112	2.4	1770 ± 280	185.5	1937	1.0
Al Rais	CR2	14,300 ± 3,900	2658	6,261	0.3	1740 ± 350	146.3	3480	0.005
Murchison	CM2	1,740 ± 280	712	738	4.3	n.m.	n.m.	n.m.	n.m.
Bells	Anomalous CM2	9,700 ± 2,100	3283	5,702	0.3	3200 ± 700	415.3	2844	0.11
				Matrix					
Al Rais	CR2	6,200 ± 650		867	6.2	2000 ± 200		637	0.03
Tagish Lake	Ungrouped C2	8,600 ± 1,000		3,963	2.9	410 ± 130		1234	0.10

isotope anomalies and exchanged them with isotopically normal matter. The detection of isotope anomalies indicates that the pristine character of the IOM has not been entirely lost.

Until now, the most extreme enrichments in D (*8*) and ^{15}N (*9*) have been found in so-called hotspots (regions that are extremely isotopically enriched relative to the surrounding matter) in anhydrous cluster IDPs, which may originate from comets. In contrast, IOM from meteorites, whose parent bodies are in the asteroid belt, showed bulk isotope anomalies that were relatively small relative to those in IDP hotspots (*6*, *10*). This difference was assumed to be the result of the more severe parent body alteration and possibly nebular processing [e.g., (*11*)] experienced by meteorites. However, very few analyses [e.g., (*12*)] on meteorites have been carried out on the same spatial scales as the IDP studies.

Here we report D and ^{15}N hotspots in meteoritic IOM that are comparable to, or even exceed, those reported in IDPs. Thus, organic matter that is as primitive as that found in IDPs survives in some meteorites (Table 1), despite the more extensive alteration experienced by the meteorites on their parent bodies. This means that large samples of primitive organic matter can be prepared from meteorites for studies that would not be possible with IDPs, which typically have masses on the order of 10^{-12} g.

We analyzed matrix fragments from two carbonaceous chondrites (Al Rais and Tagish Lake) and IOM separates from five carbonaceous chondrites [Grosvenor Mountains (GRO) 95577, Elephant Moraine (EET) 92042, Al Rais, Murchison, and Bells] (Table 1) by imaging secondary ion mass spectrometry (*13*). All samples exhibited large isotopic heterogeneities [δD ~1700 to 19,400 per mil (‰), $\delta^{15}N$ ~400 to 3200‰; the δ notation gives measured isotopic ratios as deviations from terrestrial standards] on scales comparable to the spatial resolutions of the instruments (Table 1) (*13*). The most extreme D/H values were found in pure IOM separates. Because the hotspots survive the chemical separation procedure and exhibit a range of compositions, the hotspots appear to be robust units that formed in a range of environments. Figure 1A is a D/H map of an IOM sample from EET 92042 (a Renazzo-type, or CR2, chondrite recovered in Antarctica) that contains two large D hotspots and several smaller ones. The δD values for one of these (16,300 ± 2100‰) and for a similar hotspot in GRO 95577 (19,400 ± 4600‰) are the largest ever reported for meteoritic material. In total, D hotspots in EET 92042 IOM made up ~1.5% of the area analyzed (Table 1). Note that the bulk IOM has a δD value of ~3000‰ (*14*),

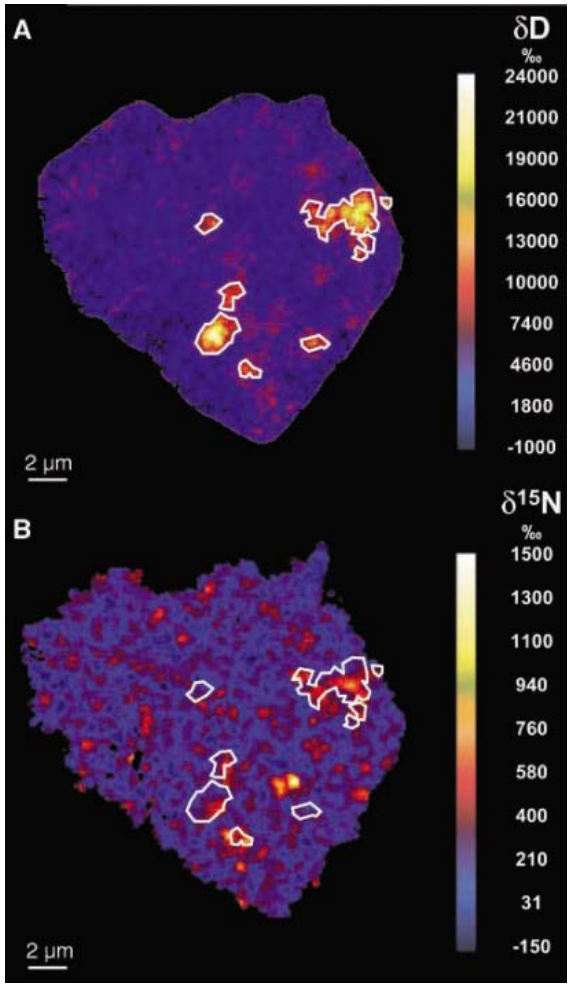

Fig. 1. Maps of (**A**) δD and (**B**) $\delta^{15}N$ in a sample of IOM from the CR2 chondrite EET 92042. Most D and ^{15}N hotspots in EET 92042 (δD up to 16,300% and $\delta^{15}N$ up to 1770‰) are not spatially associated.

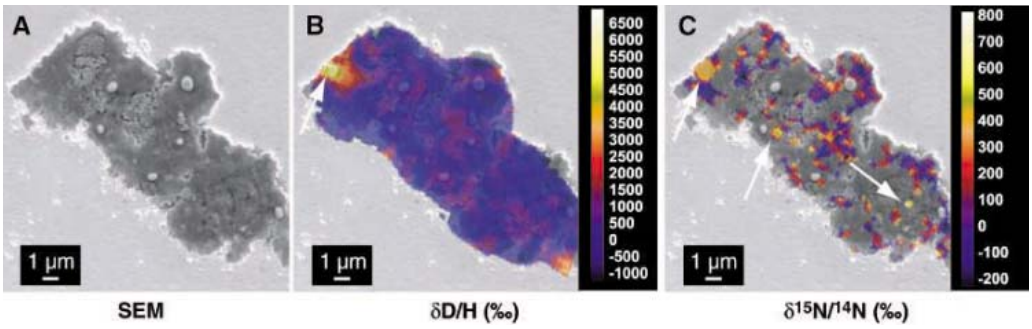

Fig. 2. (**A**) Scanning electron micrograph (secondary image) of a matrix fragment of Tagish Lake. (**B**) The overlaid δD map shows two D hotspots. (**C**) The overlaid $^{15}N/^{14}N$ map shows hotspots with $\delta^{15}N$ values up to ~400‰ (arrows). The largest of these [at upper left, arrow in (B)] is also D-rich and is spatially related to a round carbonaceous region discernable in (A). These hotspots likely correspond to the "nano-globules" observed in this meteorite (*13*, *30*).

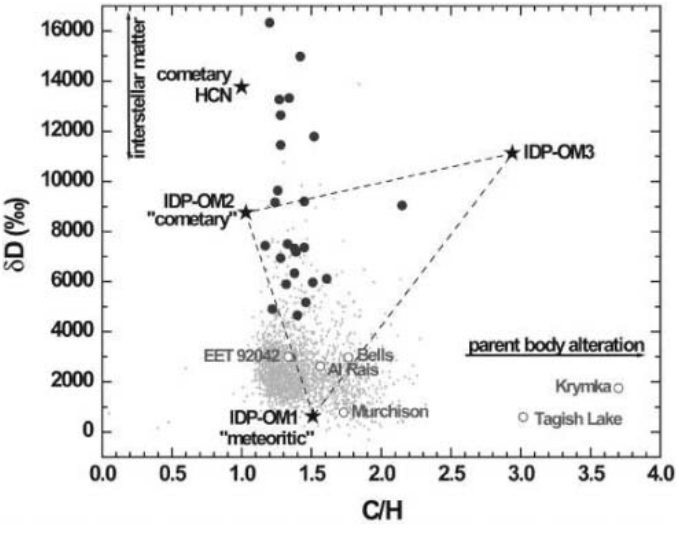

Fig. 3. δD and C/H (atomic) in the IOM of EET 92042. The most D-rich regions ("hotspots," solid circles) exhibit δD values between 4500 and 16,300‰. These values exceed those of suggested end members in the organic matter of IDPs (stars, OM1 to OM3) (*28*) and reach the δD value of cometary HCN ice (*31*). The average of automatically defined image subregions 2 μm in diameter (gray dots) (*13*) is 2613‰, close to 3004‰ given for EET 92042 bulk IOM (open circle) (*14*), which indicates that sputtering equilibrium is reached and terrestrial contamination was not important for the EET 92042 measurements. Data from bulk IOM analyses of the same meteorites that are analyzed here are given for comparison (open circles) (*14*). Thermal alteration results in higher C/H values and ultimately homogeneous and low δD values.

and therefore these hotspots make only a small contribution to the bulk composition. This is true of all analyzed IOM. Regions that are highly D-enriched have also been found in matrix fragments of Al Rais and Tagish Lake (Fig. 2).

The meteoritic IOM and matrix fragments also exhibit substantial spatial heterogeneity in their N isotopic compositions (Fig. 1B). EET 92042 has a bulk $\delta^{15}N$ of 185‰ (*14*) but has numerous regions with higher values up to $\delta^{15}N = 1770 \pm 280$‰. Bells IOM shows even larger enrichments in ^{15}N than does EET 92042, both in bulk (415‰) and in several hotspots with extreme $\delta^{15}N$ values between 2000 and 3200‰. These values are the highest ever reported for extraterrestrial material, except in presolar circumstellar grains (*15*). Note that the $\delta^{15}N$ values are relative to terrestrial atmospheric N, but the Sun has isotopically lighter N [$\delta^{15}N \leq -240$‰, e.g., (*16*)]. The enrichments reported here are therefore even larger relative to the solar value (2100 to 5400‰). The δD values given here are relative to ocean water, which is also isotopically much heavier than was the initial solar H [$\delta D \approx -870$‰ (*17*)].

There is no general spatial correlation between H and N isotopes in any of the measured samples (Fig. 1). Although some D hotspots are relatively ^{15}N-enriched, the largest ^{15}N enrichments of >1000‰ are not spatially related to D hotspots; this indicates that the most extreme anomalies are generally in different molecular carriers and probably formed through different chemical pathways.

Our data show that highly anomalous matter survived essentially unaltered in the parent bodies of primitive meteorites. δD values of up to ~19,000‰ and $\delta^{15}N$ values above 3000‰ indicate that a complete homogenization of the pristine IOM did not occur. D enrichments comparable to those found in the IOM of the CR chondrites (Table 1) were previously observed only in two fragments of a cluster IDP (*8*, *18*). Also, the highest observed $\delta^{15}N$ hotspot values (~2000 to 3200‰ in Bells, 1770‰ in EET 92042) far exceed the highest value of 1270 ± 25‰ found in IDPs (*9*, *19*). The parent bodies of the cluster IDPs (possibly Kuiper Belt comets) have been assumed to contain the most primitive matter in solar system objects (*8*). The new results imply that the parent bodies of both meteorites and IDPs acquired a comparably primitive assemblage of organic matter that survives in meteorites despite the more extensive processing that they experienced.

The largest D enrichment previously reported in a meteorite (δD ~8000‰) was found by ion microprobe imaging of a matrix fragment of the CR2 chondrite Renazzo (*12*). We found comparable D enrichments in Al Rais (CR2) matrix, and even higher δD values (>14,000‰) in IOM separates from three CR chondrites. These observations support the view, based on N isotopes in bulk samples, that CR chondrites are the carbonaceous chondrite group that preserved the most primitive organic matter (*6*). Bells IOM is even more isotopically anomalous than that of the CR chondrites, but Bells appears to be unique among the CM chondrites. The presence of D and ^{15}N hotspots in the matrix of the ungrouped C2 chondrite Tagish Lake (Table 1) shows that primitive organics have survived in this meteorite, even though nuclear magnetic resonance studies (*20*) have revealed that bulk Tagish Lake IOM has been substantially altered by oxidation and is less primitive than the CR2 IOM. Microscopic analyses are necessary to fully understand the survival and alteration of pristine organics in meteorites; our micro-scale isotope examination of meteoritic components allows for the localization of these primitive organic components for further investigation.

The isotopic anomalies observed here must have originated either in cold interstellar clouds, where large δD values have been observed and large $\delta^{15}N$ values have been predicted (*2*–*6*), or in the outer regions of the protoplanetary disk (*7*), where large D enrichments have been predicted for gas-phase molecules. Viable mechanisms for producing large δD and $\delta^{15}N$ values in either environment are low-temperature (~10 K) ion-molecule reactions in the gas phase and catalytic processes on dust grains. An interstellar origin is supported by the similarity of the IOM infrared and ultraviolet (UV) spectra to interstellar medium features of refractory organics (*21*, *22*). Moreover, the presence of circumstellar grains in meteorites and IDPs shows that interstellar

matter did survive the formation of the solar system. Finally, it has yet to be demonstrated that isotope anomalies formed in simple molecules in the outer protoplanetary disk could be transferred into the large amounts of complex organics eventually incorporated into the chondrite parent bodies. Therefore, we favor an interstellar origin. Regardless of where the anomalous material originated, the decoupled H and N systems indicate a variety of formation processes for the components of the organic matter.

The ^{15}N enrichments observed here in the IOM of Bells and EET 92042 and in IDPs (*9*) far exceed the maximum model predictions for interstellar chemistry [$\delta^{15}N \sim 800‰$ in certain molecules relative to the starting composition, (*3*, *4*)]. A stellar, nucleosynthetic origin of these ^{15}N enrichments is unlikely because, with one exception (*13*, *23*), the C isotopic compositions of ^{15}N hotspots did not exhibit the extreme anomalies indicative of nucleosynthesis ($^{12}C/^{13}C \approx 0.01$ to 100 × solar ratio) typically found in meteoritic presolar grains (*15*). It is also unlikely that isotopically anomalous N from circumstellar grains has been redistributed into interstellar organic matter with essentially normal C isotopic composition. Likewise, ^{13}C anomalies associated with ^{15}N enrichments in IDPs are rare (*9*). Stellar sources of ^{15}N-rich dust, such as novae, are only minor contributors to the dust in the Galaxy, and most (>90%) N-bearing circumstellar dust grains found in meteorites are enriched in ^{14}N (*15*).

The $\delta^{15}N$ values between 1000‰ and 3200‰ reported here require a new mechanism for enriching ^{15}N. Elevated $^{15}N/^{14}N$ values could have been produced by UV self-shielding in regions of the solar nebula (*24*) or protosolar cloud, where, because of the much greater abundance of ^{14}N, the $^{14}N_2$ UV absorption lines are saturated but not the $^{15}N^{14}N$ and $^{15}N_2$ lines. However, the potential magnitude of the enrichments that would ultimately be transferred to the IOM is unknown. Oxygen isotope anomalies in meteoritic minerals have been attributed to UV self-shielding, but these anomalies are only on the order of 50‰. Much larger O isotope anomalies measured in rare silica grains located in organic separates from Murchison (*25*) have been attributed to particle irradiation of matter by the early active Sun. However, such a scenario cannot explain the D enrichments in organic matter. This and the mostly uncorrelated occurrence of D and ^{15}N hotspots suggest that different mechanisms were responsible for the isotope anomalies found in H, N, and O.

Whether the D and ^{15}N enrichments in the IOM were established in the protosolar cloud or the protoplanetary disk, the presence of similar material in both meteorites and IDPs provides insights into the conditions that prevailed during the formation of the asteroid belt. The parent bodies of the chondritic meteorites probably formed in restricted regions within the asteroid belt at ~3 AU from the Sun. The organic molecules are much more fragile than the presolar circumstellar grains found in meteorites. The presence of organic C shows that the ambient temperature in the asteroid belt was low at the time of asteroid accretion, and that (i) the ambient temperature was always low, or (ii) the organics were introduced when the ambient temperatures in the asteroid belt were sufficiently low for their survival. The introduction of organic matter into the asteroid belt could be the result of continuing infall of interstellar material onto the protoplanetary disk, or transport of material from greater radial distances in the disk [e.g., through turbulent mixing (*26*)]. Radial mixing of organic matter into the asteroid belt would be consistent with the inference, based on the observation of crystalline silicates in comets, that such mixing was important in the early solar system [e.g., (*26*, *27*)]. The cometary and asteroidal parent bodies of IDPs and primitive meteorites may have sampled to varying degrees the same reservoirs of presolar material (interstellar organic matter, amorphous silicates, and circumstellar grains) and crystalline silicate-dominated material that was processed in the inner solar nebula (*13*).

Although the IOM in primitive meteorites is isotopically very heterogeneous on a scale of ~0.1 to 1.5 μm (Fig. 1), as is the case for IDPs (*8*, *9*), the most extreme D and ^{15}N hotspots have C/H abundances that are typical of the bulk IOM (Fig. 3). However, isotopic imaging of IDPs has led to the suggestion that extraterrestrial organic matter is a mixture of three components (labeled OM1 to OM3) with distinct H and N isotopic compositions and C/H ratios [(*28*) and references therein]. These observations are not reproduced by meteoritic IOM (Fig. 3). The bulk IOM in many primitive meteorites is already much more D-rich [up to $\delta D \sim 3000‰$ (*14*)] than the OM1 component in IDPs ($\delta D \sim 630‰$) that has been suggested to resemble typical IOM in carbonaceous chondrites. All D hotspots show C/H ratios that are similar to those of the bulk IOM of the respective meteorites (Fig. 3). This is not the result of a more thorough mixing of the various organic phases in meteorites relative to IDPs, because the highest values for δD and $\delta^{15}N$ in meteorites found here are more extreme than those of OM2 and OM3. IOM in meteorites is not represented by the three end-member components deduced from IDPs.

References and Notes

1. I. Gilmour, in *Treatise on Geochemistry, Volume 1—Meteorites, Comets, and Planets*, H. D. Holland, K. K. Turekian, A. M. Davis, Eds. (Elsevier-Pergamon, Oxford, 2003), pp. 269–290.
2. S. A. Sandford, M. P. Bernstein, J. P. Dworkin, *Meteorit. Planet. Sci.* **36**, 1117 (2001).
3. R. Terzieva, E. Herbst, *Mon. Not. R. Astron. Soc.* **317**, 563 (2000).
4. S. B. Charnley, S. D. Rodgers, *Astrophys. J.* **569**, L133 (2002).
5. Y. Aikawa, E. Herbst, *Astrophys. J.* **526**, 314 (1999).
6. C. M. O'D. Alexander *et al.*, *Meteorit. Planet. Sci.* **33**, 603 (1998).
7. Y. Aikawa, G. J. van Zadelhoff, E. F. van Dishoeck, E. Herbst, *Astron. Astrophys.* **386**, 622 (2002).
8. S. Messenger, *Nature* **404**, 968 (2000).
9. C. Floss *et al.*, *Science* **303**, 1355 (2004).
10. F. Robert, *Space Sci. Rev.* **106**, 87 (2003).
11. G. R. Huss, A. P. Meshik, J. B. Smith, C. M. Hohenberg, *Geochim. Cosmochim. Acta* **67**, 4823 (2003).
12. Y. Guan, A. Hofmeister, S. Messenger, R. M. Walker, *Lunar Planet. Sci.* **XXIX**, 1760 (1998).
13. See supporting material on *Science* Online.
14. C. M. O'D. Alexander, M. L. Fogel, G. D. Cody, *Meteorit. Planet. Sci.* **40**, A15 (2005).
15. L. R. Nittler, *Earth Planet. Sci. Lett.* **209**, 259 (2003).
16. K. Hashizume, M. Chaussidon, B. Marty, F. Robert, *Science* **290**, 1142 (2000).
17. J. Geiss, G. Gloeckler, *Space Sci. Rev.* **106**, 3 (2003).
18. S. Messenger, F. J. Stadermann, C. Floss, L. R. Nittler, S. Mukhopadhyay, *Space Sci. Rev.* **106**, 155 (2003).
19. Large ^{15}N enrichments (up to $\delta^{15}N \sim 2500‰$) have been found in CB and CH chondrites [e.g., (*29*)]. However, the origin of these anomalies is unknown and their carriers may be secondary phases.
20. G. D. Cody, C. M. O'D. Alexander, *Geochim. Cosmochim. Acta* **69**, 1085 (2005).
21. Y. J. Pendleton, S. A. Sandford, L. J. Allamandola, A. G. G. M. Tielens, K. Sellgren, *Astrophys. J.* **437**, 683 (1994).
22. J. Bradley *et al.*, *Science* **307**, 244 (2005).
23. One 5-μm^2 region in EET 92042 IOM is isotopically anomalous in both N and C ($\delta^{15}N = 1150 \pm 40‰$, $\delta^{13}C = -113 \pm 14‰$), a composition closely similar to a putative interstellar C grain reported in an IDP (*9*). All other observed C anomalies originate from presolar SiC grains (*15*) embedded in the samples.
24. R. N. Clayton, *Lunar Planet. Sci.* **XXXIII**, 1326 (2002).
25. J. Aléon, F. Robert, J. Duprat, S. Derenne, *Nature* **437**, 385 (2005).
26. H.-P. Gail, *Astron. Astrophys.* **378**, 192 (2001).
27. D. H. Wooden, D. E. Harker, A. J. Brearley, *ASP Conf. Ser.* **341**, 774 (2005).
28. J. Aléon, F. Robert, *Icarus* **167**, 424 (2004).
29. N. Sugiura, S. Zashu, *Meteorit. Planet. Sci.* **36**, 515 (2001).
30. K. Nakamura, M. E. Zolensky, S. Tomita, S. Nakashima, K. Tomeoka, *Int. J. Astrobiol.* **1**, 179 (2002).
31. R. Meier *et al.*, *Science* **279**, 1707 (1998).

32. Supported by grants from NASA's Cosmochemistry and Origins of the Solar System program (C.M.O'D.A., L.R.N.) and by the NASA Astrobiology Institute. We thank the NASA Meteorite Working Group for the Antarctic meteorites, M. Zolensky for providing the Tagish Lake sample, G. Cody for sample preparation assistance, E. Gröner for technical assistance with NanoSIMS, and two anonymous reviewers for their helpful constructive comments. A.F.Y. thanks B. Minarik for support through a NSF Research Experience for Undergraduates program at the Carnegie Institution of Washington.

Supporting Online Material

www.sciencemag.org/cgi/content/full/312/5774/727/DC1
Materials and Methods
SOM Text
References

14 December 2005; accepted 6 March 2006
10.1126/science.1123878

Lower Cambrian Vendobionts from China and Early Diploblast Evolution

D.-G. Shu,[1,2]* S. Conway Morris,[3]* J. Han,[1] Y. Li,[4] X.-L. Zhang,[1] H. Hua,[1] Z.-F. Zhang,[1] J.-N. Liu,[1] J.-F. Guo,[1] Y. Yao,[1] K. Yasui[5]

Ediacaran assemblages immediately predate the Cambrian explosion of metazoans and should have played a crucial role in this radiation. Their wider relationships, however, have remained refractory and difficult to integrate with early metazoan phylogeny. Here, we describe a frondlike fossil, *Stromatoveris* (*S. psygmoglena* sp. nov.), from the Lower Cambrian Chengjiang Lagerstätte (Yunnan, China) that is strikingly similar to Ediacaran vendobionts. The exquisite preservation reveals closely spaced branches, probably ciliated, that appear to represent precursors of the diagnostic comb rows of ctenophores. Therefore, this finding has important implications for the early evolution of this phylum and related diploblasts, some of which independently evolved a frondose habit.

Ediacaran assemblages represent Earth's earliest complex macroscopic organisms in the history of life (*1*). They lack skeletal hard parts but are relatively diverse (*1*, *2*), have a defined community structure (*3*), and show a global distribution (*2*). Yet their phylogenetic interpretation remains highly controversial. Radical reassignments to lichens (*4*) and fungi (*5*) have won little support (*1*, *6*), but the traditional assignments to animals (*7*) remain problematic. A few taxa can be compared, with varying degrees of reliability, to known animal groups, including sponges (*8*), cnidarians (*9*), mollusks (*10*), and arthropods (*11*). Most, however, remain in phylogenetic limbo because comparisons to either extant phyla or putative stem groups are frustratingly imprecise. The provocative vendobiont hypothesis (*12*–*14*) seeks to unify disparate taxa, including forms otherwise assigned to groups as separate as cnidarians and arthropods, on the basis of a distinctive body plan with a modular quilted construction and possibly syncytial tissue. If correct, this hypothesis has two major implications. First, did at least some vendobionts derive independently from protistans, or are they a sister group of either animals (*15*) or even diploblasts? Crucial in this respect are various frondlike fossils, some of which have been compared to the cnidarians, specifically the pennatulaceans (*7*, *16*), whereas others are clearly akin to other vendobionts (*12*, *17*).

Here, we describe eight specimens of *Stromatoveris psygmoglena* gen. sp. nov., (*18*) a frondose fossil from the Lower Cambrian Chengjiang Lagerstätte near Kunming, Yunnan, and interpret them as a new vendobiont (Figs. 1 and 2). Five of them, including the holotype, were collected near Meishucun, whereas the other three are from Jianshan, near Haikou. Specimens show preservation typical of other soft-bodied fossils from Chengjiang and therefore provide exceptional morphological detail. Presumably they were rapidly buried by storm events, and most are oriented at a shallow angle to the bedding plane. The split between part and counterpart is therefore oblique, necessitating composite reconstructions of each specimen (Figs. 1, C to E, and 2, B and C).

The body is foliate, with a bluntly terminating stalk that lacks obvious attachment structures (Figs. 1; A, C, D, and F; and 2; A, B, and D). Body length ranges between 2.5 and 7.5 cm. Orientations were adopted for convenience and imply no direct homologies with other organisms. Upper and lower surfaces are markedly different. The former bears prominent branches with quite pronounced relief. Most specimens are too incomplete to count the precise number of branches [typical width was circa (ca.) 1 mm], but in the holotype about 15 are visible on either side of the midline. The latter is defined by a relatively narrow groove (Figs. 1A and 2, A and E). The most proximal branches arise along an adaxially inclined line, but all branches

Fig. 1. The Cambrian vendobiont *S. psygmoglena*, gen. sp. nov. (**A**, **B**, and **G**) Holotype, ELI-Vend-05-001. (A) Upper surface, (B) fragment (counterpart) of lower surface, and (G) enlargement of the boxed area in (A). (**C** and **D**) ELI-Vend-05-002. (C) Composite photograph of upper and lower surfaces and (D) distal part of upper surface removed to reveal lower surface. (**E**) ELI-Vend-05-003, composite photo of part and counterpart to show both upper and lower surfaces. (**F**) ELI-Vend-05-004, composite photograph of part and counterpart to show upper surface and axial rod located between upper and lower surfaces.

[1]Early Life Institute and Key Laboratory of Continental Dynamics, Northwest University, Xi'an 710069, China. [2]School of Earth Sciences and Resources, China University of Geosciences, Beijing 100083, China. [3]Department of Earth Sciences, University of Cambridge, Downing Street, Cambridge CB2 3EQ, UK. [4]College of Earth Science and Land Resources, Chang'an University, Xi'an 710054, China. [5]Marine Biological Laboratory, Graduate School of Science, Hiroshima University, 2445 Mukaishima-cho, Onomichi, Hiroshima 722-0073, Japan.

*To whom correspondence should be addressed. E-mail: elidgshu@nwu.edu.cn (D.-G.S.); sc113@esc.cam.ac.uk (S.C.M.)

are parallel and fan distally at a shallow angle to the midline. Branches are mostly single, but occasionally they bifurcate or fuse in an irregular fashion (Figs. 1A and 2, A and E). In some specimens, branches were filled with sediment, suggesting that during life they were hollow tubes. The lateral margins of the branches show occasional short prongs or spurs. These may represent interconnections either between the branches or possibly into the interior of the frond. Branch numbers appear to have shown only a modest increase with body size, and differences in relative width in larger specimens suggest that the individual branches continued to grow. Distally, however, new branches can be seen to differentiate from the surface of the blade (Figs. 1A and 2, A and E).

The branches were evidently firmly attached to the body, but some branches show slight imbrication. The branches bear transverse, closely spaced striations (Figs. 1, A and G, and 2, A and B, and fig. S1, A and D), but there is no evidence for zooids. The regions between the branches were narrow and recessed, and in some specimens there are associated dark strands (Fig. 1; A, C, and E to G; and fig. S1; A, B, F, and G). These may have been discrete structures, possibly canal-like and presumably located in the body wall. They have irregular margins (Fig. 1E), which may have been extensions connecting to other regions of the body wall. Distal to the branches the surface of the frond is smooth, although a continuation of the midline occurs as a narrow meandering groove (Figs. 1A and 2A). This region was quite elongate (Figs. 1F and 2D) and in the living animal probably acutely tapered. Basal to the branches the midline area rapidly widens to define a more or less smooth stalk.

The lower region broadly appears to be divisible into two regions. More distally an ovoid central smooth area is strongly concave (Figs. 1D and 2B), but adjacent there are subdued ridges that run slightly oblique to the body margin and in the opposite direction to the branches on the upper surface. In addition, there is a diffuse ornamentation, roughly ovoid. More basally there is subdued ribbing and a prominent leopard-skin ornamentation, at least near the margin (Figs. 1B and 2A). The lower surface becomes smooth toward the basal region. One specimen (fig. S1, C and E) shows striking arcuate structures on the stem. Although these might be another type of surface ornamentation, they are interpreted as body-wall support, possibly collagenous.

The interior contains a substantial sediment fill (Figs. 1, C to E, and 2, C and D, and fig. S1B), more pronounced in the stalk, suggesting its cross section was approximately circular, whereas the blade was somewhat compressed. As with the branches, this sediment infill suggests the interior was largely hollow and possibly fluid-filled during the organism's life. An axial structure (ca. 0.4 mm across), with apparently ferruginous preservation, is located nearer to the upper surface. In one specimen (Figs. 1F and 2D), it has been partially excavated, and toward the base a similar structure occurs, but it runs transversely and possibly was rotated to its present position as a result of decay.

The organism was benthic and embedded in the seafloor by the stalk. Whether it lived upright or recumbent is less clear. The apparent rigidity of the axial structure would suggest the former orientation, whereas the subdued morphology of the lower surface, particularly the ovoid strongly concave smooth area (Figs. 1D and 2B), could be consistent with a recumbent mode. Mode of feeding is conjectural and depends in part on phylogenetic comparisons. Given the absence of definitive zooids, one possibility is that the branches were ciliated and served to transport food particles via the narrow grooves between the branches. Assuming a density of cilia comparable to typical suspension feeders, this would provide a highly effective trap. What appear to be interconnections between the branches (Figs. 1; A, E, and G; and 2; A and D) suggest an exchange system that presumably also connected to the interior. During the organism's life, the interior was presumably filled with fluid or gelatinous tissue. The central axis (Figs. 1F and 2D), analogous to the axial rod of pennatulaceans, presumably provided additional support, but no other internal organs are discernible.

Although it cannot be placed in any known genus, in overall form *Stromatoveris* is similar to a number of Ediacaran frondlike fossils. It is most similar to the otherwise poorly documented *Khatyspytia* (*19*), but the latter is more slender and has a larger number of shorter branches. General resemblances also exist with the fronds *Vaizitsinia* (*19*), *Charniodiscus* (*16*, *20*), *Glaessnerina* (*16*), and, more remotely, such forms as *Charnia* (*19*, *20*). The phylogenetic position of these Ediacaran fronds (and by implication *Stromatoveris*) is controversial (*21*), with opposing views favoring cnidarians, especially pennatulaceans (*7*, *16*), or vendobionts (*12*, *14*). Key points in these differing interpretations include attachment of the branches to the frond and absence of unequivocal evidence for zooids, both of which are inconsistent with the pennatulacean hypothesis. The axial structure has an obvious counterpart in pennatulaceans, but on functional grounds this could be convergent. *Stromatoveris*

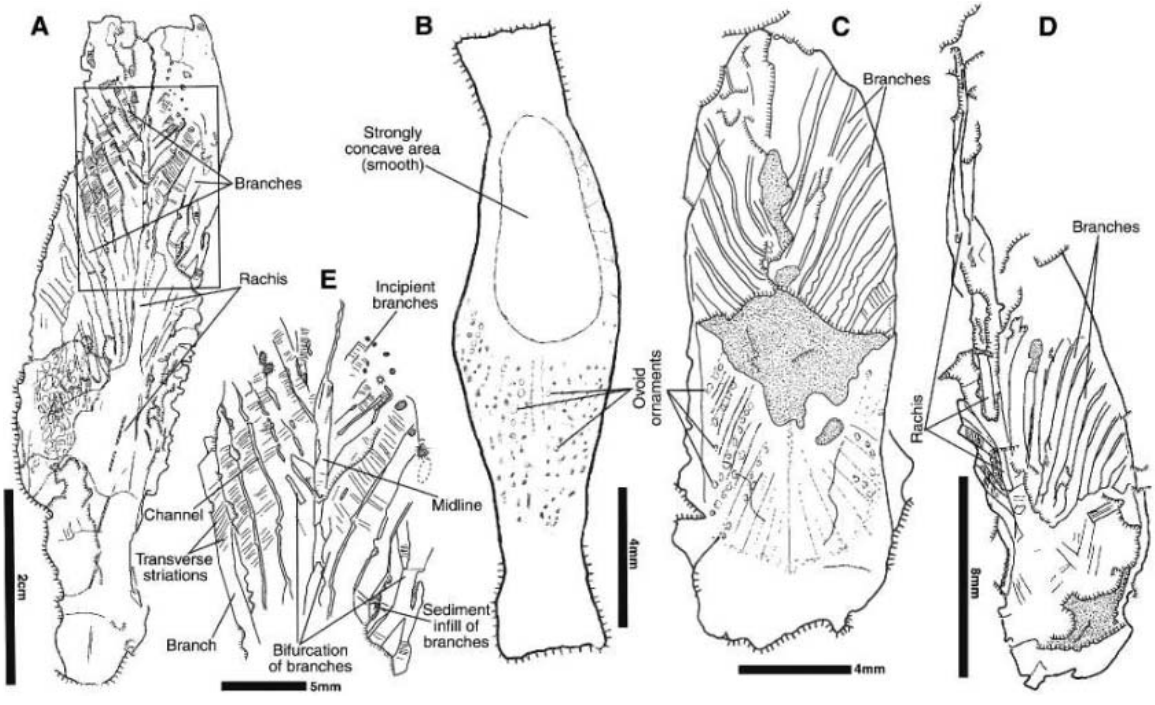

Fig. 2. Camera lucida drawings of *S. psygmoglena*, gen. sp. nov. (compare with Fig. 1). The interpretative drawings are composite, with the counterpart reversed and superimposed on the part. Correspondences are as follows: (**A**) and (**E**) correspond to Fig. 1, A, B, and G [(E) is enlargement of boxed area in (A)]; (**B**), to Fig. 1, C and D; (**C**), to Fig. 1E; and (**D**), to Fig. 1F.

also has some similarities to the mid-Cambrian *Thaumaptilon* (*22*), a possible Ediacaran survivor. This taxon was provisionally identified as a pennatulacean, in part on the basis of zooids. The discovery of a more convincing pennatulacean from the Chengjiang Lagerstätte (fig. S2) suggests that if *Thaumaptilon* is a cnidarian (assuming the zooids are correctly identified), then it is more primitive than the anthozoans (Fig. 3). In any event, *Thaumaptilon* and *Stromatoveris* are unlikely to be closely related. The latter taxon lacks obvious zooids and has a markedly different branching pattern. Branching in *Stromatoveris* also shows various irregularities [perhaps consistent with a less constrained morphogenetic program (*21*)] and has possible interbranch connections, and most importantly the distal branches differentiate from within the upper surface. The latter arrangement is unlike growth in pennatulaceans (or other colonial metazoans). Such a style of growth, although inferred in many frondose vendobionts, may bear reexamination, especially because at least some taxa show other distinctive characteristics, including a striking fractal growth (*17*).

The level of organization seen in *Stromatoveris* (and equivalent Ediacaran fossils) seems to transcend protistan complexity. It seems likely, therefore, that the vendobionts as currently recognized (*12*, *14*) are not monophyletic. Taxa such as *Ernietta* and *Pteridinium*, built on simple modular units and apparently with an infaunal mode of life, may well be giant protistans (*14*). The frondlike fossils, however, are interpreted as metazoans, specifically diploblasts (Fig. 3). The pronounced disparity within the diploblasts, notably between cnidarians and ctenophores, has made their early evolution highly speculative. Dzik (*23*), however, has hypothesized a link between Ediacaran fronds and Cambrian ctenophores. Although it is difficult to accommodate, for instance, taxa such as *Dickinsonia* and *Thaumaptilon* in this scheme, the fine transverse structures seen on the branches of *Stromatoveris* are similar to those seen in Cambrian ctenophores (Fig. 3) despite their otherwise disparate body plans. In *Stromatoveris*, the ciliated branches are closely spaced and attached to the frond. In Cambrian ctenophores, the branches became separated and the body more globular. Both were probably benthic, using the ciliated rows for suspension feeding, whereas in contrast extant ctenophores are highly derived. This evolutionary transition is marked by a shift to a pelagic existence, acquisition of a gelatinous body plan, and co-opting of the ciliary rows from feeding to locomotion.

Stromatoveris joins a select group of Ediacaran survivors (*22*–*25*). In comparison to those Cambrian survivors showing typical Ediacaran-like preservation (*24*, *25*), the material shows new features unobservable in the coarser host matrix. Quality of preservation matches that of *Thaumaptilon* (*22*), but as noted the similarities between the two taxa are evidently convergent (Fig. 3). The possible example of an Ediacaran survivor, reported earlier from Chengjiang (*26*), has no similarity to the example described here, and its wider relationships are uncertain.

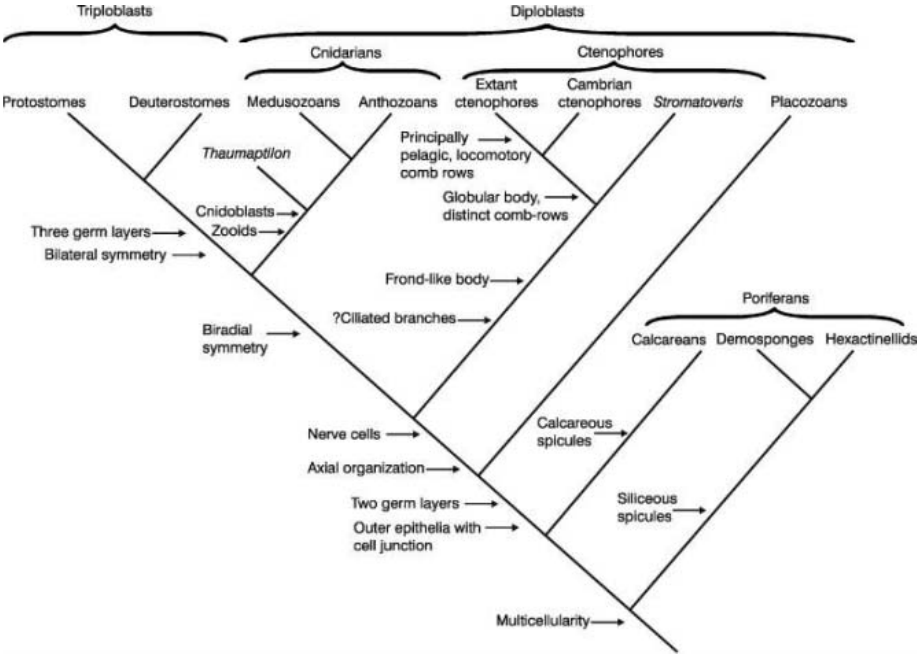

Fig. 3. Outline of metazoan phylogeny, showing proposed position of *Stromatoveris* and *Thaumaptilon* (*22*) as primitive ctenophores and cnidarians, respectively, so implying convergent evolution of a frondlike habit. Metazoan phylogeny is still in a state of flux, but here sponges are taken to be basal, with the calcareans possibly a sister group of all other metazoans (*28*). The position of the placozoans is controversial, but here they are treated as primitive diploblasts (*29*), evolving before the invention of nerve cells (*30*). Ctenophores are monophyletic (*31*) and are taken to be the sister group of cnidarians plus triploblasts (*28*). As argued in the text, ctenophores were primitively frondlike (vendobionts) before acquiring a globular body with separate comb rows that eventually were used in a pelagic existence. Although ctenophores have a biradial symmetry, this has a unique rotational element and may be derived and effectively unrelated to the biradial symmetry that may be primitive to cnidarians. Cnidarians are also monophyletic and are divided into anthozoans and medusozoans (*32*). Although previously ctenophores have been argued to be the sister group of all bilaterians, it is now widely accepted that cnidarians are the sister group (*33*). The triploblasts are composed of deuterostomes and protostomes.

References and Notes

1. G. M. Narbonne, *Annu. Rev. Earth Planet. Sci.* **33**, 421 (2005).
2. D. Grazhdankin, *Paleobiology* **30**, 203 (2004).
3. M. E. Clapham, G. M. Narbonne, J. G. Gehling, *Paleobiology* **29**, 527 (2003).
4. G. J. Retallack, *Paleobiology* **20**, 523 (1994).
5. K. J. Peterson, B. Waggoner, J. W. Hagadorn, *Integr. Comp. Biol* **43**, 127 (2003).
6. B. M. Waggoner, *Paleobiology* **21**, 393 (1995).
7. M. F. Glaessner, *The Dawn of Animal Life: A Biohistorical Study* (Cambridge Univ. Press, Cambridge, 1984).
8. J. G. Gehling, J. K. Rigby, *J. Paleontol.* **70**, 185 (1996).
9. A. Y. Ivantsov, M. A. Fedonkin, *Palaeontology* **45**, 1219 (2002).
10. M. A. Fedonkin, B. M. Waggoner, *Nature* **388**, 868 (1997).
11. X.-L. Zhang, J. Han, Z.-F. Zhang, H.-Q. Liu, D.-G. Shu, *Palaeontology* **46**, 447 (2003).
12. A. Seilacher, *J. Geol. Soc. London* **149**, 607 (1992).
13. A. Yu. Zhuravlev, *Neues Jahrb. Geol. Paläontol. Abh.* **180**, 299 (1993).
14. A. Seilacher, D. Grazhdankin, A. Legouta, *Paleontol. Res.* **7**, 43 (2003).
15. L. W. Buss, A. Seilacher, *Paleobiology* **20**, 1 (1994).
16. R. J. F. Jenkins, J. G. Gehling, *Rec. South Aust. Mus.* **17**, 347 (1978).
17. G. M. Narbonne, *Science* **305**, 1141 (2004); published online 15 July 2004 (10.1126/science.1099727).
18. Systematic paleontology is as follows: Stem group Ctenophora (in part Vendobionta). Order "Charniomorpha" (*27*). Family Stromatoveridae Shu, Conway Morris, and Han fam. nov. genus *Stromatoveris* Shu, Conway Morris, and Han gen. nov. *Stromatoveris psygmoglena* Shu, Conway Morris, and Han sp. nov. Etymology: Generic name is compound, based on mattress (Greek *stromatos*) and Spring (Latin *veris*), oblique references to the mattresslike fossil and its discovery near the city of Kunming, nicknamed Spring City; specific name implies wonderful (Greek *glenos*) fan (Greek *psygma*). Holotype: ELI-Vend-05-001. Other material: ELI-Vend-05-002 to 008. Stratigraphy and locality: Heilinpu (formerly Qiongzhusi) Formation, Yu'anshan Member (*Eoredlichia* zone), Lower Cambrian. Specimens collected in Meishucun and Jianshan areas. Diagnosis: Foliate, divided into basal stalk with rounded termination and flatter frond that tapers distally. Body strongly differentiated, both between upper and lower surfaces and also along axis of both upper and lower surfaces. Upper surface with prominent attached branches in midregion, strongly acute insertion, separated by central groove, branches differentiate from surface in distal region. Branches bear fine transverse structures. Basal and distal regions of upper surface smooth. Distally lower surface has a medial elliptical smooth area from which radiate lines with ovoid ornamentation. Basal region bears subdued ribbing and prominent oval ornamentation, but toward basal tip becomes smooth.
19. M. A. Fedonkin, in *The Vendian System*, B. S. Sokolov, A. B. Iwanowski, Eds. (Springer-Verlag, Berlin, 1990), vol. 1, pp. 71–120.

20. T. D. Ford, *Proc. Yorks. Geol. Soc.* **31**, 211 (1958).
21. B. N. Runnegar, *Neues Jahrb. Geol. Paläontol. Abh.* **195**, 303 (1995).
22. S. Conway Morris, *Palaeontology* **36**, 593 (1993).
23. J. Dzik, *J. Morphol.* **252**, 315 (2002).
24. S. Jensen, J. G. Gehling, M. L. Droser, *Nature* **393**, 567 (1998).
25. J. W. Hagadorn, C. M. Fedo, B. M. Waggoner, *J. Paleontol.* **74**, 731 (2000).
26. W.-T. Zhang, L. Babcock, *Acta Palaeontol. Sinica* **40** (Suppl.), 201 (2001).
27. The phylogenetic questions associated with Ediacaran taxa have largely precluded a higher-level taxonomy. This ordinal designation would include both the taxon described here and such genera as *Charniodiscus*, *Glaessnerina*, *Khatyspytia*, *Vaizitsinia*, and possibly *Charnia*.
28. M. Medina, A. G. Collins, J. D. Silberman, M. L. Sogin, *Proc. Natl. Acad. Sci. U.S.A.* **98**, 9707 (2001).
29. A. Ender, B. Schierwater, *Mol. Biol. Evol.* **20**, 130 (2003).
30. T. Hadrys, R. DeSalle, S. Sagasser, N. Fischer, B. Schierwater, *Mol. Biol. Evol.* **22**, 1569 (2005).
31. M. Podar, S. H. D. Haddock, M. L. Sogin, G. R. Harbison, *Mol. Phyl. Evol.* **21**, 218 (2001).
32. A. G. Collins *et al.*, *Syst. Biol.* **55**, 97 (2006).
33. K. J. Peterson, M. McPeek, D. A. D. Evans, *Paleobiology* **2** (Suppl.), 36 (2005).
34. We thank Y. Ji, M. Cheng, and J. Zhai at the Early Life Institute; S. Last, S. Capon, and V. Brown at Cambridge for technical assistance; and N. Butterfield and three anonymous referees for critical remarks. The work is supported by the National Natural Science Foundation of China, Ministry of Science and Technology of China, Program for Changjiang Scholars and Innovative Research Team in University (PCSIRT), the Cowper-Reed Fund, and St. John's College, Cambridge.

Supporting Online Material
www.sciencemag.org/cgi/content/full/312/5774/731/DC1
Figs. S1 and S2

4 January 2006; accepted 31 March 2006
10.1126/science.1124565

Defective Lipolysis and Altered Energy Metabolism in Mice Lacking Adipose Triglyceride Lipase

Guenter Haemmerle,[1] Achim Lass,[1] Robert Zimmermann,[1] Gregor Gorkiewicz,[2] Carola Meyer,[5] Jan Rozman,[5] Gerhard Heldmaier,[5] Robert Maier,[3] Christian Theussl,[6] Sandra Eder,[1] Dagmar Kratky,[4] Erwin F. Wagner,[6] Martin Klingenspor,[5] Gerald Hoefler,[2] Rudolf Zechner[1]*

Fat tissue is the most important energy depot in vertebrates. The release of free fatty acids (FFAs) from stored fat requires the enzymatic activity of lipases. We showed that genetic inactivation of adipose triglyceride lipase (ATGL) in mice increases adipose mass and leads to triacylglycerol deposition in multiple tissues. ATGL-deficient mice accumulated large amounts of lipid in the heart, causing cardiac dysfunction and premature death. Defective cold adaptation indicated that the enzyme provides FFAs to fuel thermogenesis. The reduced availability of ATGL-derived FFAs leads to increased glucose use, increased glucose tolerance, and increased insulin sensitivity. These results indicate that ATGL is rate limiting in the catabolism of cellular fat depots and plays an important role in energy homeostasis.

Adipose tissue mass in mammals is determined by the dynamic equilibrium of lipid synthesis and lipid catabolism. Disruptions of this balance underlie metabolic diseases such as obesity and type II diabetes (*1*–*3*). Hormone-sensitive lipase (HSL) was once thought to be the major enzyme responsible for the lipolytic breakdown of cellular fat stores (*4*–*6*). However, HSL-deficient mice are lean, and they efficiently mobilize FFAs from triacylglycerol (TG) stores (*7*, *8*), suggesting that other TG hydrolases play an important role. Recently, we and others reported the discovery of an enzyme that we named in accordance with its physiological activity: adipose triglyceride lipase (ATGL) (*9*–*11*). Other designations for this enzyme have been: transport secretion protein (TTS), desnutrin (*10*), calcium-independent phospholipase A2z (iPL-A2z) (*11*), adiposome triglyceride lipase (ATGL) (*12*), and patatin-like phospholipase domain–containing protein 2 (PNPLP2). ATGL specifically hydrolyses long-chain fatty acid TG (*9*, *11*) and is predominantly expressed in adipose tissue and, to a lesser extent, in cardiac muscle, skeletal muscle, testis tissue, and other tissues. The finding that ATGL mRNA expression is regulated by fasting/feeding (*10*) as well as hormones and cytokines (*13*, *14*), and that the inhibition of ATGL in vitro (*9*, *12*) markedly decreases TG catabolism, imply that the enzyme plays an important role in lipolysis.

To elucidate the physiological function of ATGL during lipid mobilization in vivo, we inactivated the *Atgl* gene in mice by replacing the first exon, including the translational start codon and the lipase consensus sequence motif (GXSXG, where G is Gly, S is Ser, and X is any amino acid), with a neomycin expression cassette (fig. S1). *Atgl*(−/−) mice showed accumulation of neutral lipid to supraphysiological levels in most tissues, suggesting an essential role for ATGL in cellular TG catabolism (table S1). The TG content in tissues of *Atgl*(+/−) mice resembled that of wild-type (WT) mice, except for cardiac muscle where there was a twofold increase. Compared with WT mice, *Atgl*(−/−) animals were heavier (Fig. 1A and fig. S2A), displayed a twofold increase in whole body fat mass, and exhibited enlarged adipose fat depots (Fig. 1B and fig. S2, B and C). The mutants had an increased wet weight of gonadal (2.1-fold) and inguinal white adipose tissue (WAT) (1.6-fold), as well as intrascapular brown adipose tissue (BAT) (8.5-fold). Ad libitum food intake [3.6 ± 0.6 g in *Atgl*(−/−) mice and 3.3 ± 0.7 g in WT mice] and lean body mass (Fig. 1A) were similar in mice of both genotypes. Consistent with increased adipose weight, plasma leptin levels were elevated in fed (2.1-fold) and fasted (4.4-fold) *Atgl*(−/−) mice (table S2). The leptin/fat mass ratio, however, was similar in mutant and control mice. Morphological analyses of adipose tissue from *Atgl*(−/−) mice (fig. S2C) revealed enlarged lipid droplets in white [4690 ± 235 μm^2 for *Atgl*(−/−) versus 3382 ± 90 μm^2 for WT] and brown adipocytes [1395 ± 119 μm^2 for *Atgl*(−/−) versus 67 ± 10 μm^2 for WT; n = 100 cells analyzed, $P < 0.001$]. The multilocular lipid droplets normally observed in BAT became unilocular and strongly resembled white fat in appearance. Thus, the absence of ATGL in mice causes fat cell hypertrophy and mild obesity.

In cardiac muscle, ATGL deficiency caused severe TG accumulation (Fig. 1, C and E). At the age of 12 weeks, mice had a TG content in myocytes more than 20 times higher in *Atgl*(−/−) mice than in WT controls, causing a 1.4-fold increase in heart weight [193 ± 18 mg for *Atgl*(−/−) versus 131 ± 12 mg for WT, $P < 0.001$, n = 8]. Histological analyses revealed an age-dependent increase of lipid droplets in number and size in cardiomyocytes, starting with microvesicular lipid accumulation at the age of 6 weeks and progressing to the accumulation of large droplets at the age of 18 weeks (Fig. 1E). This massive lipid buildup led to severe cardiac insufficiency. In echocardiography (Fig. 1E and table S3), the ejection fraction of the left ventricle was drastically reduced in *Atgl*(−/−) mice (40.2 ± 26.5%) compared with WT (80.5 ± 17.1%, $P < 0.001$). Additionally, a marked disturbance of cardiac texture and increased fibrosis was noted (Fig. 1E). The interventricular septum (1.9 ± 0.6 mm)

[1]Institute of Molecular Biosciences, University of Graz, Austria. [2]Institute of Pathology; [3]Department of Cardiology; [4]Institute of Molecular Biology and Biochemistry, Center of Molecular Medicine, Medical University of Graz, Austria. [5]Department of Animal Physiology, Faculty of Biology, Philipps-University Marburg, Germany. [6]Research Institute of Molecular Pathology, Vienna, Austria.

*To whom correspondence should be addressed. E-mail: rudolf.zechner@uni-graz.at

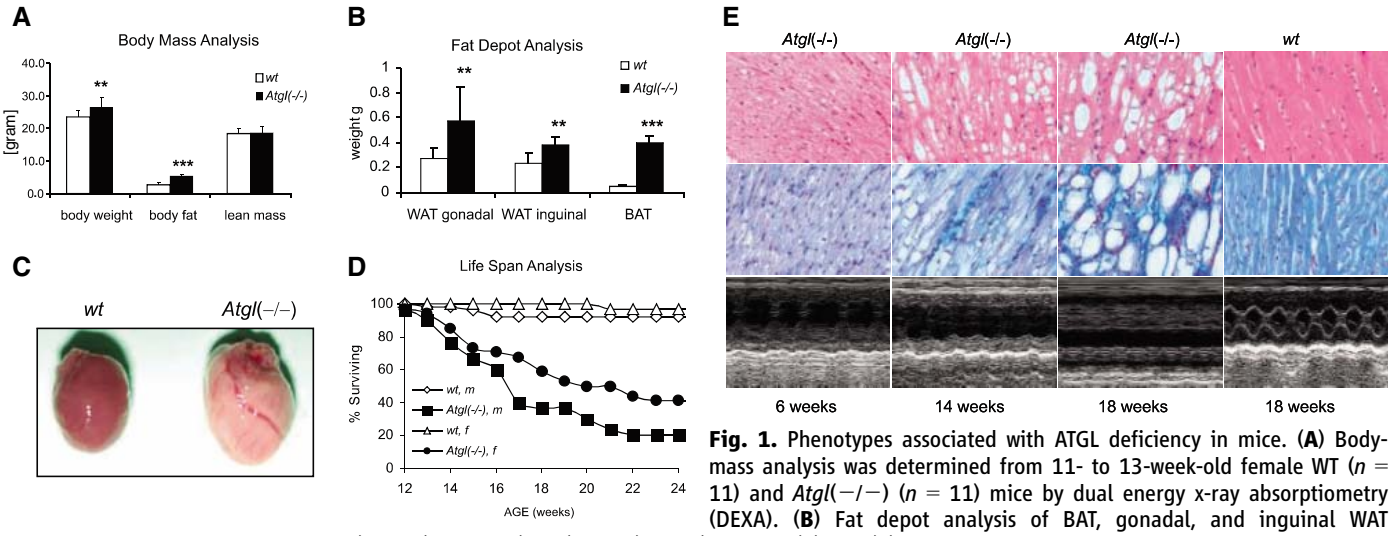

Fig. 1. Phenotypes associated with ATGL deficiency in mice. (**A**) Body-mass analysis was determined from 11- to 13-week-old female WT (n = 11) and *Atgl*(−/−) (n = 11) mice by dual energy x-ray absorptiometry (DEXA). (**B**) Fat depot analysis of BAT, gonadal, and inguinal WAT dissected from 14- to 16-week-old WT (n = 12) and *Atgl*(−/−) mice (n = 11). Data in (A) and (B) are shown as mean ± SD. Statistical significance was determined by a two-tailed Student's t-test comparing WT and *Atgl*(−/−) mice (**P < 0.01, ***P < 0.001). (**C**) Photographs of hearts from 14-week-old WT and *Atgl*(−/−) mice. Note the yellow discoloration due to lipid accumulation in the heart of *Atgl*(−/−) mice. (**D**) Kaplan-Meier plot showing the cumulative survival of WT (m, males n = 53; f, females n = 33) and *Atgl*(−/−) mice, (males n = 30, females n = 34) over a period of 24 weeks. (**E**) Heart histology and echocardiographic analysis. *Atgl*(−/−) mice show progressing triglyceride accumulation in cardiomyocytes (hematoxilin/eosin stain, top row) and myocardial fibrosis indicated by fiber specific staining (chromotrope aniline blue stain, dark blue, middle row) increasing with age. WT animals show none of these alterations (right column). Echocardiography of *Atgl*(−/−) mice revealed increasing concentric left-ventricular hypertrophy and impairment of left-ventricular systolic function (M-mode imaging, bottom row).

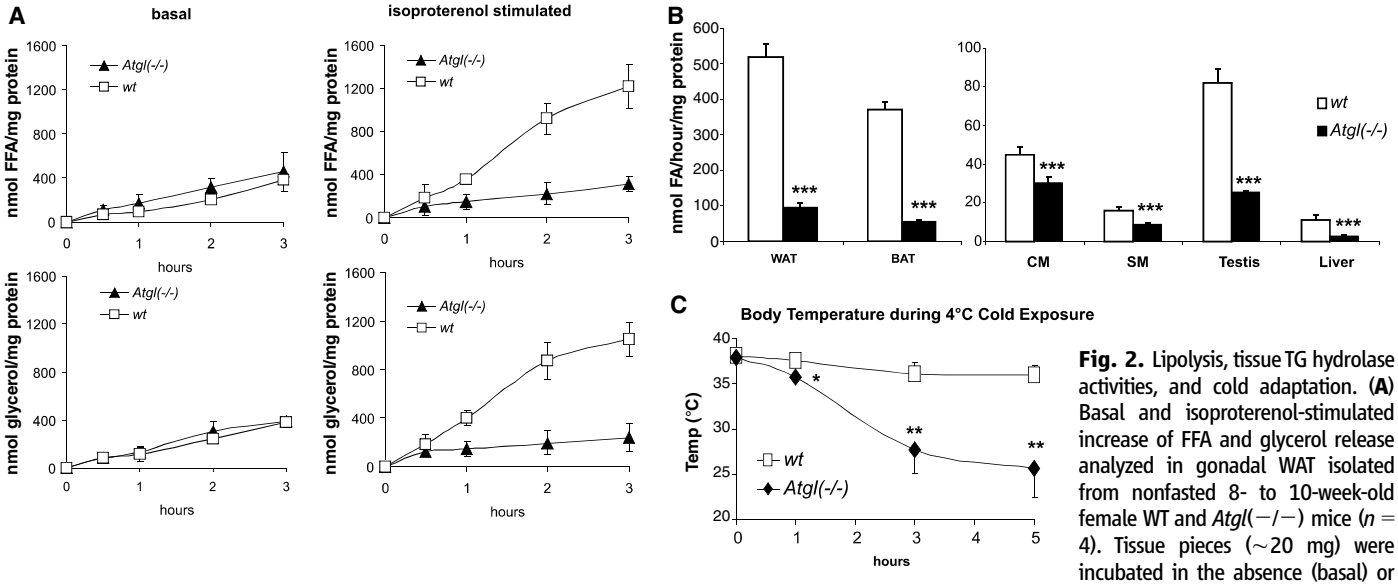

Fig. 2. Lipolysis, tissue TG hydrolase activities, and cold adaptation. (**A**) Basal and isoproterenol-stimulated increase of FFA and glycerol release analyzed in gonadal WAT isolated from nonfasted 8- to 10-week-old female WT and *Atgl*(−/−) mice (n = 4). Tissue pieces (~20 mg) were incubated in the absence (basal) or presence of 10 μM isoproterenol (isoproterenol-stimulated). Isoproterenol-mediated increase was calculated by the subtraction of basal values. (**B**) TG-hydrolase activities were determined in cytosolic fractions of tissues from fasted 10- to 12-week-old female WT and *Atgl*(−/−) mice (n = 5). CM, cardiac muscle; SM, skeletal muscle; (**C**) Body temperature of 11- to 12-week-old male WT and *Atgl*(−/−) mice was determined during exposure to 4°C for 5 hours. Three mice were used for each time point and genotype. All data are shown as mean ± SD (*P < 0.05, **P < 0.01, ***P < 0.001).

and the posterior wall of the left ventricle (1.8 ± 0.6 mm) were significantly thicker in *Atgl*(−/−) hearts than in controls (1.2 ± 0.2 mm, P < 0.005, and 1.2 ± 0.4 mm, P < 0.05, respectively) and increased with age. Consistent with tissue damage, a moderate (less than 1% of cells) induction of apoptosis was noted in *Atgl*(−/−) mice by caspase 3 immunohistochemistry (fig. S3A). Signs of inflammation were not detected. The pronounced cardiac dysfunction resulted in premature death of male and female *Atgl*(−/−) mice. As shown in the Kaplan-Meier plot (Fig. 1D), the first *Atgl*(−/−) mice died around 12 weeks after birth. Male mice died earlier (50% after 16 weeks) than females (50% after 20 weeks). In contrast, male and female *Atgl*(+/−) mice had a normal life expectancy. At dissection, deceased *Atgl*(−/−) mice exhibited typical features of congestive heart failure. These included marked dilatation of both left and right ventricles, congestion of pulmonary blood vessels and edema (fig. S3), pleural as well as cardiac effusions (fig. S4), and extensive blood congestion of organs (fig. S3). None of these features were present in control animals or *Atgl*(−/−) mice analyzed morphologically before the age of 14 weeks.

Table 1. Comparison of plasma parameters in WT mice, heterozygous [*Atgl*(+/−)], and homozygous ATGL-deficient [*Atgl*(−/−)] mice. Plasma lipids, glucose, insulin, and metabolites were measured in fed or fasted (overnight fast) female 10- to 12-week-old mice. Essentially similar data were observed for male *Atgl*(−/−) mice. FFA, free fatty acids; TG, triacylglycerols; KB, ketone bodies; TC, total cholesterol. Data are shown as mean ± SD from at least six mice per genotype and measurement condition. Mean values of each plasma component are compared between WT and *Atgl*(−/−) mice and WT and *Atgl*(+/−) mice, respectively. Statistical significance was determined by a two-tailed Student's *t*-test (**P* < 0.05, ***P* < 0.01, ****P* < 0.001). n.d., not determined.

	WT		*Atgl*(+/−)		*Atgl*(−/−)	
	Fed	Fasted	Fed	Fasted	Fed	Fasted
FFA (mmol/L)	0.40 ± 0.07	0.79 ± 0.32	0.37 ± 0.14	0.93 ± 0.35	0.28 ± 0.05*	0.30 ± 0.08**
TG (mg/dl)	81.5 ± 14.7	60.5 ± 19.6	84.7 ± 28.5	48.6 ± 15.6	79.8 ± 13.6	20.2 ± 8.0**
KB (mmol/L)	n.d.	2.09 ± 0.30	n.d.	1.72 ± 0.37	n.d.	0.60 ± 0.25***
TC (mg/dl)	105.8 ± 21.1	91.9 ± 10.5	94.1 ± 12.6	95.1 ± 6.0	98.1 ± 19.0	71.5 ± 12.1*
Glucose (mg/dl)	142.1 ± 8.6	82.2 ± 10.8	140.6 ± 9.5	81.6 ± 5.1	136.6 ± 16.4	78.6 ± 11.8
Insulin (ng/ml)	0.82 ± 0.28	0.20 ± 0.06	0.93 ± 0.46	0.24 ± 0.11	0.48 ± 0.21*	0.25 ± 0.11

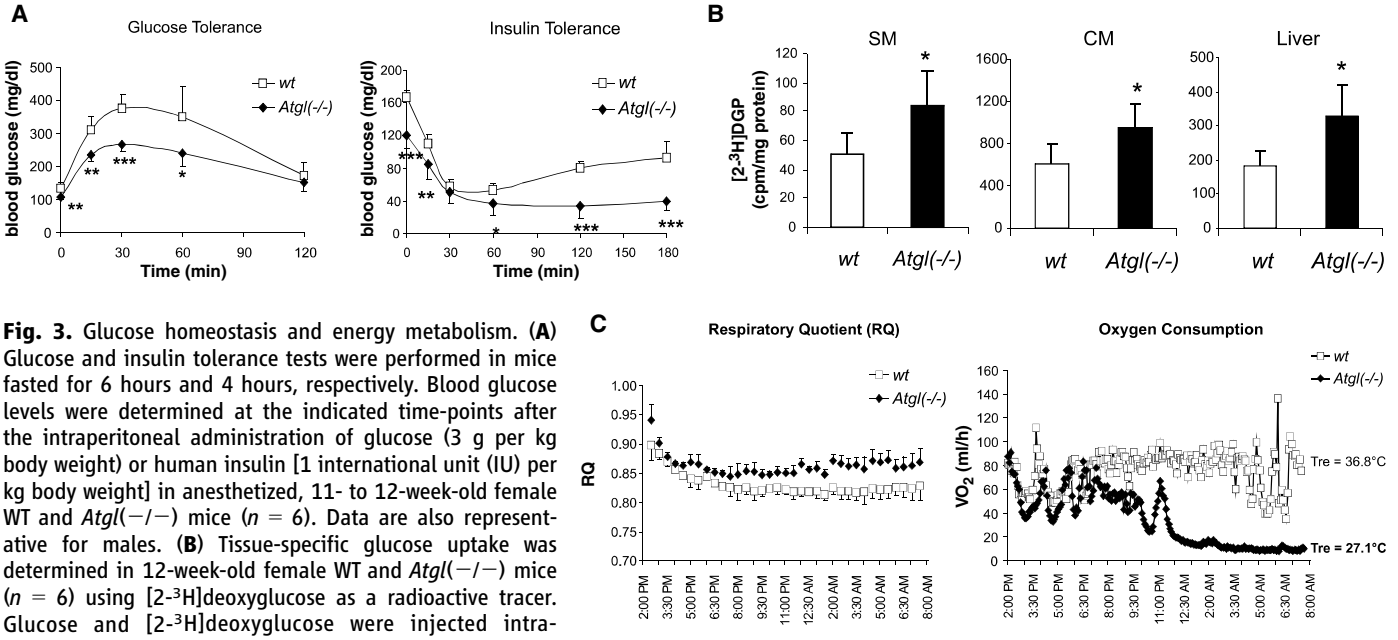

Fig. 3. Glucose homeostasis and energy metabolism. (**A**) Glucose and insulin tolerance tests were performed in mice fasted for 6 hours and 4 hours, respectively. Blood glucose levels were determined at the indicated time-points after the intraperitoneal administration of glucose (3 g per kg body weight) or human insulin [1 international unit (IU) per kg body weight] in anesthetized, 11- to 12-week-old female WT and *Atgl*(−/−) mice (n = 6). Data are also representative for males. (**B**) Tissue-specific glucose uptake was determined in 12-week-old female WT and *Atgl*(−/−) mice (n = 6) using [2-^{3}H]deoxyglucose as a radioactive tracer. Glucose and [2-^{3}H]deoxyglucose were injected intraperitoneally under the conditions described for the glucose tolerance test, and the accumulation of [2-^{3}H]deoxyglucose-6-phosphate ([2-^{3}H]DGP) was determined in skeletal muscle (SM), cardiac muscle (CM), and the liver. (**C**) Time course of the RQ and oxygen consumption (VO_2) in 12- to 13-week-old female WT and *Atgl*(−/−) mice (n = 8) during 18 hours of food deprivation at 24°C. Mean RQ ± SD values were significantly lower in WT mice than in *Atgl*(−/−) mice ($P < 0.01$) after 3 hours of food removal. VO_2 (measured every 5 min) was significantly decreased in *Atgl*(−/−) mice compared with WT mice ($P < 0.01$) after 5 hours of food removal. A representative plot for one *Atgl*(−/−) and one WT mouse is shown for VO_2. Hypometabolism is also reflected by decreased rectal temperature (T_{re}) in *Atgl*(−/−) mice mesasured immediately after removal of the mice from the metabolic cage. Data are shown as mean ± SD. Statistical significance was determined in a two-tailed Student's *t*-test (for glucose measurements) or by analysis of variance (ANOVA) (RQ and VO_2 analysis) (**P* < 0.05, ***P* < 0.01, ****P* < 0.001).

Thus, the functional, histological, and pathological observations indicate that *Atgl*(−/−) mice die from cardiac insufficiency caused by a mechanical contraction defect resulting from the massive accumulation of lipids.

In other nonadipose tissues, the most pronounced accumulation of TG (>10-fold) occurred in the testis and kidney (table S1), although smaller increases in fat content (1.5- to 4-fold) were observed in essentially all tissues, including the liver. Thus, an important lipolytic function of ATGL is generally implied for nonadipose tissues. TG deposition in the kidney was not associated with lipiduria or increased plasma creatinine or urea levels in *Atgl*(−/−) mice, indicating normal renal function.

To identify the biochemical defect caused by ATGL-deficiency, we analyzed the β-adrenergic stimulated lipolytic capacity of normal and ATGL-deficient WAT. Explants of gonadal white fat were incubated in the presence or absence of isoproterenol, and the release of FFAs and glycerol was determined hourly. As shown in Fig. 2A, the basal release of FFAs and glycerol from *Atgl*(−/−) WAT was similar to that from WT tissue. In contrast, isoproterenol-stimulated lipolysis was drastically reduced in *Atgl*(−/−) WAT. After a 2-hour incubation period, 74% fewer FFAs and 78% less glycerol were released from mutant versus WT WAT. Similarly, the TG hydrolase activity in *Atgl*(−/−) WAT and BAT was decreased by 82% and 85%, respectively (Fig. 2B). Lipolytic activities were also reduced in cardiac muscle (–31%), skeletal muscle (–44%), the testis (–69%), and the liver (–73%) of *Atgl*(−/−) mice. Thus, alternative lipases such as HSL or triglyceride hydrolase (TGH) (*15*) cannot efficiently compensate for the absence of ATGL in adipose and other peripheral tissues. These results also support the hypothesis that HSL might be more important as a diacylglycerol hydrolase than as a TG hydrolase (*9*, *16*).

Impaired catabolism of TG in BAT caused a severe defect in thermoregulation in *Atgl*(−/−) mice. Upon cold exposure for 5 hours, *Atgl*(−/−) mice suffered from life-threatening hypothermia (body temperature, 25°C) (Fig. 2C). This phenotype resembles that of β-adrenergic receptor–deficient mice (*17*) and suggests that in the absence of ATGL, insufficient amounts of FFAs are released as energy substrate for uncoupled mitochondrial respiration. Consistent with the observed defect in adaptive thermogenesis, peroxisome proliferator activated receptor-γ coactivator-1α (PGC-1α) and uncoupling protein-1 (UCP-1) expression were decreased by 80% and 53% in *Atgl*(−/−) mice compared with WT mice, respectively (fig. S5). Thus, HSL cannot compensate for the defective lipolysis in BAT of *Atgl*(−/−) mice. In contrast, HSL-deficient mice expressing normal amounts of ATGL are not cold sensitive (*7*), indicating that ATGL provides adequate amounts of FFAs for thermogenesis. Additionally, both male and female *Atgl*(−/−) mice are fertile, whereas HSL-deficient male mice are sterile (*18*).

Table 1 summarizes measurements of plasma lipid metabolism and carbohydrate metabolism in *Atgl*(−/−), *Atgl*(+/−), and WT mice. Coherent with the observed defective lipolysis in WAT, *Atgl*(−/−) mice exhibited reduced plasma FFA concentrations in both the fed and in the fasted state (–30 and –62%, respectively). Plasma concentrations for TG (–66%), β-hydroxy-butyrate (–71%), and total cholesterol (–22%) were also lower in fasted *Atgl*(−/−) mice. The decrease in plasma TG and cholesterol concentrations in *Atgl*(−/−) mice was due to reduced plasma very low–density lipoprotein (VLDL) and high-density lipoprotein levels (HDL), respectively (fig. S6). Reduced FFA, TG, VLDL, and β-hydroxy-butyrate levels were also reported for HSL-deficient mice (*19*) and might result from lower transport rates of FFAs to the liver in both animal models, leading to decreased hepatic VLDL synthesis and ketogenesis (*19*). In contrast with HSL-deficient mice exhibiting increased HDL-cholesterol levels, *Atgl*(−/−) animals had reduced plasma concentrations of HDL cholesterol.

A reciprocal relationship exists between the use of FFAs and glucose as substrates for energy production (*20*). Elevated uptake, storage, and oxidation of FFAs in muscle is associated with increased insulin resistance, resulting in increased plasma glucose and insulin levels (*21*–*23*). This adverse effect of FFAs in nonadipose tissues is commonly referred to as "lipotoxicity" (*24*, *25*). According to the view that FFAs and acyl–coenzyme A (CoA) derivatives, and not fat per se, exert "lipotoxic" effects (*26*, *27*), the reduced release of FFAs from stored fat in adipose tissue and (cardiac) muscle of ATGL-deficient mice should promote "antilipotoxic" effects, such as decreased FFA oxidation, increased glucose use, and increased glucose tolerance. Consistent with this hypothesis, in fed *Atgl*(−/−) mice, plasma insulin levels were reduced by 42%, whereas plasma glucose concentrations were similar to those in WT animals (Table 1). No significant changes in glucose or insulin levels were observed in heterozygous *Atgl*(+/−) mice when compared with control animals. In the fasted state (overnight fast), insulin and glucose concentrations were similar in mice of all three genotypes. In glucose tolerance tests (Fig. 3A), 6-hour fasted *Atgl*(−/−) mice exhibited significantly lower basal glucose values and displayed a markedly improved glucose tolerance compared with WT mice. In insulin tolerance tests (Fig. 3A), the maximal decline of blood glucose levels was more pronounced in *Atgl*(−/−) mice (34 mg/dl) than in WT mice (53 mg/dl) and persisted over the whole measurement period of 3 hours. In WT mice, a rebound of glucose values occured after 60 min. Glucose uptake experiments revealed that the accumulation of 2-deoxyglucose was markedly elevated in skeletal muscle (68%), cardiac muscle (54%), and in the liver (78%) (Fig. 3B) of *Atgl*(−/−) mice. Thus, glucose uptake and insulin sensitivity/resistance may be determined by the capacity of ATGL to mobilize FFA.

Consistent with increased glucose uptake and utilization, the respiratory quotient (RQ) of *Atgl*(−/−) mice deviated from that of WT during fasting (Fig. 3C). During ad libitum feeding and the first 2 hours of fasting, RQ values were similar in *Atgl*(−/−) and WT mice. With increasing fasting time, the RQ in WT mice decreased further, which is indicative of increased lipid oxidation, whereas the RQ in *Atgl*(−/−) mice remained at a constant elevated level. Simultaneously, a gradual decrease in oxygen consumption indicating reduced energy expenditure was observed in *Atgl*(−/−) mice (Fig. 3C). After 18 hours of fasting, oxygen consumption was only 25% of that found in control mice. Furthermore, the body temperature dropped to 28.4 ± 2.2°C in *Atgl*(−/−) mice, compared with 35.4 ± 1.8°C in WT mice in response to prolonged fasting.

Our studies suggest that in mice, ATGL is the rate-limiting enzyme for the initiation of TG catabolism in adipose and many nonadipose tissues. The association of ATGL deficiency with increased glucose tolerance, increased insulin sensitivity, and increased RQ during fasting provides compelling evidence that the decreased availability of FFAs promotes the use of glucose as metabolic fuel despite the presence of massive amounts of fat in adipose tissue and muscle. The inability to mobilize these fat stores leads to energy starvation, resulting in reduced energy expenditure, a decline in body temperature, and premature death when *Atgl*(−/−) animals are stressed by cold exposure or food deprivation. Thus, ATGL plays a crucial role in energy homeostasis in mice. The observations that ATGL contributes to adipocyte lipolysis in human adipose tissue (*28*) and that genetic variation in the human *ATGL* gene is associated with plasma FFA, TG, and type II diabetes (*29*) suggest that our findings in mice may also be relevant for human physiology.

References and Notes

1. B. B. Kahn, J. S. Flier, *J. Clin. Invest.* **106**, 473 (2000).
2. B. M. Spiegelman, J. S. Flier, *Cell* **104**, 531 (2001).
3. G. I. Shulman, *J. Clin. Invest.* **106**, 171 (2000).
4. D. M. Raben, J. J. Baldassare, *Trends Endocrinol. Metab.* **16**, 35 (2005).
5. H. Mulder *et al.*, *Diabetes* **48**, 228 (1999).
6. V. Large *et al.*, *J. Lipid Res.* **39**, 1688 (1998).
7. J. Osuga *et al.*, *Proc. Natl. Acad. Sci. U.S.A.* **97**, 787 (2000).
8. G. Haemmerle *et al.*, *J. Biol. Chem.* **277**, 4806 (2002).
9. R. Zimmermann *et al.*, *Science* **306**, 1383 (2004).
10. J. A. Villena, S. Roy, E. Sarkadi-Nagy, K. H. Kim, H. S. Sul, *J. Biol. Chem.* **279**, 47066 (2004).
11. C. M. Jenkins *et al.*, *J. Biol. Chem.* **279**, 48968 (2004).
12. E. Smirnova *et al.*, *EMBO Rep.* **7**, 106 (2006).
13. S. Kralisch *et al.*, *Mol. Cell. Endocrinol.* **240**, 43 (2005).
14. E. E. Kershaw *et al.*, *Diabetes* **55**, 148 (2006).
15. K. G. Soni *et al.*, *J. Biol. Chem.* **279**, 40683 (2004).
16. G. Haemmerle *et al.*, *J. Biol. Chem.* **277**, 4806 (2002).
17. E. S. Bachman *et al.*, *Science* **297**, 843 (2002).
18. J. Osuga *et al.*, *Proc. Natl. Acad. Sci. U.S.A.* **97**, 787 (2000).
19. G. Haemmerle *et al.*, *J. Biol. Chem.* **277**, 12946 (2002).
20. P. J. Randle, P. B. Garland, C. N. Hales, E. A. Newsholme, *Lancet* **1**, 785 (1963).
21. J. D. McGarry, R. L. Dobbins, *Diabetologia* **42**, 128 (1999).
22. M. Roden *et al.*, *J. Clin. Invest.* **97**, 2859 (1996).
23. G. Boden, X. Chen, J. Ruiz, J. V. White, L. Rossetti, *J. Clin. Invest.* **93**, 2438 (1994).
24. Y. T. Zhou *et al.*, *Proc. Natl. Acad. Sci. U.S.A.* **97**, 1784 (2000).
25. R. H. Unger, *Annu. Rev. Med.* **53**, 319 (2002).
26. L. L. Listenberger *et al.*, *Proc. Natl. Acad. Sci. U.S.A.* **100**, 3077 (2003).
27. H. C. Chiu *et al.*, *J. Clin. Invest.* **107**, 813 (2001).
28. D. Langin *et al.*, *Diabetes* **54**, 3190 (2005).
29. V. Schoenborn *et al.*, *Diabetes,* in press.

30. We thank H. Braunias, A. Haumer, A. Hermann, B. Juritsch, H. Reicher, C. Schober, R. Schreiber, and G. Szerencsi for administrative and technical assistance; Siemens Medical Solutions for providing the echo machine and transducer; and E. Zechner for critically reviewing the manuscript. Supported by the Austrian Fonds zur Förderung der Wissenschaftlichen Forschung (SFB-Biomembranes F00701 and F00713) and the Austrian Federal Ministry of Education, Science, and Culture (GEN-AU project Genomics of Lipid-associated Disorders–GOLD), and the NGFN2 Neuronet Obesity and Related Disorders (FKZ01GS0483).

Supporting Online Material

www.sciencemag.org/cgi/content/full/312/5774/734/DC1
Materials and Methods
SOM Text
Figs. S1 to S6
Tables S1 to S3
References

16 December 2005; accepted 5 April 2006
10.1126/science.1123965

B Cell Ligand Discrimination Through a Spreading and Contraction Response

S. J. Fleire,[1] J. P. Goldman,[2,3] Y. R. Carrasco,[1] M. Weber,[1] D. Bray,[3] F. D. Batista[1]*

B cells recognize foreign antigens by virtue of cell surface immunoglobulin receptors and are most effectively activated by membrane-bound ligands. Here, we show that in the early stages of this process, B cells exhibit a two-phase response in which they first spread over the antigen-bearing membrane and then contract, thereby collecting bound antigen into a central aggregate. The extent of this response, which is both signaling- and actin-dependent, determines the quantity of antigen accumulated and hence the degree of B cell activation. Brownian dynamic simulations reproduce essential features of the antigen collection process and suggest a possible basis for affinity discrimination. We propose that dynamic spreading is an important step of the immune response.

B cells are lymphocytes that make soluble antibodies. They are triggered, or activated, by foreign antigens, typically those presented on the surface of other cells. Activation leads to selective proliferation and differentiation into mature antibody-secreting cells and the selection of high-affinity B cells. Membrane-anchored antigens are known to be very effective in driving B cell activation (*1*, *2*) and may constitute the dominant form of antigen responsible for B cell stimulation in vivo (*3*–*7*). When a B cell recognizes antigens tethered on the surface of a target cell, a cluster of the B cell receptor (BCR) and its cognate ligand forms at the site of contact (*8*). Simultaneously, membrane proteins are reorganized on the cell surface, leading to the formation of an immunological synapse. This structure is characterized by a central cluster of BCR/antigen complex surrounded by a ring of adhesion molecules LFA-1/ICAM-1 (*9*) and is similar to the synaptic structure originally described for T cells (*10*–*12*).

A functional B cell synapse, however, can form in the absence of integrins (*8*), and this provides an opportunity to quantitatively study the early stages of recognition of membrane-bound antigens. Thus, we observed by scanning electron microscopy (SEM) that when transgenic B cells carrying a BCR specific for hen egg lysozyme (HEL) (*13*) recognize this antigen on the surface of target cells, they rapidly spread over the target membrane before slowly contracting (Fig. 1A). To follow these morphological changes and relate them to the localization of antigen in real time, we labeled B cell membranes with a lipid soluble dye, PKH26, and expressed the HEL antigen as a fusion protein with green fluorescent protein (GFP) (*8*). Three-dimensional (3D) time-lapse fluorescence

[1]Lymphocyte Interaction Laboratory, London Research Institute, Cancer Research UK, 44 Lincoln's Inn Fields, London, WC2A 3PX, UK. [2]Computing Laboratory, University of Kent, Canterbury CT2 7NF, UK. [3]Physiology, Development, and Neuroscience, University of Cambridge, Downing Street, Cambridge CB2 3DY, UK.

*To whom correspondence should be addressed. E-mail: facundo.batista@cancer.org.uk

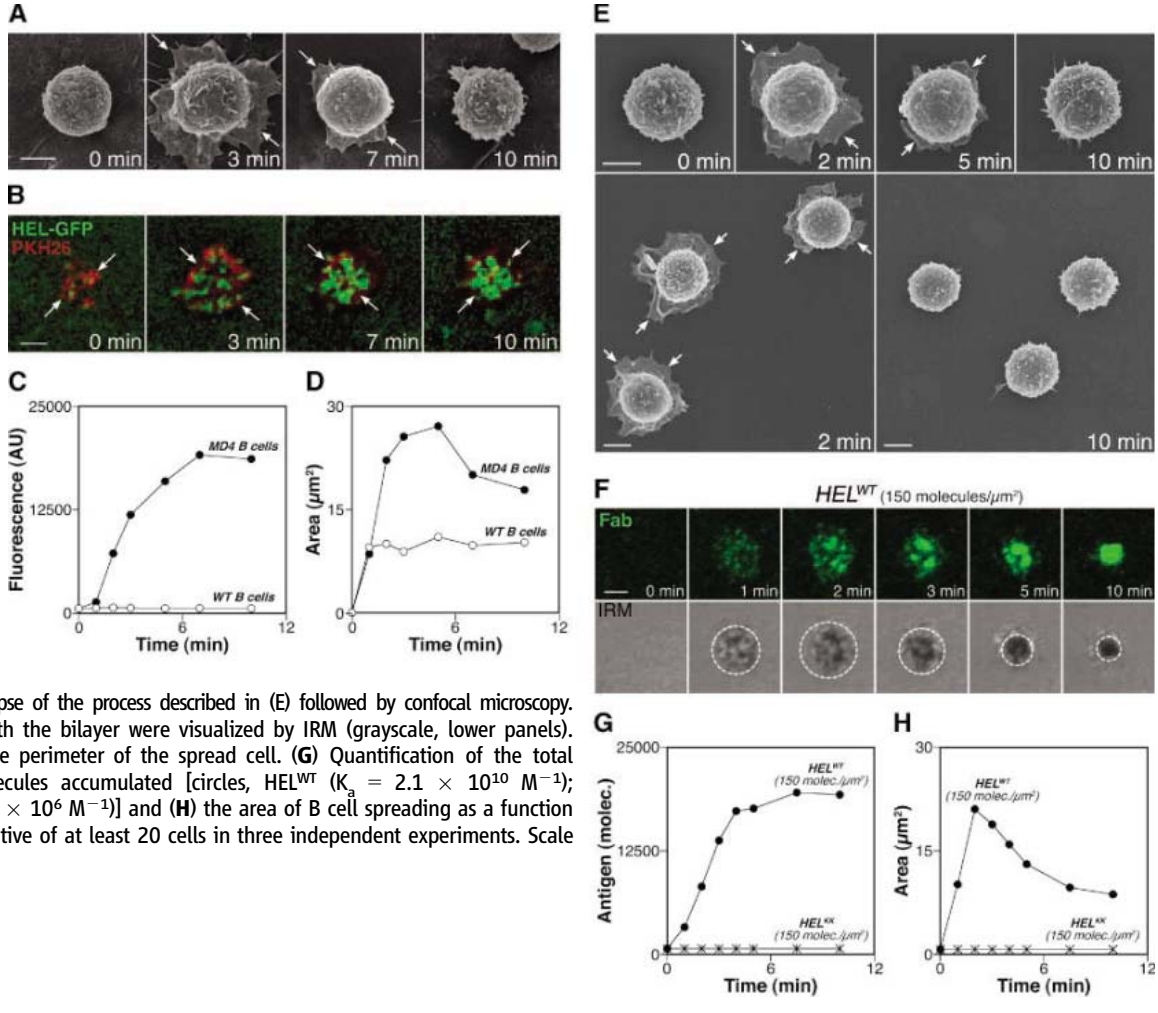

Fig. 1. Antigen recognition through the BCR triggers cell spreading. Images of MD4 transgenic B cells interacting with COS-7 cells expressing a membrane form of HEL-GFP obtained using (**A**) SEM of fixed cells or (**B**) time-lapse wide-field fluorescence microscopy [antigen (green) and B cell membrane (red)]. White arrows indicate the limits of the B cell membrane. (**C**) Quantification of the total antigen accumulated in fluorescence units and (**D**) the area of B cell contact as a function of time. (**E**) SEM images of fixed MD4 B cells settled onto planar lipid bilayers bearing HEL^{WT} (density = 150 molecules/μm^2) at different times. (**F**) Time lapse of the process described in (E) followed by confocal microscopy. Contacts of the B cell with the bilayer were visualized by IRM (grayscale, lower panels). Dotted circles indicate the perimeter of the spread cell. (**G**) Quantification of the total number of antigen molecules accumulated [circles, HEL^{WT} ($K_a = 2.1 \times 10^{10}$ M^{-1}); asterisks, HEL^{KK} ($K_a < 0.4 \times 10^6$ M^{-1})] and (**H**) the area of B cell spreading as a function of time. This is representative of at least 20 cells in three independent experiments. Scale bars, 2 μm.

microscopy revealed that during the spreading phase (2 to 4 min after contact) several small clusters of GFP-HEL of approximately 0.5 to 1 μm in diameter appeared within the area of interaction (Fig. 1B). The flattening B cells reached a maximum surface area of contact of approximately 25 μm^2 before gradually starting to contract (Fig. 1, B and C). During this second phase, which lasted for ~5 to 7 min, the antigen was gathered into a central defined cluster, with an eventual area of 16 μm^2 (Fig. 1D).

Similar morphological changes and kinetics of antigen accumulation were seen when B cells settled on glass-supported planar lipid bilayers (Fig. 1, E to H). In this case, the lysozyme antigen was tethered by a fluorescently labeled glycosylphosphatidylinositol (GPI)-anchored single-chain Fab, which binds to a nonoverlapping epitope of the HEL (fig. S1A). Fluorescence and interference reflection microscopy (IRM), used to examine the dynamics of antigen accumulation and correlate them with changes in cell shape, revealed that this is a general phenomenon that could also be observed with other HEL specific transgenic (*14*) or transfected B cells (*15*) (Fig. 1F and fig. S2, A and B).

The cell response was dependent on specific immunological recognition, because the same experiment performed with a null HEL mutant (HEL^{KK}) (table S1) with no detectable affinity for the BCR failed to reveal antigen aggregation, contact formation (as assessed by IRM), or any sign of B cell spreading (Fig. 1, G and H). Transgenic B cells carrying a signaling-deficient chimaeric BCR ($IgM/\beta^{Y>L}$) with high affinity binding for the lysozyme (*14*) or B cells transfectants expressing signaling deficient BCRs (*15*) also showed a complete lack of spreading, and their capacity to accumulate antigen was severely compromised (Fig. 2, A to C, and fig. S2, A to E). Cells carrying the same chimaeric receptor but with a functional immunoreceptor tyrosine-based activation motif (ITAM) (*16*) regained the ability to spread and form antigen aggregates (Fig. 2, A to C). These processes were also blocked when wild-type transgenic B cells were treated with inhibitors of tyrosine kinase or actin polymerization (Fig. 2D). Immunostaining of fixed cells also revealed an accumulation of phosphotyrosine and actin that was coincident with antigen at earliest time points but later moved to the periphery (fig. S2F). Taken together, these results indicate that this is an actin-mediated phenomenon in which both the BCR-antigen binding and functional B cell signaling are required.

The B cell response was sensitive to both the density of antigen in the presenting membrane and the strength of the BCR/antigen interaction. A twofold reduction in the starting density of antigen caused a marked diminution of spreading, and a 10-fold reduction abolished it entirely (Fig. 3A). Using a set of mutant lysozymes with a 20,000-fold range of affinity for BCR (table S1), we found that a Ka value of about $10^6\ M^{-1}$ is the lower threshold for triggering cell spreading. Above this, the maximum area attained by the B cell increased with its affinity up to a Ka value of $5 \times 10^7\ M^{-1}$ (Fig. 3A). Above the upper threshold, further increases in affinity did not result in additional spreading. Similar results were obtained if we measured the total amount of antigen accumulated (Fig. 3B) or the intracellular calcium levels of the B cells (Fig. 3C). Thus, the magnitude of the signal determines the extent of spreading and ultimately the total amount of antigen accumulated at the end of the response.

The capacity of B cells to extract antigen was assessed using flow cytometry after incubation with HEL–fluorescein isothiocyanate bearing membranes for 2 hours. In these experiments, the amount of antigen acquired was found to be proportional to the total amount of antigen accumulated (Fig. 3D). The ability of B cells to present antigen-derived peptides to T cells was also dependent on the amount of antigen tethered on the membrane (Fig. 3E). Similar results were obtained when the antigen was presented at different densities on the surface of transfected cells (fig. S3, A to C). Thus, a direct correlation appeared to exist between the amount of antigen accumulated and the capacity of a B cell to extract and present it to T cells.

We next explored the question of how cell spreading enables the cell to detect a wide range of binding affinities using a stochastic computer program in which protein molecules are represented as dimensionless points with Cartesian coordinates and binding radii that determine their interactions during the simulation (*17*) (Movies S1 to S4). Antigen molecules moved by Brownian diffusion within a square field representing a portion of the lipid bilayer, with periodic boundaries to avoid edge effects. The area of contact between the B cell and the bilayer was represented by a circle, initially small, within which receptors were assigned random positions. These receptors remained fixed in place but, through reversible mass action kinetics, were accessible to diffusing antigens leading to associ-

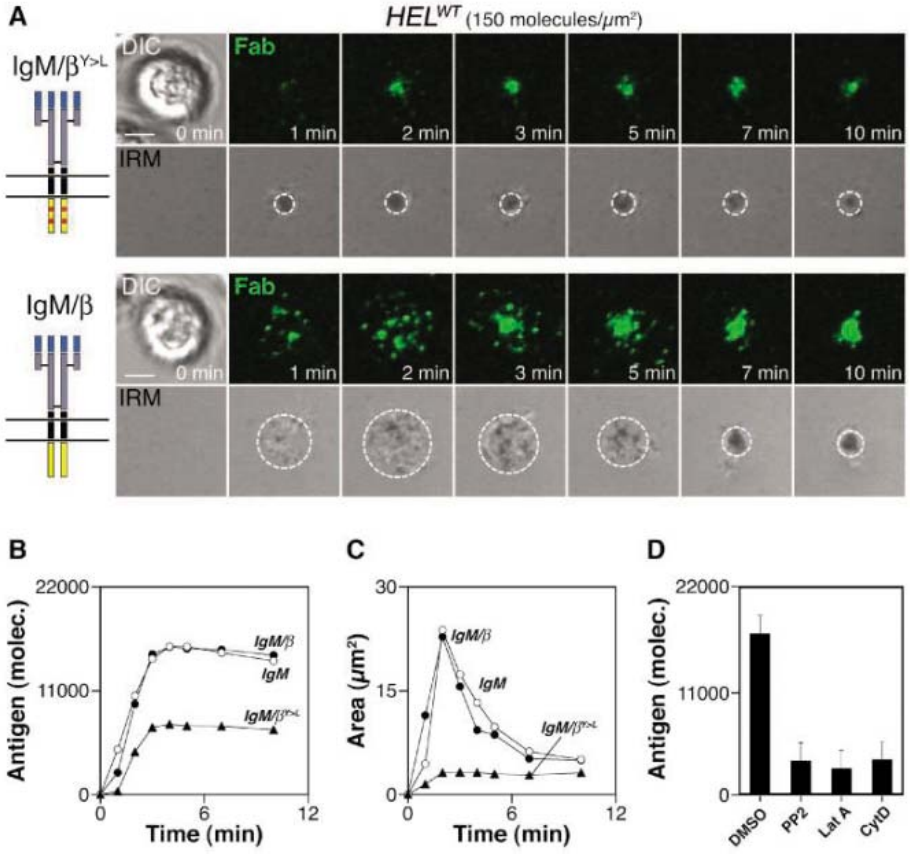

Fig. 2. BCR signaling is required for cell spreading and effective antigen collection. (**A**) Time lapse of the interaction of $IgM/\beta^{Y>L}$ (top two panels) and IgM/β (bottom two panels) transgenic naïve B cells with artificial lipid bilayers loaded with HEL^{WT} antigen (density = 150 molecules/μm^2) as followed by confocal microscopy (green) and IRM (gray). Dotted circles indicate the perimeter of the spread cell. Scale bars. 2 μm. (**B**) Quantification of the total amount of HEL aggregated and (**C**) the area of B cell spreading for the different transgenic B cells as a function of time. Filled circles, IgM/β; open circles, IgM; triangles, $IgM/\beta^{Y>L}$). (**D**) Total amount of accumulated HEL at 10 min when MD4 B cells were treated with the indicated inhibitors. DMSO, dimethylsulfoxide (control); PP2, tyrosine kinase inhibitor; LatA, latrunculin A (actin inhibitor); CytD, cytochalasin D (actin inhibitor).

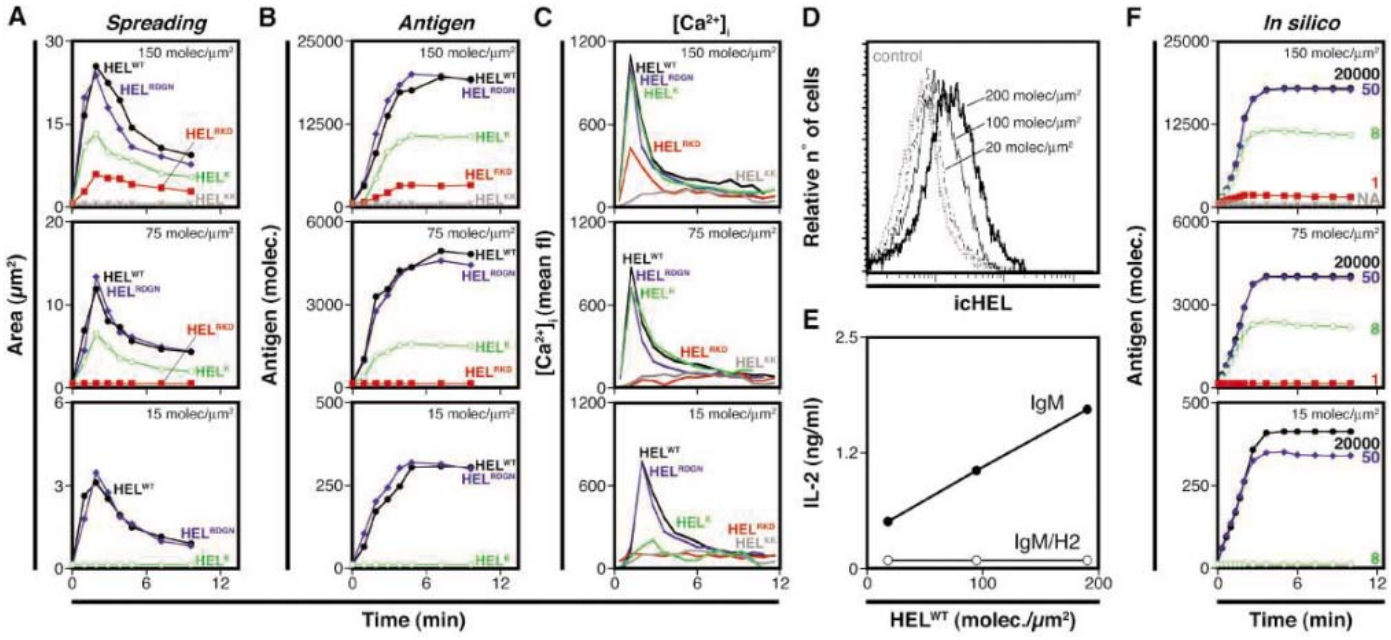

Fig. 3. The extent of B cell spreading depends on both the density and the affinity of the BCR for antigen and correlates with B cell activation. Kinetics of (**A**) B cell spreading, (**B**) antigen accumulation, and (**C**) the intracellular calcium response when MD4 transgenic B cells were settled on artificial planar bilayers loaded at the indicated densities with mutant HELs. Filled circles, HEL^{WT} ($K_a = 2.1 \times 10^{10}\ M^{-1}$); Diamonds, HEL^{RDGN} ($K_a = 5.2 \times 10^{7}\ M^{-1}$); open circles, HEL^{K} ($K_a = 8.7 \times 10^{6}\ M^{-1}$); Squares, HEL^{RKD} ($K_a = 0.8 \times 10^{6}\ M^{-1}$); Asterisks, HEL^{KK} ($K_a < 0.4 \times 10^{6}\ M^{-1}$). (**D**) Uptake of Alexa488-conjugated HEL^{WT} (icHEL) by MD4 B cells was evaluated by flow cytometry after incubation on antigen-bearing membranes at the specified densities. (**E**) Antigen presentation of HEL-derived peptides by IgM (closed symbols) or IgM/H2 (open symbols) transfectants when settled together with HEL-specific 2G7 hybridoma T cells on lipid bilayers containing HEL^{WT} at different densities. T cell activation was monitored by measuring interleukin-2 production after 24 hours. (**F**) Kinetics of antigen aggregation derived from the stochastic model. Antigen affinities are given as the affinity constant (K_a) in μM^{-1} units. See also fig. S4.

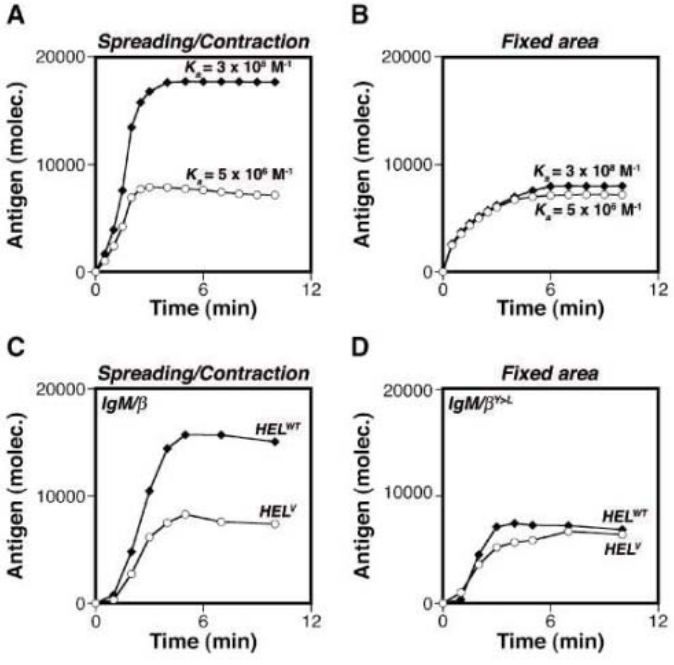

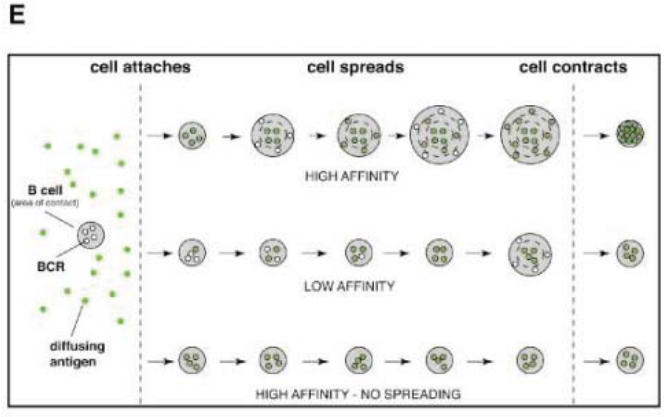

Fig. 4. B cell spreading and contraction enhances antigen affinity discrimination. (**A** and **B**) Stochastic model. (A) Shows an effective discrimination of ligand affinities when the spreading-contraction algorithm is implemented. (B) However, antigen discrimination is severely impaired if the spreading-contraction algorithm is disabled. (**C** and **D**) This prediction is supported experimentally by comparing the kinetics of interaction of HEL^{WT} (diamonds, $K_a = 3 \times 10^{8}\ M^{-1}$) and HEL^{V} (circles, $K_a = 5 \times 10^{6}\ M^{-1}$) by (C) IgM/β cells, which are able to spread normally, and (D) IgM/$\beta^{Y>L}$ transgenic B cells in which spreading is defective. See Fig. 2. (**E**) Conceptual basis for affinity discrimination. On the left, a B cell is shown that has just attached to a surface carrying diffusing antigens. If the interaction between antigen and BCR is of high affinity (upper row), rapid binding of antigen occurs. The high occupancy induces the cell to spread over the surface and expose more receptors, which in turn bind more antigen, leading to further spreading. After 2 min, the cell contracts and collects the receptor/ligand complexes into a central aggregate. However, if the interaction between antigen and receptors is of low affinity (middle row), binding occurs more slowly and the number of spreading events is much reduced. Consequently, when contraction takes place many fewer receptor-antigen complexes are collected. The lower row illustrates the situation in which the B cell is unable to spread because of a signaling-impaired BCR mutation. Even if high-affinity binding occurs, it cannot lead to an elevated accumulation of antigen.

ation of the two. All kinetic parameters were either directly determined, or derived from experimental measurements (supporting online text).

To model the spreading response, the area of contact between cell and bilayer increased in a series of small steps. The dependence on antigen binding was obtained by stipulating that each successive increment of cell area took place only if the receptor occupancy reached 75%. If this critical occupancy was not attained 1 min after initial attachment (an indication of insufficient antigen or avidity) then the cell "detached" and the simulation was aborted. As soon as receptor occupancy reached 75%, the area of cell attachment was increased by a fixed amount and a new cohort of receptors added. Iterated application of this strategy continued until 2 min after the initial contact with the lipid bilayer, when the area of cell contact began to shrink at a rate based on experimental measurements. Receptor-antigen pairs were collected into the central area (supporting online text).

We found that, given suitable parameters, this simple model was able to reproduce the essential features of the B cell response (Fig. 3F and fig. S4). It had a similar time course of spreading and contraction and it had a comparable capacity to discriminate between different antigen densities and affinities. The quantity of antigen accumulated showed a nonlinear relationship with affinity and density over a wide range (fig. S5A). However, if the spreading mechanism was inactivated in the program, for example by giving the B cell a fixed area of contact, then the amount of antigen accumulated was closely similar for both high- and low-affinity antigens (Fig. 4, A and B)—a result that we also found using the experimental set-up (Fig. 4, C and D, and fig. S2, G and H). These results are consistent with the notion that a quantitative relationship between receptor occupancy and cell spreading may influence the observed cellular response (Fig. 4E). Mechanistic details of this linkage—the role played by the small focal clusters of receptors and how these are coupled to actin accumulation and tyrosine phosphorylation and hence the extension of lamellipodia—will require further collaboration between experiment and theory.

The B cell spreading reported here shares some similarities to the one observed in T cells (*18*–*21*). Both processes are sensitive to inhibitors of signaling and actin polymerization (*20*) and could represent an active process common to lymphocytes in general. In T cells, the process of antigen recognition has been the subject of extensive quantitative studies combined with computer models (*22*–*25*). However, the gathering of antigen by B cells is responsive to a much wider range of antigen affinities than T cells. It will occur in the absence of adhesion molecules without compromising the fundamental features of the antigen-specific responses. This highly reduced experimental system can then be modeled using a simple stochastic algorithm based on the binding interactions between antigen and cell receptors. In this way, we have been able to clarify the basis of the powerful discriminatory ability of B cells.

References and Notes

1. D. M. Russell *et al.*, *Nature* **354**, 308 (1991).
2. S. B. Hartley *et al.*, *Nature* **353**, 765 (1991).
3. J. G. Tew, M. H. Kosco, G. F. Burton, A. K. Szakal, *Immunol. Rev.* **117**, 185 (1990).
4. M. Wykes, A. Pombo, C. Jenkins, G. G. MacPherson, *J. Immunol.* **161**, 1313 (1998).
5. A. M. Haberman, M. J. Shlomchik, *Nat. Rev. Immunol.* **3**, 757 (2003).
6. M. H. Kosco-Vilbois, *Nat. Rev. Immunol.* **3**, 764 (2003).
7. A. Bergtold, D. D. Desai, A. Gavhane, R. Clynes, *Immunity* **23**, 503 (2005).
8. F. D. Batista, D. Iber, M. S. Neuberger, *Nature* **411**, 489 (2001).
9. Y. R. Carrasco, S. J. Fleire, T. Cameron, M. L. Dustin, F. D. Batista, *Immunity* **20**, 589 (2004).
10. C. R. Monks, B. A. Freiberg, H. Kupfer, N. Sciaky, A. Kupfer, *Nature* **395**, 82 (1998).
11. A. Grakoui *et al.*, *Science* **285**, 221 (1999).
12. M. F. Krummel, M. D. Sjaastad, C. Wulfing, M. M. Davis, *Science* **289**, 1349 (2000).
13. C. C. Goodnow *et al.*, *Nature* **334**, 676 (1988).
14. Y. M. Teh, M. S. Neuberger, *J. Exp. Med.* **185**, 1753 (1997).
15. G. T. Williams, C. J. Peaker, K. J. Patel, M. S. Neuberger, *Proc. Natl. Acad. Sci. U.S.A.* **91**, 474 (1994).
16. M. Reth, *Nature* **338**, 383 (1989).
17. S. S. Andrews, D. Bray, *Phys. Biol.* **1**, 137 (2004).
18. S. C. Bunnell *et al.*, *J. Cell Biol.* **158**, 1263 (2002).
19. S. C. Bunnell, V. Kapoor, R. P. Trible, W. Zhang, L. E. Samelson, *Immunity* **14**, 315 (2001).
20. P. A. Negulescu, T. B. Krasieva, A. Khan, H. H. Kerschbaum, M. D. Cahalan, *Immunity* **4**, 421 (1996).
21. M. V. Parsey, G. K. Lewis, *J. Immunol.* **151**, 1881 (1993).
22. N. J. Burroughs, C. Wulfing, *Biophys. J.* **83**, 1784 (2002).
23. K. H. Lee *et al.*, *Science* **302**, 1218 (2003).
24. S. J. Lee, Y. Hori, J. T. Groves, M. L. Dustin, A. K. Chakraborty, *Trends Immunol.* **23**, 500 (2002).
25. Q. J. Li *et al.*, *Nat. Immunol.* **5**, 791 (2004).

26. We thank P. Bates and his group, J. Lewis, K. Lipkow, V. Silva-Vargas, and C. Reis e Sousa for critical reading of this manuscript. We also thank the Electron Microscopy Unit at the London Research Institute. This work was funded by National Institute of General Medical Sciences grant G64713 (D.B.), Cancer Research UK, and the European Molecular Biology Organization Young Investigator Program (F.D.B.).

Supporting Online Material

www.sciencemag.org/cgi/content/full/312/5774/738/DC1
Materials and Methods
SOM Text
Figs. S1 to S5
Table S1
References
Movies S1 to S4

16 December 2005; accepted 13 March 2006
10.1126/science.1123940

Structure of the Multidrug Transporter EmrD from *Escherichia coli*

Yong Yin,* Xiao He,* Paul Szewczyk, That Nguyen, Geoffrey Chang†

EmrD is a multidrug transporter from the Major Facilitator Superfamily that expels amphipathic compounds across the inner membrane of *Escherichia coli*. Here, we report the x-ray structure of EmrD determined to a resolution of 3.5 angstroms. The structure reveals an interior that is composed mostly of hydrophobic residues, which is consistent with its role transporting amphipathic molecules. Two long loops extend into the inner leaflet side of the cell membrane. This region can serve to recognize and bind substrate directly from the lipid bilayer. We propose that multisubstrate specificity, binding, and transport are facilitated by these loop regions and the internal cavity.

The advent of medicinal antibiotics heralded an unprecedented breakthrough in the treatment of infectious disease, but the emergence of drug-resistant bacteria is threatening to undermine this achievement. Multidrug resistance (MDR) develops partially through direct drug efflux by integral membrane transporters. There are two classes of MDR transporters: adenosine 5′-triphosphate (ATP)–binding cassette (ABC) proteins that directly couple drug efflux to ATP hydrolysis and secondary transporters that use energy derived from electrochemical gradients across the cell membrane. The secondary transporters include four families: the Resistance/Nodulation/Division superfamily (RND), the Multiple Antimicrobial Toxin Extrusion family, the Small Multidrug Resistance family, and the Major Facilitator Superfamily (MFS). The MDR transporters from the MFS family (MDR MFS) are among the most prevalent in microbial genomes and diverse in their substrate specificities (*1*).

One MDR MFS transporter, EmrD, is a proton-dependent secondary transporter from *Escherichia coli*. EmrD was first identified as an efflux pump for uncouplers of oxidative phosphorylation (*2*), which can rapidly arrest growth in bacteria by depleting the H^+ gradient (*3*). Some of these uncouplers are structurally unrelated, such as meta–chloro carbonylcyanide

The Scripps Research Institute, Department of Molecular Biology, 10550 North Torrey Pines Road, CB-105, La Jolla, CA 92037, USA.

*These authors contributed equally to this work.
†To whom correspondence should be addressed. E-mail: gchang@scripps.edu

phenylhydrazone (CCCP) and tetrachlorosalicylanilide. It was later discovered that EmrD could also transport detergents such as benzalkonium and sodium dodecylsulfate (*4*). Sequence alignment suggests that EmrD is a close homolog to other MDR MFS transporters (*5*), including NorA from *Staphylococcus aureas* (with 19% identity and 41% similarity), LmrP from *Lactococcus lactis* (22 and 40%), FlorR from *S. enterica* (24 and 45%), Bmr from *Bacillus subtilis* (20 and 40%), and the *E. coli* transporters MdfA (26 and 39%) and Bcr (24 and 44%) (fig. S1). EmrD *E. coli* has 394 amino acids and a molecular weight of ~42.2 kD. Hydropathy analysis indicates that EmrD has 12 transmembrane α helices, and phylogenetic studies have suggested that it is a drug/H^+ antiporter (DHA) from the DHA12 drug efflux subfamily within the MFS (*6*).

The general model for substrate efflux by secondary transporters involves an alternating access mechanism, and most non-MDR MFS transport systems, such as the lactose (LacY) and glycerol-3-phosphate (GlpT) permeases, typically transport a relatively narrow range of structurally related substrates (*7*, *8*). MDR MFS transporters, such as EmrD, differ significantly in that they are able to export a broad spectrum of hydrophobic compounds (*9*). How do they recognize this wide range of structurally distinct substrates and what are the conformational rearrangements within the MFS necessary for hydrophobic drug efflux? To elucidate the molecular basis of MDR MFS transport, we determined the x-ray structure of EmrD to 3.5 Å resolution by anomalous dispersion methods.

Crystals of EmrD were grown in the presence of β-dodecyl-maltoside. X-ray diffraction data was collected from a native crystal and a gold thiomalate derivative (table S1). After density modification and phase extension, the electron density map clearly showed two identical molecules in the asymmetric unit with densities corresponding to side chains (Fig. 1A and fig. S2). The crystal lattice contacts between the two copies of EmrD are small (<250 $Å^2$), and we believe that the packing arrangement of the dimer is nonphysiological. We designate the transmembrane helices in each monomer as H1 to H12 and the connecting loops L1-2 to L11-12.

The overall structural topology of EmrD is reminiscent of LacY and GlpT. Twelve transmembrane helices form a compact structure that spans ~50 Å in the plane of the lipid bilayer and ~45 Å along the membrane normal (Fig. 1, B and C). The transmembrane helices facing away from the interior (H3, H6, H9, and H12) demonstrate an organization similar to LacY and GlpT. The remaining transmembrane helices form the internal cavity, but their relative orientations show substantial deviation from those observed in LacY and GlpT. This structural arrangement may reflect a general architecture of MDR MFS transporters.

Unlike the LacY and GlpT structures, which are both in the configuration facing the cytoplasm, this EmrD structure is not in a V shape and probably represents an intermediate state. The periplasmic loops in EmrD are more imbedded in the cell membrane, and the central loop L6-7 is considerably shorter. A molecular two-fold axis relates the N- and C-terminal halves of EmrD (H1 to H6 and H7 to H12; average root mean square deviation of 0.78 Å for 116 carbon alpha positions) and supports the notion that the MFS arose from recurrent gene duplication of an ancestral six-helix domain (*9*, *10*). The two halves of EmrD, however, are less symmetric than those of LacY or GlpT, and the most notable internal asymmetry is localized to the loop regions on the periplasmic side. For example, L3-4 (residues 92 to 99) is actually a bent helix, whereas L9-10 (residues 285 to 289) is a short loop. Compared with LacY, H6 in

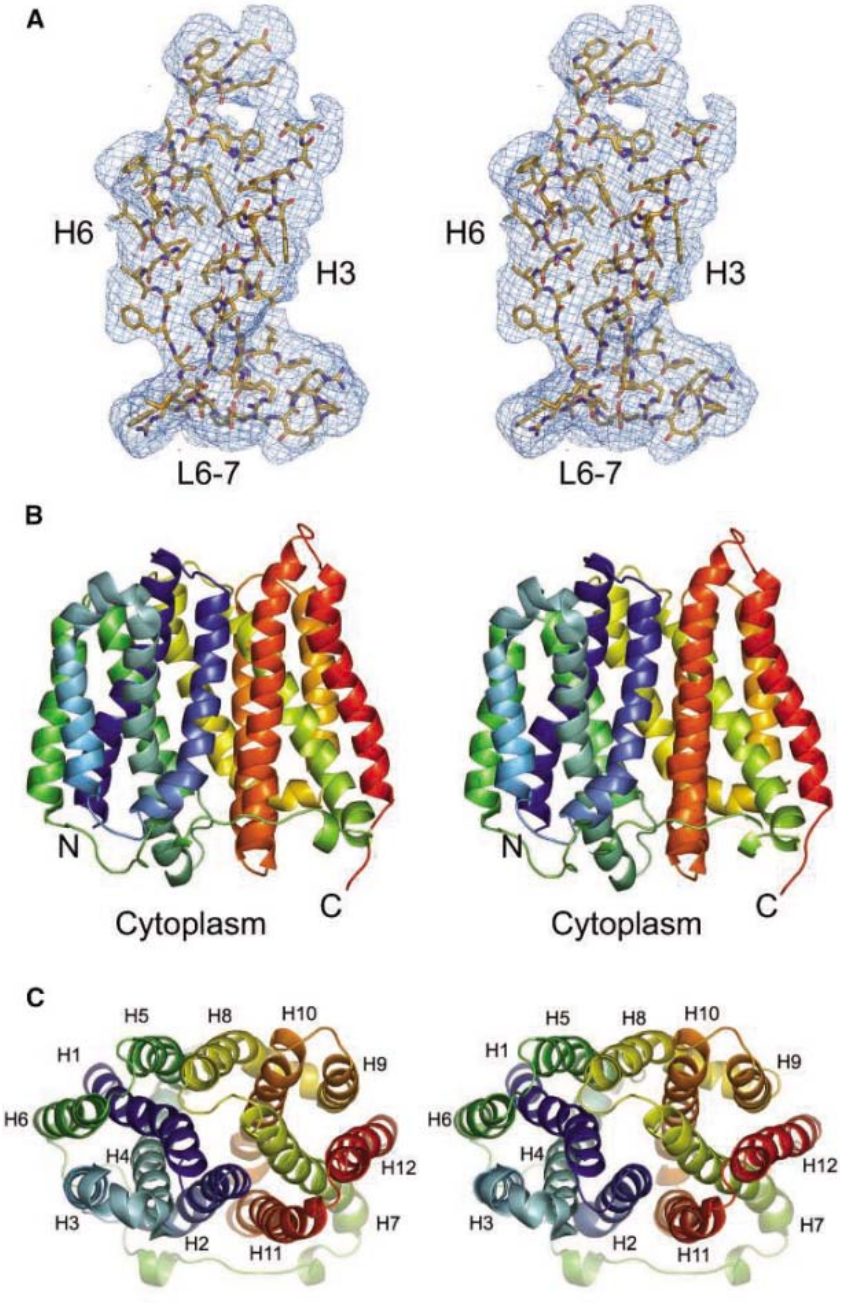

Fig. 1. Stereoimages of crystallography and structure of EmrD. (**A**) A portion of the experimental electron density map is shown for H3, H6, and L6-7. The map is contoured to 1σ. (**B**) Side view of EmrD. The N and C termini are indicated. (**C**) View of EmrD looking toward the cytoplasm showing the molecular two-fold axis relating the N- and C-terminal halves. Transmembrane helices are indicated. The images were created by PyMol (*33*).

EmrD is shorter, whereas H11 is substantially longer.

The most notable difference between the structure of EmrD and the structures of LacY and GlpT is in the internal cavity. Whereas LacY and GlpT have hydrophilic interiors, the internal cavity of EmrD comprises mostly hydrophobic residues, consistent with its function of transporting lipophilic compounds. Several of these residues are bulky and aromatic (Ile^{28}, Ile^{217}, Ile^{253}, Tyr^{52}, Tyr^{56}, Trp^{300}, and Phe^{249}), and some are conserved in other MDR MFS transporters (fig. S1 and Fig. 2, A and B). This type of hydrophobic core has been previously proposed and also observed in the recent x-ray structure of EmrE with substrate (*11*, *12*). These residues likely contribute to a general mechanism of substrate translocation and may play an important role in dictating a level of drug specificity either through steric or aromatic interactions. The internal cavity also has several uncharged polar residues, such as glutamines (Gln^{21}, Gln^{24}, Gln^{46}, and Gln^{60}), and a basic arginine residue (Arg^{118}) that is located closer to the cytoplasmic side. On the periplasmic side lie a threonine (Thr^{25}), an aspartate (Asp^{33}), and a glutamate residue (Glu^{227}) that could easily reorient into the cavity during the transport cycle and may participate in H^+ translocation.

The hydrophobic interior of EmrD provides a generalized pathway and mechanism for transporting a variety of different substrates in drug efflux systems (*11*). EmrD possesses two pairs of stacked aromatic groups (Tyr^{52}/Tyr^{56} and Trp^{300}/Phe^{249}) that could play a key role in multisubstrate binding, given their ability to stack with aromatic drugs (Fig. 2B). In Bmr, two phenylalanines have been implicated in substrate recognition (*13*), whereas the multidrug binding site of the transcriptional repressor QacR uses several aromatic and polar residues (*14*, *15*). The energetic cost of transporting charged amphipathic compounds may be compensated by these types of hydrophobic interactions (*11*).

The structure of EmrD reveals another region that could provide additional substrate specificity. There are two long helical regions (H4, L4-5, H5 and H10, L10-11, and H11) located on the cytoplasmic side that are arranged much closer to the central cavity and extend farther into the cytoplasm than do LacY and GlpT (Fig. 2C). The cytoplasmic end of H4 also has a number of charged residues (Arg^{118}, Arg^{122}, Asp^{123}, Glu^{126}, Arg^{127}, and Arg^{131}), which may play a role both in defining the topology of the transporter and in substrate recognition (*9*). Here, we refer to this region as the selectivity filter. Functional studies of the EmrD homolog MdfA have indicated that several residues in this region are important for substrate recognition. For example, residues in the cytoplasmic halves of H4, H5, and H6 in MdfA are protected by substrate against alkylation by *N*-ethylmaleimide (NEM) (*16*) (Fig. 2C and fig.

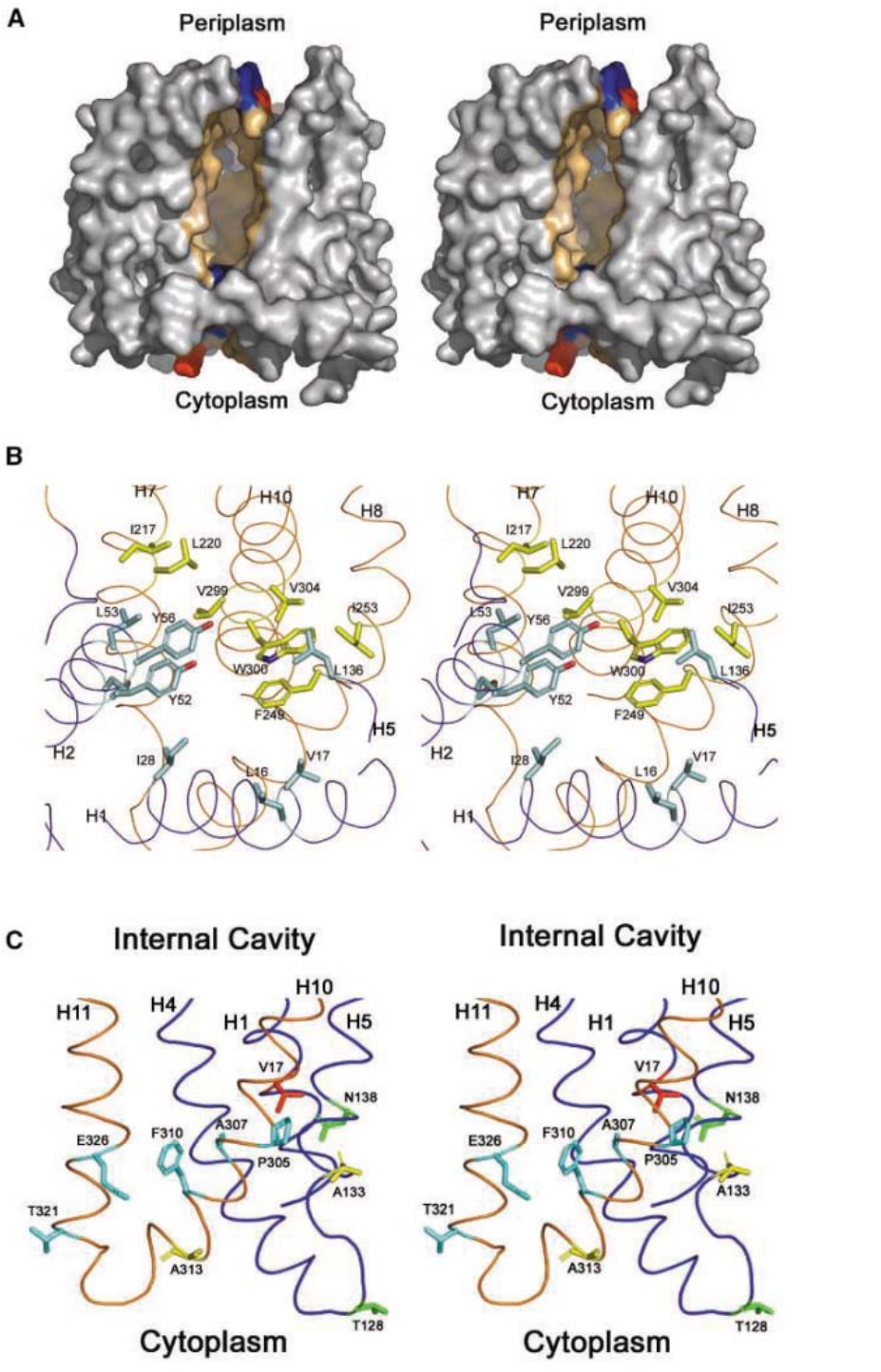

Fig. 2. (**A**) Stereoimage cut-away view of the hydrophobic internal cavity of EmrD. For clarity, residues 43 to 67 were omitted. Hydrophobicity is shown as a gradation from low (light brown) to high (brown). Regions that are positive and negative are shown in blue and red, respectively. (**B**) Stereoimage inside view of the internal cavity of EmrD, characterized by the lining of hydrophobic residues (*34*). The N- and C-terminal halves of EmrD and the corresponding residues are colored blue and orange, respectively. (**C**) Stereoimage close view of the selectivity filter region of EmrD. The positions of residues that are involved in substrate recognition based on protein sequence homology to other MDR MFS transporters are marked in fig. S1. Residues colored in light blue correspond to those in MdfA that, when mutated into cysteines, either reduce or abolish resistance. Residues in yellow correspond to positions in LmrP that are important for substrate recognition. Val^{17}, shown in red, corresponds to Glu^{26} in MdfA and Asp^{23} in FlorR, which are both important for drug recognition. Residues shown in green correspond to cysteine mutations in MdfA that are protected from NEM labeling by substrate. The relative position of the cytoplasm and the internal cavity are indicated.

S1). In addition, certain single-site mutations in the cytoplasmic halves of H10 and H11 as well as L10-11 of MdfA either abolish or substantially reduce MDR (*17*, *18*) (Fig. 2C and fig. S1). Biochemical studies on LmrP, another close homolog of EmrD, also suggest that substantial conformational changes occur in this region. In LmrP, single-site mutations at positions corresponding to 133 and 313 in EmrD show that negative charges in this region are not critical for transport function but are important for drug recognition (Fig. 2C). Further studies on LmrP using fluorescein maleimide labeling upon substrate binding suggest movement of this region from a nonpolar to a polar environment (*18*).

Helix 1 in EmrD might also be important for drug recognition. Studies in MdfA and FlorR have implicated a key residue (Glu^{26} in MdfA and Asp^{23} in FlorR) corresponding to Val^{17} in EmrD that is important for recognizing substrate (*19*, *20*). If this residue is changed to a valine in MdfA, the transporter loses its ability to recognize cationic compounds but still retains wild-type resistance to the neutral antibiotic chloramphenicol (*16*). Interestingly, some other MDR MFS transporters that have small hydrophobic residues at this position are also known to transport neutral hydrophobic compounds. In this EmrD structure, Val^{17} points toward the internal cavity but is also partially accessible from the inner membrane leaflet side (Fig. 2, B and C).

Based on the structure and homology to other MDR MFS transporters, we propose that EmrD intercepts CCCP on the inner membrane leaflet as it crosses toward the cytoplasm (Fig. 3). In the absence of drug efflux, CCCP diffuses across the inner membrane from the periplasmic space in the protonated form, disrupting the pH differential as it moves into the cytoplasm (*3*). The molecule then quickly releases its proton to become a lipophilic soluble anion that rapidly diffuses back to the periplasm (*21*). Binding of CCCP on the inner leaflet side is likely facilitated by the selectivity filter and hydrophobic interactions within the internal cavity of EmrD. Structural rearrangement favoring the outward facing conformation would be coupled to H^+ antiport by a rocker-switch mechanism similar to those previously proposed, but this remains to be proven (*7*, *8*). Based on the structure of EmrD, we speculate that proton translocation and drug transport may occur at different locations, which has also been proposed for MdfA (*11*).

What happens to CCCP when it enters the periplasmic space? There are at least two possibilities. Several MDR MFS systems have an adaptor protein that facilitates the transport of substrate through the periplasmic space; possibly using an apparatus similar to the TolC-adaptor RND efflux systems (*22*–*24*). Perhaps the best known example is the EmrAB efflux system, in which EmrB operates as the MDR MFS transporter and EmrA is an accessory protein (*1*, *25*). In this case, the CCCP would be expelled out of the bacterial cell. However, no such adaptor protein or TolC-like apparatus has been identified that is associated with EmrD or any other 12-TMS MDR MFS transporter. If EmrD acts alone, as do LmrP and Bmr in Gram-positive bacteria, then CCCP would be expelled into the periplasmic space in *E. coli*.

The intracellular loop region of EmrD is reminiscent of the intracellular domain of MsbA, which is a bacterial homolog of MDR ABC transporters (*26*). In MsbA, these helices are thought to recognize head groups of the substrates as well as to transmit structural changes caused by ATP hydrolysis and substrate binding (*27*–*29*). Functional studies on the MDR ABC transporter LmrA suggest a model in which drug recognition by MDR transporters occurs in the inner leaflet of cell membrane bilayer (*30*). The lateral diffusion of hydrophobic substrate has also been proposed for the RND transporter AcrAB/TolC efflux system (*22*, *31*), and access from the inner membrane leaflet is evident in the recent x-ray structures of both EmrE and MsbA with substrate (*12*, *28*). Both of these structures also have hydrophobic pockets. In addition, mutational and biochemical studies on the cytoplasmic side of MdfA and LmrP suggest a model where drugs could diffuse laterally from the inner membrane leaflet (*16*–*18*, *32*). This type of diffusion can be a common theme not only for the MDR MFS but also among all the MDR transporter families.

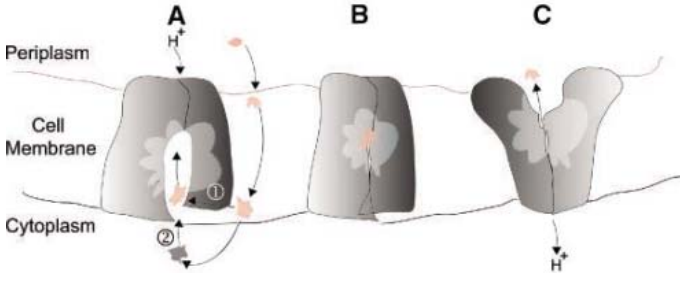

Fig. 3. A potential mechanism for hydrophobic substrate transport by EmrD. (**A**) The drug can enter the internal cavity of the transporter either through the inner membrane leaflet (path 1) or through the cytoplasm (path 2). Substrate recognition and binding may be facilitated through the selectivity filter and the internal cavity containing hydrophobic residues. (**B**) The drug is transported through a rocker-switch alternating-access model coupled with H^+ antiport. (**C**) The drug is transported across the lipid bilayer.

References and Notes

1. M. Putman, H. W. van Veen, W. N. Konings, *Microbiol. Mol. Biol. Rev.* **64**, 672 (2000).
2. V. Naroditskaya, M. J. Schlosser, N. Y. Fang, K. Lewis, *Biochem. Biophys. Res. Commun.* **196**, 803 (1993).
3. T. A. Krulwich, P. G. Quirk, A. A. Guffanti, *Microbiol. Rev.* **54**, 52 (1990).
4. K. Nishino, A. Yamaguchi, *J. Bacteriol.* **183**, 5803 (2001).
5. I. T. Paulsen, M. H. Brown, R. A. Skurray, *Microbiol. Rev.* **60**, 575 (1996).
6. M. H. Saier Jr., C. V. Tran, R. D. Barabote, *Nucleic Acids Res.* **34**, D181 (2006).
7. J. Abramson *et al.*, *Science* **301**, 610 (2003).
8. Y. Huang, M. J. Lemieux, J. Song, M. Auer, D. N. Wang, *Science* **301**, 616 (2003).
9. S. S. Pao, I. T. Paulsen, M. H. Saier, *Microbiol. Rev.* **62**, 1 (1998).
10. M. H. Saier, *Mol. Microbiol.* **48**, 1145 (2003).
11. I. T. Paulsen, K. Lewis, *Microbial Multidrug Efflux* (Horizon Press, Norfolk, 2002).
12. O. Pornillos, Y. J. Chen, A. P. Chen, G. Chang, *Science* **310**, 1950 (2005).
13. K. A. Klyachko, S. Schuldiner, A. A. Neyfakh, *J. Bacteriol.* **179**, 2189 (1997).
14. D. S. Murray, M. A. Schumacher, R. G. Brennan, *J. Biol. Chem.* **279**, 14365 (2004).
15. M. A. Schumacher, M. C. Miller, R. G. Brennan, *EMBO J.* **23**, 2923 (2004).
16. J. Adler, E. Bibi, *J. Biol. Chem.* **279**, 8957 (2004).
17. J. Adler, E. Bibi, *J. Biol. Chem.* **280**, 2721 (2005).
18. P. Mazurkiewicz, W. N. Konings, G. J. Poelarends, *J. Biol. Chem.* **277**, 26081 (2002).
19. R. Edgar, E. Bibi, *EMBO J.* **18**, 822 (1999).
20. M. Braibant, J. Chevalier, E. Chaslus-Dancla, J. M. Pages, A. Cloeckaert, *Antimicrob. Agents Chemother.* **49**, 2965 (2005).
21. J. Kasianowicz, R. Benz, S. McLaughlin, *J. Membr. Biol.* **82**, 179 (1984) (Historical Archive).
22. S. Murakami, R. Nakashima, E. Yamashita, A. Yamaguchi, *Nature* **419**, 587 (2002).
23. J. A. Fralick, *J. Bacteriol.* **178**, 5803 (1996).
24. V. Koronakis, A. Sharff, E. Koronakis, B. Luisi, C. Hughes, *Nature* **405**, 914 (2000).
25. K. Nishino, T. Latifi, E. A. Groisman, *Mol. Microbiol.* **59**, 126 (2006).
26. A. B. Chang, R. Lin, W. K. Studley, C. V. Tran, M. H. Saier, *Mol. Membr. Biol.* **21**, 171 (2004).
27. G. Chang, C. B. Roth, *Science* **293**, 1793 (2001).
28. C. L. Reyes, G. Chang, *Science* **308**, 1028 (2005).
29. B. Woebking *et al.*, *J. Bacteriol.* **187**, 6363 (2005).
30. H. Bolhuis *et al.*, *EMBO J.* **15**, 4239 (1996).
31. E. W. Yu, G. McDermott, H. I. Zgurskaya, H. Nikaido, D. E. Koshland Jr., *Science* **300**, 976 (2003).
32. H. Bolhuis *et al.*, *J. Biol. Chem.* **271**, 24123 (1996).
33. W. L. Delano, PyMol molecular visualization system (http://pymol.sourceforge.net).
34. Single-letter abbreviations for the amino acid residues are as follows: A, Ala; C, Cys; D, Asp; E, Glu; F, Phe; G, Gly; H, His; I, Ile; K, Lys; L, Leu; M, Met; N, Asn; P, Pro; Q, Gln; R, Arg; S, Ser; T, Thr; V, Val; W, Trp; and Y, Tyr.

35. We thank S. Lieu for general lab support and the staff at the Stanford Synchrotron Radiation Laboratory (SSRL) and the Advanced Light Source (beamlines BL821 and BL831) for assistance with data collection and crystal screening. We thank P. Wright, R. Milligan, M. Saier, C. Reyes, S. Aller, and A. Ward for carefully reading and making valuable suggestions to the manuscript. This study was supported by grants from the NIH (GM70480 and GM65798), NASA (NAG8-1834), a NIH Presidential Early Career Award, and the Skaggs Institute for Chemical Biology. Coordinates have been deposited in the Protein Data Bank (PDB code 2GFP).

Supporting Online Material

www.sciencemag.org/cgi/content/full/312/5774/741/DC1
Materials and Methods
Figs. S1 and S2
Table S1
References

31 January 2006; accepted 7 April 2006
10.1126/science.1125629

Signal Recognition Particle Receptor Exposes the Ribosomal Translocon Binding Site

Mario Halic,[1*] Marco Gartmann,[1*] Oliver Schlenker,[2] Thorsten Mielke,[3] Martin R. Pool,[4] Irmgard Sinning,[2] Roland Beckmann[1,3*†]

Signal sequences of secretory and membrane proteins are recognized by the signal recognition particle (SRP) as they emerge from the ribosome. This results in their targeting to the membrane by docking with the SRP receptor, which facilitates transfer of the ribosome to the translocon. Here, we present the 8 angstrom cryo–electron microscopy structure of a "docking complex" consisting of a SRP-bound 80*S* ribosome and the SRP receptor. Interaction of the SRP receptor with both SRP and the ribosome rearranged the S domain of SRP such that a ribosomal binding site for the translocon, the L23e/L35 site, became exposed, whereas Alu domain–mediated elongation arrest persisted.

Most secretory or membrane proteins carry N-terminal signal sequences that bind to the SRP, a conserved ribonucleoprotein complex (*1*). After binding SRP, the resulting complex is targeted in a guanine nucleotide triphosphate (GTP)–dependent manner to the plasma membrane in bacteria or the endoplasmic reticulum in eukaryotes via the SRP receptor (SR). This GTP-dependent docking reaction coordinates the presence of a signal sequence on the ribosome with the presence of a vacant translocon (*2*). The transfer of the ribosome nascent chain complex (RNC) from SRP to the translocon occurs before GTP hydrolysis (*3*, *4*). A direct interaction between SR and the translocon has been demonstrated in prokaryotic cells (*5*), and an interaction between SR and the ribosome is suggested in eukaryotic (*6*) and prokaryotic cells (*7*).

In eukaryotes, SR is a heterodimeric complex formed by two GTPase subunits, SRα (FtsY in *Escherichia coli*) and the integral membrane protein SRβ. SRα consists of an N-terminal X domain, which interacts with SRβ (X1), and, connected by a positively charged linker region (X2), a conserved GTP-binding NG domain (*8*), which is homologous to the NG domain of SRP54 (Ffh in *E. coli*).

The SRP-SR interaction involves primarily the NG domains of SRP54 and SRα. A prerequisite for stable complex formation is GTP binding by both NG domains interacting in a twinlike conformation (*9*, *10*). Both NG domains act as mutual GTPase-activating proteins (GAPs) (*11*), and GTP hydrolysis leads to dissociation (*3*).

Crystal structures of the SRαX1-SRβ complex (*8*, *12*) show GTP present in the active site, suggesting catalytic inactivity of SRβ in complex with SRα. The interaction between SRαX and SRβ is GTP dependent, and GTP hydrolysis would result in dissociation (*8*).

It is not known how SR interacts with SRP in the context of the SRP-RNC targeting complex. The targeting complex itself is unable to interact directly with the translocon (*13*) due to overlapping binding sites of SRP (*14*) and translocon at the ribosomal tunnel exit (*15*). The presence of SR, however, allows translocon binding (*13*) and leads to structural rearrangements of SRP, which suggests a distinct mode of ribosome binding (*16*). The question thus remains: How does SR prime the SRP-RNC targeting complex to allow the transfer of the signal sequence and RNC to the translocon?

The SR-SRP-RNC complex was reconstituted in vitro (*14*, *17*). Stalled RNCs were used for the reconstitution with excess amounts of purified mammalian SRP and recombinant SR [lacking the transmembrane domain of SRβ (*18*)]. Sucrose density gradient centrifugation confirmed

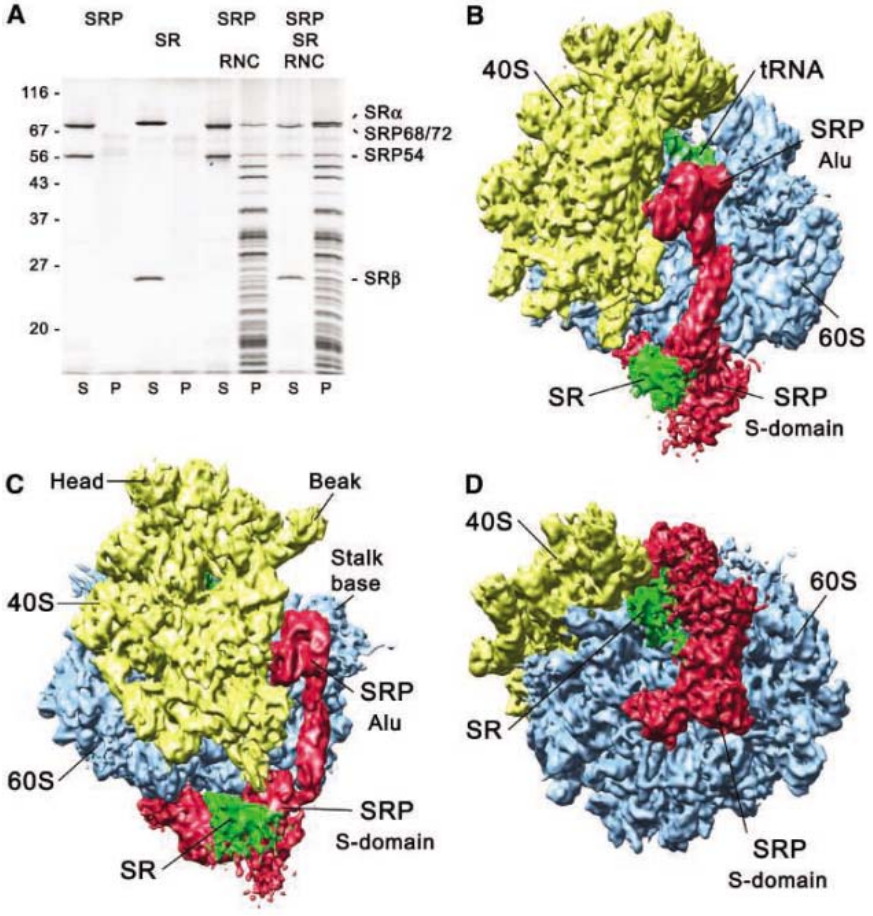

Fig. 1. Reconstitution and cryo-EM structure of the 80*S* ribosome-SRP-SR docking complex. (**A**) Binding assay using purified RNCs (RNC) with an excess of purified SRP and SR in the presence of GMP-PNP. Supernatant (S) and pellet (P) fractions were analyzed by SDS–polyacrylamide gel electrophoresis and Coomassie blue staining. SRP and SR bind stably to RNCs, and both subunits of SR, SRα and SRβ, are detectable in the bound fraction. (**B**) Cryo-EM reconstruction of the 80*S* RNC-SRP-SR complex. The 40*S* small ribosomal subunit is shown in yellow, 60*S* large subunit is in blue, P-site tRNA is in green, and SRP is in red. Additional density at the S domain of SRP is shown in bright green. Landmark features are indicated. (**C**) Same as (B), rotated by 45° around the central vertical axis. (**D**) Same as (B), rotated by 90° backward around a central horizontal axis.

[1]Institute of Biochemistry, Charité, University Medical School Berlin, Monbijoustrasse 2, 10117 Berlin, Germany. [2]Heidelberg University Biochemistry Center (BZH), Im Neuenheimer Feld 328, D-69120 Heidelberg, Germany. [3]UltraStructureNetwork, USN, Max Planck Institute for Molecular Genetics, Ihnestrasse 63-73, 14195 Berlin, Germany. [4]University of Manchester, Faculty of Life Sciences, Michael Smith Building, Oxford Road, Manchester M13 9PT, UK.

*Present address: Gene Center, University of Munich, Department of Chemistry and Biochemistry, Feodor-Lynen-Strasse 25, 81377 Munich, Germany.

†To whom correspondence should be addressed. E-mail: beckmann@lmb.uni-muenchen.de

specific and high-affinity binding of SRP and both subunits of SR to RNCs with a near one-to-one-to-one stoichiometry (Fig. 1). No substantial SRP-SR interaction was observed in the absence of either GTP or GMP-PNP (β, γ-imidoguanosine 5′-triphosphate), as expected.

The cryo–electron microscopy (cryo-EM) map shows the 80*S* ribosome at 7.4 Å resolution (fig. S1), with additional density stretching from the peptide exit site to the intersubunit space (Fig. 1). A difference in the domain appearance between Alu and S domains of SRP (*14*) probably reflects the higher flexibility of the S domain in the newly formed complex after SR interaction. Consequently, the α-helical secondary structure of proteins is well resolved in the ribosome and the SRP Alu domain but not in density corresponding to the SR and S domain of SRP.

The Alu domain is rigidly bound to the ribosome in the exact same position in both the SRP-RNC complex (*14*) and the SR-SRP-RNC complex. Thus, the elongation retardation induced by the Alu domain (*19*) appears to persist during the docking phase and may be released only after successful transfer of the RNC to the translocon.

A clear difference between this reconstruction and the structure of the SRP-RNC complex (*14*) is the additional density visible on the S domain of SRP near the previously described connection C4. In difference calculations, a strong signal appeared in this region and can, thus, be assigned to additional density provided by SR (Fig. 2A). It contacts both the S domain of SRP and the 60*S* ribosomal subunit, confirming a "dual" binding mode of SR to both SRP and the ribosome (*6*). This density corresponds very well to the structure of the mammalian SRαX1-SRβ heterodimer (*12*), for which two alternative orientations related by a 180° rotation are possible. The best-fitting model (correlation coefficient of 0.82 versus 0.78) positions the SRαX1-SRβ heterodimer such that the SRβ subunit interacts with 7*S* RNA of SRP and also with two ribosomal components, protein L31 and helix 99 of 25*S* ribosomal RNA (rRNA) (Fig. 2, B and C). This is in agreement with cross-linking data showing a ribosomal protein of 21 kD (possibly representing L31) in the immediate vicinity of SRβ (*18*). The linker between the globular domain of the SRβ subunit and the transmembrane helix comprises seven amino acids and is long enough to span a maximum distance of about 25 Å between the observed position of SRβ and the membrane. In this position, the SRαX1 domain interacts only with the 7*S* RNA of SRP and the SRP68/72 protein heterodimer and is close to but does not participate directly in the interaction with the ribosome, as suggested (*6*). Involvement of the SRP68/72 heterodimer may explain the observation that alkylation of SRP68/72 yields

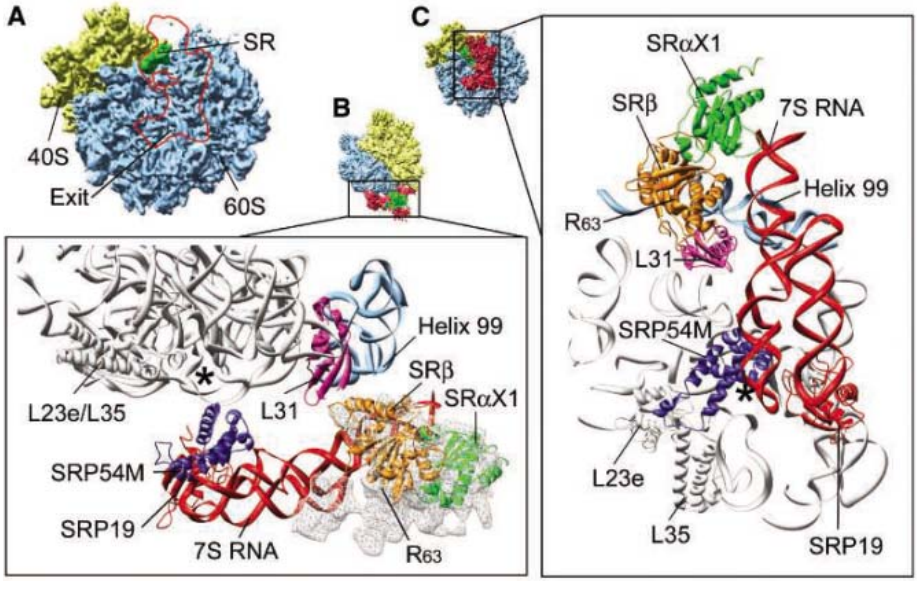

Fig. 2. Difference map and docking of the SRαX1-SRβ heterodimer. (**A**) Bottom view of the EM map of the RNC-SRP-SR complex together with the difference map (green, SR) indicating additional density as compared with the RNC-SRP map. The contour of the SRP S domain/SR density is shown as a red line. (**B**) Molecular models docked into the EM densities (side view). White mesh, extra density in the RNC-SRP-SR complex; green and orange, mammalian SRαX1-SRβ heterodimer; white ribbons, 25*S* rRNA and proteins L23e/L35; bright blue, helix 99 of 25*S* rRNA; pink, ribosomal protein L31; red ribbons, RNA of SRP S domain and SRP19 protein; dark blue, SRP54M domain. R63 indicates the N-terminal Arg^{63} of the reconstituted SRβ construct, in the wild-type protein, connecting with the transmembrane domain. Asterisk indicates the tunnel exit. (**C**) Same as (B) but oriented as in (A).

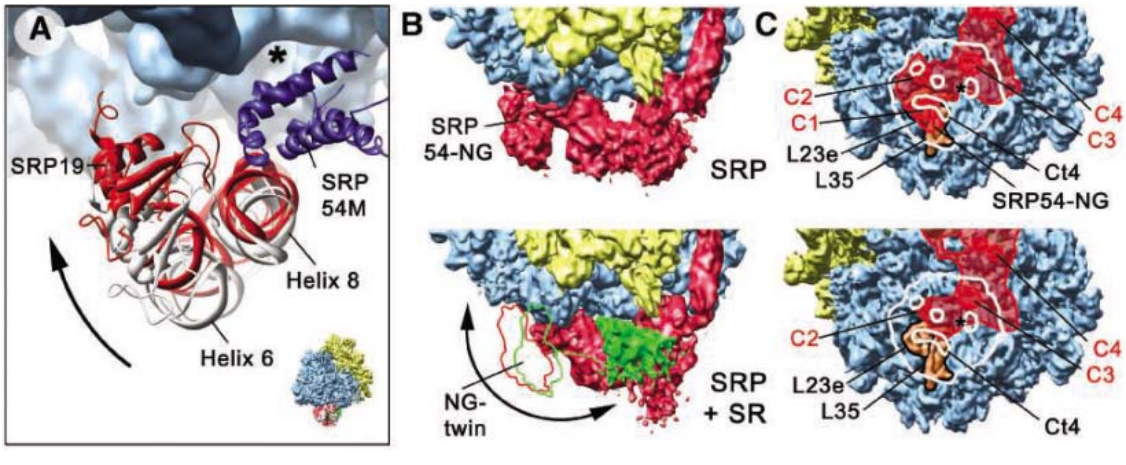

Fig. 3. Rearrangement of SRP S domain and exposure of translocon binding site. (**A**) The 60*S* subunit is shown together with molecular models for the SRP S-domain RNA and SRP19 in the absence (white) or presence of SR (red). The arrow indicates the rotation toward the ribosome. The SRP54 M domain is shown in dark blue, and the inset indicates the orientation. (**B**) Comparison of the RNC-SRP (top) and the RNC-SRP-SR (bottom) reconstructions, with color code as in Fig. 1. The position of the SRP54 NG domain (top) and of the expected position of the SRP/SR NG twin (bottom, red and green contour) is indicated. The arrow indicates the possible movements of the delocalized NG twin and the dashed green line the linker (SRαX2) between the SR NG domain and SRαX1. (**C**) The map of the ribosome is shown together with the SRP S domain (transparent red area with red contour) in the absence (top) and presence of SR (bottom). L23e and L35 are shown in orange. C1 to C4 (red) point to the connections between SRP and the ribosome. The translocon and its ribosomal connections are indicated by an white contour; Ct4 points to the main connection described previously (*15*). The ribosomal tunnel exit is indicated by an asterisk in (A) and (C). The L23e/L35 adaptor site is exposed in the presence of SR.

a particle that no longer interacts functionally with SR (*20*). Additional density indicates that the positively charged SRαX2 linker domain stretches from the position of the SRαX1-SRβ heterodimer parallel along the SRP RNA toward the M domain.

To address the possibility that the targeting complex serves as a GAP for SRβ (*21*), resulting in dissociation of SRβ from SRα, we used a mutant SRβ containing a GTPase-inactivating point mutation H119A (replacement of His^{119} with Ala) (*22*). However, the absence of major differences between the mutant cryo-EM structure (at 9 Å) (fig. S2) and the wild type suggests that no substantial GTP hydrolysis by SRβ and no SR dissociation take place under the conditions in our study. This indicates that the SRP-RNC complex is not sufficient to act as a GAP for SRβ (*6*).

Another difference between the SR-SRP-RNC structure and the SRP-RNC complex (*14*) is the overall behavior and position of the SRP S domain. It is not as rigidly bound to the ribosome as it is without SR, and it rearranges with respect to the 60*S* ribosomal subunit by a rotation of ~10° toward the ribosome (Fig. 3A). The axis of the rotation runs from SRP connection C4 to connections C2/C3 parallel to helix 8 of SRP RNA. As a result, the S domain moves away from the peptide exit site and, at the same time, closer to the ribosome (Fig. 3A). No rearrangements beyond connection C4 toward the Alu domain of SRP could be identified, which implies that within the observed limits the conformations of Alu and S domain can be uncoupled due to the flexibility of hinge 1 (*14*).

The third and most prominent difference between the docking and the targeting complex is the apparent delocalization of both NG domains and loss of connection C1 (Fig. 3B). As one possibility, we expected to recognize a twin-like arrangement, as observed in the complex formed by the isolated NG domains of bacterial SRP and SR (*9*, *10*). However, although the SR binding is GTP dependent and SRα and SRP54 can be detected as full-length proteins in the reconstitution assay (Fig. 1A), density for the two NG domains is completely absent. Thus, the suggested interaction of the two NG domains is likely to lead to delocalization of the flexible SRP54 NG domain (*23*), possibly due to rearrangement of the ribosome-interacting N domain of SRP54 as observed in isolated NG heterodimer structures (*9*, *10*). As a result, SRP breaks its connection with the ribosome (C1), and a site composed of the ribosomal proteins L23e and L35 (L23p and L29p in *E. coli*) is exposed (Fig. 3, B and C). This is in agreement with the cross-link pattern between SRP54 and L23e/L35, which changes in response to SR interaction (*16*). Moreover, several lines of biochemical evidence also point to a conformational change of SRP54 upon SR interaction, and distinct conformations of the SRP-SR complex have been suggested (*24*–*26*). However, the results are not directly comparable.

The SRP binding site (C1) cleared by the NG delocalization is the universal ribosomal adaptor site used by many factors that interact with the emerging nascent chain (*14*–*16*, *27*, *28*). In particular, the two ribosomal proteins L23e and L35 provide a major binding site (Ct4) for the translocon in eukaryotes (*15*) and also in prokaryotes (*29*). Although additional translocon binding sites (*15*, *29*) are still covered, exposure of this site thus allows initial spatial access of the translocon (Fig. 3C). When interacting with this site, the translocon would not only be close to the ribosomal tunnel exit, but it would also be in the immediate vicinity of the signal sequence–binding M domain of SRP54, a position suitable for direct transfer of the signal sequence from SRP.

Taken together, our results explain how SR interacts with both the ribosome and SRP, rendering the targeted RNC competent to interact with the translocon and primed for transfer of the signal sequence (Fig. 4): The Alu domain of SRP stays firmly bound to the ribosome to maintain elongation arrest, whereas the entire S domain is destabilized. Most important, after interaction of the NG domains, a major translocon binding site is exposed by a conformational change that results in the SRP54 NG domain being disconnected from the universal adaptor site. It remains to be shown how the presence of a translocon coordinates subsequent signal sequence transfer and triggers GTP hydrolysis by the SRP system (*4*) and subsequent SRP-SR dissociation.

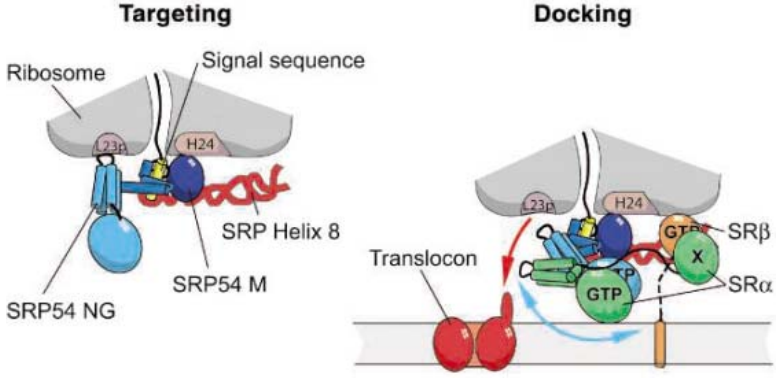

Fig. 4. Dynamic behavior of SRP upon SR interaction. SR interaction with RNC and SRP induces rearrangement of the S domain but leaves the Alu domain unchanged: The NG domain of SRP54 is delocalized after NG-twin formation (cyan arrow), resulting in exposure of the L23e/L35 universal ribosomal adaptor site and access of the translocon to its ribosomal binding site Ct4 (red arrow).

References and Notes

1. R. J. Keenan, D. M. Freymann, R. M. Stroud, P. Walter, *Annu. Rev. Biochem.* **70**, 755 (2001).
2. M. Halic, R. Beckmann, *Curr. Opin. Struct. Biol.* **15**, 116 (2005).
3. P. J. Rapiejko, R. Gilmore, *Cell* **89**, 703 (1997).
4. W. Song, D. Raden, E. C. Mandon, R. Gilmore, *Cell* **100**, 333 (2000).
5. S. Angelini, S. Deitermann, H. G. Koch, *EMBO Rep.* **6**, 476 (2005).
6. E. C. Mandon, Y. Jiang, R. Gilmore, *J. Cell Biol.* **162**, 575 (2003).
7. A. A. Herskovits, E. Shimoni, A. Minsky, E. Bibi, *J. Cell Biol.* **159**, 403 (2002).
8. T. Schwartz, G. Blobel, *Cell* **112**, 793 (2003).
9. P. F. Egea *et al.*, *Nature* **427**, 215 (2004).
10. P. J. Focia, I. V. Shepotinovskaya, J. A. Seidler, D. M. Freymann, *Science* **303**, 373 (2004).
11. T. Powers, P. Walter, *Science* **269**, 1422 (1995).
12. O. Schlenker, A. Hendricks, I. Sinning, K. Wild, *J. Biol. Chem.* **281**, 8898 (2006).
13. I. Moller *et al.*, *Proc. Natl. Acad. Sci. U.S.A.* **95**, 13425 (1998).
14. M. Halic *et al.*, *Nature* **427**, 808 (2004).
15. R. Beckmann *et al.*, *Cell* **107**, 361 (2001).
16. M. R. Pool, J. Stumm, T. A. Fulga, I. Sinning, B. Dobberstein, *Science* **297**, 1345 (2002).
17. Materials and methods are available as supporting material on *Science* Online.
18. T. A. Fulga, I. Sinning, B. Dobberstein, M. R. Pool, *EMBO J.* **20**, 2338 (2001).
19. V. Siegel, P. Walter, *Nature* **320**, 81 (1986).
20. V. Siegel, P. Walter, *Cell* **52**, 39 (1988).
21. G. Bacher, M. Pool, B. Dobberstein, *J. Cell Biol.* **146**, 723 (1999).
22. K. R. Legate, D. Falcone, D. W. Andrews, *J. Biol. Chem.* **275**, 27439 (2000).
23. K. Wild, M. Halic, I. Sinning, R. Beckmann, *Nat. Struct. Mol. Biol.* **11**, 1049 (2004).
24. I. Buskiewicz, A. Kubarenko, F. Peske, M. V. Rodnina, W. Wintermeyer, *RNA* **11**, 947 (2005).
25. F. Chu *et al.*, *Proc. Natl. Acad. Sci. U.S.A.* **101**, 16454 (2004).
26. R. J. Spanggord, F. Siu, A. Ke, J. A. Doudna, *Nat. Struct. Mol. Biol.* **12**, 1116 (2005).
27. S. Q. Gu, F. Peske, H. J. Wieden, M. V. Rodnina, W. Wintermeyer, *RNA* **9**, 566 (2003).
28. I. Buskiewicz *et al.*, *Proc. Natl. Acad. Sci. U.S.A.* **101**, 7902 (2004).
29. K. Mitra *et al.*, *Nature* **438**, 318 (2005).

30. We thank G. Bozkurt for preparation of the mutant SR (SRβ H119A). This work was supported by grants from the VolkswagenStiftung (R.B.) and the Deutsche Forschungsgemeinschaft SFB449 (R.B.) and SFB638 (I.S.); by the Royal Society (M.R.P.); and by the European Union and Senatsverwaltung für Wissenschaft, Forschung und Kultur Berlin (UltraStructureNetwork). Coordinates have been deposited in the RCSB (Research Collaboratory for Structural Bioinformatics) Protein Data Bank with accession number 2GO5. The cryo–EM map has been deposited at the 3D-EM database (European Molecular Biology Laboratory–European Bioinformatics Institute, Cambridge, UK) with accession number EMD-1217.

Supporting Online Material

www.sciencemag.org/cgi/content/full/312/5774/745/DC1
Materials and Methods
Figs. S1 and S2
References

11 January 2006; accepted 3 April 2006
10.1126/science.1124864

Recognition of Histone H3 Lysine-4 Methylation by the Double Tudor Domain of JMJD2A

Ying Huang,[1*] Jia Fang,[2] Mark T. Bedford,[3] Yi Zhang,[2] Rui-Ming Xu[1*†]

Biological responses to histone methylation critically depend on the faithful readout and transduction of the methyl-lysine signal by "effector" proteins, yet our understanding of methyl-lysine recognition has so far been limited to the study of histone binding by chromodomain and WD40-repeat proteins. The double tudor domain of JMJD2A, a Jmjc domain–containing histone demethylase, binds methylated histone H3-K4 and H4-K20. We found that the double tudor domain has an interdigitated structure, and the unusual fold is required for its ability to bind methylated histone tails. The cocrystal structure of the JMJD2A double tudor domain with a trimethylated H3-K4 peptide reveals that the trimethyl-K4 is bound in a cage of three aromatic residues, two of which are from the tudor-2 motif, whereas the binding specificity is determined by side-chain interactions involving amino acids from the tudor-1 motif. Our study provides mechanistic insights into recognition of methylated histone tails by tudor domains and reveals the structural intricacy of methyl-lysine recognition by two closely spaced effector domains.

Posttranslational modifications of histones have a profound influence on fundamental biological processes such as transcriptional regulation and epigenetic inheritance (*1*, *2*). However, the mechanisms by which covalent histone modifications are recognized and deciphered remain poorly understood. Currently, both the recognition of acetylated histones by the bromo domain (*3*, *4*) and the binding of methylated histone tails by the chromo domain and a WD40-repeat protein, WDR5, are the only modified histone/protein interactions understood in any detail (*5*–*10*). The chromodomain is a member of the tudor domain "royal family," which includes the tudor, plant Agenet, chromo, PWWP, and MBT domains. Many of the proteins containing these domains are associated with chromatin (*11*). Using a protein-array approach, we recently showed that in addition to chromo domains, certain tudor and MBT domains specifically bind to methylated histone tails (*12*). Here we focus on the tudor domains of JMJD2A, which is a member of a conserved family of Jmjc domain–containing proteins (Fig. 1, A and B) belonging to the Jmjc domain histone demethylase superfamily (*13*). JMJD2A has been reported to interact with histone deacetylase complexes and Rb and to function as a transcription repressor (*14*, *15*).

Previous structural studies of the tudor domain of survival motor neuron (SMN) revealed that it contains a binding site for a symmetrically dimethylated arginine (*16*). The double tudor domain of 53BP1, a p53 binding protein, has been implicated in binding methylated Lys^{79} of histone H3 (*17*), methylated Lys^{20} of histone

[1]W. M. Keck Structural Biology Laboratory, Cold Spring Harbor Laboratory, Cold Spring Harbor, NY 11724, USA. [2]Howard Hughes Medical Institute and Department of Biochemistry and Biophysics, Lineberger Comprehensive Cancer Center, University of North Carolina at Chapel Hill, Chapel Hill, NC 27599–7295, USA. [3]The University of Texas M. D. Anderson Cancer Center, Science Park-Research Division, Post Office Box 389, Smithville, TX 78957, USA.

*Present address: Structural Biology Program, Skirball Institute of Biomolecular Medicine and Department of Pharmacology, New York University School of Medicine, New York, NY 10016, USA.

†To whom correspondence should be addressed. E-mail: rmxu@saturn.med.nyu.edu

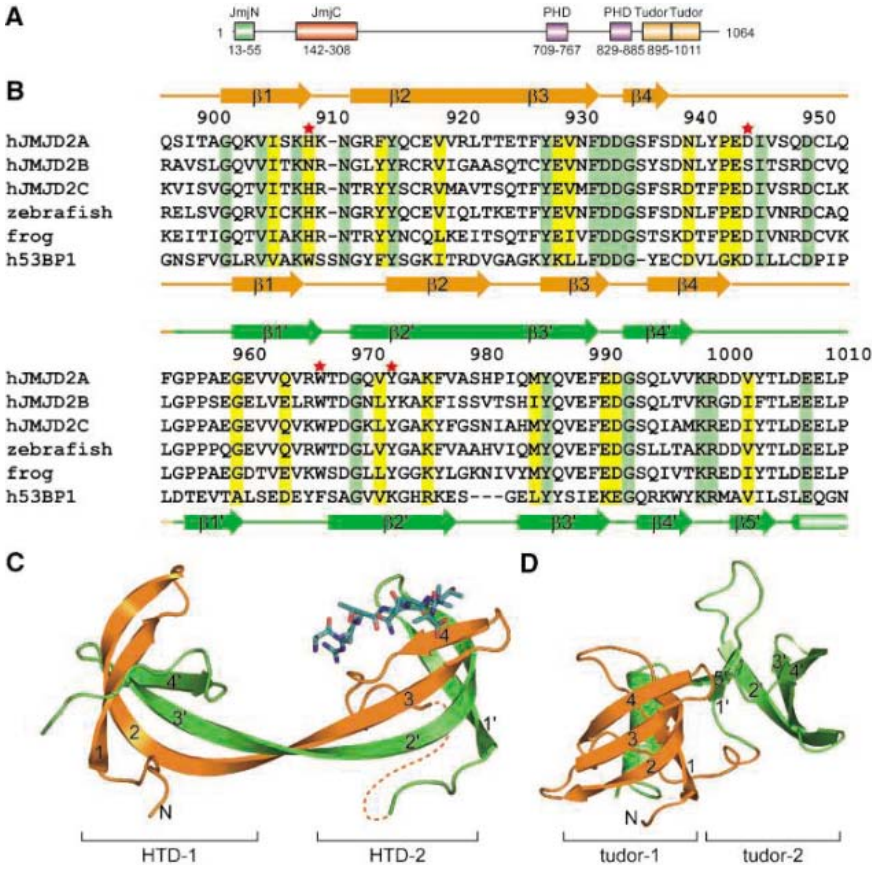

Fig. 1. JMJD2A structure. (**A**) A schematic drawing of the domain structure of JMJD2A. (**B**) Alignment of the double tudor domain sequences of three human JMJD2 homologs, one from zebrafish (Ensemble ID: DARP00000024692) and another from frog (Ensemble ID: XETP00000001152), and human 53BP1. Secondary-structure elements (orange and green for the first and second tudor motifs, respectively), their nomenclature, and the amino acid numbering of JMJD2A are shown above the sequences. The secondary-structure elements of the 53BP1 double tudor domain are delineated below the sequences. JMJD2A residues subjected to mutational studies are indicated by stars. (**C**) The structure of the JMJD2A double tudor domain (ribbon representation) in complex with a trimethylated H3K4 peptide (ball-and-stick model). Regions spanning the first and second tudor motifs are colored orange and green, respectively. The dotted line indicates a segment of seven disordered residues. (**D**) The structure of the double tudor domain of 53BP1 shown in a ribbon representation. Secondary-structure elements in (C) and (D) are colored as in (B).

H4 (*12*), as well as DNA and arginine-glycine–rich sequences (*18*). However, the structural basis for ligand binding by tudor domains is not understood. JMJD2A contains two tandem tudor domains, and the double tudor domain is known to bind methylated histone H3-K4 or H4-K20 (*12*). To gain insights into the structural basis for binding methylated histone tails, we have solved the crystal structure of the double tudor domain of JMJD2A both in the presence and absence of a trimethylated H3-K4 peptide (H3K4Me3). A detailed description of structure determination and data statistics can be found in the supporting online material.

Surprisingly, the 2.1 Å structure revealed that the two tudor domains interdigitate and form a bilobal, saddle-shaped structure with each lobe resembling the canonical tudor domain structure (Fig. 1C). We term these tudorlike lobes hybrid tudor domain 1 and 2 (HTD-1 and HTD-2). The methyl-H3-K4 peptide is bound in a cleft of HTD-2 (Fig. 1C). The interdigitated folding of the double tudor domain of JMJD2A differs appreciably from the structure of the homologous double tudor domain of 53BP1, which comprises two independently folded tudor domains (Fig. 1D) (*17*, *18*). The hybrid-tudor domains are formed by the exchange of the third and fourth β strands with respect to the canonical tudor domain. The swapped β3 forms a long, contiguous strand with the nonswapped β2, which we call β2β3, and the two long strands, β2β3 and β2'β3' (an apostrophe indicates secondary-structure elements of the second tudor motif, as denoted in Fig. 1B), bridge the two compact HTDs (Fig. 1, B and C).

Compared to the corresponding surface area of HTD-1, the surface of HTD-2 surrounding a cluster of aromatic residues has a more negatively charged electrostatic potential, consistent with its role in binding the positively charged H3K4Me3 peptide (Fig. 2A). Three aromatic residues, Trp^{967} and Tyr^{973} of the tudor-2 motif and Phe^{932} of the tudor-1 motif, form an open cage that accommodates the binding of trimethylated Lys^4 (Fig. 2B). The binding buries a total accessible surface area of 1039 $Å^2$. In addition, a negatively charged residue, Asp^{934}, lines up at the edge of the aromatic cage (Fig. 2C). This arrangement of aromatic residues and the negatively charged amino acid is reminiscent of the H3K9Me3 binding site of the HP1 chromo domain (Fig. 2B) (*5*, *6*). The aromatic cage is required for binding methylated lysines: Changing Tyr^{973} to an alanine (Y973A) or Trp^{967} to a histidine (W967H) abolishes the binding of H3K4Me3, whereas the wild-type double tudor domain binds the peptide with an apparent equilibrium dissociation constant (K_d) of 10.4 μM. The binding constants were determined using surface plasmon resonance (SPR) (Fig. 3, A and B).

A number of side chain-side chain interactions between HTD-2 and the H3K4Me3 peptide contribute to their binding specificity. In contrast to the binding of methylated histone peptides by chromo domains (*5*–*9*), there are only two β sheet–like main-chain hydrogen bonds between the H3K4Me3 peptide and HTD-2, which involve the main-chain atoms of Gln^5 of the histone peptide and Phe^{937} of HTD-2. In the present structure, Arg^2 of the histone H3 peptide interacts with Asp^{945} of HTD-2 through ionic and hydrogen bonds (Fig. 2C). Thr^3 of the peptide forms a hydrogen bond with Asn^{940}, and the peptide Gln^5 interacts with Phe^{937} through van der Waals contacts. In addition, the terminal amino group of the peptide interacts with HTD-2 through two weak hydrogen bonds (both ~3.4 Å), one with the hydroxyl group of Tyr^{942} and another with the carbonyl group of Ala^{941}. It should be noted that all of the HTD-2 residues involved, except the ones in the methyl-lysine binding aromatic cage, belong to the tudor-1 motif (Fig. 2C), which explains the observation that tudor-2 alone cannot bind H3K4Me3 (Fig. 3B).

Because Arg^2 of the H3K4Me3 peptide plays a prominent role in the interaction with the double tudor domain of JMJD2A, we tested the binding effect of mutations of Arg^2 and its interaction partner, Asp^{945} of HTD-2, by changing Arg^2 to an alanine (R2A) and changing Asp^{945} to an alanine (D945A) or an arginine (D945R). The wild-type double tudor domain binds the R2A H3K4Me3 peptide with a K_d of 127.9 μM, which is ~$^1/_{12}$th the level of binding to the wild-type H3K4Me3 peptide (Fig. 3). The D945A mutant binds to the wild-type H3K4Me3 peptide with a K_d of 118.4 μM, a level comparable to that between the wild-type double tudor domain and the R2A H3K4Me3 peptide, and the D945R mutant no longer binds the peptide. In the vicinity of Lys^9, Lys^{27}, and Lys^{36} of histone H3, either an alanine or a glycine occupies the position corresponding to that of Arg^2 (Fig. 3D). These small residues cannot efficiently interact with Asp^{945} of JMJD2A, which is likely to account for the preferential binding of the JMJD2A double tudor domain to H3K4Me3 over other histone H3 methyl-lysine marks.

As pointed out earlier, the double tudor domain can also bind methylated H4-K20 (*12*). A trimethylated H4-K20 peptide binds the double tudor domain of JMJD2A with a K_d of ~25 μM, and our study shows that the same binding pocket is involved in binding H3K4Me3 and methylated H4-K20, because the W967H and Y973A HTD-2

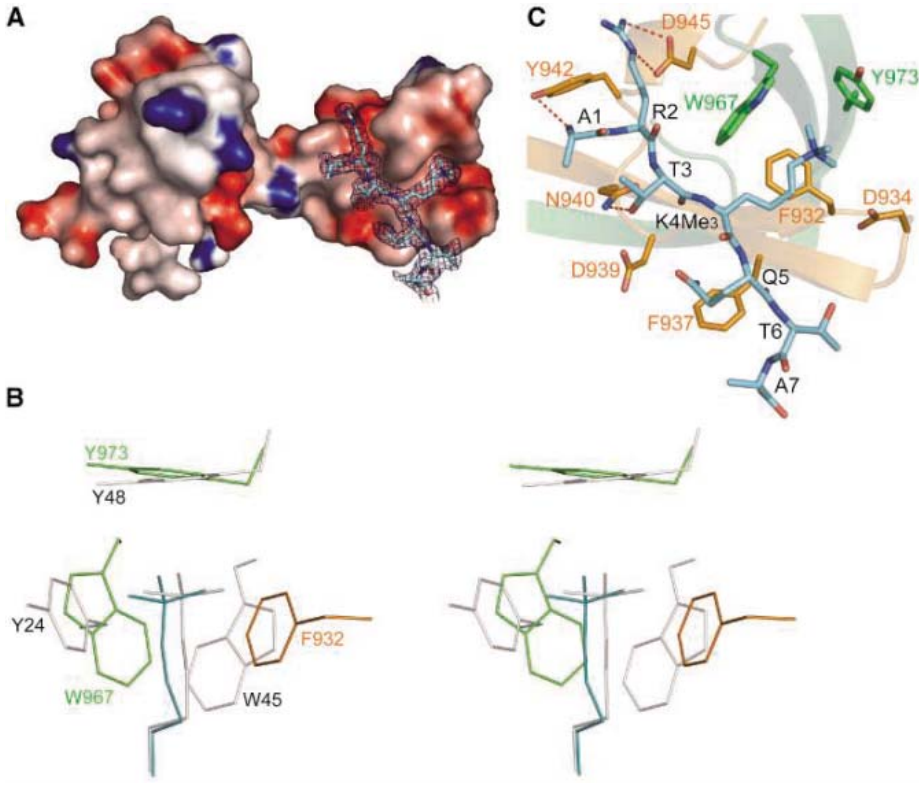

Fig. 2. JMJD2A double tudor domain–H3K4Me3 peptide interactions. (**A**) The double tudor domain as seen in a surface representation with electrostatic potential distribution colored red for negatively charged, white for neutral, and blue for positively charged areas. The peptide is shown as a stick model superimposed with the surrounding $2F_o - F_c$ electron density map (displayed at 1.2σ contour level). (**B**) A stereo view of the methyl-H3K4 (colored cyan) binding aromatic cage superimposed with the methyl-lysine binding aromatic cage of the chromo domain of HP1 (gray). Tudor-1 and Tudor-2 residues are colored orange and green, respectively. (**C**) A detailed view of JMJD2A-H3K4Me3 interactions. The peptide and the HTD-2 residues involved are shown in a stick model. Dashed lines indicate hydrogen bonds. The same coloring scheme as in Fig. 1 is used.

aromatic cage mutants also lost the ability to bind methylated H4-K20. In a H4-K20 peptide, the residue corresponding to Arg^2 is a histidine (Fig. 3D), which cannot interact with Asp^{945} as does Arg^2 of histone H3 but should still be able to bind favorably in the area formed by Leu^{941}, Tyr^{942}, and Asp^{945} (Fig. 2C). Furthermore, the HTD-2 region surrounding the methyl-lysine binding site is quite negatively charged (Fig. 2A), which provides a favorable environment for the binding of three positively charged arginine residues near H4-K20 (Fig. 3D).

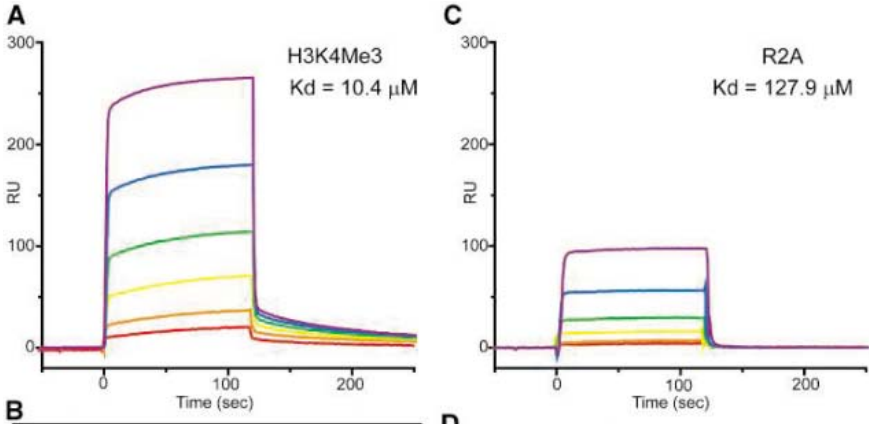

B

Protein	Immob. Peptide	Kd (μM)
wt	Btn-H3K4Me3	10.4
wt	Btn-H3K4	n/d
Y973A	Btn-H3K4Me3	n/d
W967H	Btn-H3K4Me3	n/d
W967H/H909W	Btn-H3K4Me3	n/d
Tudor2	Btn-H3K4Me3	n/d
D945A	Btn-H3K4Me3	118.4
D945R	Btn-H3K4Me3	n/d
wt	Btn-R2A	127.9

D

	-2	0	
H3K4	A	R	TKQTA
H3K9	T	A	RKSTG
H3K27	A	A	RKSAP
H3K36	G	G	VKKPH
H4K20	R	H	RKVLR

Fig. 3. Binding of the JMJD2A double tudor domain to histone H3 peptides. (**A**) Representative binding curves for the wild-type double tudor domain and a biotinylated H3K4Me3 peptide (Btn-H3K4Me3) as measured using SPR. Curves represent measurements with an increasing concentration of the protein used. From bottom to top: 1 μM (red), 2 μM (orange), 5 μM (yellow), 10 μM (green), 20 μM (blue), and 40 μM (magenta). The vertical and horizontal axes show the Biacore response unit (RU) and the time scale (seconds). (**B**) Tabulation of pairwise protein-peptide interactions measured. The wild-type or mutant JMJD2A double tudor domains used are shown in the first column, and the peptide used is indicated in the second column. Btn-H3K4: an H3K4 peptide with an unmethylated Lys^4; Btn-R2A: an H3K4Me3 peptide with an alanine in place of Arg^2. The derived equilibrium dissociation constants are shown in the third column, where n/d denotes bindings too weak to be reliably quantitated. (**C**) Representative binding curves of the wild-type double tudor domain with the Btn-R2A peptide. (**D**) Alignment of amino acid sequences encompassing known methylated lysine residues of histone H3 and H4. The position of methyl-lysines is designated position 0. Both the 0 and −2 positions are highlighted in red.

The two HTDs share ~23 and ~44% sequence identity and similarity, respectively, and the main chains of the two domains can be superimposed with a root mean square (RMS) deviation of 1.05 Å. In particular, a HTD-1 aromatic cage differs from that of HTD-2 only by one residue, a histidine (His^{909}) instead of a tryptophan (Trp^{967}). Superimposition of the two HTD domains reveals that His^{909} occupies a position that occludes the binding of a methyl-lysine (Fig. 4A). To determine whether His^{909} is solely responsible for the inability of HTD-1 to bind H3K4Me3, we changed the histidine to a tryptophan while at the same time changing Trp^{967} of HTD-2 to a histidine. As described earlier, the latter mutation alone precludes HTD-2 from binding H3K4Me3. The W967H/H909W double mutant does not bind H3K4Me3 (Fig. 3B). Thus, residues outside the aromatic cage are also important for the functional differences between HTD-1 and HTD-2. It is possible that HTD-1 could be involved in binding yet unidentified ligands.

There is little conformational change between the H3K4Me3 bound and free double tudor domain structures of JMJD2A, showing that the interdigitated structure is not due to H3K4Me3 binding and that conformational dynamics do not play a major role in regulating histone binding (fig. S1). HTDs and canonical tudor domains have similar secondary structural arrangements: HTD-1 and HTD-2 can be superimposed with the tudor domain of SMN (*16*) with RMS deviations of 1.26 and 0.87 Å, respectively. The locations of the aromatic cages in both HTDs also generally coincide with the sites in SMN and 53BP1 implicated in binding dimethylated arginine and methylated histone H3-K79, respectively (*16*, *17*). A comparison of the tudor domain structures reveals that the loop connecting β1 and β2, in which two of the three aromatic residues reside, has the most notable conformational variation among

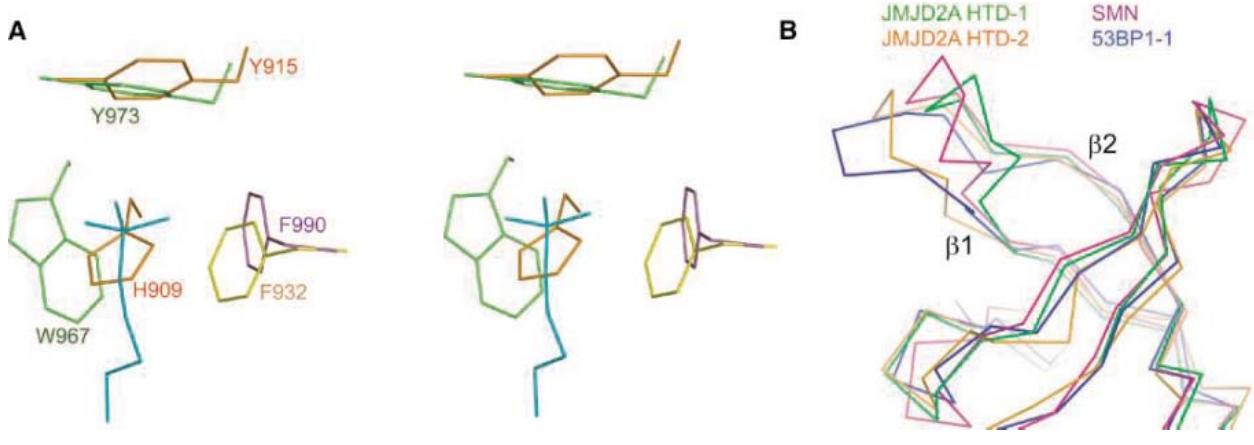

Fig. 4. Tudor domain ligand binding sites. (**A**) A stereo view of superimposed HTD-2 and HTD-1 aromatic clusters. The latter is formed by His^{909} and Tyr^{915} of the tudor-1 motif (orange) and Phe^{990} of tudor-2 (magenta). His^{909} clashes with the superimposed methyl-H3K4. (**B**) Conformational differences of the β1-β2 loop among HTD-1 (green) and HTD-2 (orange) of JMJD2A, SMN tudor (magenta), and the first tudor domain of 53BP1 (blue). Two of the aromatic residues implicated in binding methylated lysine, or arginine for SMN tudor, reside in this loop.

different tudor domains (Fig. 4B), perhaps reflecting the structural flexibility needed for accommodating different binding partners.

Because of the involvement in transcription regulation, it is tempting to speculate that the double tudor domain is responsible for directing JMJD2A to chromatin regions enriched with H3-K4 or H4-K20 methylation. However, alternative scenarios are also possible, and the functional relation between methyl-histone binding by the double tudor domain and histone demethylation by JMJD2A in a physiological context remains to be established. Nevertheless, our results demonstrate that the hybrid-tudor domain structure of JMJD2A is required for the formation of a functional methyl-histone H3 binding module. The unusual fold requires two tudor domain motifs in tandem, which is only present in a subset of tudor domain–containing proteins including JMJD2 family members and 53BP1. It will be extremely interesting to understand the principle underlying the distinct folding of the double tudor domains of JMJD2A and 53BP1 despite their sequence similarity. Many chromatin-associated proteins have closely spaced tandem repeats of effector domains implicated in histone binding, including the bromo, chromo, MBT, Agenet, and tudor domains. Our discovery reveals the potential for forming novel histone binding modules from the familiar effector domains.

References and Notes

1. T. Jenuwein, C. D. Allis, *Science* **293**, 1074 (2001).
2. C. Martin, Y. Zhang, *Nat. Rev. Mol. Cell Biol.* **6**, 838 (2005).
3. C. Dhalluin *et al.*, *Nature* **399**, 491 (1999).
4. R. H. Jacobson, A. G. Ladurner, D. S. King, R. Tjian, *Science* **288**, 1422 (2000).
5. S. A. Jacobs, S. Khorasanizadeh, *Science* **295**, 2080 (2002).
6. P. R. Nielsen *et al.*, *Nature* **416**, 103 (2002).
7. J. Min, Y. Zhang, R. M. Xu, *Genes Dev.* **17**, 1823 (2003).
8. W. Fischle *et al.*, *Genes Dev.* **17**, 1870 (2003).
9. J. F. Flanagan *et al.*, *Nature* **438**, 1181 (2005).
10. J. Wysocka *et al.*, *Cell* **121**, 859 (2005).
11. S. Maurer-Stroh *et al.*, *Trends Biochem. Sci.* **28**, 69 (2003).
12. J. Kim *et al.*, *EMBO Rep.* **7**, 397 (2006).
13. Y.-i. Tsukada *et al.*, *Nature* **439**, 811 (2006).
14. D. Zhang, H. G. Yoon, J. Wong, *Mol. Cell. Biol.* **25**, 6404 (2005).
15. S. G. Gray *et al.*, *J. Biol. Chem.* **280**, 28507 (2005).
16. R. Sprangers, M. R. Groves, I. Sinning, M. Sattler, *J. Mol. Biol.* **327**, 507 (2003).
17. Y. Huyen *et al.*, *Nature* **432**, 406 (2004).
18. G. Charier *et al.*, *Structure* **12**, 1551 (2004).

19. We thank D. Schneider and A. Heroux for help at the X26C beamline of the National Synchrotron Light Source (Brookhaven National Laboratory), and L. Henry and S. Shaw for comments on the manuscript. The coordinates and the structure factors have been deposited with the RCSB (Research Collaboratory for Structural Bioinformatics) Protein Data Bank with accession codes 2GFA (H3K4Me3 bound) and 2GF7 (free). The work was supported in part by the W. M. Keck foundation (R.-M.X.), the Howard Hughes Medical Institute (Y.Z.), and NIH grants GM 63718 (R.M.X.), GM68804 (Y.Z.), and DK62248 (M.T.B.). Y.Z. is an Investigator of the Howard Hughes Medical Institute.

Supporting Online Material

www.sciencemag.org/cgi/content/full/1125162/DC1
Materials and Methods
Fig. S1
Table S1
References

19 January 2006; accepted 27 March 2006
Published online 6 April 2006;
10.1126/science.1125162
Include this information when citing this paper.

The Embryonic Vertebrate Heart Tube Is a Dynamic Suction Pump

Arian S. Forouhar,[1] Michael Liebling,[2] Anna Hickerson,[1] Abbas Nasiraei-Moghaddam,[1] Huai-Jen Tsai,[4] Jay R. Hove,[5] Scott E. Fraser,[1,2] Mary E. Dickinson,[2,6] Morteza Gharib[1,3]*

The embryonic vertebrate heart begins pumping blood long before the development of discernable chambers and valves. At these early stages, the heart tube has been described as a peristaltic pump. Recent advances in confocal laser scanning microscopy and four-dimensional visualization have warranted another look at early cardiac structure and function. We examined the movement of cells in the embryonic zebrafish heart tube and the flow of blood through the heart and obtained results that contradict peristalsis as a pumping mechanism in the embryonic heart. We propose a more likely explanation of early cardiac dynamics in which the pumping action results from suction due to elastic wave propagation in the heart tube.

The cardiovascular system is the first functional organ system to develop in vertebrate embryos. In its earliest stages, it consists of a primitive heart tube that drives blood through a simple vascular network. Cardiac physiologists have long conjectured that the valveless embryonic heart tube drives circulation by means of peristaltic contractions (*1*, *2*), a pumping mechanism that pushes blood through the heart tube by progressively reducing the tube volume (*3*). Confirmation of this pumping mechanism requires in vivo visualization and quantification of both heart wall motion and blood cell motion, which are difficult with traditional imaging modalities. The zebrafish offers a powerful vertebrate model for cardiogenetic studies (*4*–*7*) with multiple advantages for in vivo imaging: Eggs are externally fertilized; embryos are nearly transparent, providing optical access to the earliest stages of cardiogenesis; and many GFP (green fluorescent protein)-labeled transgenic strains have been derived.

Recent improvements in confocal microscopy and four-dimensional (three spatial dimensions plus time) reconstruction protocols (*8*) permit us to take full advantage of these qualities and revisit the pumping mechanism of the early embryonic heart tube. We tested three implications of peristaltic pumping in the heart, namely that (i) there should be a unidirectional wave traveling along the endocardial layer, (ii) blood cell velocities should be bounded in magnitude by the instantaneous traveling wave speed through the heart tube wall, and (iii) cardiac output should increase linearly with heart rate.

To test the nature of cardiac pumping, we used in vivo high-speed confocal imaging of zebrafish hearts before valve formation. Optical sections through 26–hours postfertilization (hpf) *Tg(gata1:GFP)* zebrafish hearts expressing GFP in blood cells, endocardium, and myocardium were reconstructed into four-dimensional data sets (*8*) (Fig. 1A and movie S1), which provided direct three-dimensional data on the position of myocardial and endocardial cells throughout the cardiac cycle (Figs. 1B and 2 and movies S1 to S3). By tracking the position of the trailing edge of the endocardial wave crest during the cardiac cycle, we identified the speed and the direction of the traveling wave through the heart wall. The wave originates in myocardial cells positioned near the inflow tract of the heart tube (Fig. 2), and upon contraction a bidirectional wave propagates axially along the heart tube wall (Fig. 1 and movies S1 and S2). The proximity of the pacemaker cells to the venous boundary of the heart tube, along with the speed of the traveling wave, combine to make this bidirectional wave undetectable through traditional imaging modalities.

In a peristaltic heart tube model, the net flow is exactly equal to the volume displaced during contractions. This dynamic imposes a direct relationship between the upstream blood velocity and the local traveling wave velocity. Specifically, because peristalsis is governed by static pressure rather than dynamic pressure (*3*),

[1]Option in Bioengineering, [2]Biological Imaging Center, Beckman Institute, [3]Graduate Aeronautical Laboratories, California Institute of Technology (Caltech), Pasadena, CA 91125, USA. [4]Institute of Molecular and Cellular Biology, National Taiwan University, Taiwan. [5]Genome Research Institute, University of Cincinnati, Cincinnati, OH 45221, USA. [6]Department of Molecular Physiology and Biophysics, Baylor College of Medicine, Houston, TX 77030, USA.

*To whom correspondence should be addressed. E-mail: mgharib@caltech.edu

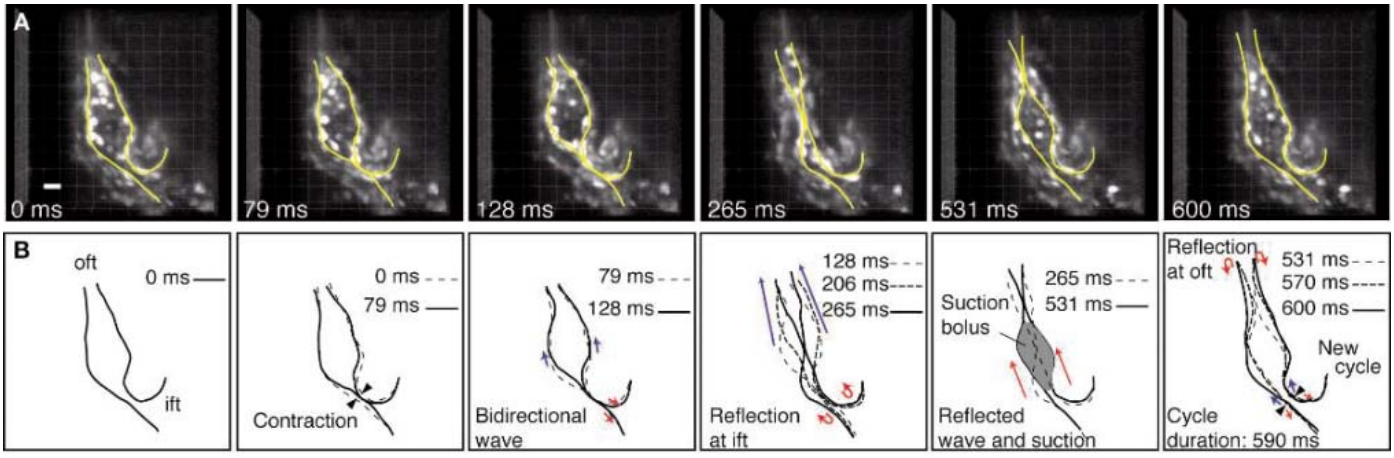

Fig. 1. Biomechanics of embryonic heart tube contractions contradicts peristalsis as the main pumping mechanism. (**A**) Three-dimensional reconstructions of a 26-hpf *Tg(gata1:GFP)* zebrafish heart tube at six time points. Yellow lines denote the shape of the endocardial layer. (**B**) Superimposed outlines of different time points highlight bidirectional traveling wave (red and blue arrows). Black arrowheads indicate contraction location. Shaded gray region indicates suction bolus. Regions of mismatched impedance at the inflow tract (ift) and outflow tract (oft) of the heart tube are reflection sites. Grid spacing is 20 μm.

it would imply that the upstream blood velocity in the zebrafish heart does not exceed the simultaneous local traveling wave velocity. However, in each of the cases observed (n = 5), the maximum velocity of the upstream blood accelerated to velocities exceeding the wall wave speed (Fig. 3, A to C).

To investigate how the cardiac output varied with the contractile wave frequency in vivo, we altered temperature to manipulate heart rates and tracked blood cells to determine flow rates. In this temperature range (24°C to 34°C), fish develop normally, and we do not expect a nonlinear change in blood viscosity. If the heart tube were a peristaltic pump, the cardiac output should increase linearly with the contractile wave frequency. However, we found that the blood velocity response, and thus the net flow rate response, to a monotonic heart rate change is nonlinear (Fig. 3D).

These three observations indicate that the embryonic heart tube does not act as a peristaltic pump; instead, they seem consistent with a previously investigated hydro-impedance pump model (*9*). In this model of valveless pumping, the pumping action results from elastic wave propagation and reflection in the heart tube; resonance conditions arise at certain frequencies where the phase speed permits constructive interference between the incident and reflected pressure waves. Mechanical properties of the system such as diameter, length, elasticity, and pressure dictate wave speed as well as attenuation and reflection coefficients in the system. The impedance pump model exhibits a sensitivity of the generated flow to the activation frequency that is similar in many ways to our in vivo observations (Fig. 3D), including nonlinear flow with frequency, domains of negative slope, and resonance frequencies that allow higher flow rates than peristalsis.

The impedance pump model requires mismatches in impedance to induce wave reflections at the boundaries of the pump element and to build up suction and induce net flow (*9*). In zebrafish, many mechanical properties of the heart tube boundaries contribute to mismatched impedance. The most prominent feature at the inflow boundary of the heart tube is a drastic change in diameter (Fig. 4, A and B). The heart tube stems from the surface of the spherical yolk sac, acutely narrows to about 30 μm, and becomes lined by an additional layer of cells (myocardium) and cardiac jelly that alters the elasticity of the heart tube at the inflow boundary (Fig. 4, A and B). Our four-dimensional data confirmed that this region of mismatch impedance is indeed a site of wave reflections. Pacemaker cell contractions initiate axial waves that travel along the heart tube until they reach the heart tube boundaries. When these waves reach the inflow and outflow boundaries, they reflect in the form of sudden expansions and begin to travel back through the heart tube (movies S1 and S2).

The sudden expansions of the cardiac lumen at the reflection sites create low-pressure zones and suck blood through the heart tube (movie S1). In order to describe this suction mechanism in vivo, we looked at the pressure-flow relationship through the heart tube during the

Fig. 2. Heart tube contractions convey active and passive regions. (**A**) Three-dimensional reconstruction of a 26-hpf *Tg(cmlc2:GFP)* embryo. Myocytes are fluorescently labeled, and their three-dimensional trajectories during two complete cardiac cycles are shown. The red double-arrow line indicates the active pacemaker region and the double-arrow white line, the passive region. The orthogonal scale bar triplet indicates 20 μm in each direction. (**B**) The active pacemaker region spans the first 20 μm of the heart tube. It was identified by calculating the time difference between the moment myocardial cells at a given position along the tube experience a 10 to 13% strain rate with neighboring cells and the time at which they each reach 90% of their maximal displacement. When this time difference is nearly zero, the region experiences active contraction.

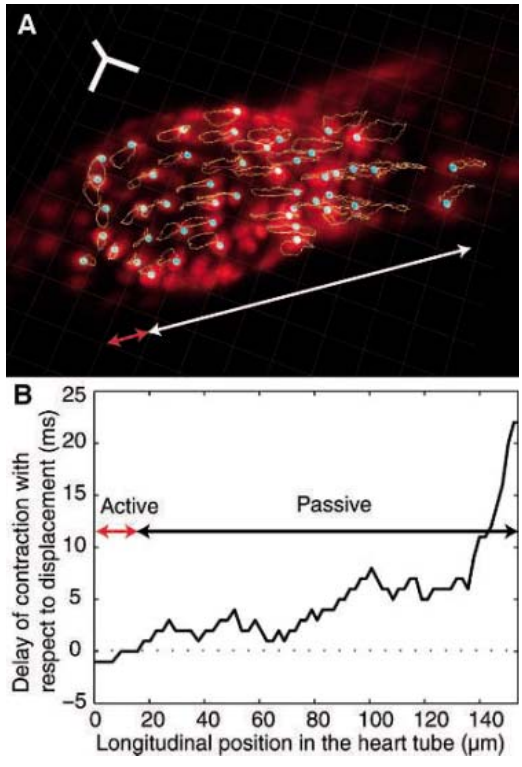

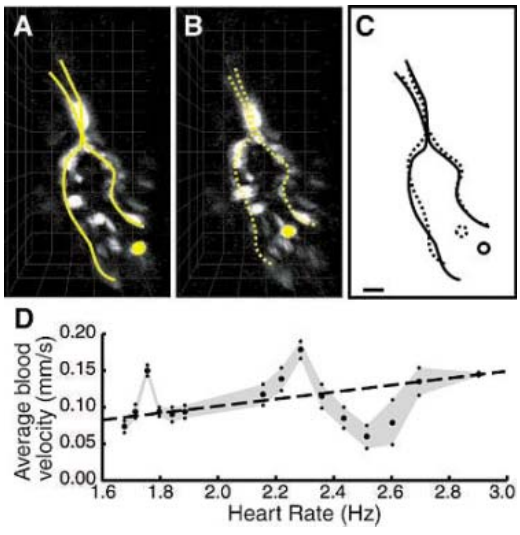

Fig. 3. Blood cell motions demonstrate nonperistaltic pumping mechanism in the embryonic heart tube. (**A** and **B**) Reconstruction of a 26-hpf Tg(*gata1*::GFP) embryo. The endocardial layer, along with a blood cell, have been marked in yellow in each image. (**C**) Superposition of schematics in (A) and (B). Blood cell displacement is much greater than traveling wave crest displacement, indicating that blood cells do not passively follow the traveling wave. Scale bar indicates 20 μm. (**D**) Nonlinear frequency-flow relationship for 26-hpf zebrafish heart tube (Materials and Methods). Resonance peaks in the observed average blood velocity at 1.75 and 2.3 Hz exceed the expected estimate for peristaltic pumping (dashed line).

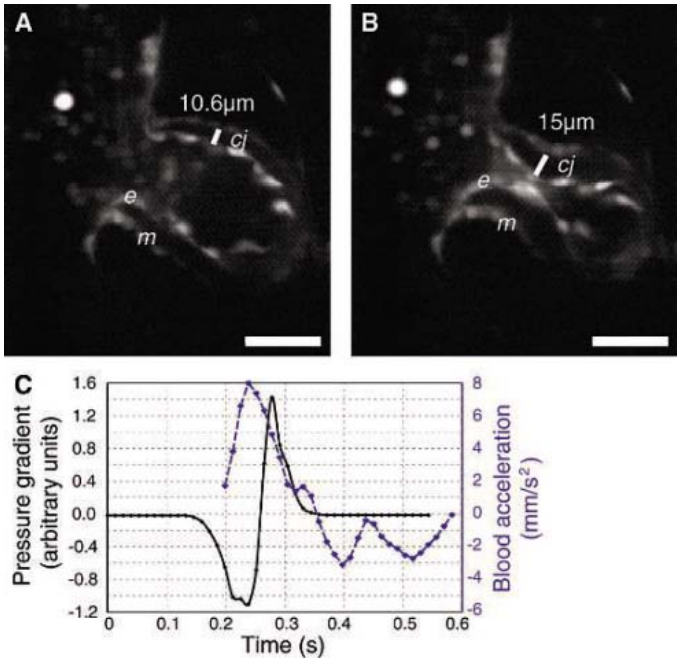

Fig. 4. Hydroelastic-based suction mechanism in the embryonic heart tube. (**A**) Inflow region of a 26-hpf embryo. The distance between the myocardial (m) and endocardial (e) layers is marked (short diagonal white bars). (**B**) Upon contraction, this distance increases. The expansion of the cardiac jelly (cj) at the site of contraction illustrates the elastic nature of the heart wall, a requirement of the impedance pump model. This observation contradicts the muscularly driven peristaltic mechanism because the concentric rings of endocardium and myocardium do not approach each other during contraction. Scale bars, 50 μm. (**C**) Blood cell accelerations and estimated pressure gradient as a function of time (Materials and Methods). The maximum acceleration occurs when the pressure gradient is negative, indicating that the embryonic heart tube acts as a suction pump.

cardiac cycle. By measuring the radius of the cardiac lumen at two cross sections a short distance apart, we deduced the pressure gradient at a point (*10*) (Fig. 4C and movie S4). In this region, blood cells first begin to accelerate when the pressure gradient is negative, analogous to drinking liquid through a straw. Blood cells continue to accelerate, reaching a maximum as the pressure gradient climbs from negative values toward zero. As the pressure gradient continues to increase from zero to positive values, blood cells continue to move forward but with decreasing accelerations. Lastly, when the pressure gradient reaches a maximum and begins to decrease, blood cells decelerate until they finally reach a resting point. Importantly, a phase difference between the maximum acceleration and the maximum pressure gradient exists. Specifically, blood reaches a maximum acceleration a short time after there is a local minimum in the pressure gradient. This time lag between suction pressure and flow in the embryonic heart resembles the pressure-flow relationship of a fluid dynamic pump (*3*) rather than a peristaltic mechanism, where such a time lag should not exist.

By using new in vivo imaging tools, we have taken a closer look at early cardiac structure and function and identified three biomechanical properties of embryonic heart tube contractions that contradict cardiac peristalsis: (i) a bidirectional, as opposed to unidirectional, wave traverses the endocardial layer, (ii) blood cell trajectories do not follow local endocardial wave trajectories and exhibit velocities greater than those of the traveling wave, and (iii) the frequency-flow relationship is nonlinear and exceeds the maximum flow rate possible for a peristaltic pump. Furthermore, we observed (i) resonance peaks in the frequency-flow relationship; (ii) mismatched impedance at inflow and outflow tracts and visible wave reflections at the heart tube boundaries; and (iii) a pressure-flow relationship that exhibits a phase difference between the maximum acceleration of blood and the maximum local pressure gradient. Thus, the valveless embryonic heart does not drive circulation through peristalsis. Instead, these observations suggest a hydroelastic impedance pump model based on elastic wave propagation and reflection (*9*). The simple mechanism we propose requires only a single actuation site rather than complete synchrony throughout the heart tube. The frequency-dependent sensitivity of this pumping mechanism itself suggests that such valveless pumping may not be suitable for post-embryonic circulation in ectotherms. The presented characterization of early cardiac biomechanics should provide the foundation to revisit many aspects of embryonic cardiogenesis and provides evidence for an embryonic root to the observed suction action of the adult heart (*11*).

References and Notes

1. M. C. Fishman, K. R. Chien, *Development* **124**, 2099 (1997).
2. S. F. Gilbert, *Developmental Biology* (Sinauer, Sunderland, MA, 2000).
3. S. Vogel, *Life in Moving Fluids* (Princeton Univ. Press, Princeton, NJ, 1994), pp. 323–329.
4. M. Fishman, *Science* **294**, 1290 (2001).
5. J. R. Hove *et al.*, *Nature* **421**, 172 (2003).
6. D. Y. Stainier, *Nat. Rev. Genet.* **2**, 39 (2001).
7. D. Yelon, *Dev. Dyn.* **222**, 552 (2001).
8. M. Liebling, A. S. Forouhar, M. Gharib, S. E. Fraser, M. E. Dickinson, *J. Biomed. Opt.* **10**, 054001 (2005).
9. A. I. Hickerson, D. Rinderknecht, M. Gharib, *Exp. Fluids* **38**, 534 (2005).
10. W. W. Nichols, M. F. O'Rourke, *McDonald's Blood Flow in Arteries* (Oxford Univ. Press, New York, 1988), pp. 98–102.
11. G. D. Buckberg *et al.*, *Semin. Thorac. Cardiovasc. Surg.* **13**, 342 (2001).
12. We thank J. Dabiri, M. Milano, J. Vermot, and J. Pierce for comments on the paper; S. Megason and L. Trinh for help with zebrafish and imaging techniques; and S. Lin for providing the *Tg(gata1:GFP)* zebrafish line. This work was supported by American Heart Association grant 03665071Y (J.R.H.), NIH grant 5R01HL078694 (S.E.F., M.E.D., and M.L.), and Swiss National Science Foundation grants PBEL2-104418 and PA002-111433 (M.L.).

Supporting Online Material

www.sciencemag.org/cgi/content/full/312/5774/751/DC1
Materials and Methods
Figs. S1 and S2
Movies S1 to S4

13 December 2005; accepted 6 April 2006
10.1126/science.1123775

Neurobiological Substrates of Dread

Gregory S. Berns,* Jonathan Chappelow, Milos Cekic, Caroline F. Zink, Giuseppe Pagnoni, Megan E. Martin-Skurski

Given the choice of waiting for an adverse outcome or getting it over with quickly, many people choose the latter. Theoretical models of decision-making have assumed that this occurs because there is a cost to waiting—i.e., dread. Using functional magnetic resonance imaging, we measured the neural responses to waiting for a cutaneous electric shock. Some individuals dreaded the outcome so much that, when given a choice, they preferred to receive more voltage rather than wait. Even when no decision was required, these extreme dreaders were distinguishable from those who dreaded mildly by the rate of increase of neural activity in the posterior elements of the cortical pain matrix. This suggests that dread derives, in part, from the attention devoted to the expected physical response and not simply from fear or anxiety. Although these differences were observed during a passive waiting procedure, they correlated with individual behavior in a subsequent choice paradigm, providing evidence for a neurobiological link between the experienced disutility of dread and subsequent decisions about unpleasant outcomes.

Making decisions about gains and losses is one of the archetypal problems that all animals face, but when the outcome is temporally delayed from the decision, the problem becomes considerably more complex than simply choosing the course of action with the better expected outcome. Standard economic theory posits that preferences for outcomes that occur at different times can be represented by an expected utility of the future outcomes discounted by the amount of time one must wait for them (*1*). These theories typically apply discounting under the assumption that people care less about outcomes that are more remote in the future than those that are more imminent, which leads to the prediction that people should want to expedite desired experiences and delay undesirable experiences for as long as possible. A wide range of findings, however, shows that people often exhibit the opposite pattern: They prefer to delay gratifications and to speed up the occurrence of unpleasant outcomes. If people do, indeed, discount the future, then why do they so often exhibit patterns of preference that are the opposite of the predictions of time discounting? The answer, we suggest, lies in the fact that the act of waiting may itself bring subjective benefits or costs, such as the joyous anticipation of waiting for a birthday present or the misery of waiting for a dentist's appointment. In the case of bad outcomes, the problem can be reduced to the utility of dread (*2*).

In contrast to standard discounted utility theory, another type of decision-making model posits that waiting enters the utility function separately from the outcome (*3*, *4*). Here, an individual's preference for waiting at any point in time reflects the relative weight of two considerations: the effect of time discounting on the present value of the outcome itself, and the effect of changes in timing on the length of the period of anticipation. The latter effect can explain why people sometimes delay pleasant outcomes and expedite unpleasant ones.

This is not the only possible reason that people might want to delay or expedite outcomes. It is also possible that delaying or speeding up an outcome could either increase the utility or disutility of an outcome at the time when it is experienced. For example, sensitization mechanisms in the central nervous system could modulate one's hedonic reaction to an outcome, depending on how long one has to wait for it (*5*). If this were the case, then people might prefer to get unpleasant outcomes over with quickly, not because they dislike the dread associated with waiting, but because the outcome itself is more unpleasant after one has waited for it. Mechanisms producing anticipatory adaptation, on the other hand, could decrease one's response to an outcome as a function of how long one waits for it, which would have the opposite effect on preferences for timing.

Although the cognitive and emotional processes of waiting are multidimensional, these economic models predict a specific shape for the time course of utility while an individual waits for an outcome, and each of the aforementioned theories makes a different prediction. Here, we used functional magnetic resonance imaging (fMRI) in the context of waiting for an adverse event—a cutaneous electrical shock—to identify which brain regions display time courses consistent with a theoretical model of dread and whether activity in these regions differentiates individuals based on their predilection to wait. Previous neuroimaging studies of pain have found evidence for anticipatory responses in nearly all elements of the "pain matrix" of the brain, although none has specifically linked these responses to the flow of dread in the context of an intertemporal choice (*6*–*8*). The pain matrix is a generally accepted network of brain regions that responds to noxious stimuli, and its elements have been variously associated with different aspects of the pain experience. For example, the somatosensory aspect of pain has been associated with activity in the primary somatosensory cortex (SI), the secondary somatosensory cortex (SII), and the posterior insula, whereas the visceral and emotional aspects of pain have been associated with activity in the anterior insula, rostral anterior cingulate cortex (ACC), and amygdala. Preparation for a withdrawal response has been linked to activity in mid-ACC and supplementary motor area (SMA), and the effects of attention have been observed in SII, the posterior insula, and the caudal ACC (*9*–*11*). Consequently, we hypothesized that dread would manifest in some components of the pain matrix and both the location and time course of these components would yield insight into the nature of dread itself.

To test our hypothesis that dread follows a time course of activity in the pain matrix consistent with utility theory, we used a delay-conditioning paradigm with different levels of shock and delay. Participants (n = 32) were presented with a series of 96 passive trials inside the scanner (*12*). Each trial began with the presentation of a cue that indicated both the voltage level and the amount of time one would have to wait for the outcome (Fig. 1). Shocks were delivered to the dorsum of the left foot on a 100% reinforcement schedule (*12*). After the passive delay-conditioning procedure, but while still in the scanner, the utility of voltage and delay was estimated through a series of forced-choice options. In this phase, participants were presented with pairs of voltage and delay—e.g., "90% in 3 seconds" or "60% in 27 seconds"—and they had to choose which of the two offerings they would prefer to receive. The choices were real, not hypothetical, and participants received their preferred shock at the chosen voltage level and time. Choosing the shorter delay could not speed up the experiment, as each trial lasted the length of the longer of the two choices (when the shorter duration was chosen, the extra time was added to the intertrial interval after the shock).

When the voltages between the choices were identical, participants generally chose the shorter delay (mean = 78.9% of these types of choices, range = 0 to 100%). Out of the 32 participants, 27 chose the shorter delay more than 50% of the time, indicating that the majority of individuals dreaded waiting for a shock. Some individuals dreaded so much that they were often willing to take the next higher voltage level to avoid waiting the longest delay, even though doing so would not cause the next trial to appear any sooner. Consistent with microeconomic theory, we take these revealed preferences as a measure of expected utility and then ask what neurobiological aspect of the passive experience correlates with this expected utility. Based on an individual's preferences during the choice procedure, we constructed an ordinal ranking of voltage-delay combinations (Fig. 2A). The shape of the ranking curve tells us the relative im-

Department of Psychiatry and Behavioral Sciences, Emory University School of Medicine, 101 Woodruff Circle, Suite 4000, Atlanta, GA 30322, USA.

*To whom correspondence should be addressed. E-mail: gberns@emory.edu

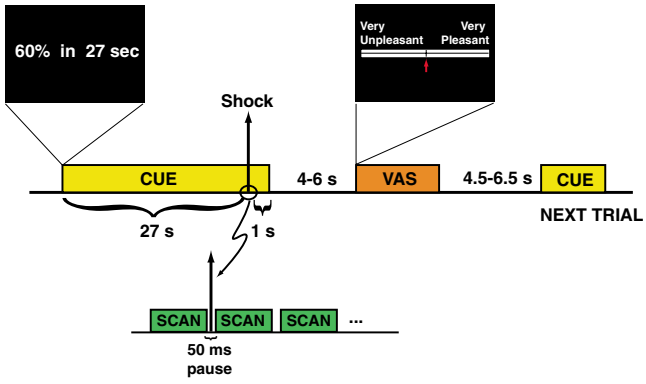

Fig. 1. Functional MRI trial design. Each trial followed a delay-conditioning procedure, in which a cue was presented for the duration of the trial, up to and beyond the delivery of an aversive stimulus in the form of a brief cutaneous electric shock (10 to 15 ms in duration). At the beginning of each trial, a cue was displayed that indicated the level of shock (expressed as a percentage of the individual's maximum tolerable voltage) and the time until that shock would be delivered. Four voltage levels [10, 30, 60 (shown), and 90%] and four time delays [1, 3, 9, and 27 s (shown)] were used in all 16 possible combinations. To avoid shock-induced artifacts on the fMRI images, a 50-ms pause between scan volumes was introduced, and each shock was delivered during this pause. Following the shock, the cue remained visible for another 1 s to prevent conditioning to the cue offset. A visual analog scale (VAS) was then presented in which the individual moved an arrow to indicate their subjective experience for the entire preceding trial, including the waiting time.

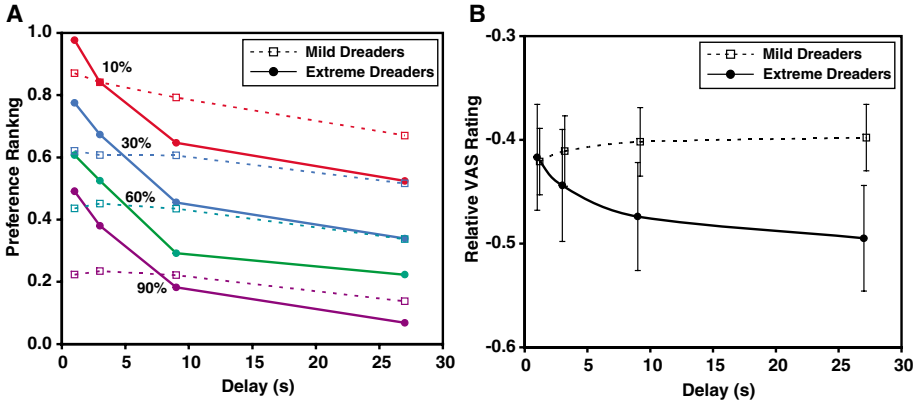

Fig. 2. Ratings of aversive experience. (**A**) Ratings, as a function of voltage and delay, obtained by forced-choice preference procedure after the fMRI session. Participants were offered a series of choice pairs in which they had to choose between different voltage and delay combinations. An ordinal ranking was computed based on these choices (0 is worst and 1 is best), and participants were categorized as either "mild dreaders" (prefer to receive shock as soon as possible, but not so much as to take more voltage to do so) and "extreme dreaders" (really dislike waiting, as evidenced by choosing more voltage to receive the shock quickly). There was a significant effect on preference by both voltage [$F(3,90) = 709.9$, $P < 0.0001$] and delay [$F(3,90) = 32.4$, $P < 0.0001$] as well as the interaction of group (mild versus extreme dreader) and delay [$F(3,90) = 12.0$, $P < 0.0001$]. (**B**) Visual analog scale (VAS) ratings as a function of delay, normalized to each individual's minimum rating (–1 is the worst rating and 0 is neutral) and averaged across the four voltage levels. Error bars show SEM across participants. There was a significant interaction between group and delay [repeated measures analysis of variance: $F(3,90) = 4.4$, $P = 0.007$], with the extreme dreaders indicating that the shock experience after a longer delay was significantly worse than the equivalent voltage at a shorter delay. This was not the case for the mild dreaders.

portance of voltage and delay for each individual. A useful metric for characterizing this relationship is the marginal rate of substitution (MRS) of voltage for delay (*13*). The MRS tells us the value of time to that individual in terms of how much the voltage would have to be decreased for each added second of delay. The higher the MRS, the more a person dreads waiting (*12*). We used each individual's MRS value as a behavioral metric of dread and then used a clustering procedure to divide the cohort of participants into two categories: extreme dreaders ($n = 9$) and mild dreaders ($n = 23$). The extreme dreaders were those individuals who preferred more voltage sooner to less voltage later, and the mild dreaders were those who dreaded only to the extent of shortening the delay at a given voltage but were not willing to take more voltage just to get the shock over with. Comparing the brain responses between these two groups during the shock-waiting period allowed us to test the predictions made by a utility-based theory of waiting about the biological flow of dread.

Although MRS was calculated based on the forced-choice procedure, it was possible that the act of choosing changed the subjective experience of each trial from the passive condition. To verify the generalizability of the choice-based categorization of the individuals outside a decision-making paradigm, we examined how the two groups rated their experiences on the passive trials. Confirming the subjective equivalence of passive and active experiences, extreme dreaders rated trials with long waits as significantly more unpleasant than trials with shorter waits, but mild dreaders did not show this effect (Fig. 2B).

To determine whether dreading behavior that resulted from waiting altered the response to the outcome, we examined the fMRI response to the shock itself. We identified brain regions sensitive to shock amplitude by a linearly increasing contrast across voltage levels and then subjected 12 subregions of this map that intersected the pain matrix to further analysis on the ex-post effect of waiting on the shock itself (Fig. 3). A voltage-weighted contrast on the response to the instantaneous shock revealed a map consistent with previous reports of the pain matrix. Although a significant effect of the length of delay was observed in the right SII, the predominant pattern in the pain matrix was that waiting did not change the response to the shock itself, nor was there a differential voltage sensitivity between mild and extreme dreaders. Therefore, whatever differentiated the two groups must have occurred during the waiting period. It does not appear that the preference for expediting negative outcomes results from any impact of waiting on the utility of the outcome itself.

To understand how the brain response differed between mild and extreme dreaders during the waiting period, we performed a time-series analysis on the regions of interest (ROIs). We used Loewenstein's model for the utility of anticipation to test the hypothesis that the distinguishing characteristic between mild and extreme dreaders lies in the prospective response to future outcomes (*3*). In this model, the present value of a delayed act of consumption is divided into two components: the utility from consumption and the utility from anticipation (dread). Assuming instantaneous consumption at the time (T) of shock delivery, the present value at time (t) of a future act of consumption is the utility of consumption U discounted by an exponential function with rate $r = Ue^{-r(T-t)}$ (*1*). In addition to the discounted consumption utility, anticipation—i.e., dread—confers utility in and of itself. For the sake of simplicity, we assumed that the instantaneous intensity of dread was constant and that the present value was this constant, α, multiplied by the time remaining until the shock. Thus, combining the terms for dread and discounted consumption, the present value $U(V,t) = U(V) \times [\alpha(T-t) + e^{-r(T-t)}]$, where $U(V)$ is the utility of the shock (a function of voltage V) occurring at time T; α is the

dread factor, and r is the discount rate. According to this theory, differences in the utility of dread should be measurable as differences in the dread factor α. A dread factor that is significantly positive would manifest as an early increase in the time course of activity (as opposed to a slow increase as the shock approached in time).

All of the contralateral (right hemisphere) ROIs and the caudal ACC displayed time courses with dread factors significantly different from zero, but this was an effect observed primarily in the extreme dreaders and not the mild dreaders (compare with the early, sustained, increases in Fig. 4). Both SI and SII showed marked elevations in activity after the presentation of the cue—an elevation which continued to rise in advance of the shock. But the initial elevation in SI, SII, and right posterior insula, which was measured by the dread factor, was significantly greater in the extreme dreaders (*12*). The time course in the caudal ACC displayed a significant dread factor for only the extreme dreaders. The right amygdala had a significant dread factor for both groups but was not significantly different between mild and extreme dreaders. From the time course of the response in these regions, coupled with its predominance in individuals who showed the most extreme behavioral evidence of not wanting to wait, we conclude that the component of anticipation that can be specifically attributed to dread is manifest in the posterior elements of the cortical pain matrix (SI, SII, the posterior insula, and the caudal ACC) and not the anterior ones (the anterior insula and the rostral ACC).

The manifestation of dread in the more posterior elements of the pain matrix informs our understanding of what dread is and how it impacts decision-making. The pain matrix can be divided broadly into somatosensory, attentive, movement, and emotional divisions. Although dread is usually thought of as an emotion based on fear and anxiety (*14*), our localization of dread to the posterior elements of the matrix suggests that dread has a substantial attentive component. Both the mild and extreme dreaders displayed time courses of activity in SI, SII, the caudal ACC, and the posterior insula that were consistent with the utility-based theory of dread. The more anterior, "emotional" components (e.g., the anterior insula, the rostral ACC, and the amygdala) did not have such time courses. Moreover, it was the significantly different dread factor in the posterior divisions that most clearly distinguished mild from extreme dreading behavior when individuals subsequently had to make decisions regarding wait times. Both SI and SII have generally been associated with the physical intensity of noxious stimulation (*9*, *10*, *15*), whereas the caudal ACC has been associated with the attentive component of pain (*16*). With regard to nociceptive inputs, both SI and SII receive afferent signals from the posterior portion of the ventromedial nucleus of the thalamus, whereas the ACC receives input from the mediodorsal nucleus (*10*). As the terminal fields from the spinothalamic system, these regions naturally show activations that track stimulation voltage. But increasing stimulation intensity also elicits increased attention, and SII has been associated with the spatial localization of noxious stimuli (*17*). In the context of waiting, however, increased activity in this region suggests increased attention toward the location of the impending shock. The caudal ACC (also termed the posterior mid-cingulate cortex) is a key region for the modulation of inputs coming from the spinothalamic pathway through both SI and SII, and the caudal ACC is closely associated with sensory orientation and preparatory motor responses (*16*, *18*). We found that the caudal ACC showed a significantly greater early response in the extreme dreaders than in the mild dreaders. Interestingly, the amygdala, whose role in aversive conditioning is well known (*19*), displayed a significant dread response on the right side, but this was not significantly different between the mild and extreme dreaders. This suggests that although the amygdala may contribute to the emotional component of dread, it does not differentiate mild from extreme dreaders.

Taken together, the anatomical locations of dread responses suggest that the subjective experience of dread that ultimately drives an individual's behavior comes from the attention devoted to the expected physical response (SI, SII, the caudal ACC, and the posterior insula) and not simply a fear or anxiety response. Indeed, this finding would be consistent with the theory that dread comes from the integral of future expected utility—a cognitive operation that would depend on attentional resources to make such a projection possible. In contrast, distracting an individual's attention from the affected part of the body would be predicted to decrease dread, a finding supported by the use of hypnotic suggestion to decrease pain (*20*).

Because we collected fMRI data during the passive experience and not during the choice

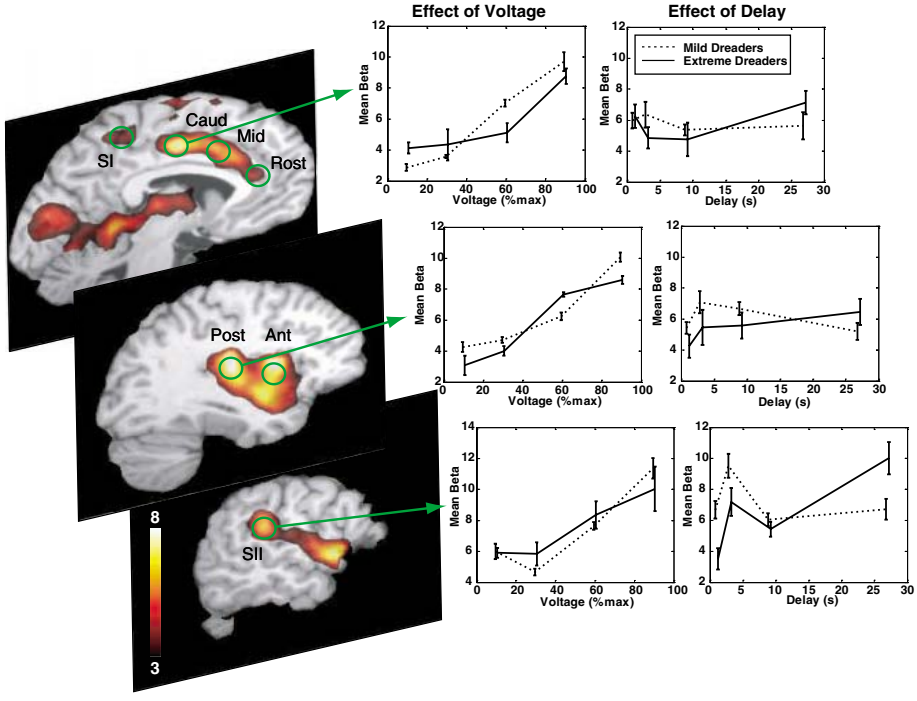

Fig. 3. Effect of voltage and delay on the brain response to the shock itself. Statistical parametric map of the voltage-sensitive response to shock (left), identified by a linearly weighted contrast across the four voltage levels ($P < 0.001$, uncorrected). ROIs (green) were defined on the basis of this functional map in conjunction with anatomical masks within the cortical pain matrix (*6*–*11*): SI for the foot, SII (*32*, *33*), anterior (Ant) and posterior (Post) insular cortex, caudal ACC (Caud), middle ACC (Mid), rostral ACC (Rost), and amygdala (not shown). There was a significant positive effect of voltage on the amplitude of response to the shock itself in all of the ROIs (middle, shown for caudal ACC, right posterior insula, and right SII), and this was not significantly different for the mild and extreme dreaders. With the possible exception of the right SII, the length of the preceding delay had minimal, if any, effect on the response to the shock itself (right) and was not significantly different between mild and extreme dreaders (*12*). The trials with 1-s and 3-s delays, however, did not allow complete separation of the cue response from the shock response, and so these beta values are not exactly equivalent to the 9-s and 27-s values. The general lack of an effect of delay on the instantaneous response to the shock itself suggested that the utility of the outcome was not affected by how long one had to wait for it. Given this evidence, the differentiation of mild and extreme dreaders must have occurred during the waiting period (Fig. 4).

procedure, any correlations with dread cannot be due to the decision-making process itself. Unlike previous reports of neurobiological processes during intertemporal choice (*21*), the imaging data reported here were acquired passively—when no choices were offered and no decisions were required. Thus, the regions of fMRI activity that differentiated two patterns of decision-making must be related to the experiential utility of dread. To our knowledge, this is the first time that experiential utility has been linked directly, and biologically, to decision utility, even though the two forms are assumed to be related (*22*).

Although the idea of utility is fundamental to rational choice theories, utility has been surprisingly difficult to measure, other than through the act of choosing. Thus, the demonstration of activity traces in the brain that follow a time course consistent with that predicted by a model based on utility theory is a notable validation for one of the basic constructs of economics (*23*). However, specifically attributing such patterns to the flow of utility, versus some other time-dependent process, depends both on the specificity of the model's predictions and how well the data fit these predictions.

For the subjective experience of dread, the model used here is quite specific. The distinguishing feature of this model is the additional utility (or disutility) conferred by the act of waiting (*3*). Simpler models of decision-making that do not account for dread cannot explain why people should hasten the occurrence of an unpleasant outcome. Nearly all of the individuals studied in our experiment, however, exhibited this behavior, and the degree to which they did so was correlated with the early increase in activity in the posterior parts of the pain matrix. As instantiated in our modification of the Loewenstein model, anticipated dread is computed as the forward-looking integral from the present moment to the time of the expected outcome, which is maximal at the beginning of a trial and decreases monotonically to zero at the outcome. The outcome, even if unpleasant, thus affords relief from the dread. This type of time course is not generally accounted for by other theories of anticipation. Indeed, apart from the requirement that an expectation of an outcome is formed, few theories predict the nature of anticipation. Trial-based models of learning, such as Rescorla-Wagner (*24*) and temporal difference (*25*) suggest that the learning of an association between cue and outcome is driven by the mismatch between expectation and outcome but say little about what form the expectation should take leading up to the outcome. Other theories suggest that anticipation is, in part, based on the recollection of past experience, but again, say little about the time course of transmuting recollection into anticipation (*26*). Even other rational choice models do not consider the passage of time to have utility in and of itself.

Indeed, the notion of "anticipation" can be sharpened by separately mapping neurobiological traces onto two major components (*3*). The consumptive element of anticipation is conceptually identical to the expected outcome term of associative learning theories but exponentially discounted in time. The defining characteristic of this process is an exponential growth up to the outcome. We found ample evidence for this process throughout the cortical pain matrix, a result consistent with previous studies of pain anticipation (*6*, *7*, *27*–*31*). Unlike previous studies, we are now able to identify neurobiological substrates associated specifically with a second component of anticipation: dread. Although there are potentially a wide variety of theoretical models that could explain dread, the approach described here allows for the principled comparison of one against another, as well as in brain regions outside the pain matrix. For example, comparing the dread model with a simple discounting model, we found the former to be a better fit to the fMRI data, suggesting that the dread term is necessary to account for the responses observed here (*12*).

In addition to suggesting a neurobiological substrate for the utility of dread, our results have implications for another assumption of utility theory: the origin of preferences. It seems likely that an individual's relative preference for waiting for something unpleasant derives from previous experience. In our experiment, participants presumably had well-established preferences for waiting, although it is unlikely that they had previous experience with foot shocks. We thus observed the construction of waiting preference in the specific context of foot shocks without any choices being offered. That the activity patterns in the brain regions associated with the pain ex-

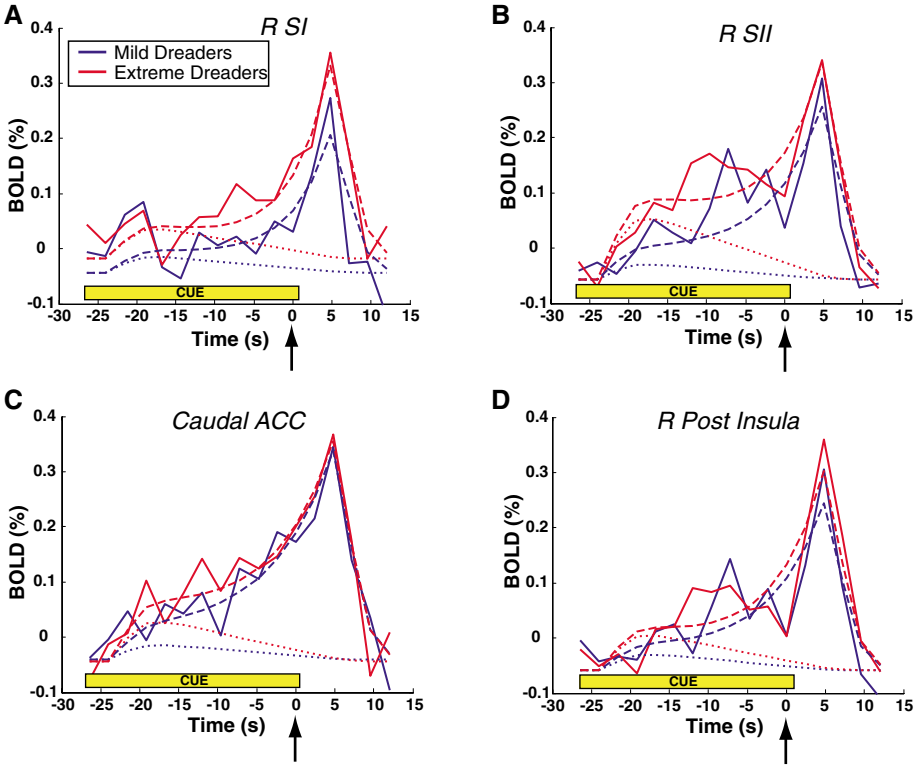

Fig. 4. Flow of dread in selected brain regions while waiting for shocks. Solid lines were averaged from 60 and 90% voltage trials (27-s trials only) in mild dreaders (solid blue) and extreme dreaders (solid red). The trial began with the cue at $t = -27$ s, and the shock occurred at $t = 0$ (arrow). During the waiting period (cue), the extreme dreaders displayed earlier and more sustained activity increases than the mild dreaders. BOLD, blood oxygenation level–dependent response as percentage change from baseline. To determine whether these differences were based predominately in an early prospective response or a later anticipation of consumption, a theoretical model of waiting was fit to the data (dashed lines). This model was comprised of two terms that were convolved with a hemodynamic response function: a declining dread term (dotted lines) and an exponentially increasing time-discounted consumption term (not shown for clarity). The dread term was calculated as the forward-looking integral from time t to the shock (i.e., $-\alpha t$), which has the characteristic of being maximal at the beginning of the trial and decreasing linearly to zero at the time of the shock. Significantly positive values for the dread factor α are associated with the experience of disutility from waiting itself. The four ROIs that had significantly greater ($P \leq 0.001$) dread factors in the extreme dreaders compared with those of the mild dreaders were (**A**) the right SI; (**B**) the right SII; (**C**) the caudal ACC; and (**D**) the right posterior insula. The difference between mild and extreme dreaders is seen most clearly by the early increase in activity, especially in the right SII and the caudal ACC and noted by the difference between the two dotted lines.

perience correlate with subsequent choices offers strong evidence for the existence of intrinsic preferences. Although it is not clear how malleable these preferences are, their existence may have health implications for the way in which individuals deal with events that are known to be unpleasant—for example, going to the doctor for painful procedures. The neurobiological mechanisms governing dreading behavior may hold clues for both better pain management and improvements in public health.

References and Notes

1. P. A. Samuelson, *Rev. Econ. Stud.* **4**, 155 (1937).
2. The opposite of utility is generally referred to as disutility, but for the sake of clarity, we refer to "utility" as possessing both positive and negative domains.
3. G. Loewenstein, *Econ. J.* **97**, 666 (1987).
4. A. Caplin, J. Leahy, *Q. J. Econ.* **116**, 55 (2001).
5. R.-R. Ji, T. Kohno, K. A. Moore, C. J. Woolf, *Trends Neurosci.* **26**, 696 (2003).
6. A. Ploghaus *et al.*, *Science* **284**, 1979 (1999).
7. T. Koyama, J. G. McHaffie, P. J. Laurienti, R. C. Coghill, *Proc. Natl. Acad. Sci. U.S.A.* **102**, 12950 (2005).
8. T. T. Raij, J. Numminen, S. Narvanen, J. Hiltunen, R. Hari, *Proc. Natl. Acad. Sci. U.S.A.* **102**, 2147 (2005).
9. I. Tracey, *Curr. Opin. Neurobiol.* **15**, 478 (2005).
10. A. D. Craig, *Annu. Rev. Neurosci.* **26**, 1 (2003).
11. R. Peyron, B. Laurent, L. Garcia-Larrea, *Neurophysiol. Clin.* **30**, 263 (2000).
12. Materials and methods are available as supporting material on *Science* Online.
13. H. R. Varian, *Intermediate Microeconomics: A Modern Approach* (Norton & Co., New York, ed. 6, 2002).
14. K. C. Berridge, in *Well-Being. The Foundations of Hedonic Psychology*, D. Kahneman, E. Diener, N. Schwarz, Eds. (Russell Sage Foundation, New York, 1999), pp. 525–557.
15. P. Petrovic, K. M. Petersson, P. Hansson, M. Ingvar, *Neuroimage* **16**, 1142 (2002).
16. B. A. Vogt, *Nat. Rev. Neurosci.* **6**, 533 (2005).
17. D. E. Bentley *et al.*, *Clin. Neurophysiol.* **115**, 1846 (2004).
18. D. E. Bentley, S. W. G. Derbyshire, P. D. Youell, A. K. P. Jones, *Pain* **102**, 265 (2003).
19. E. A. Phelps, *Annu. Rev. Psychol.* **57**, 27 (2006).
20. P. Rainville, B. Carrier, R. K. Hofbauer, M. C. Bushnell, G. H. Duncan, *Pain* **82**, 159 (1999).
21. S. M. McClure, D. I. Laibson, G. Loewenstein, J. D. Cohen, *Science* **306**, 503 (2004).
22. D. Kahneman, P. P. Wakker, R. Sarin, *Q. J. Econ.* **112**, 375 (1997).
23. C. Camerer, G. Loewenstein, D. Prelec, *J. Econ. Lit.* **43**, 9 (2005).
24. R. A. Rescorla, A. R. Wagner, in *Classical Conditioning 2: Current Research and Theory*, A. H. Black, W. F. Prokasy, Eds. (Appleton Century-Crofts, New York, 1972), pp. 64–69.
25. R. S. Sutton, *Mach. Learn.* **3**, 9 (1988).
26. C. K. Morewedge, D. T. Gilbert, T. D. Wilson, *Psychol. Sci.* **16**, 626 (2005).
27. A. Ploghaus *et al.*, *Proc. Natl. Acad. Sci. U.S.A.* **97**, 9281 (2000).
28. A. Ploghaus, L. Becerra, C. Borras, D. Borsook, *Trends Cogn. Sci.* **7**, 197 (2003).
29. T. V. Salomons, T. Johnstone, M.-M. Backonja, R. J. Davidson, *J. Neurosci.* **24**, 7199 (2004).
30. T. D. Wager *et al.*, *Science* **303**, 1162 (2004).
31. C. A. Porro *et al.*, *J. Neurosci.* **22**, 3206 (2002).
32. A. Ferretti *et al.*, *Neuroimage* **23**, 1217 (2004).
33. U. Bingel *et al.*, *Neuroimage* **23**, 224 (2004).

34. We thank C. M. Capra, C. Noussair, A. Rangel, and A. Rustichini for comments on this paper. Supported by grants from the National Institute on Drug Abuse (DA00367 and DA016434).

Supporting Online Material

www.sciencemag.org/cgi/content/full/312/5774/754/DC1
Materials and Methods
Figs. S1 to S6
Tables S1 to S3
References

12 December 2005; accepted 17 March 2006
10.1126/science.1123721

Conjunctive Representation of Position, Direction, and Velocity in Entorhinal Cortex

Francesca Sargolini,[1] Marianne Fyhn,[1] Torkel Hafting,[1] Bruce L. McNaughton,[1,2] Menno P. Witter,[1,3] May-Britt Moser,[1] Edvard I. Moser[1]*

Grid cells in the medial entorhinal cortex (MEC) are part of an environment-independent spatial coordinate system. To determine how information about location, direction, and distance is integrated in the grid-cell network, we recorded from each principal cell layer of MEC in rats that explored two-dimensional environments. Whereas layer II was predominated by grid cells, grid cells colocalized with head-direction cells and conjunctive grid × head-direction cells in the deeper layers. All cell types were modulated by running speed. The conjunction of positional, directional, and translational information in a single MEC cell type may enable grid coordinates to be updated during self-motion–based navigation.

The MEC is the hub of a widespread brain network for spatial navigation (*1*–*11*). Layer II of the MEC contains a two-dimensional (2D), ensemble-encoded metric map of relative spatial location (*6*–*8*) that is independent of the specific environment and the external sensory cues (*7*, *11*). The elements of the map are "grid" cells, which fire whenever the animal's position coincides with the vertices of a periodic triangular grid spanning the complete surface of the environment, with different cells having different firing coordinates on the unit grid (*7*, *12*). The regular structure of the grid field, and the environmentally invariant relationships among simultaneously recorded grid fields (*13*), implicates the grid cell as part of a universal, path-integration–based spatial metric, but its interaction with other cell types in MEC is not understood. To investigate the integration of metric spatial information in the multilayered entorhinal network (*10*, *14*, *15*), we compared the activity of cell populations in its four principal cell layers while rats were running in a 2D environment (*16*). Recordings were made from the most dorsal 23% of MEC in 17 rats (Fig. 1).

Grid cells with tessellating firing fields (*7*) were observed in all principal cell layers (Fig. 1, A and B). To compare their prevalence, we estimated the periodicity of the rate map of each cell by computing a 2D autocorrelation matrix for the rate distribution (Fig. 1C, left), rotating the autocorrelation map in steps of 6°, and calculating the correlation between each rotated map and the original. Grid structure was apparent as a sinusoidal modulation of this correlation, with peaks recurring at multiples of 60° (Fig. 1C, right, and fig. S1) (*12*). The degree of "gridness" was expressed as the difference between the correlations at the expected peaks (60° and 120°) and the expected troughs (30°, 90°, and 150°) of the function. The proportion of cells with a sinusoidal modulation was layer-dependent (Fig. 1D and table S1). Whereas most well-separated layer II cells had strongly periodic firing fields, only a smaller proportion of the deeper neurons had such characteristics; however, the range of "gridness" among those cells was not different from that of the layer II cells.

To compare the geometric structure of grids in different layers, we defined grid cells as the subset of cells that had higher correlations at 60° and 120° of rotation than at 30°, 90°, and 150° (gridness > 0) (*16*). All 203 neurons that passed this criterion had stable periodic firing patterns both within and between trials (figs. S1 and S2). Irrespective of layer, the scale of the grid in these cells increased by a factor of 1.5 to 2 from the dorsalmost to the ventralmost recording location, such that cells near the postrhinal border had the densest spacing (~35 to 40 cm) and the smallest firing fields (~500 cm^2) (fig. S3). The correlations between distance from the

[1]Centre for the Biology of Memory, Norwegian University of Science and Technology, 7489 Trondheim, Norway. [2]Arizona Research Laboratories Division of Neural Systems, Memory, and Aging, University of Arizona, Tucson, AZ 85724, USA. [3]Research Institute Neurosciences, Department of Anatomy and Neurosciences, Vrije Universiteit University Medical Center, Amsterdam, Netherlands.

*To whom correspondence should be addressed. E-mail: edvard.moser@ntnu.no

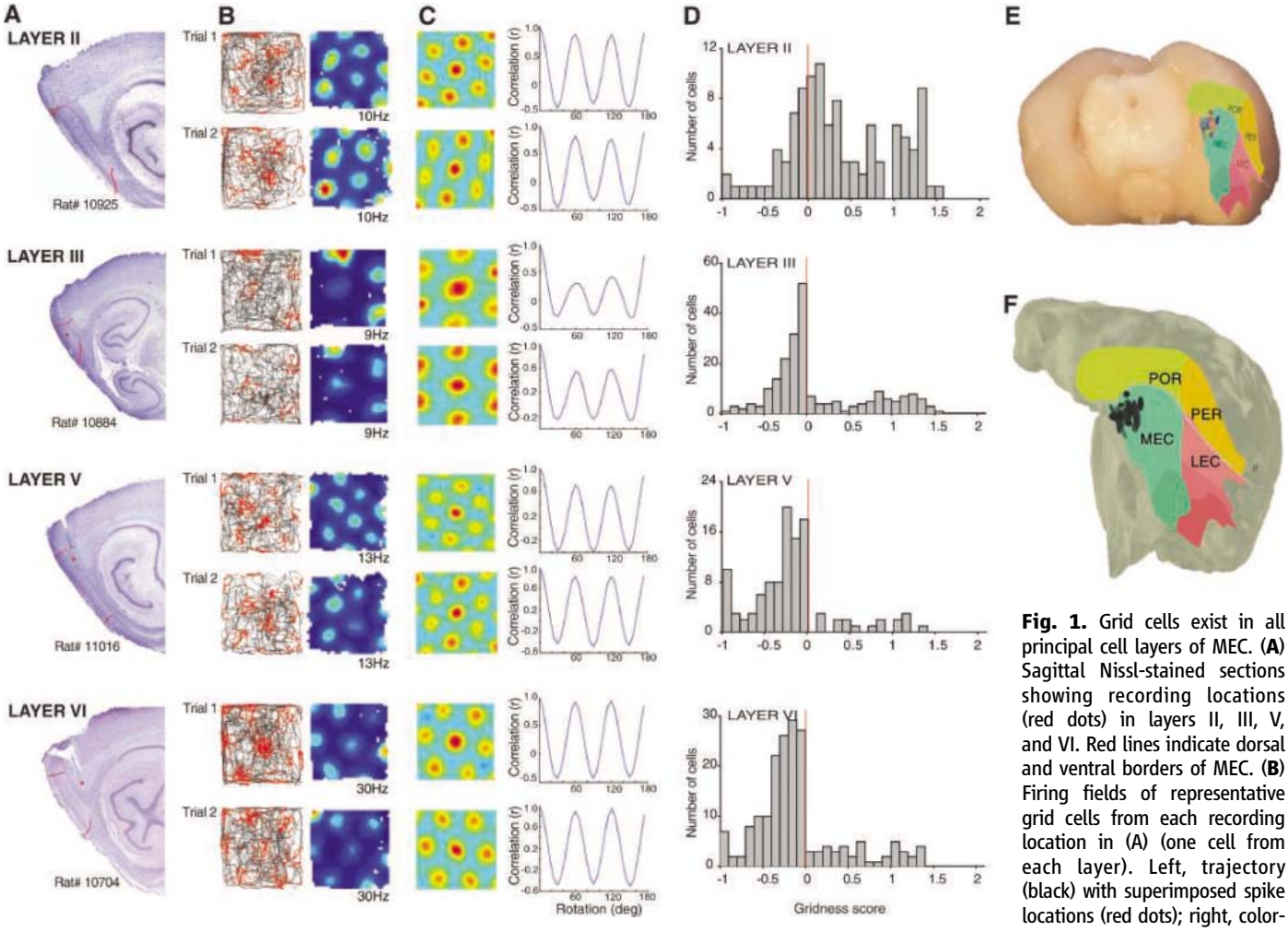

Fig. 1. Grid cells exist in all principal cell layers of MEC. (**A**) Sagittal Nissl-stained sections showing recording locations (red dots) in layers II, III, V, and VI. Red lines indicate dorsal and ventral borders of MEC. (**B**) Firing fields of representative grid cells from each recording location in (A) (one cell from each layer). Left, trajectory (black) with superimposed spike locations (red dots); right, color-coded rate map with the peak rate indicated. Red is maximum, dark blue is zero. Pixels not covered are white. Spike activity was recorded during two trials of running in a square box (10 min each, 10 min interval). (**C**) Periodic firing structure of the grid cells shown in (B). Left, autocorrelation matrix for the rate map. The color scale is from blue ($r = -1$) through green ($r = 0$) to red ($r = 1$). The distance scale of the autocorrelogram is the same as for the rate map; only the central part of the autocorrelogram is shown. Right, periodicity of the autocorrelation matrix. We rotated the autocorrelation map in steps of 6° and computed the correlation between each rotated map and the original. Correlations are 1 at 180° because of the mirror symmetry of the autocorrelation matrix. (**D**) Frequency distribution of gridness for all cells recorded in all cell layers of the MEC. (**E**) Ventral-posterior view of a whole rat brain, indicating the position of the reconstructed region in (F). The orientation of the brain in (E) and (F) is similar. (**F**) Three-dimensional reconstruction of the posterolateral surface of one hemisphere showing the complete range of recording locations in all 17 animals. For each animal, the position and dorsoventral extent of the tetrode tract is indicated as a black ellipsoid. Note clustering of recording locations in the most dorsomedial quarter (23%) of the MEC (dark and light green), with the majority of tetrodes positioned in the dorsal 5 to 15%. Recording locations were clustered dorsally for the practical reason that, at deeper levels, the grid scale becomes too large for quantitative analysis given the limited size of the apparatus. LEC, lateral entorhinal cortex; POR, postrhinal cortex; PER, perirhinal cortex; gray line, rhinal fissure (rf). Subdivisions of MEC (green) and LEC (red) are indicated by light and dark colors.

postrhinal border on the one hand and spacing and field size on the other were significant in all layers (spacing, $0.46 \leq r \leq 0.94$; field size, $0.44 \leq r \leq 0.94$; all, $P < 0.005$) (*17*). In all layers, the phase of the grid was distributed, i.e., the vertices of most nearby grid cells were offset relative to each other, but the orientation of the grids was consistent across all simultaneously recorded cells.

Beneath layer II, grid cells were colocalized with head-direction cells whose general properties were similar to those of head-direction cells in other brain areas (*18*–*21*) (Fig. 2). In these neurons, firing increased from a low background rate (typically < 0.5 Hz) to a high maximum rate (5 to 40 Hz) whenever the rat's head faced a certain range of directions (Fig. 2D, fig. S4, and table S1). The preferred firing direction varied among cells. The degree of directional tuning was quantified for each cell by comparing the distribution of the rat's orientation at the time of firing with the distribution of orientations across the entire trial, using Watson's U^2 test statistic (*20*). When these distributions differed significantly and the directional bias was significantly correlated across blocks of the trial, the cell was classified as a head-direction cell. No head-direction cells were found in layer II (Fig. 2E). In contrast, a large proportion of the cells in layers III to VI had directional preferences (273 of 385 cells) (Fig. 2E). The breadth of tuning was not significantly different between layers III, V, and VI (mean U^2 values, 18.2, 25.2, and 18.3, respectively; mean angular standard deviations, 55.9°, 52.2°, and 58.2°; $P > 0.05$) (fig. S4). The entire range of head directions was represented in all three layers (Fig. 2F). When several head-direction cells were recorded simultaneously in the same area, their peak firing directions were widely distributed (Fig. 2G and fig. S5). Head-direction cells were usually encountered together with grid cells (fig. S6). Directional tuning curves were always stable across trials (circular correlation, $r = 0.84$, $P < 0.001$).

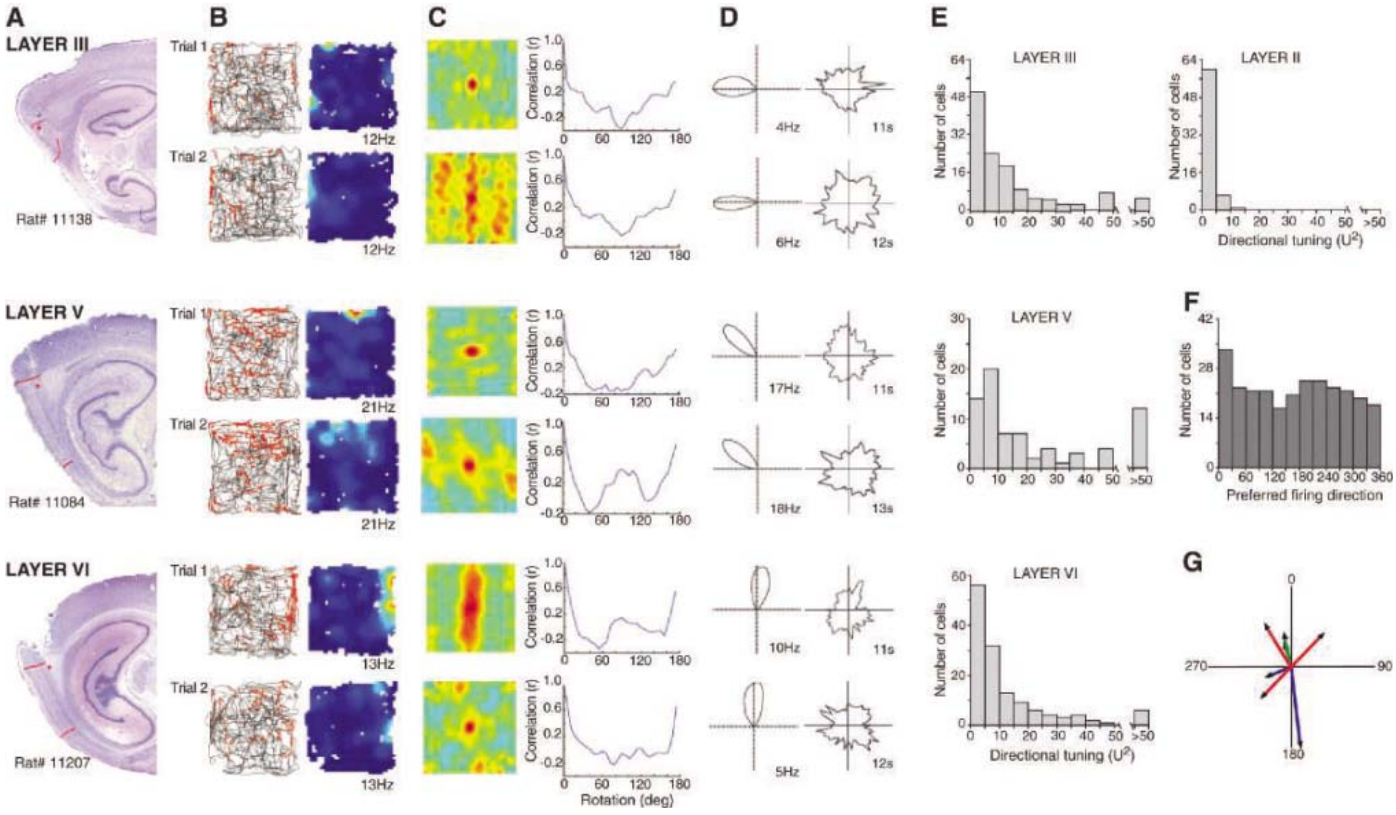

Fig. 2. Head-direction cells in the MEC. (**A**) Sagittal Nissl-stained sections from three rats showing recording locations in layers III, V, and VI. (**B**) Trajectory with spike locations (left) and color-coded rate maps (right) for three representative head-direction cells, one from each location in (A). Two trials are shown. Symbols as in Fig. 1B. (**C**) Color-coded autocorrelation matrices (left) and periodicity of the autocorrelation (right) for the same three cells as in (B). Note lack of periodicity. The correlation at 180° reflects the mirror symmetry of the autocorrelation matrix. Symbols and computations as in Fig. 1C. (**D**) Polar plots indicating strong directional tuning of firing rate in the cells shown in (B) and (C). Left, firing rate as a function of head direction. Right, amount of time that the rat faced each direction. Bin sizes were 6°. Peak firing rate and peak dwell time are indicated. Watson's U^2 values for these cells ranged from 23 to 33. (**E**) Frequency distribution of head-direction tuning for all cells recorded in all layers. Directional tuning is expressed by Watson's U^2 test statistic (*19*). (**F**) Distribution of peak firing direction relative to a common external reference for the entire sample of head-direction cells (all layers). (**G**) Vector representation of firing direction (angle) and firing rate (length) of 7 colocalized head-direction cells in layer VI (mean vectors for each cell). Cells from the same tetrode have the same color. There was no significant clustering of the mean vectors in this recording (Watson's U^2 test, U^2 = 0.01, critical value 0.18, n.s.) (see also fig. S5).

Grid cells and head-direction cells formed overlapping populations. The 2D distribution of gridness and directional tuning was continuous, such that some grid cells were directionally tuned and some head-direction cells had grid correlates (Fig. 3, A to D, and fig. S7). The proportion of grid cells with conjunctive properties was layer-dependent (table S1). The largest proportion was encountered in layers III and V, where 66% and 90% of the grid cells had dual response properties, respectively. In layer VI, the proportion was 28%. No conjunctive cells were observed in layer II. Differences between layers were significant (all four cell layers, $\chi(3) = 28.4$, $P < 0.001$; layers III to VI, $\chi(2) = 6.2$, $P < 0.05$). The degree of directional tuning in cells that met selection criteria for both gridness and directionality was not significantly different from that of pure head-direction cells (mean U^2 values, 18.0 and 19.4, respectively; $P > 0.05$) (Fig. 3, D and E). Cells with different degrees of gridness and directionality always responded as a coherent ensemble during environmental manipulations such as the rotation of a polarizing cue card (Fig. 3F and fig. S8) (*22*).

Cells with conjunctive grid and head-direction properties may update the representation of spatial location by integrating position and direction information as the animal moves around; however, translocation of the position vector between grid cells with shifted firing vertices may require additional information about the animal's instantaneous speed of movement (*23*–*27*). We thus asked whether speed was expressed in the firing rates of any of the cells that we recorded (Fig. 4). Because all position points were used in this analysis, including those outside the firing fields, the correlation between speed and rate was generally low (Fig. 4A). Yet, regression analyses showed a consistent positive speed-rate relation in nearly all grid cells (141/150 cells, $P < 0.001$), head-direction cells (153/220 cells, $P < 0.001$) and grid × head-direction cells (45/53 cells, $P < 0.001$), suggesting that a substantial proportion of the network expressed information about how fast the animal was moving (Fig. 4B). The slope of the regression line was steeper for conjunctive cells and grid cells than for head-direction cells [$F(2,422) = 5.5$, $P < 0.005$; conjunctive versus head-direction, $P = 0.009$; grid versus head-direction, $P = 0.01$; conjunctive versus grid, $P = 0.60$; Tukey HSD test). The *y*-intercept of the regression line was positive in 422 out of 423 cells (Fig. 4C). Average rates at the lowest velocity (0 to 3 cm/s) were 2.26 ± 0.03 Hz (grid cells), 2.50 ± 0.02 Hz (head-direction cells) and 2.39 ± 0.05 Hz (grid × head-direction cells). Thus, grid structure and directional tuning can be maintained during brief stops along the rat's trajectory. Few stops were longer than 5 s.

These results imply that, despite the differential hippocampal and neocortical connections of superficial and deep layers of the MEC (*10*, *28*), all layers together operate as an integrated unit, with considerable interaction between grid cells, present in all principal cell

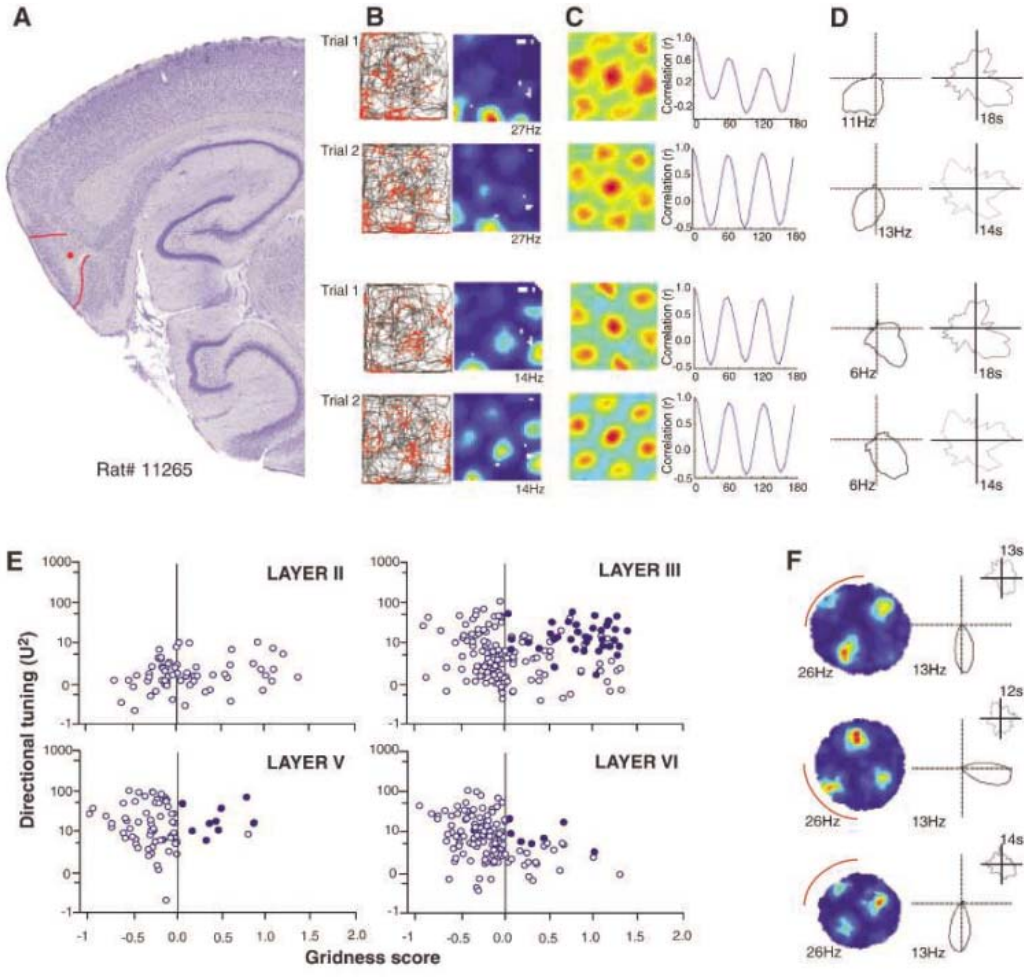

Fig. 3. Conjunctive representation of position and direction. (**A** to **D**) Firing correlates of two simultaneously recorded cells with conjunctive grid and head-direction properties in layer III of MEC in one rat. Two trials are shown; note consistent discharge profile. (A) Sagittal Nissl-stained section showing recording location in layer III of the dorsocaudal MEC. (**B**) Trajectory with spike locations (left) and color-coded rate map (right). (**C**) Color-coded spatial autocorrelation matrix (left) and the periodicity of the matrix (right). (**D**) Polar plots showing directional tuning of firing rate (left) and distribution of dwell time across head directions (right). Symbols and computations as in Fig. 2, B to D. (**E**) Scatterplot showing relation between gridness (Fig. 1D) and degree of head-direction tuning (Watson's U^2, logarithmic scale; Fig. 2E) in all cells for which head direction was tracked. Each circle refers to one cell. Filled circles indicate cells that passed criteria for conjunctive firing. Note the high proportion of conjunctive cells in layers III and V. (**F**) Rate map for a grid cell (left) and polar plot for a head-direction cell (right) recorded simultaneously in layer VI of MEC after rotation of a polarizing cue card on the wall of the circular environment (red arc). Top and bottom, cue card in original position. Middle panel, cue card rotated 90°. Insets show distribution of time across head directions. Three other head-direction cells were recorded simultaneously; all of these rotated 90° (fig. S8).

layers, and head-direction cells, present in layers III to VI. Principal neurons from layer II to layer V have apical dendrites that extend up to the pial surface (*14*, *29*). Layer V cells have extensive axonal connections to the superficial layers (*14*, *15*), and local axons of layer II and III cells may contact the dendrites of deeper cells (*30*). This implies that visuospatial and movement-related signals from the postrhinal and retrosplenial cortices (*10*, *28*) and directional signals from the dorsal presubiculum (*18–20*, *31–34*) may activate the entire MEC circuit even when the axonal input is specific to one or a few layers.

The results show that the spatial map in MEC comprises both grid cells and head-direction cells. These cell types form a continuous population, with grid cells expressing variable degrees of directional modulation and head-direction cells expressing variable degrees of grid structure. Conjunctive representations among input variables appear in many theoretical models for neural systems that perform coordinate transformations, and similar conjunctions of head direction and location have been observed in some cells in the dorsal presubiculum (*35*). Analogous conjunctive cells may be involved in the computation of head-centered coordinates from retinal-location and eye-position data ("gain fields") in the posterior parietal cortex (*36*, *37*) and in the continuous updating of head direction cells on the basis of conjunctions between current head direction and head angular velocity (*38*, *39*). Our results suggest that, as the animal moves, the position vector may be updated through integration of position, direction, and speed signals in the grid-cell network (*23–27*). Conjunctive cells are likely to play a critical role in this process. The conjunctive cells are located predominantly in layers III and V, where principal neurons have extensive axonal projections to the grid-cell population in layer II (*14*, *15*). The ability of superficial cells to read out signals carried by these axons may be critical for translating activity over the population of grid cells, i.e., between cells with a different spatial phase, in a manner consistent with the rat's motion. The direction of translation may be determined by the head-direction input; the distance may be controlled by the speed modulation. In essence, this mechanism would perform path integration in the MEC network.

The integration of directional and positional information is strongly facilitated by the intermingled localization of the grid cells and the head-direction cells and the distributed representation of spatial phase (*7*) and head orientation in these cell types. Within a diameter of a few hundred micrometers or less, the complete range of positions and distances appears to be represented. It remains to be determined whether the integration of position, direction, and velocity is confined to the local circuitry, as in the columns of the isocortex (*40*), or extends across the entire entorhinal sheet of grid cells, spanning all grid spacings.

References and Notes

1. J. O'Keefe, L. Nadel, *The Hippocampus as a Cognitive Map* (Clarendon Press, Oxford, 1978).
2. G. J. Quirk, R. U. Muller, J. L. Kubie, J. B. Ranck Jr., *J. Neurosci.* **12**, 1945 (1992).
3. A. D. Redish, D. S. Touretzky, *Hippocampus* **7**, 15 (1997).
4. A. D. Redish, *Beyond the Cognitive Map: From Place Cells to Episodic Memory* (MIT Press, Cambridge, 1999).
5. P. E. Sharp, *Hippocampus* **9**, 432 (1999).
6. M. Fyhn, S. Molden, M. P. Witter, E. I. Moser, M.-B. Moser, *Science* **305**, 1258 (2004).
7. T. Hafting, M. Fyhn, S. Molden, M.-B. Moser, E. I. Moser, *Nature* **436**, 801 (2005).
8. E. L. Hargreaves, G. Rao, I. Lee, J. J. Knierim, *Science* **308**, 1792 (2005).

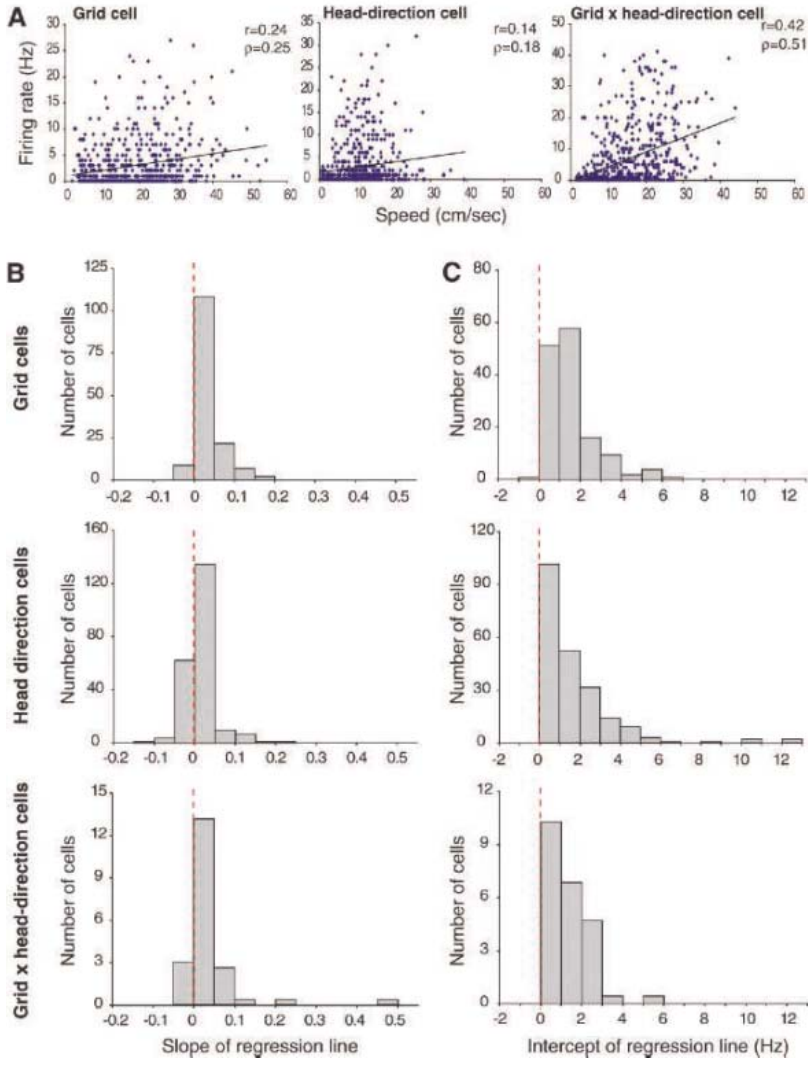

Fig. 4. Velocity modulation of grid cells, head-direction cells, and conjunctive cells. (**A**) Scatterplot showing relation between velocity and firing rate in three representative cells (grid cell, head-direction cell, and grid × head-direction cell; one plot for each cell). Dots refer to individual spikes. Linear regression line and correlation values are indicated (Pearson's product-moment correlation and Spearman's rank correlation). (**B**) Frequency distribution for the slope of the rate/velocity function. Analyses were based on the entire set of videotracker positions, irrespective of whether they were inside or outside the positional or directional firing fields of the cell. Nearly all grid cells, head-direction cells, and grid × head-direction cells had positive slope values, i.e., the firing rate increased with velocity. (**C**) Frequency distribution for the estimated firing rate at zero velocity (the *y*-intercept of the regression line). All cells except one had positive intercepts, implying that the activity of the network was not interrupted by brief stops on the rat's trajectory.

9. D. A. Nitz, *Neuron* **49**, 747 (2006).
10. M. P. Witter, D. G. Amaral, in *The Rat Nervous System, 3rd Edition*, G. Paxinos, Ed. (Academic Press, San Diego, 2004), pp. 637–703.
11. C. Parron, E. Save, *Exp. Brain Res.* **159**, 349 (2004).
12. The firing field of a grid cell has the form of a regular grid whose unit cell is a pair of inverted equilateral triangles or a rhombus with interior angles of 60 and 120°. Firing rate is maximal at the vertices of the grid and minimal at the center of each triangle. Rotations of the firing rate map (or its 2D autocorrelation function) come into correspondence with the unrotated map every 60°.
13. M. Fyhn, T. Hafting, A. Treves, M.-B. Moser, E. I. Moser, *Soc. Neurosci. Abstr.* **31**, 198.6 (2005).
14. T. van Haeften, T. L. Baks-te-Bulte, P. H. Goede, F. G. Wouterlood, M. P. Witter, *Hippocampus* **13**, 943 (2003).
15. F. Kloosterman, T. van Haeften, M. P. Witter, F. H. Lopes da Silva, *Eur. J. Neurosci.* **18**, 3037 (2003).
16. Materials and methods are available as supporting material on *Science* Online.
17. If this linear trend persists throughout the dorsal-to-ventral extent of MEC, it predicts grids with spacings of about 2 m in the most ventral portions of MEC.
18. J. S. Taube, R. U. Muller, J. B. Ranck Jr., *J. Neurosci.* **10**, 420 (1990).
19. J. S. Taube, *Prog. Neurobiol.* **55**, 225 (1998).
20. A. Johnson, K. Seeland, A. D. Redish, *Hippocampus* **15**, 86 (2005).
21. J. J. Knierim, H. S. Kudrimoti, B. L. McNaughton, *J. Neurosci.* **15**, 1648 (1995).
22. A similar coupling has been reported for thalamic head-direction cells and hippocampal place cells (*21*).
23. B. L. McNaughton *et al.*, *J. Exp. Biol.* **199**, 173 (1996).
24. K. Zhang, *J. Neurosci.* **16**, 2112 (1996).
25. A. Samsonovich, B. L. McNaughton, *J. Neurosci.* **17**, 5900 (1997).
26. J. O'Keefe, N. Burgess, *Hippocampus* **15**, 853 (2005).
27. M. C. Fuhs, D. S. Touretzky, *J. Neurosci.* **26**, 4266 (2006).
28. M. P. Witter, H. J. Groenewegen, F. H. Lopes da Silva, A. H. Lohman, *Prog. Neurobiol.* **33**, 161 (1989).
29. B. N. Hamam, T. E. Kennedy, A. Alonso, D. G. Amaral, *J. Comp. Neurol.* **418**, 457 (2000).
30. T. Iijima *et al.*, *Science* **272**, 1176 (1996).
31. M. Caballero-Bleda, M. P. Witter, *Exp. Brain Res.* **101**, 93 (1993).
32. T. van Haeften, F. G. Wouterlood, B. Jorritsma-Byham, M. P. Witter, *J. Neurosci.* **17**, 862 (1997).
33. Y. Honda, N. Ishizuka, *J. Comp. Neurol.* **473**, 463 (2004).
34. F. G. Wouterlood *et al.*, *Brain Res.* **1013**, 1 (2004).
35. F. Cacucci, C. Lever, T. J. Wills, N. Burgess, J. O'Keefe, *J. Neurosci.* **24**, 8265 (2004).
36. R. A. Andersen, G. K. Essick, R. M. Siegel, *Science* **230**, 456 (1985).
37. J. Xing, R. A. Andersen, *J. Cogn. Neurosci.* **12**, 601 (2000).
38. W. E. Skaggs, J. J. Knierim, H. S. Kudrimoti, B. L. McNaughton, in *Advances in Neural Information Processing Systems 7*, G. Tesauro, D. Touretzky, T. Leen, Eds. (MIT Press, Cambridge, 1995), pp. 173–180.
39. L. L. Chen, L. H. Lin, E. J. Green, C. A. Barnes, B. L. McNaughton, *Exp. Brain Res.* **101**, 8 (1994).
40. V. B. Mountcastle, *Brain* **120**, 701 (1997).

41. We thank S. Molden and A. Treves for discussion and A. M. Amundsgård, K. Haugen, K. Jenssen, E. Sjulstad, R. Skjerpeng, and H. Waade for technical assistance. This work was supported by a Centre of Excellence grant from the Norwegian Research Council.

Supporting Online Material

www.sciencemag.org/cgi/content/full/312/5774/758/DC1
Materials and Methods
Figs. S1 to S9
Table S1

30 January 2006; accepted 30 March 2006
10.1126/science.1125572

Automated Plate Sealer

The TriSeal automated heat sealer is designed to produce an accurate and tight seal on any standard microplate from 5 mm to 47 mm in height. Offering adjustable-temperature heat sealing from 50°C to 185°C, TriSeal operates optimally with most foil and film seals. A unique turntable design that allows simultaneously loading, unloading, and sealing permits the TriSeal to seal 12 plates per minute. It can be used for stand-alone operation or integrated via RS-232 connection with most robotic plate stackers and automated equipment lines. A 610-m sealing film roll enables up to 5,000 plates to be sealed without intervention.

Porvair Sciences For information +44 1932 240255 www.porvair-sciences.com

Plant Protease Inhibitor

Plant ProteaseArrest is a plant-specific protease inhibitor cocktail comprising agents to inhibit serine, cysteine, and plant-specific proteases, including aminopeptidases and metalloproteases. Plant ProteaseArrest contains both irreversible and reversible protease inhibitors. An optional EDTA solution is provided for enhanced inhibition of metalloproteases. The reagent is suitable for the protection of proteins during preparation of samples and protein purification from plant tissues.

G-Biosciences/Genotech For information 314-991-6034 www.GBiosciences.com

Proteome Enrichment Chemistry

The second-generation ProteomeLab IgY-12 Partitioning Chemistries dramatically increase the throughput capacity of its columns. Based on avian-generated antibodies bound to inert microbeads, ProteomeLab IgY-12 liquid chromatography and spin columns selectively partition 12 highly abundant proteins (up to 96% of the protein mass) from primate serum or plasma. Each column can now partition twice as much plasma or serum per cycle as the original version—from 20 μl to 250 μl per cycle. The capacity of the ProteomeLab IgY-HSA spin columns has also been doubled to 40 μl plasma or serum per cycle.

Beckman Coulter For information 800-742-2345 www.beckmancoulter.com

Plasma Protein Removal

One of the most significant challenges facing scientists in clinical proteomics is the inability to detect the majority of low abundance proteins, which are the mediators of disease or drug efficacy, in plasma. The patent-pending ProteoPrep 20 Plasma Immunodepletion Kit removes 99% of 20 high abundant plasma proteins through the use of a proprietary multivalent antibody affinity medium in a convenient spin column format, resulting in removal of 97% of the overall protein mass. The unique high-density antibody affinity medium enhances the ability to visualize low abundance proteins in the plasma proteome using standard analysis technology. In addition, the multivalent antibody resin features novel recombinant antibodies that allow for a significantly higher density of conjugation, and hence efficiency of depletion with minimal sample loss or dilution.

Sigma-Aldrich For information 800-521-8956 www.sigma-aldrich.com

DNA Methylation Analysis

The MethylDetector Bisulfite Modification Kit simplifies DNA methylation analysis by providing optimized reagents for performing DNA conversion along with time-saving DNA purification columns and positive control polymerase chain reaction primers. Because the control primers anneal only to converted DNA, they can be used to assess the success of conversion before spending time and money on sequencing or other costly analysis.

Active Motif For information 877-222-9543 www.activemotif.com

Hydrophobic Protein Columns

The HiTrap Butyl-S FF (1 ml and 5 ml) prepacked columns are designed to meet the growing need for pure proteins in research and process development. These new columns enable convenient purification or removal of highly hydrophobic proteins.

GE Healthcare For information 732-457-8082 www.gehealthcare.com

High-Speed Microscope System

The Cell Observer HS is for users of light microscopes with digital microscope cameras who want to analyze fast processes in biomedical research; cellular, neurological, and developmental biology; zoology; and virology. It allows the acquisition of time-lapse movies reaching the speed limits of what is technically feasible. The AxioCam HSm digital camera, a major component of the new design, allows image rates between 60 and 300 images per second. The Fast Image Acquisition module allows camera data to be stored directly on the hard drive. The system enables fast recording in more than one fluorescence channel, with up to 85 dual-channel images per second, and fast recording in a transmitted-light channel, with up to 300 images per second. It is possible to combine transmitted-light and fluorescence channels with up to 30 time points per second and to record Z-stacks of living cells to gather three-dimensional information with about 1 Z-stack per second in more than one channel. These high speeds are facilitated by a xenon light source with rapidly changeable excitation wavelengths.

Zeiss For information +49 3641 64-2770 www.zeiss.de/micro

Newly offered instrumentation, apparatus, and laboratory materials of interest to researchers in all disciplines in academic, industrial, and government organizations are featured in this space. Emphasis is given to purpose, chief characteristics, and availability of products and materials. Endorsement by *Science* or AAAS of any products or materials mentioned is not implied. Additional information may be obtained from the manufacturer or supplier by visiting www.science.labvelocity.com on the Web, where you can request that the information be sent to you by e-mail, fax, mail, or telephone.

TaKaRa

GENE EXPRESSION

Single Protein Production System

SPP System™

Takara Bio Introduces:

Takara Bio, in collaboration with Dr. Masayori Inouye, introduces the SPP System™ (Single Protein Production System). This *E. coli*-based system exploits the unique properties of MazF, a bacterial ssRNA and ACA-specific endoribuclease. Expression of this endoribonuclease along with an engineered ACA-less target protein results in high-level target gene synthesis and dramatically reduced background. In addition, *csp*A-based cold-temperature expression increases protein solubility and stability, and easily aggregated proteins can be expressed.

SPP System™ offers:

- **Exceptional Signal to Noise Ratios:** Degradation of cellular mRNAs leads to virtual absence of background protein synthesis.
- **Expression of Difficult Proteins:** Easily aggregated proteins can be successfully expressed.
- **Increased Protein Stability and Solubility:** Cold-temperature expression suppresses protease activity and increases protein solubility.
- **Excellent for Labeling Applications (i.e. NMR):** High-level (up to 90%) target gene expression simplifies structural analysis of proteins.

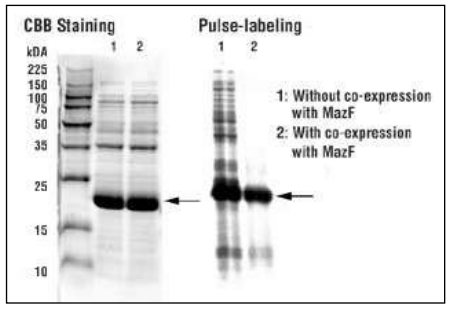

Synthesis of *csp*A-Promoter Expressed envAB with and without MazF. *E. coli* BL21 cells co-expressing MazF and pCold™ I (SP-4) envZB showed good envZB expression and extremely low background synthesis of host proteins, with M9 glucose medium.

Ref: Suzuki, M.; *et. al. Molecular Cell,* 2005, 18, 253-261.

TAKARA BIO INC.
The Biotechnology Company™

Otsu, Shiga, Japan
Phone: +81 77-543-7247
Fax: +81 77-543-9254

USA: Takara Mirus Bio Inc. Phone: 888-251-6618 • www.takaramirusbio.com
Europe: Takara Bio Europe S.A.S. Phone: +33 1 3904 6880 • www.takarabioeurope.com
Korea: Takara Korea Biomedical Inc. Phone: +82 31 739 3300 • www.takara.co.kr
China: Takara Biotechnology (Dalian) Co., Ltd. Phone: +86 411 8764 1681 • www.takara.com.cn

For more information and a list of Takara distributors worldwide, please visit our website today!

www.takara-bio.com

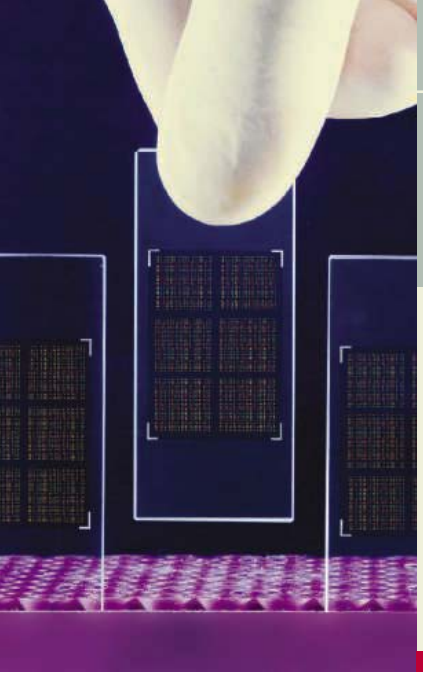

Life Science Technologies

Biochips and Lab-on-a-Chip Devices:
CHIPS WITH EVERYONE

With their ability to analyze large amounts of information in small volumes, microarrays and microfluidic devices exert a growing influence on studies of genotyping, gene expression, and protein interactions. Much of the recent improvement in the technologies stems from collaborations between vendors and among vendors and their customers. **By Peter Gwynne and Gary Heebner**

Microarrays and microfluidic devices provide miniature laboratories for studies of genomics and proteomics. Researchers typically apply microarrays to genotyping, mutation screening, gene expression, and protein-interaction studies. And they use microfluidic devices for processing or testing thousands of samples under nearly identical conditions in an automated environment. The key to the effectiveness of both devices is high density. In recent years, steady advances in technology have produced smaller, denser devices.

"The main improvement in microarrays is ever more information per experiment," says Walter Koch, head of research at **Roche Molecular Diagnostics**. "We get smaller feature sizes and more probes per array, and can ask increasingly complex questions." Tom Willis, vice president of DNA marketing for **Affymetrix**, puts the improvement into context. "We have reduced feature size to five microns, allowing experimentalists to collect 400 times more information from each microarray than they could in 1994 with the first commercial high-density microarray," he explains. "We have also made great improvements in the development of biochemical assays that enhance the power of these arrays."

Dramatic Steps

Microfluidic technology has taken similarly dramatic steps. "We have created tremendous traction by developing a lot of assays, particularly biochemical assays such as proteases or kinase profiling" says Kevin Hrusovsky, president and CEO of **Caliper Life Sciences**. "The next stage will be to broaden our portfolio of cellular assays."

Those improvements stem in large part from formal and informal cooperative ventures, both among vendors and between vendors and their customers. "We see a lot of collaboration in this area," says Criss Walworth, product director for gene expression at **Applied Biosystems**. "It really helps to move things forward as the area is so complex, involving materials science, chemistry, manufacturing methodology, optics, and other fields. For one organization to specialize in every area would be very challenging."

Inclusion of companies in this article does not indicate endorsement by either AAAS or *Science*, nor is it meant to imply that their products or services are superior to those of other companies.

Roland Green, vice president and chief technology officer for **NimbleGen Systems**, explains the value of customers in perfecting new technology. "Whenever we develop a new application we look to leaders in the field – usually academics – to help develop it," he says. "They have the expertise on the biology side." Jamie Wibbenmeyer, microarray marketing manager in **Bio-Rad**'s Gene Expression division, expands that point. "It lends so much more credibility to have collaborating researchers do the experiments and show their data," she explains.

Some companies still prefer to go it alone in advancing microarrays and microfluidics devices. "We observe the needs to capture proteins and try to imagine what kinds of development are necessary for unmet needs," says Eqisto Boschetti, **Ciphergen Biosystems**' vice president of research and development. But many vendors keep in touch with changing technical needs by word of mouth. "Discussions are ongoing between consumables manufacturers and equipment manufacturers, working on compatibility issues," says Varshal Davé, director of marketing microarray technology at **Molecular Devices**. The conversations extend to customers. "In the design of the AB array, genes were selected through a rigorous process from all the available information in public databases, as well as the Celera database," says Chris Streck, associate product manager for microarrays at Applied Biosystems.

Five-Micron Features

Affymetrix, which developed the original technology needed to produce very high-density DNA microarrays in the early 1990s, now offers the GeneChip Mapping 500K Array Set with a feature size of five microns. "This enables researchers to conduct larger scale studies in large populations for the first time," Willis says. "It provides a more comprehensive view of the human genetic variations that contribute to common diseases, by enabling researchers to perform whole-genome association studies across tens of thousands of samples." **continued ›**

IN THIS ISSUE:

The company has sought help to perfect applications of its new system. "Since the second half of last year, we have announced several groundbreaking collaborations with leading research organizations, including the Broad Institute of MIT and Harvard, the Genetic Association Information Network, GlaxoSmithKline, and the Wellcome Trust," Willis continues. "These partnerships will help Affymetrix to develop additional laboratory, informatics, and statistical methods for using the new 500K set."

NimbleGen Systems has developed another approach to fabricating DNA microarrays, based on patented technology from **Texas Instruments** that uses micromirrors to direct oligonucleotide synthesis on a solid matrix. "These types of microarrays can assay the full complexity of the human genome," Green explains. "That enables comparative genomic hybridization experiments; you can put different genomes on the same plate without any more preparation." The company specializes in custom arrays for clients studying organisms for which no arrays exist and for researchers who want to undertake focused, high-resolution studies. "We have arrays that can zoom in on custom regions of the genome with ultrahigh resolution," Green says. "The real value of our rapid custom design capability is for enabling rapid development of innovative new products."

Collaboration has helped to drive improvements in NimbleGen's technology. "It has been a critical part of the process for us as we're a fairly small company," Green says. "In every single product that we develop, we always work through these collaborations."

From Genes to SNPs

Scientists often use DNA microarrays to measure differential gene expression in different cells or tissues. **SuperArray** has decided to provide application-specific arrays that allow researchers to take in-depth looks at the specific gene expression involved in the pathways they study. The company provides low-density nylon membrane–based arrays, called GEArrays, that cover such areas as cell cycling, signal transduction, cytokines, and inflammatory response.

CombiMatrix group, meanwhile, has launched a series of microarrays specifically designed for analyzing microRNAs. These highly conserved RNAs regulate the expression of genes and are believed to be critical to controlling physiology in areas that include neural development, viral disease, and cancer.

Closer to the clinic, Roche Molecular Diagnostics offers the AmpliChip CYP450 Test, the world's first pharmacogenetic microarray–based test approved for clinical use. Clinical testing based on the chip, which is powered by Affymetrix technology, provides comprehensive coverage of gene variations, including deletions and duplications, for the CYP2D6 and CYP2C19 genes, which play a major role in the metabolism of an estimated 25 percent of all prescription drugs. The test helps physicians to individualize the choice and doses of drugs metabolized through those genes.

Researchers also foresee physicians testing single nucleotide polymorphisms (SNPs) to determine which drugs at which doses will best suit individual patients. "In a perfect world you would run a test for any drug, but that would need a huge budget," Koch explains. "So I think it will be introduced stepwise in particular therapeutic areas where it has a chance to make a big impact. We're focusing on psychiatry – helping people with severe depression or schizophrenia to manage their diseases.

The effort provides another example of collaboration. "We work with Affymetrix as a strategic partner because of its capability of manufacturing these microarrays for us," Koch explains. "And we have collaborations with pharmas such as Roche itself and Lilly to work on codeveloping diagnostics and therapeutics."

Two Prizes on Offer

Within the next two months, young scientists can apply for two US$25,000 prizes offered by this publication and commercial partners: the Eppendorf & *Science* Prize for Neurobiology (entries due by 15 June 2006) and the GE Healthcare & *Science* Prize for Young Life Scientists (entries due by 15 July 2006). For more information on these and other awards go to:

http://www.sciencemag.org/help/about/awards.dtl

Two Types of Protein Chip

Protein chips, which emerged a few years after DNA microarrays, come in two main types. Capture chips grab proteins of interest in much the same way that DNA chips capture their counterpart DNA sequences, while interaction chips use immobilized proteins, peptides, or other small molecules to study the interaction of proteins in a sample.

Capture chips from **Clontech**, **RayBiotech**, and **Zyomyx**, among other vendors, can use antibodies, antibody mimics, or aptamers. The chips can hunt down cytokines, identify which standard proteins a sample contains, and even determine whether a particular protein has been activated by phosphorylation.

Ciphergen bases its ProteinChip Systems on proprietary surface enhanced laser desorption/ionization (SELDI) technology, which enables a combination of miniaturized technologies on a single, unified platform. "People often think of protein microarrays in terms of conventional microarrays," points out director of biology Lee Lomas. "What our technology does is help you to identify both specific molecules that you're looking for and species in cases where you don't know what you're looking for. It uses direct detections based on mass spectrometry." The system enables protein capture, purification, analysis, and processing from complex biological mixtures directly on protein array surfaces. "The most important application of protein chip arrays is the discovery of proteins from biological extracts," Lomas's colleague Boschetti explains. "We can also see patterns of proteins to find biomarkers of interest in people with diseases. And we can discover toxicity markers in the development of new drugs."

Researchers can also use protein microarrays to study the interactions between proteins or peptides. The relatively small number of companies that have moved into this business include **Biacore** and **Jerini**. continued ›

Protein interaction analysis

from discovery to quality control

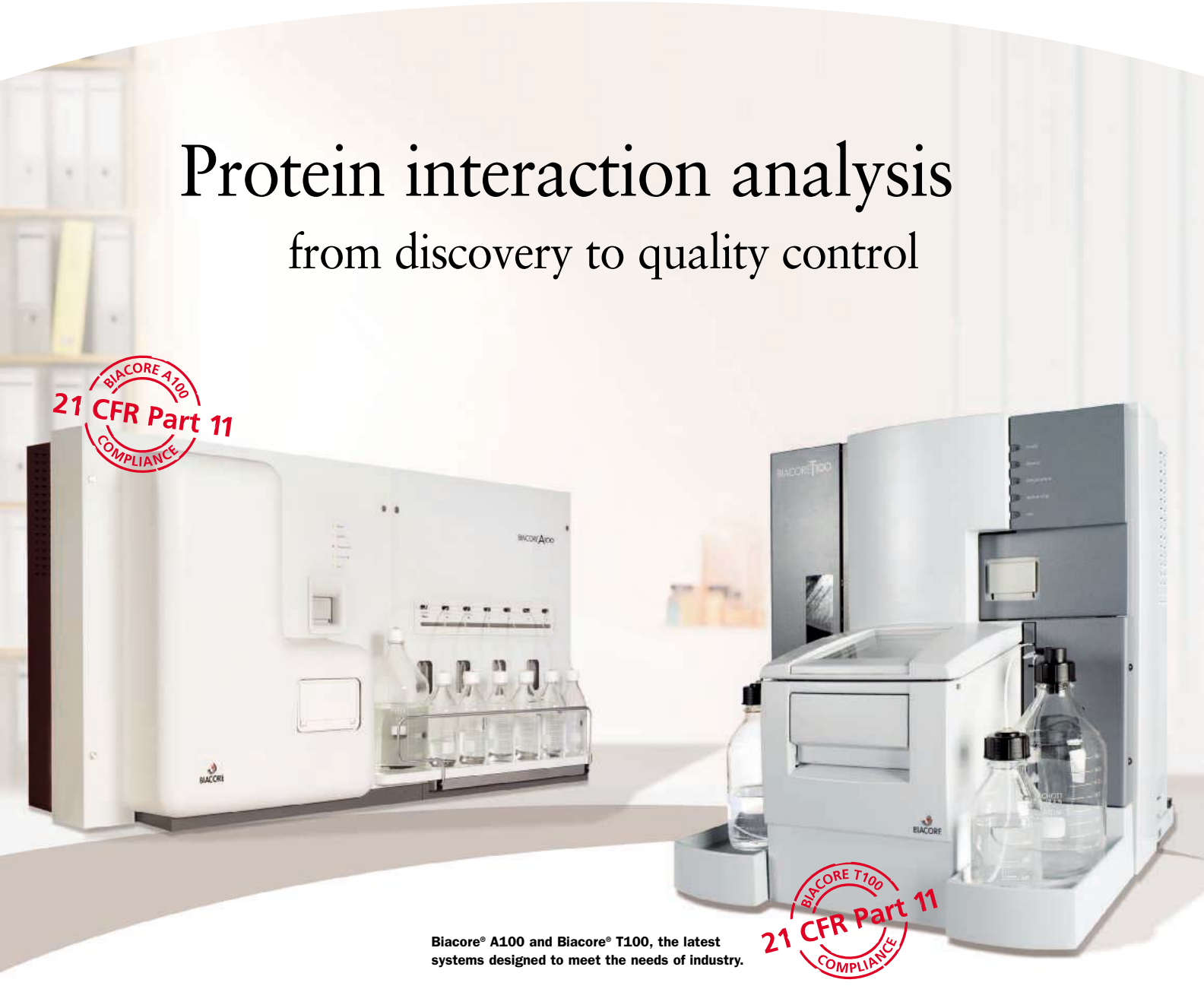

Biacore® A100 and Biacore® T100, the latest systems designed to meet the needs of industry.

The name Biacore is synonymous with the high quality, information-rich protein interaction analysis needed throughout drug discovery and development, biotherapeutic development, manufacturing and QC.

Biacore systems are used in the world's leading pharmaceutical and biotechnology companies.

Unique insights into protein interactions ensure confident decision-making at every stage, resulting in greater productivity, reduced development costs, improved safety and efficacy, as well as shortened timelines.

For screening, selection, characterization and quality control in:

- **Development of biotherapeutics**
- **LMW drug discovery and development**
- **Preclinical and clinical immunogenicity studies**
- **In-process control and release testing**

Define · Decide

BIACORE

www.biacore.com

Life Science Technologies: BIOCHIPS AND LAB-ON-A-CHIP DEVICES

Another Miniaturized Methodology

In recent years several companies have developed microfluidic devices for preparing samples and conducting massively parallel chemical reactions. These devices range from chip-like systems to cartridges to compact discs (CDs).

Companies such as Applied Biosystems, Caliper Life Sciences, and **Cepheid** have developed microfluidic devices for genomics research. Applied Biosystems offers the TaqMan Low Density Array, a microfluidic card that can perform up to 384 different real-time PCR assays simultaneously. The array streamlines the reaction set-up process by eliminating the need for liquid-handling robotics, minimizing pipetting steps, and is supplied preloaded with TaqMan Gene Expression Assays. "It's a very robust product line that runs on a real-time PCR system," Walworth says. "People are thinking about using it for tasks previously done only on a microarray platform. You get better data in terms of higher sensitivity, higher specificity, and a wider dynamic range. You can also do very large numbers of samples without the need for robotics."

Flexibility also gives this technology particular appeal to researchers. "The TaqMan Array runs on the 7900HT system, a platform that can also run standard 384- and 96-well microplates," says Chris Grimley, the company's product director for real-time PCR and microarray systems. "Researchers can have a single platform that can accommodate multiple assay formats and multiple applications, including gene expression and genotyping."

Until recently, studies of proteins' structures have remained the province of expert crystallographers, and hence too esoteric and expensive for routine use in drug discovery and development. But **Fluidigm** has developed a microfluidic cartridge that scientists can use to crystallize proteins. Another approach to microfluidic technology, **Gyros**'s lab-on-a-compact disc, also permits researchers to carry out protein characterization and drug discovery. The Gyrolab Bioaffy CD microlaboratory enables protein quantification at the nanoliter scale.

Electrophoretic Separation

Microfluidic devices can simplify the electrophoretic separation of tiny amounts of protein, DNA, or RNA. Caliper uses microfluidic technology in its LabChip 90 Electrophoresis System for automated analysis of proteins and nucleic acid fragments. This system uses the company's proprietary sipper process to move samples into the chamber for processing.

Probably the best-known microfluidic device for life science research is the 2100 Bioanalyzer that **Agilent** has developed for DNA and RNA analysis, protein analysis, and even flow cytometric analysis of cells. A prominent example of collaboration among vendors, the bioanalyzer uses Caliper's LabChip devices. "Agilent has placed about 4,000 instruments with our chips. It's a nice commercial engine for our technologies that started in 2000," Caliper's Hrusovsky says. Agilent isn't Caliper's only partner. "Bio-Rad now offers an electrophoresis system as well, and is investigating a new microfluidics-based platform that we believe will be different from anything currently out there," Hrusovsky continues. "In addition, Affymetrix has the idea of using our chip to feed their chip and has licensed our microfluidics technology for future product development."

Caliper has also begun to shift microfluidics into another field. "We've just entered an agreement to acquire Xenogen, whose technology uses luciferase to light up the inside of mice," Hrusovsky reports. "We believe that by linking our innovative in vitro technologies like microfluidics to in vivo technologies, we can cross the in vitro–in vivo bridge and provide much needed platforms for drug discovery research. Ultimately we plan to go into models for human prediction."

Detection and Analysis

No microarray or microfluidic experiment is complete until the signals that the technology creates have been detected and analyzed. The detection method used with DNA chips depends on the type of label – fluorescent, radioactive, or enzymatic – used in an experiment. Most researchers opt for fluorescent labels from companies such as **GE Healthcare**, **Invitrogen**'s Molecular Probes division, and **Sigma-Aldrich**, which are detected with laser scanners specifically designed for use with DNA microarrays. The scanners often include software for analyzing and interpreting the data. Affymetrix, **Hitachi Genetic Systems**, **PerkinElmer**, and other companies offer detectors of that type.

Tecan has developed what it calls a highly flexible scanning technology. It allows researchers to scan multiple samples on different substrates, from glass slides to microtiter plates, without having to switch scanners or make extensive adjustments each time the format type or size changes. The LS Series of laser scanners can operate up to four excitation lasers and 28 emission filters. "It operates on customized chips and formats, especially microplates for arrays, minigels, and microfluidic chips that use fluorescence, in addition to standard and special coated slides," says Ralph Beneke, microarray product manager at Tecan Austria. "It has high reproducibility and walkaway time for customers. And it contains LaserCheck, a unique tool that permits the user to run quality control of the complete scanning system, including its electronics, optics, and mechanical parts."

Look for these upcoming Life Science Technology articles

Pharmacogenomics	28 July
Mass Spectrometry	1 September
Functional Genomics	29 September
Aging and Neuroscience	6 October
Nanobiotechnology	3 November

Or, access past articles at http://www.sciencemag.org/products/articles.dtl

Laboratory Automation	13 January
Combinatorial and Computational Chemistry	17 March
Cell Signaling in Cancer Research	24 March
Proteomics	14 April

Molecular Devices has its own technological wrinkle, in the form of the nonconfocal scanning technology that underlies its GenePix scanners for microarray analysis. "The idea was to give maximum usable focal depth to detection capabilities," Davé explains. "Another key strength is our ease of use. Not only is our GenePix 4000B the fastest two-laser scanner in the world, but our GenePix software controls both acquisition and analysis for fast and straightforward operation." Suitable for low- and high-density arrays, the GenePix scanners are compatible with all 25x75mm slide arrays, including those from Agilent, CombiMatrix, GE Healthcare, **Illumina**, and **Whatman**, as well as lab-printed slides.

A Matter of Interpretation

Because they often contain thousands of samples or spots, microarrays can produce huge volumes of data. Storing and analyzing the data can create a serious bottleneck in laboratory research. So companies such as **BioDiscovery**, **Gene Logic**, Invitrogen, and **Rosetta Biosoftware** offer software for microarray analysis.

Bio-Rad's VersArray analyzer 5.0 is a powerful software program that analyzes the images captured by any microarray scanner. "It is not a bioinformatics program; it's just an image analysis software," Wibbenmeyer explains. "What I really like about it is that it has a wizard. It walks you through all the steps, and the data output is there on a spreadsheet format. Our approach, especially with the introduction of the BioOdyssey Calligrapher miniarrayer, is to make microarrays a tool that can be easily used in every laboratory."

Affymetrix, meanwhile, uses collaborations to provide its customers with soup-to-nuts service, which includes data analysis as well as the original DNA microarrays. "The Affymetrix GeneChip-compatible Applications Program provides customers with a broad spectrum of software solutions for biomedical research and development seamlessly integrated with the GeneChip platform," Willis says. "Under this program, leading software developers collaborate with us to deliver software solutions that apply data on gene expression and genetic variations to translational medicine, discovery research, and systems biology."

DNA microarraying has proven its utility as a valuable experimental platform for research in several areas, including expression profiling, SNP analysis, and tumor subtyping. Researchers working with microfluidics continue to develop better methods of moving small volumes of samples through these miniaturized laboratories. As new methods emerge for both technologies, companies will move fast to collaborate with fellow vendors and with customers to adapt each new method into valuable applications for the laboratory and the clinic.

Peter Gwynne (pgwynne767@aol.com) is a freelance science writer based on Cape Cod, Massachusetts, U.S.A. Gary Heebner (gheebner@cell-associates.com) is a marketing consultant with Cell Associates in St. Louis, Missouri, U.S.A.

ScienceCareers.org

Classified Advertising

For full advertising details, go to **www.sciencecareers.org** and click on **For Advertisers,** or call one of our representatives.

United States & Canada

E-mail: advertise@sciencecareers.org
Fax: 202-289-6742

JILL DOWNING
(CT, DE, DC, FL, GA, MD, ME, MA, NH, NJ, NY, NC, PA, RI, SC, VT, VA)
Phone: 631-580-2445

KRISTINE VON ZEDLITZ
(AK, AZ, CA, CO, HI, ID, IA, KS, MT, NE, NV, NM, ND, OR, SD, TX, UT, WA, WY)
Phone: 415-956-2531

KATHLEEN CLARK
Employment: AR, IL, LA, MN, MO, OK, WI
Canada; Graduate Programs; Meetings & Announcements (U.S., Canada, Caribbean, Central and South America)
Phone: 510-271-8349

EMNET TESFAYE
(Display Ads: AL, IN, KY, MI, MS, OH, TN, WV; Line Ads)
Phone: 202-326-6740

GABRIELLE BOGUSLAWSKI
(U.S. Recruitment Advertising Sales Director)
Phone: 718-491-1607

Europe & International

E-mail: ads@science-int.co.uk
Fax: +44 (0) 1223-326-532

TRACY HOLMES
Phone: +44 (0) 1223-326-525

HELEN MORONEY
Phone: +44 (0) 1223-326-528

CHRISTINA HARRISON
Phone: +44 (0) 1223-326-510

SVITLANA BARNES
Phone: +44 (0) 1223-326-527

JASON HANNAFORD
Phone: +81 (0) 52-789-1860

To subscribe to *Science*:
In U.S./Canada call 202-326-6417 or 1-800-731-4939
In the rest of the world call +44 (0) 1223-326-515

Science makes every effort to screen its ads for offensive and/or discriminatory language in accordance with U.S. and non-U.S. law. Since we are an international journal, you may see ads from non-U.S. countries that request applications from specific demographic groups. Since U.S. law does not apply to other countries we try to accommodate recruiting practices of other countries. However, we encourage our readers to alert us to any ads that they feel are discriminatory or offensive.

ScienceCareers.org
We know science AAAS

Careers in Translational Medicine

Advertising Supplement

Be sure to read this special ad supplement devoted to translational medicine opportunities in the upcoming **26 May issue of *Science*.**

Find translational medicine jobs and other career resources online at **www.sciencecareers.org.**

For advertising information, contact:

U.S. Daryl Anderson, phone: 202-326-6543, e-mail: danderso@aaas.org

Europe and International, Tracy Holmes, phone: +44 (0) 1223 326 500, e-mail: ads@science-int.co.uk

Japan Jason Hannaford, phone: +81 (0) 52 789-1860, e-mail: jhannaford@sciencemag.jp

ScienceCareers.org
We know science AAAS

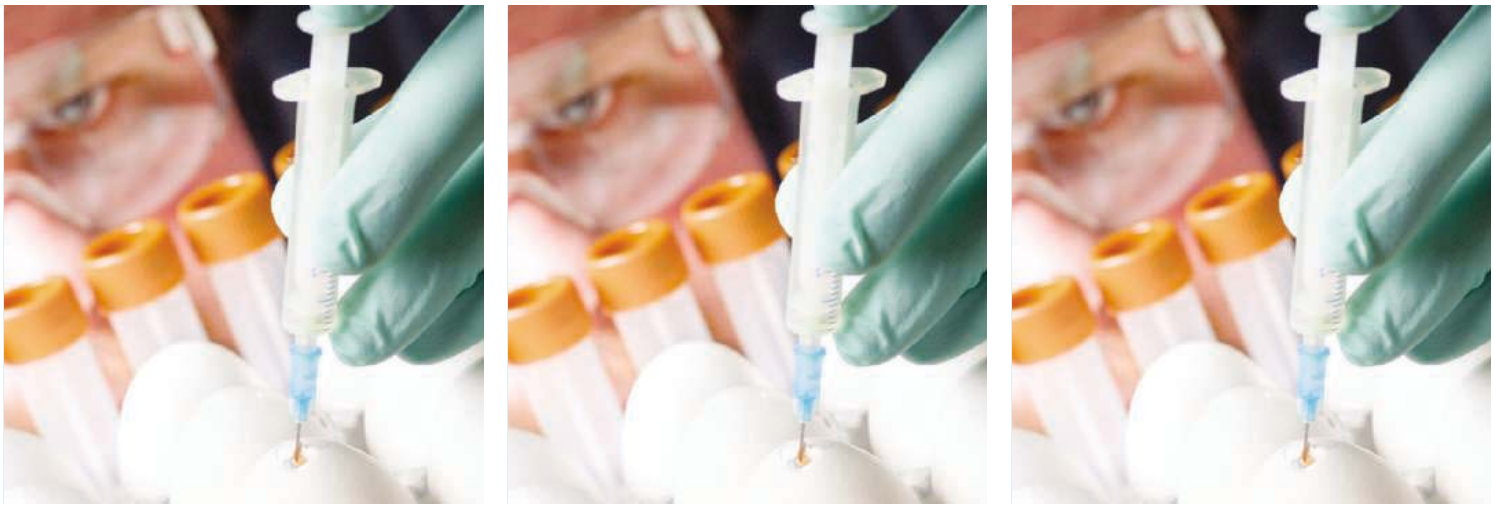

FOCUS ON CAREERS

Immunology & Infectious Disease

Healthy Careers

There is ongoing work in academics and industry on old infectious diseases—such as tuberculosis and malaria—and more recent ones—such as avian influenza and human immunodeficiency virus (HIV). In addition, immune mediated diseases cause problems throughout the developing and developed worlds. Consequently, the fields of immunology and infectious diseases generate many positions in the life science job market. BY MIKE MAY

Infectious and immune mediated diseases create problems around the world. In "Protecting the Nation's Health in an Era of Globalization: CDC's Global Infectious Disease Strategy," the authors write: "It is not possible to adequately protect the health of our nation without addressing infectious disease problems that occur elsewhere in the world." In addition, immune mediated diseases—such as allergies, asthma, and autoimmune disorders—impact many people. These international concerns create a world of opportunities in research on immunology and infectious diseases.

Daniel Rotrosen, director of the division of allergy, immunology, and transplantation at the U.S. National Institutes of Health's National Institute of Allergy and Infectious Diseases, says the infectious diseases that cause the most concern today include: emerging and reemerging infectious disease, such as avian influenza, SARS, HIV/AIDS, and West Nile virus; diseases that cripple the developing world, such as tuberculosis and malaria; multiple drug resistant pathogens; and bioterrorism agents such as anthrax. He adds that immune mediated diseases are important in many ways: the number of affected individuals, the chronicity of these diseases, the disabilities that they cause, and their costs to society. He says, "There are close to 100 autoimmune diseases affecting just about every organ system, and a large number of rare, but interesting primary immunodeficiencies."

In addition, scientists at GlaxoSmithKline point out drug resistant bacteria. David Pompliano, vice president, biology, at GlaxoSmithKline's Microbial, Musculoskeletal, and Proliferative Diseases Center of Excellence for Drug Discovery, says, "Infectious diseases from resistant bacteria top the Pharmaceutical Gaps list compiled by the World Health Organization. Examples include methicillin-resistant *Staphylococcus aureus*, penicillin-resistant *Streptococcus pneumoniae*, vancomycin-resistant enterococci, and fluoroquinolone-resistant *Pseudomonas aeruginosa*." So Pompliano points out the pressing need for new antibiotics.

The fields of immunology and infectious diseases will also face surprises on a regular basis. "HIV came out of nowhere in the early 1980s and appears to be here to stay," says Eric von Hofe, president of Antigen Express. "Other infectious diseases can and will appear just as unexpectedly." Such surprises fuel a high demand for scientists with skills related to fighting disease.

Antigen Express
http://www.antigenexpress.com

GlaxoSmithKline
http://www.gsk.com

National Institute of Allergy and Infectious Diseases
http://www3.niaid.nih.gov

University of California, Irvine
http://www.uci.edu

Advancing Integration

Rotrosen says that the growing understanding of how the immune system responds to infection or autoantigens as well as how it is regulated provides the basis for some of the most interesting recent discoveries. One important example is the evolving interface between innate and adaptive immunity and its application to infectious diseases and vaccine development. Another area of interest builds on the success of novel approaches to achieve relatively durable, antigen specific immune tolerance in rodents—and increasingly in large animal models—and the long-term potential of such approaches to prevent, arrest, or reverse the immune mediated diseases.

Overall, von Hofe thinks that understanding the entire immune system and its interrelationships is vitalizing the CONTINUED »

FOCUS ON CAREERS

Immunology and Infectious Disease


ALAN BARBOUR

development of a wide range of treatment options. "We are discovering how the various components of the immune system fit together and work," he says. "This knowledge is now at a level where it can be exploited for both novel vaccine development and immunotherapy strategies."

Equally interesting work pushes ahead the understanding of infectious diseases. According to Alan Barbour, professor of microbiology and molecular genetics and medicine in the School of Medicine at the University of California, Irvine, the evolutionary biology of microbes and mathematical modeling of infections and epidemics make up the most exciting recent advances in infectious disease research.

Pompliano also sees great value in research on new antibiotics. "Not every large pharmaceutical company is sticking with antibiotics research, but GlaxoSmithKline has decided to sustain its commitment," Pompliano says. "Some of the antibiotics of the future may bring only modest financial returns, but we believe we have a responsibility to our patients to create novel antibiotics in time to protect future generations. We are beginning to see the results of our commitment." In February, for example, GlaxoSmithKline filed with the U.S. Food and Drug Administration for Altabax, a topical formulation of a new class of antibiotics called pleuromutilins.


ERIC VON HOFE

Targeting the Market

Translational or applied research will capture increasing funds in the near future, according to Barbour. For example, he says, "Government agencies and nonprofit foundations, like the Bill & Melinda Gates Foundation, will remain the foremost funders of research on infectious disease, but research will tend to be more targeted." He adds, "The government will also be one of the major consumers of infectious disease products, such as vaccines and new antivirals."

Barbour adds, "There is an increased need for microbiologists in public health—environmental, clinical, veterinary. Few people are being trained for this career." He also expects an increased need for microbiologists with backgrounds in bacterial physiology for industrial microbiology and environmental remediation.

In addition, Rotrosen says, "There are many career opportunities related to immune mediated diseases and for those interested in making transplantation a safer and more widely applied therapy for end stage organ disease." Rotrosen also sees opportunities for "physicians with a strong grasp of basic and translational immunology and the ability to integrate clinical expertise across traditional medical disciplines, such as rheumatology, neurology, gastroenterology, endocrinology, transplantation, allergy, and infectious disease." He also mentions positions outside the laboratory in a variety of fields: research program directors or regulatory positions in federal agencies, industry, or private research foundations; forensics; patent law; science education and writing; and science policy analysis.


DAVID POMPLIANO

Focused Attention

To work in this field, a scientist needs a basic set of skills, such as a knowledge of biochemistry and cellular and molecular biology. "There will also be a greater need for experience or training in statistics and bioinformatics," says Barbour. "There will be a need as well for better backgrounds in mathematics and advanced methods for data analysis. Some understanding of computer programming will also be desirable."

When evaluating potential new hires for antibiotics research, Pompliano says, GlaxoSmithKline must account for the fact that "microbiology is not as popular a major as it used to be." Therefore, he says, "We look for accomplishment in related areas of biology, such as molecular biology, for our more junior positions. For senior positions, experience in this therapeutic area is a must. We look for demonstrated accomplishment—for example, publications or previous, significant roles in investigational new drug filings with regulatory agencies."

The variety of ongoing work in immunology and infectious diseases, however, also demands another skill—focus. "It is very exciting as to see the advances made in understanding how different components of the immune system work in complement with each other," says von Hofe, "but trying to apply these advances can lead to surprises and draw people into multiple areas, all requiring significant effort to sort out. At the end of the day, you've spent too little time in any one area to really accomplish something." Instead, von Hofe says, "Pick an area and stay focused on it."


DANIEL ROTROSEN

A Busy Future

With surprises such as SARS and avian influenza in recent years, scientists expect the need for extensive research in the near future. Barbour thinks that the "application of molecular and biochemical approaches to infectious disease diagnosis and clinical microbiology" will stimulate significant research ahead. He also points out that research will arise from the "effects of climate and landscape change on infectious diseases."

In many ways, the future of immunology and infectious diseases revolves around surprising proximity. "People in the world are closer together than they realize," says von Hofe. "SARS showed how infectious agents come out of nowhere and provide a wakeup call." More than 6 million children suffering from asthma in the U.S. also shows the need to fight immune mediated diseases. "This is an exciting time to go into immunology," says von Hofe. "There will be lots to do."

Mike May (mikemay@mindspring.com) is a publishing consultant for science and technology based in the state of Minnesota, U.S.A.

Gilead Sciences is a biopharmaceutical company that discovers, develops and commercializes innovative therapeutics in areas of unmet medical need. Our mission is to advance the care of patients suffering from life-threatening diseases worldwide. Headquartered in Foster City, CA, Gilead has operations in the United States, Europe and Australia. We're looking for experienced professionals to join our multi-disciplinary R&D teams.

Director/Senior Director, Biology (Biophysics/Enzymology)

Reporting to the VP - Biology, the successful candidate will direct biophysics and enzymology research at Gilead. He/she will be a key member of the Biology department and will be responsible for the development and implementation of methods to characterize the interaction of small molecule ligands with protein targets. He/she will manage a group of both Ph.D. and non-Ph.D. level scientists. He/she will participate in, or lead, interdisciplinary drug discovery teams and manage external academic and industrial collaborations as required. Publication and presentation of company research is expected. The candidate will likely be a recognized leader in biophysics, biochemistry, and/or enzymology. The position typically requires a Ph.D. with a minimum of 10 years of relevant experience. Experience in using biophysical instrumentation to study the interaction of organic ligands with protein targets and working knowledge of mass spectrometry, circular dichroism, analytical centrifugation, calorimetry and/or binding kinetics highly preferred. A strong performance focus and commitment to integrity are expected, as are problem-solving, communication and team-building skills. Industrial experience and demonstrated success in drug discovery are preferred. **(Req# BF 6-709)**

Research Scientist, Protein Chemistry

The candidate will construct, express, isolate, and characterize recombinant proteins used as target proteins in drug screening assays and crystallography. Requires a Ph.D. in Protein Chemistry, Molecular Biology, Biophysics, or related discipline; 2+ years of postdoctoral experience in academia/industry, preferably with a research focus on protein chemistry/biophysics; a proven publication record of scientific achievements; and proficiency with data analysis, molecular biology, word processing, and graphic software applications. **(Req# BF 6-591)**

Research Scientist, HIV Biology

The successful candidate will become a member of a multidisciplinary drug discovery team focused on the identification of novel antiviral drugs targeting HIV. Requires a Ph.D. in a Life Sciences discipline (Molecular Biology, Cell Biology, Microbiology, Immunology); 2+ years of postdoctoral experience in academia/industry, preferably with a research focus on virology; broad knowledge of molecular & cell biology, virology and biochemistry techniques, including assay development; a proven publication record of scientific achievements; and proficiency with data analysis, molecular biology, word processing, and graphic software applications. **(Req# BF 6-547 & BF 6-679)**

GILEAD

We're an equal opportunity employer. View complete job descriptions, reference the corresponding Req#, and apply online at

http://www.gilead.com/wt/sec/careers

The Chemistry is right.

Anadys Pharmaceuticals (NASDAQ: ANDS) is a rapidly growing biopharmaceutical company committed to advancing patient care by discovering, developing and commercializing novel small molecule medicines for the treatment of hepatitis, other serious infections, and cancer. The Company has core expertise in Toll-Like Receptor-based small molecule therapeutics and structure-based drug design coupled with medicinal chemistry. Anadys' clinical development programs include ANA975 for the treatment of HCV and HBV, and ANA380 for the treatment of HBV. Backed by strong core values and an ongoing commitment to human health, our goal is to improve the quality of life worldwide. If you share our values and our goal, consider these opportunities:

- **Head of Document & Information Management**
- **Head of Pharmaceutical Research & Development**
- **Associate Director, Analytical Chemistry**

Anadys offers excellent salaries, stock options, advancement opportunities, ongoing training, 401(k), generous vacation, and a choice of PPO or HMO options with most employee health benefits provided at no cost. For more information about the above positions or to see additional opportunities, visit: **www.anadyspharma.com**

ANADYS
PHARMACEUTICALS, INC.

We are proud to be an equal opportunity employer.

POSTDOCTORAL AND STAFF SCIENTIST POSITIONS

The Division of Viral Pathogenesis at Beth Israel Deaconess Medical Center and Harvard Medical School has postdoctoral and staff scientist positions available in the laboratory of **Dr. Dan Barouch** to study HIV/AIDS immunology and vaccine development. The successful applicant will join an outstanding team focused on AIDS virus pathogenesis and vaccine development involving both preclinical and clinical studies. The applicant should have a Ph.D. and/or an M.D. and be motivated, organized, and able to work both independently and as part of a team. At least two years experience with molecular biology, molecular virology, and/or cellular immunology is required.

Please send a letter of application and current curriculum vitae to:

Amanda P. Kelcz
Administrative Coordinator
Beth Israel Deaconess Medical Center
Division of Viral Pathogenesis
330 Brookline Avenue, E/RE-213G
Boston, MA 02215

Or via email:
akelcz@bidmc.harvard.edu

Beth Israel Deaconess Medical Center is an Equal Opportunity Employer.

IDEXX LABORATORIES

IDEXX Laboratories is a worldwide leader in the development and commercialization of innovative, technology-based products and services for veterinary, food and water applications. IDEXX employs more than 3000 employees in 45 locations worldwide and is headquartered in beautiful southern Maine, between the mountains and the ocean.

We are currently seeking PhD scientists with 3+ years industry experience for the following positions:

MATERIALS SCIENTIST: Must be skilled in organic or surface chemistry; protein conjugation and immobilization; characterizing proteins and assaying biological activities.

RESEARCH SCIENTIST, IMMUNODIAGNOSTIC PRODUCT DEVELOPMENT: Candidates with protein and antibody expertise preferred.

RESEARCH SCIENTIST, R&D TECHNICAL SUPPORT: Requires expertise in protein chemistry and biochemistry plus excellent communication skills.

APPLY ONLINE AT
WWW.IDEXX.COM

POSTDOCTORAL FELLOWSHIP
Department *of* Immunology

BCM Baylor College of Medicine

Applications are now being accepted from recent graduates for postdoctoral fellowship positions in the Department of Immunology at Baylor College of Medicine, through the NIH Training Grant, "Molecular and Cellular Mechanisms of Host Defense." Located in Houston TX, Baylor College of Medicine is a leader in biomedical research. More than eighteen distinguished mentors are available. The program provides mentorship in individual career development, curriculum in grant writing and presentation skills, as well as research opportunities in critical areas of immunology:

Lymphocyte signaling	Apoptosis
Lymphocyte development	Stem cells
Autoimmunity	Inflammation
Cytokines	HIV pathogenesis
Adhesion molecules	Dendritic and Treg cells
Gene therapy	Cancer research

Applicants must be recent graduates, as well as United States citizens or permanent residents. To apply, send a statement of research interest, C.V., and the names and email addresses of three references to:

Tse-Hua Tan, Ph.D., Program Director
Baylor College of Medicine
c/o Ms. Robin Cuthbert, at rmcuthbe@bcm.edu

www.bcm.edu/immuno
BCM is an equal EEOC/AA/EA employer

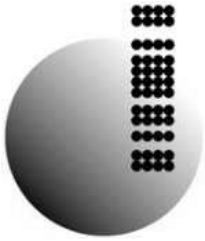

Research & Leadership Positions

Center for Genomics and Bioinformatics

Indiana University, Bloomington

The **CGB** (http://cgb.indiana.edu), a campus-wide research center, carries out research in all aspects of genomics and bioinformatics. Center scientists work both independently and in collaboration with faculty in the College of Arts and Sciences and the Schools of Medicine and Informatics. The CGB is home to the *Drosophila Genomics Resource Center* and is a leading participant in the *Daphnia Genomics Consortium*, the *Indiana Center for Insect Genomics*, and the *Indiana METACYT Initiative*. Both Indiana University (http://www.research.indiana.edu) and the State of Indiana (http://www.biocrossroads.com) have made the life sciences a priority, and the CGB is an active participant in this effort. Bloomington is routinely rated an exceptionally desirable place to live.

Expanding CGB activities have created the open leadership positions described below. These positions offer the opportunity to work in a fast-moving collegial environment and to collaborate with geneticists, molecular biologists, developmental biologists, evolutionary biologists, bioinformaticists, and mathematicians. Appointments – with competitive salary and benefits – will be at the rank of Research Associate or Assistant Scientist (a research faculty rank) based on a candidate's preparation and prior experience. In addition, there are frequent openings for post-doctoral researchers and technical staff. Inquiries about all openings should be directed to jobs@cgb.indiana.edu.

Genomics Scientists

We seek three Ph.D. level scientists to participate and/or lead aspects of the genomics laboratory's work:

The *Microarray Production Unit Leader* will manage all aspects of microarray development, fabrication, quality control, and distribution of high quality reagents for genomic research. The Unit Leader will supervise current technical staff and direct further hiring efforts as needed. The successful candidate will have prior experience in the use of microarrays and robotics.

The *Functional Genomics Unit Leader* will help guide research projects that use large-scale cDNA libraries and microarrays to characterize genomes, supervise current technical staff and also direct further hiring efforts as needed. The successful candidate will have considerable experience in the use of cDNA libraries and in molecular biology techniques.

The *Emerging Genomic Technologies Scientist* will lead efforts to devise, adopt, and/or test new technologies, e.g. on-slide oligonucleotide synthesis and novel imaging techniques. The successful candidate will have a strong background in biochemistry and/or chemistry with some experience in phosphoramidite synthesis.

The division of responsibilities among these positions may be adjusted to match the skills and preferences of applicants.

Bioinformatics Director

We seek a full-time *Bioinformatics Director*. This is a non-tenure track position involving both research and administration.

The Bioinformatics Director pursues his/her own research interests and is encouraged to develop significant extramurally funded research projects. In addition, s/he directs the efforts of core CGB biocomputing and bioinformatics staff, consults and collaborates with CGB scientists and with life sciences faculty across the campus, and plans training workshops.

The position is ideal for an experienced post-doctoral scientist who excels at devising and organizing collaborations amongst biologists, computer scientists, bioinformaticists, and statisticians.

The Bioinformatics Director will be appointed to the research faculty of the University with rank and remuneration depending upon experience. The ideal candidate will have a Ph.D. and several years of appropriate post-doctoral experience, or an equivalent combination of education and industry experience, and will be able to join us at an early date.

Positions are available immediately; applications will be accepted until positions are filled. Those received by 6/01/06 will be assured full consideration. To apply, please submit a CV and a description of your background and interests, and arrange that 3 letters of recommendation be sent directly to:

Search: *Position Name*
Center for Genomics and Bioinformatics
Indiana University
1001 E. 3rd St.
Bloomington IN 47405-3700

Indiana University is an affirmative action equal opportunity employer

Positions @ NIH

The National Institutes of Health

Scientific and Clinical Director

The National Center for Complementary and Alternative Medicine (NCCAM) seeks an accomplished, innovative neuroscientist and clinician to fill three pivotal roles: as Scientific Director and Clinical Director of its Intramural Research Program (IRP) and as Senior Investigator responsible for developing a new research program in mind-body medicine. This individual will report to the NCCAM Director and will be a member of the NCCAM leadership.

As Scientific Director, you will articulate and implement a vision and oversee research infrastructure for highly unified and mutually supportive laboratory and clinical programs in the conduct of bench-to-bedside and bedside-to-bench research related to CAM therapies.

As Clinical Director, you will chart a course and allocate resources for clinical research; recruit and oversee the activities of clinical staff and fellows; ensure appropriate design and conduct of clinical research protocols; and facilitate the integration of CAM practices into the training programs and delivery of care throughout the NIH Clinical Center.

As Senior Investigator, you will have substantial committed resources to create a cutting-edge program of clinically oriented laboratory research and clinical studies that exploit neuroscience disciplines to define the nature, mechanisms of action, safety, and efficacy of diverse CAM modalities that affect actions and interactions linking mind, body, and behavior.

This exceptional opportunity is available to a U.S. citizen, resident alien, or nonresident alien with valid employment authorization who is an accomplished neuroscientist with a U.S. medical license; a demonstrated record of senior-level management of a large, nationally recognized research program; a commitment to both basic and clinical research; and leadership skills that equip him/her to forge team efforts with colleagues within intramural programs across NIH.

Salary and benefits are commensurate with experience. Qualified individuals are encouraged to email their CV, bibliography, list of three references, and cover letter outlining their relevant experience and vision for leading the NCCAM IRP to:

nccamdirector-r@mail.nih.gov
Subject Line: Scientific and Clinical Director Search
Application Deadline: July 14, 2006

Email receipt of applications and inquiries is preferred; however, candidates needing reasonable accommodation may fax application materials to 301-402-4741.

NIH and DHHS are Equal Opportunity Employers

NCCAM
NATIONAL CENTER FOR COMPLEMENTARY AND ALTERNATIVE MEDICINE

Postdoctoral, Research and Clinical Fellowships at the National Institutes of Health

www.training.nih.gov/pdopenings

www.training.nih.gov/clinopenings

Train at the bench, the bedside, or both

Office of Intramural Training and Education
Bethesda, Maryland 20892-0240
800.445.8283

Scientific Review Administrator
National Heart, Lung and Blood Institute

The National Heart, Lung, and Blood Institute (NHLBI), a major research component of the National Institutes of Health (NIH), Department of Health and Human Services (DHHS), is seeking two Scientific Review Administrators for the Review Branch, Division of Extramural Affairs. Scientific Review Administrators organize and manage the comprehensive scientific and technical merit review of grant applications and contract proposals through interaction with established scientists in a variety of fields. Scientific Review Administrators are responsible for assuring the fairness and consistency of the review process, and for providing technical guidance to applicants, reviewers, and Institute staff.

Qualifications: Individuals with a Ph.D. or doctoral degree equivalent, and a scientific background in disciplines relevant to heart, lung, blood, or sleep disease research, are encouraged to apply. Experience in grant preparation and in the peer review process is desirable. For the basic qualification requirements, please refer to the NIH guidance for Health Scientist Administrators at http://www.nhlbi.nih.gov/about/jobs/hsaguide.htm. U.S. citizenship is required.

Salary: The current salary range is $ 65,048 to $118,828. In addition, a recruitment bonus may also be considered. Position requirements and detailed application procedures are provided on vacancy announcement **NHLBI-06-123471**, which can be obtained by accessing **http://WWW.USAJOBS.GOV**.

How to Apply: Please view the above USAJobs website for full vacancy announcement. This vacancy requires the submission of narrative Knowledge, Skills and Abilities (KSAs) as part of the application process. You may apply online at the above website or submit a Standard Form 171, Application for Federal Employment; OF-612, Optional Application for Federal Employment; current curriculum vitae/bibliography or other format to: **National Heart, Lung, and Blood Institute, Human Resources Branch G, 2115 E. Jefferson Street, Room 1-M100, Bethesda, Maryland 20892; Attn: Leanna Lomax**. All applications must be postmarked by **06/20/2006**. For additional information contact **Leanna Lomax at (301) 402-8032**.

WWW.NIH.GOV

Pre-Clinical Trials – Immunotherapy
Dr. Thomas Waldmann, M.D.

With nation-wide responsibility for improving the health and well-being of all Americans, the Department of Health and Human Services (NIH) oversees the biomedical research programs of the National Institutes of health (NIH) and those of NIH's research Institutes.

The Metabolism Branch (MB), Center for Cancer Research (CCR), National Cancer Institute (NCI), National Institutes of Health (NIH), Department of Health and Human Services (DHHS), is offering a post-doctoral research training fellowship position in the laboratory of Dr. Thomas Waldmann for an individual to investigate new therapeutic approaches directed toward receptors expressed on leukemic T-cells. There is a special emphasis on the IL-2/IL-15 receptor system and its signaling pathways. This approach exploits the observation that the high affinity IL-2R is not expressed by normal cells, but is expressed by select leukemic cells, as well as T-cells involved in allograft rejection and autoimmunity. A murine model of IL-2R expressing human Adult-T-Cell leukemia (ATL) was established by introducing cells from an ATL patient into SCID-NOD mice. Agents showing promise in this murine model may move forward into clinical trials. Humanized anti-receptor antibodies, such antibodies armed with alpha and beta emitting radionuclides, and small molecule inhibitors, are some of the agents under investigation. Another special focus of the laboratory is on IL-15, a cytokine co-discovered in the lab. IL-15 receptors are being studied in murine models of autoimmune disease. Applicants should have completed an M.D., D.V.M., or Ph.D. within the last five years, and be highly motivated individuals interested in joining a progressive Clinical Research Program at the NCI.

The salary range will be commensurate with prior training and experience. Additionally, candidates should be willing to cooperate and interact with a team approach to this project, as well as possess good interpersonal skills and a strong work ethic. To apply, interested candidates should submit a statement of research interest, curriculum vitae, bibliography, and a list of three references to: **Mrs. Jean Decker, e-mail: jrmdeck@helix.nih.gov, National Cancer Institute, 10 Center Drive, MSC 1374, Building 10, Room 3B38, Bethesda, MD 20892-1374.**

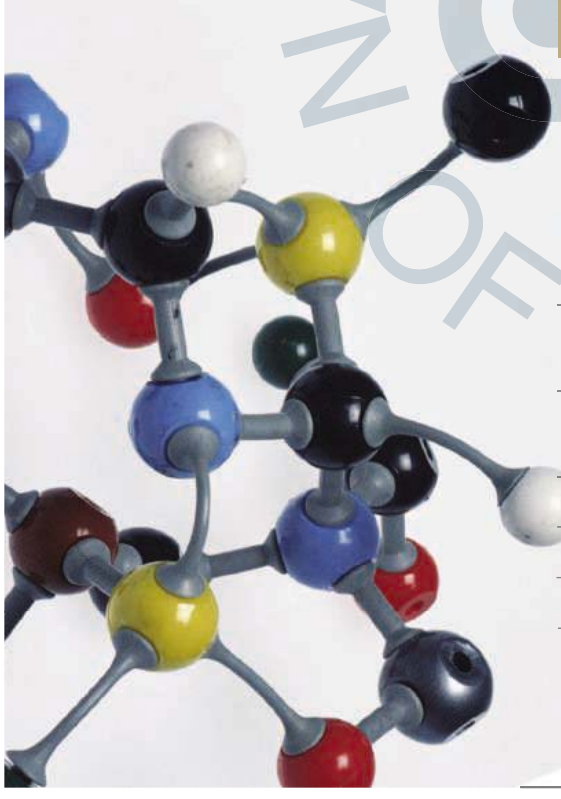

Postdoctoral Research Training at NIH

- Launch a career to improve human health
- Work in one of 1250 of the most innovative and well-equipped biomedical research laboratories in the world
- Explore new options in interdisciplinary and bench-to-bedside research
- Develop the professional skills essential for success
- Earn an excellent stipend and benefits
- Click on www.training.nih.gov

Office of Intramural Training and Education

University of Heidelberg

The **Zentrum für Molekulare Biologie** (ZMBH) at the University of Heidelberg (Germany) invites applications from scientists for two

Junior Group Leader Positions in Molecular Mechanisms of Ageing

The successful candidates will establish independent research groups. It is expected that his/her research program will contribute to the further development of research in the molecular mechanisms of ageing in the Heidelberg / Mannheim area. Funding for the group will be available for the first five years from a grant of the "Zukunftsoffensive des Landes Baden-Württemberg" / Ministerium für Wissenschaft, Forschung und Kunst. After a successful evaluation a three-year extension is possible.

The holder of the position is expected to participate in the department's teaching program.

The ZMBH presently houses 15 independent research groups and offers excellent central facilities, which include protein analysis, high performance microscopy, animal facilities, biocomputing, and centralized administrative services.

Research and teaching programs are summarized at the ZMBH's website (http://www.zmbh.uni-heidelberg.de).

The University of Heidelberg has a policy of raising the proportion of women in academic positions and therefore specifically invites the application of women scholars with the necessary qualifications.

Under German law disabled applicants with full qualifications are to be preferred.

Further details may be obtained from Prof. Dr. Bernd Bukau, telephone +49-6221-546850, telefax: +49-6221-545507.

Applications should be sent to the **Director of the ZMBH, Im Neuenheimer Feld 282, D-69120 Heidelberg, Germany** (e-mail: director@zmbh.uni-heidelberg.de) within four weeks after the publication of this advertisement.

www.cam.ac.uk/jobs/

Post-doctoral Fellowship Opportunity

Functional analyses of novel genes in diabetes and autoimmune disease

A unique and exciting research opportunity has arisen in the Juvenile Diabetes Research Foundation/Wellcome Trust Diabetes and Inflammation Laboratory (JDRF/WT DIL; http://www-gene.cimr.cam.ac.uk/todd/) for a post-doctoral research assistant owing to the recent and very rapid progress in discovering genes with polymorphisms that determine susceptibility to type 1 diabetes, one of the most common chronic diseases of children.

We are keen to identify a researcher who wants to make a difference, and can apply a range of skills in gene expression and function at the molecule, cell and whole organism level, across disciplines.

You will need a first class publication record from your PhD such that you would be highly competitive for a personal fellowship.

The position would be available in John Todd's laboratory, in collaboration with Linda Wicker and David Clayton, with world-class facilities and interactions in the Cambridge Institute for Medical Research (http://www.cimr.cam.ac.uk/), and the University, for functional analyses, including allele-specific gene expression, multicolour flow cytometry and access to blood donors and patients. Our specific aim is to correlate disease-associated genotype with phenotype in order to investigate the pathways that determine development of type 1 diabetes and other autoimmune diseases.

Persons interested in applying for a post-doctoral fellowship are encouraged to contact John Todd e-mail: john.todd@cimr.cam.ac.uk

Closing date: 30 June 2006.

UNIVERSITY OF CAMBRIDGE

The University offers a range of benefits including attractive pension schemes, professional development, family friendly policies, health and welfare provision, and staff discounts. The University is committed to equality of opportunity.

SCOTT & WHITE

College of Medicine
The Texas A&M University System Health Science Center

Pediatric Hematology-Oncologist

The Section of Pediatric Hematology/Oncology at **Scott and White Clinic** and the **Texas A&M University System Health Science Center College of Medicine** (TAMUS HSC-COM) are seeking a clinician scientist with current research grants for a faculty position in a rapidly growing program. The candidate should be BE/BC in pediatric oncology and committed to an academic career. The successful candidates will join and enhance ongoing efforts in basic and translational research, with an institutional commitment to building a world-class experimental therapeutics program. An outstanding start-up package includes high quality laboratory space, excellent benefits and competitive salaries commensurate with academic qualifications. The position guarantees 75% protected time for research activities.

Scott & White Clinic is a 500+ physician directed multi-specialty group practice that is the leading provider of cancer care in Central Texas. Scott and White Clinic and the 486 bed tertiary Scott & White Memorial Hospital is the main clinical teaching facility for TAMUS HSC-COM. Outstanding clinical practice and laboratory facilities on campus that perform state of the art molecular and cellular biology research, flow cytometry, genomics and biostatistics are in place to support the research effort.

Please contact: **Don Wilson, M.D. Professor and Chairman, Department of Pediatrics, Scott & White, 2401 S. 31st, Temple, TX 76508. (800)725-3627 dwilson@swmail.sw.org Fax (254) 724-4974.**

For more information about Scott & White, please visit www.sw.org For Texas A&M www.tamhsc.edu. Scott & White is an equal opportunity employer.

DEPARTMENT OF THE NAVY
ONR
Science & Technology

DIRECTOR, AEROSPACE SCIENCE RESEARCH DIVISION

The Office of Naval Research (ONR) is seeking an outstanding individual to serve in this Civil Service position in the Senior Executive Service (SES) with salary range from $109,808 - $152,000 Per Annum. The incumbent of this position is responsible for managing and directing extensive activities in fostering, administering, and executing an integrated program of basic research, applied research and advanced technology development in the areas of air vehicles and propulsion, aerodynamics, aircraft structures, gas turbine engines, control systems and avionics, and ship or air-launched weapons including missile systems and propellants, guidance and control, targeting, warheads and directed energy weapons.

For information on qualifications and how to apply, see the Job Announcements at our website http://www.onr.navy.mil/hr. Applications must be submitted by the closing date noted in the job announcement. For additional information contact Jill Blackwell at blackwj@onr.navy.mil.

U.S. CITIZENSHIP REQUIRED • AN EQUAL OPPORTUNITY EMPLOYER

University of Missouri Health Care

Research Faculty Position

The University of Missouri School of Medicine Department of Surgery is seeking outstanding candidates for two research faculty positions. Rank and appointment status are contingent upon qualifications.

The candidate should have experience in a field of research in which surgeons interface. This includes, but is not limited to, cancer, heart disease, inflammation, wound healing, trauma, and vascular biology. Candidate must demonstrate evidence of current or future potential for federal funding, show interests in teaching medical students and surgical residents, and have the desire to interact with surgical researchers in developing a vigorous, extramurally funded research program.

Applicants should send curriculum vitae to: **Steve Eubanks, M.D., Chairman, Department of Surgery, University of Missouri-Columbia, Health Sciences Center, One Hospital Drive, Columbia, Missouri 65212.**

E-mail: grotewielln@health.missouri.edu

Equal Opportunity/ Affirmative Action/ ADA Employer

Visit the Department of Surgery's Web site at http://www.surgery.missouri.edu/. Go to "Practice Opportunities".

COLUMBIA UNIVERSITY

Departments of Psychiatry and Pharmacology

TENURE-TRACK FACULTY POSITIONS

The Columbia University Departments of Psychiatry and Pharmacology of the College of Physicians and Surgeons invite applications for two tenure-track positions at the ASSISTANT and ASSOCIATE PROFESSOR levels. The candidates will develop research programs taking basic molecular, cellular, and/or genetic experimental approaches to solving biological problems relevant to the pathophysiology and therapeutics of schizophrenia and drug abuse. The Departments participate in a number of training programs, which provide opportunities for graduate and postgraduate training and interactions with a large group of multidisciplinary neuroscientists. The successful candidates are expected to establish an extramurally funded research program and play an integral role in new program initiatives. The positions are competitive with regard to salary, start-up funds, and laboratory space. Applicants must have a Ph.D. and/or M.D. and at least four years of relevant postdoctoral research experience.

Please e-mail a curriculum vitae, a brief statement of current and future research interests, and contact information for three references to **Douglas Drake at dod2@columbia.edu.**

http://www.cumc.columbia.edu

Columbia University is an affirmative action/ equal opportunity employer.

U.S. Environmental Protection Agency
Office of Research and Development

HIGH-LEVEL CAREER OPPORTUNITIES IN MICROBIOLOGY

EPA's Office of Research and Development (ORD) is seeking internationally recognized scientists to fill two positions: one in the National Exposure Research Laboratory (NERL) **http://www.epa.gov/nerl/** and another in the National Center for Environmental Assessment (NCEA) **http://www.epa.gov/ncea/**. Both positions are located in Cincinnati, Ohio.

ORD plans to fill these positions using EPA's Title 42 Authority, which offers up to 5-year renewable term appointments at highly competitive, market-based salaries. The positions are part of a larger EPA effort to use state-of-the-science approaches and technologies in its mission of protecting human health and the environment. The ideal candidates will have a doctoral level degree in a pertinent science discipline and extensive specialized experience. For more information about the two organizations and their respective job announcements, please refer to their websites as listed above.

Positions and major duties include:

NERL-06-42-04 Research Microbiologist

- Establishing and conducting a research program to address critical needs related to the assessment of exposure to microbiological hazards in water. An area of particular relevance to NERL is the development of innovative approaches for reliable concentration, detection and characterization of pathogens of concern to EPA. Other areas of research could involve studies to support the assessment of pathogenicity and the development of quantitative models of microbial risk.

NCEA-06-42-05 Microbial Risk Assessor

- Developing and implementing ORD's research agenda for microbial risk assessment, particularly (1) characterizing environmental exposures of humans to pathogenic microorganisms, (2) characterizing infectivity, virulence, and transmissibility of environmental microbial agents, and (3) characterizing both individual and population susceptibility to diseases caused by environmental microorganisms.
- Overseeing the conduct of microbial risk assessments which are of significant strategic importance to EPA risk management and rule-making decisions.

Responsibilities for both positions include providing leadership of ORD's microbiology research program, serving as a senior spokesperson/representative, identifying collaborative opportunities with outside organizations, and playing a vital role in the leadership of a proposed virtual EPA Institute for Environmental Microbiology.

Salary and Benefits: Salary is up to $200,000 per annum, dependent upon qualifications, experience, and other factors. The selected applicant will be eligible for full benefits including health and life insurance, retirement, and vacation and sick leave.

How to Apply: Send the following information: (a) a vision statement (1-2 pages) including your research goals and how they relate to the duties of the position for which you are applying; (b) curriculum vitae; (c) the names of three references; (d) citizenship status; and (e) compensation requirements. **Candidates must reference the specific vacancy number(s) of the position(s) for which they are applying.**

Applications should be mailed to the attention of: **Ms. Dorothy Carr, U.S. EPA, MD-C639-02, RTP, NC 27711** or sent via email to **title42@epa.gov** by **May 31, 2006**. For additional information, **Ms. Carr** can also be reached at **(800) 433-9633**. Technical questions pertaining to vacancy **NERL-06-42-04** may be addressed to **Dr. Al Dufour** at **(513) 569-7330**. Technical questions regarding vacancy **NCEA-06-42-05** may be addressed to **Dr. Glenn Suter** at **(513) 569-7808**.

The U.S. EPA is an Equal Opportunity Employer.

The Africa Centre for Health and Population Studies is a joint initiative of the University of KwaZulu-Natal and the South African Medical Research Council, with support from the Wellcome Trust and other funders, to create a global centre of research excellence in a rural area. The Centre's mission is to conduct in partnership with the community, policy-relevant health and population research in an ethical manner and to enhance the capacity of the people of sub-Saharan Africa to conduct research.

AFRICA CENTRE FOR HEALTH AND POPULATION STUDIES

The Centre is located in the rural Umkhanyakude District of KwaZulu-Natal. It has Africa's most comprehensive Demographic Information System, which monitors longitudinal vital events in a population of 90,000 and provides a rich base for health and social science research. With the arrival of the new Director, opportunities for 5 new posts have become available.

Senior Statistician (Ref. AC06/2006)

The Africa Centre wishes to recruit a Senior Statistician whose main responsibilities would be to provide statistical support to all studies within the Africa Centre and in addition would be expected to develop his/her own research area, possibly in the area of statistical modelling and to apply for funding for such research.

This responsible position requires the following qualifications, skills and attributes: ● PhD Biostatistics or a related field ● Strong publications record ● 5 years' post-doctoral experience ● Knowledge of computer programmes R/Splus or Stata ● Managerial and supervisory skills ● Good interpersonal skills.

HIV/ARV Clinician (Ref. AC07/2006)

The Africa Centre wishes to recruit an HIV/ARV Clinician whose main responsibilities would be to be involved in a one-year feasibility study to evaluate the way in which HIV-infected people are monitored in terms of clinical or biological parameters, before and after the initiation of antiretroviral therapy. Based on the results, the Clinician would develop a protocol for a trial to which additional funding would have to be obtained.

This responsible position requires the following qualifications, skills and attributes: ● Medical degree with advanced clinical training in infectious disease or similar field ● Registration with the Health Professions Council of South Africa ● Strong publications record ● Experience in HIV clinical care and clinical research ● Experience in collaborating with local and national Health Service providers ● Managerial skills ● Ability to work in a multidisciplinary team ● Good interpersonal skills.

Senior Epidemiologist (Ref. AC08/2006)

The Africa Centre wishes to recruit a Senior Epidemiologist whose main responsibilities would be to provide research capacity to the investigation and analysis of the determinants of HIV and other infections in the study population and to build a strong research portfolio relevant to this rural population.

This responsible position requires the following qualifications, skills and attributes: ● PhD in Epidemiology or a closely related field ● 5 years' post-doctoral experience ● Good publication record ● Managerial skills ● Ability to work in a multidisciplinary team ● Knowledge of statistics package ie SPSS, Stata and R/Splus ● Medical qualification and registration with the Health Professions Council would be an advantage.

Senior Social Scientist (Ref. AC09/2006)

The Africa Centre wishes to recruit a Senior Social Scientist whose main responsibilities would be to develop an integrated social science research agenda to examine social and behavioural aspects of HIV. A key area would be to develop randomised control trials to assess the effectiveness of counselling approaches designed to increase the rate of HIV testing, disclosure and adherence to ARVs.

This responsible position requires the following qualifications, skills and attributes: ● PhD in Psychology, Sociology, Demography or a related field ● Strong record of publications ● 3 years' post-doctoral experience ● Extensive knowledge of the current issues in HIV prevention and treatment ● Knowledge of qualitative research methodology ● General computer knowledge and specialised knowledge of qualitative analysis software ● Managerial skills ● Ability to work in a multidisciplinary team ● Ability to use different types of data and analytical approaches to answer social and health-related questions.

Senior Virologist (Ref. AC10/2006)

The Africa Centre wishes to recruit a Senior Virologist whose main responsibilities would be to lead a diagnostic laboratory and develop a research agenda in virology related to the research undertaken at the Africa Centre, for which funding would have to be obtained.

This responsible position requires the following qualifications, skills and attributes: ● PhD in Virology ● Strong publications record ● 5 years' post-doctoral experience ● Extensive research experience ● Managerial and supervisory skills ● Ability to work in a multidisciplinary team ● Good interpersonal skills.

Enquiries should be directed to the Director, tel. (035) 550-7500 or e-mail: mnewell@africacentre.ac.za Further details about these positions at the Africa Centre can be obtained from the HR Officer.

Unless otherwise stated, these posts will be offered initially on three-year fixed-term appointments. Extension of these posts will be dependent on funding. The remuneration offered will be dependent on the qualifications and/or experience of the successful applicants. The process of selection will commence on 16 May 2006 and will cease only after the vacancies have been filled or a decision is taken not to fill the posts.

Applicants are required to submit a Curriculum Vitae with certified copies of qualifications and details of three (3) contactable referees to: The Human Resources Officer, Africa Centre, Box 198, Mtubatuba 3935 or fax: (035) 550-7565 or e-mail to acemployment@africacentre.ac.za quoting the relevant reference number.

Human Communications 51380SM

UNITED NATIONS UNIVERSITY

TOKYO, JAPAN

RECTOR

Reference UNU/HQ/2006/001

The United Nations University (UNU) is searching for a new Rector.

The Institution: The UNU is an international community of scholars, engaged in research, postgraduate training and dissemination of knowledge in furthering the purposes and principles of the Charter of the United Nations. The mission of the UNU is to contribute, through research and capacity building, to efforts to resolve the pressing global problems that are the concern of the United Nations, its Peoples and Member States. The UNU's key goals are: to be an international community of scholars; to form a bridge between the United Nations and the international academic community; to serve as a think-tank for the United Nations system; to contribute to capacity building, particularly in developing countries; and to serve as a platform for new and creative ideas and dialogue.

The Position: The Rector is the chief academic and administrative officer of the University and has overall responsibility for the direction, organization, administration and programmes of the University. The position carries the rank of United Nations Under-Secretary-General. The Rector is appointed by the Secretary-General of the United Nations after consultation with the Director-General of UNESCO. The position requires extensive overseas travel. The continuing development and activities of the UNU places ever-increasing demands on the incumbent.

Required qualifications: Advanced university degree, preferably a PhD in a discipline related to the human sciences, sciences of life, the earth and the biosphere. The successful candidate must have a prominent academic profile with evidence of high quality research work in the course of his/her career. Demonstrated management experience as the head of a university or research centre is required. Fluency in English and a working knowledge of French are essential.

Desirable qualifications and characteristics: Experience in the academic world and with international scientific cooperation. Established profile in the international community. Successful track record of fund raising. Knowledge and appreciation of and commitment to the principles and ideals of the United Nations. A wide grasp of the problems of the modern world. Capability to maintain close cooperation with individuals, governments and with research and training institutions worldwide. Great drive and initiative to achieve the goals of UNU. Some knowledge of other UN official languages is desirable.

Address applications to: UNU Rectorship Nominating Committee, United Nations University, 53-70, Jingumae 5-chome, Shibuya-ku, Tokyo 150-8925, Japan. Nominations or letters of application, including full curriculum vitae and names and addresses and fax numbers of three referees should clearly indicate the above reference number. Applications must be sent by post to the above address. No email or fax applications will be accepted.

Application deadline: 31 July 2006.

It is expected that the appointee will take up the position by September 2007. The initial appointment will be for a five-year term, with the possibility of a second term. Applications from women candidates are particularly encouraged.

Postdoctoral Fellowships in Cell and Molecular Biology

Fellowships for the National Research Service Award Program of the National Institute of Diabetes and Digestive Kidney Diseases (NIDDK), National Institutes of Health (NIH) at Stony Brook University, are available in cell and molecular biology of metabolic diseases for candidates with Ph.D., D.Sc., M.D., or equivalent (within five years of Ph.D. for non-clinical applicants). Stipend levels are competitive. This institutional postdoctoral training program is interdisciplinary, interdepartmental, and interinstitutional by design, supported by regional interaction with Brookhaven National Laboratory and Cold Spring Harbor Laboratory. The program benefits from 25+ NIH-supported trainers with state-of-art research programs in areas of cell signaling relevant to diabetes, endocrine, and metabolic diseases.

Current research/mentor opportunities include:

Wadie Bahou: Proteases and endothelial cell pathology; **Deborah Brown:** Lipids rafts and caveolae; **Richard Clark**: Structure-function of non-enzymatic glycated fibronectin that adversely affect cell migration; **Ira Cohen**: Molecular and cellular cardiovascular research; **Howard Crawford**: Matrix metalloproteinases in pancreatic cancer; **Michael Frohman:** Phospholipase D and membrane vesicular trafficking; **Marie Gelato**: Pathogenesis of the insulin resistance and hyperlipidemia in HIV disease; **Jamie Konopka:** G protein-coupled receptors signaling in yeast; **Irwin Kurland:** Hepatic insulin action and role of the pentose shunt; **William Lennarz:** Congenital disorders of glycosylation in humans; **Christopher Lee:** Tumor immunology/cancer vaccine development; **Richard Lin:** G protein signaling and insulin resistance; **Craig Malbon**: GPCRs, scaffold proteins, and Wnt-Frizzled signaling; **Mirjana Maletic-Savatic**: Neural stem cell fate and function; biomarkers of human neurological disorders; **Stuart McLaughlin**: Biophysics of signal transduction; **Margaret McNurlan**: Insulin action in muscle; **Todd Miller:** Signal transduction by tyrosine kinases; **Jeffrey Pessin:** Insulin signaling and regulation of glucose transport; **Mario Rebecchi**: Phospholipase regulation and polyphosphoinositide metabolism; **Nancy Reich:** Cytokine signaling; **Suzanne Scarlata:** Activation of PLC by G proteins; **Ken Takemaru:** Role of beta-catenin antagonist Chibby in adipogenesis; **Fayanne Thorngate:** Apolipoprotein E and signaling in the development of atherosclerosis; **Stella Tsirka**: Neuronal-microglial interactions in the mammalian brain; **Hsien-yu Wang:** G Proteins and development.

Only U.S. citizens or permanent residents (within five years of Ph.D. for non-clinical applicants) are eligible for these NIH-supported fellowships.

Applicants should send a C.V., brief letter of research interest, and names of three references to:
Dr. Craig C. Malbon, Director-DMDRC, Pharmacology, Stony Brook University, Stony Brook, NY 11794-8651.

Fax: (631) 444-7696. For more information or to apply online visit:
www.stonybrook.edu/cjo

Equal Opportunity/Affirmative Action Employer. Women, people of color, individuals with disabilities, and veterans are encouraged to apply.

STONY BROOK

U.S. DEPARTMENT OF ENERGY
Office of Science
Office of Biological and Environmental Research
Intergovernmental Personnel Act (IPA)
Appointment for two Research Program Managers

The U.S. Department of Energy's (DOE) Office of Biological and Environmental Research (OBER), Office of Science, is soliciting applications from university scientists interested in a 2-year assignment (with an option for an additional 2 years) under an Intergovernmental Personnel Act (IPA) assignment. The respective incumbents will serve as research program managers in the Climate Change Research Division of OBER located in Germantown, Maryland. One assignee would serve as the research program manager for the Terrestrial Carbon Sequestration Research Program and manage selected components of DOE's Terrestrial Carbon Cycle Research Program. Information on these two programs is available at: **http://cdiac2.esd.ornl.gov/index.html** and **http://www.science.doe.gov/ober/CCRD/tcp.html**, respectively. A second IPA assignee would manage DOE's Integrated Assessment Research Program. Information on the Integrated Assessment Research Program is available at: **http://www.science.doe.gov/ober/CCRD/ia.html**. To ensure that research sponsored by these programs is effectively coordinated within and among these and other Climate Change Research Programs in DOE, the incumbents would be expected to work in a team setting with other program managers in OBER.

An IPA assignment is a temporary transfer of skilled personnel between the Federal Government and State or local governments, institutions of higher education, Native American tribal governments, and eligible non-Federal "other organizations," including Federally Funded Research and Development Centers. Assignments are implemented through written Assignment Agreements between DOE, the non-Federal employer, and the assignee. For information on Intergovernmental Personnel Act assignments, please refer to the DOE Directive on IPAs at **http://www.directives.doe.gov/cgi-bin/explhcgi?qry1347894433;doe-110**.

Individuals interested in either IPA assignment position are requested to send their resume to: **Dr. Jerry W. Elwood, Director, Climate Change Research Division, Department of Energy, SC-23.3/Germantown Building, 1000 Independence Avenue, SW, Washington, DC 20585-1290 (Phone: 301-903-3281, email: (jerry.elwood@science.doe.gov)**. Applicants are requested to describe their expertise and experience that would enable them to effectively manage the Terrestrial Carbon Sequestration Research and Carbon Cycle Research Program or manage the Integrated Assessment Research Program. These vacancies will remain open until filled. Prior to submitting an application, prospective applicants should know whether their employer would approve the temporary assignment through the IPA Assignment Agreement.

Looking for a great science career?

Get the experts behind you.
Visit www.ScienceCareers.org

Your career is too important to leave to chance. So to find the right job or get career advice, turn to the experts. At ScienceCareers.org we know science. And we are committed to helping take your career forward. Our knowledge is firmly founded on the expertise of *Science*, the premier scientific journal, and the long experience of AAAS in advancing science around the world. Put yourself in the picture with the experts in science. Visit www.ScienceCareers.org.

POSITIONS OPEN

FACULTY POSITION
Assistant/Associate/Full Professor

The Department of Pharmaceutical Sciences at Texas Tech University Health Sciences Center (TTUHSC) seeks applicants for two tenure-track faculty positions at the Assistant/Associate/Full Professor level to join a growing and active group of extramurally funded researchers with interests in receptor biology, cancer, brain/vascular, and pharmaceutical science. Areas of research interest for these two positions include pharmacology, drug delivery, pharmacokinetics, pharmaceutical chemistry, pharmaceutics, or signal transduction. The Department currently has 23 full-time faculty and will grow by six more over the next several years. TTUHSC in Amarillo includes the School of Pharmacy, School of Medicine, and the Harrington Cancer Research Center. For further details on our Department, please visit our **website: http://www.ttuhsc.edu/sop/PharmSci/.** Applicants must have an earned doctorate with relevant postdoctoral experience. In addition to maintaining an extramurally funded research program, the successful candidate will teach in the basic science components of the Pharm.D. and Ph.D. curriculum, and mentor graduate students. Competitive startup packages and space are available. Applicants should submit documents online by July 5, 2006, at **website: http://jobs.texastech.edu** (job requisition number 61359). Please include curriculum vitae, a summary of research and teaching interests, and names and addresses of three references. For questions, contact the **Search Committee Chair: Dr. Margaret Weis, Texas Tech University School of Pharmacy, 1300 Coulter, Amarillo, TX 79106; e-mail: margaret.weis@ttuhsc.edu; fax: 806-356-4034.** *TTUHSC is an Equal Opportunity/Affirmative Action Institution. Minorities and women are encouraged to apply.*

FACULTY POSITIONS
Lung Pathobiology

The Ohio State University, Division of Pulmonary, Allergy, Critical Care and Sleep Medicine **(website: http://www.internalmedicine.osu.edu/pulmonary/index.cfm)** and the Dorothy Davis Heart and Lung Research Institute **(website: http://heartlung.osu.edu/)** are seeking four basic science faculty working in areas related to human genetics of lung disease, acute lung injury/sepsis, or chronic inflammation and repair of the lung. Ph.D. scientists or physician-scientist candidates with a strong record of publications and grant support are encouraged to apply. Send curriculum vitae, statement of research interests and direction, three reference contacts, and cover letter to: **Dr. Clay Marsh, Division Director, The Ohio State University, Pulmonary Critical Care, Allergy and Sleep Medicine, 201 HLRI, 473 W. 12th Avenue, Columbus, OH 43210. Telephone: 614-247-7707; e-mail: clay.marsh@osumc.edu.** *The Ohio State University is an Equal Opportunity/Affirmative Action Employer. Qualified women, minorities, Vietnam era veterans, and individuals with disabilities are encouraged to apply.*

FACULTY POSITION
Anatomy/Cell Biology

The Edward Via Virginia College of Osteopathic Medicine (VCOM) invites applications for a tenure-track, open rank Faculty position in the discipline of anatomy. VCOM is a postbaccalaureate professional medical college located in Blacksburg, Virginia. For more information on this position, please visit our **website: http://www.vcom.vt.edu.**

RESEARCH ASSOCIATE with experience in molecular cell biology. Send resume to: **Dr. Man Sun Sy, Case Western Reserve University, 2103 Cornell Road, Cleveland, OH 44106.** Must reference job code FF3006. *Equal Opportunity Employer.*

POSITIONS OPEN

University of California San Francisco
UCSF
School of Medicine
Office of the Dean

CHAIR, DEPARTMENT OF MEDICINE
School of Medicine
University of California, San Francisco

The School of Medicine at University of California, San Francisco (UCSF) seeks an outstanding individual to lead its Department of Medicine. The successful candidate will have exceptional administrative and organizational skills and a national reputation as a leader in academic medicine in the areas of medical education and research. The individual chosen will have major responsibilities in the overall direction of this distinguished Department. Applicants must be qualified for appointment as a tenured professor in the Department of Medicine.

Please send your curriculum vitae no later than July 10, 2006, to:

Johanna Atienza
School of Medicine,
Univeristy of California, San Francisco
Office of the Dean
513 Parnassus Avenue, Room S-224
San Francisco, CA 94143-0410

Or submit via **e-mail: atienzaj@medsch.ucsf.edu.**

UCSF is an Affirmative Action/Equal Opportunity Employer. The University undertakes affirmative action to assure equal employment opportunity for underutilized minorities and women, for persons with disabilities, and for Vietnam-era veterans and special disabled veterans.

ASSISTANT PROFESSOR
Plant Ecological Genomics
School of Integrative Biology
University of Illinois at Urbana, Champaign

The School of Integrative Biology and the Department of Plant Biology seek an outstanding early career scientist with a background in interdisciplinary research involving aspects of plant ecology, ecosystem biology, plant environmental physiology, genomics, and statistics and/or bioinformatics for a nine-month, tenure-track faculty position at the **ASSISTANT PROFESSOR** level. Candidates must have a Ph.D. The ideal candidate will have extensive familiarity with plant ecology, the ability to develop and implement statistical protocols for complex data analysis, and experience with appropriate genomic and informatic tools to address ecosystem level issues. This new faculty member is expected to develop an externally funded research program to investigate environmentally sensitive genes and processes that shape ecological interactions. The School has a particular interest in interactive responses of plants to abiotic stresses with anthropogenic changes and has world-class facilities for research in this area.

The successful candidate will have the opportunity to be part of a dynamic and well- established life science faculty, as well as a broadly based genomics community forming around the Institute for Genomic Biology, housed in a new state-of-the art facility. Teaching obligations include participation in appropriate graduate and undergraduate instruction, including introductory level biology as well as upper level offerings in ecological genomics and related topics. The proposed starting date is January 2007, or negotiable after closing date; salary is commensurate with experience.

To ensure full consideration, applicants must submit curriculum vitae and statements of research and teaching interests and arrange for three letters of reference to be sent no later than June 30, 2006. Applicants may be interviewed before the closing date; however, no hiring decision will be made until after the closing date. Please send materials to: **The Ecological Genomics Search Committee, School of Integrative Biology, University of Illinois, 286 Morrill Hall, 505 South Goodwin Avenue, Urbana, IL 61801 (telephone: 217-333-3044; fax: 217-244-1224; e-mail: sib@life.uiuc.edu).**

The University of Illinois is an Affirmative Action, Equal Opportunity Employer.

POSITIONS OPEN

ASSISTANT PROFESSOR/ASSOCIATE PROFESSOR. Over the next three to five years, the Hormel Institute, a research unit of the University of Minnesota, expects to double its current research capacity including the construction of a new, state-of-the-art research facility. At this time, we invite applications for one or two faculty appointments at the level of Assistant or Associate Professor. Qualifications: Candidates must demonstrate the ability to establish an independent, extramurally funded research program of biomedical relevance that will complement ongoing programs. Preference will be given to applicants with a strong background in molecular/cell biology, and a highly successful research record in one of the following areas: signal transduction, gene expression, functional genomics, molecular carcinogenesis, chemoprevention, or the regulation of membrane-dependent cellular processes. A Ph.D. (or equivalent) degree and two to three years of postdoctoral experience are required. Individuals with additional research experience and with excellent organizational, supervisory, and communication skills are desired. Please submit curriculum vitae, a research plan, and the names of three references no later than June 15, 2006, to: **Dr. Zigang Dong, The Hormel Institute, 801 16th Avenue N.E., Austin, MN 55912,** or an e-mail Word document attachment to **e-mail: ambode@hi.umn.edu.** *The University of Minnesota is committed to the policy that all persons shall have equal access to its programs, facilities, and employment without regard to race, color, creed, religion, national origin, sex, age, marital status, disability, public assistance status, veteran status, or sexual orientation.*

WESTERN COLLEGE OF VETERINARY MEDICINE

CANADA: The Department of Veterinary Microbiology is seeking applications for a tenure-track faculty position in Public Health and Food Safety. Candidates should have a Ph.D. and research experience in exploring the connection between livestock and human disease. A degree in veterinary medicine (DVM or equivalent) would be desirable. The successful candidate will be expected to teach undergraduate courses in public health and food safety and introductory epidemiology, collaborate with other epidemiologists and microbiologists in graduate training and set up an externally funded independent or collaborative research program.

Requests for further details may be made to:

Vikram Misra, Head
Department of Veterinary Microbiology
Western College of Veterinary Medicine
University of Saskatchewan
52 Campus Drive
Saskatoon SK
CANADA, S7N5B4

Tel: 306-966-7218
Fax: 306-966-7244
e-mail: vikram.misra@usask.ca

Director

Center for Comparative Medicine and Translational Research (CCMTR)
College of Veterinary Medicine
North Carolina State University
Raleigh, NC

The College of Veterinary Medicine at North Carolina State University in Raleigh, North Carolina is seeking a Director of the newly established Center for Comparative Medicine and Translational Research (CCMTR). The successful applicant will have primary responsibility for directing the CCMTR, but will also have the opportunity to continue his or her research program. The CCMTR, representing over seventy faculty in fourteen academic departments across four colleges, engages in collaborative approaches for the comparative study of diseases. The mission of the CCMTR is to enhance collaborative, translational, interdisciplinary approaches for the comparative study of animal and human diseases and to facilitate the movement of innovative discoveries from the bench to the clinics. The members of the center recognize that complex issues affecting human and animal health are better addressed by interdisciplinary, "one medicine", approaches that combine both clinical and non-clinical expertise. This includes interactions between different laboratories as well as interactions with private groups. The ability to provide unique animal models, unique training and expertise, and an environment of innovation will facilitate the development of novel approaches to diagnose and treat human and animal disease. In addition, one of the goals of the center is to establish cooperative agreements with industrial partners in areas of mutual interest. Additional information on the CCMTR is available at **http://www.cvm.ncsu.edu/research/ccmtr/index.htm**.

The successful candidate should be a senior level faculty (Full Professor preferred) with a demonstrated record of research accomplishment and experience in providing programmatic organization and leadership. D.V.M. and/or PhD or equivalent degree is required. To apply or for further information go to **http://jobs.ncsu.edu** and search by Position Number **B-64-0601**. Applicants will complete an electronic applicant profile and should attach a curriculum vitae, a letter in which professional goals are outlined, and the names and addresses of three references the committee may contact. Review of applications will commence **May 22, 2006** and continue until the position is filled. Questions about the position can be directed to: **Dr. Jorge A. Piedrahita, Search Committee Chair, College of Veterinary Medicine, North Carolina State University, 4700 Hillsborough St., Raleigh, NC 27606; jorge_piedrahita@ncsu.edu**.

North Carolina State University is an Equal Opportunity and Affirmative Action Employer. In addition, NC State University welcomes all persons without regard to sexual orientation.

Careers in Biotechnology & Pharmaceuticals 2

Advertising Supplement

Be sure to read this special ad supplement devoted to opportunities in biotechnology & pharmaceuticals in the upcoming **16 June issue of *Science*.**

You can also read it online on **www.sciencecareers.org.**

For information, contact:

U.S. Daryl Anderson
phone: 202-326-6543
e-mail: danderso@aaas.org

Europe and International
Tracy Holmes
phone: +44 (0) 1223 326 500
e-mail: ads@science-int.co.uk

Japan Jason Hannaford
phone: +81 (0) 52 789-1860
e-mail: jhannaford@sciencemag.jp

ScienceCareers.org
We know science AAAS

Tenure-Track Faculty Position in Zoonotic Diseases

The Western College of Veterinary Medicine invites applications for a tenure-track faculty position in zoonotic diseases. This new position has been created specifically to enhance the College's program in public health and to participate in an exciting new interdisciplinary Master of Public Health (MPH) program. The ideal candidate will possess a DVM, MD, or equivalent degree. Advanced training to the PhD level with research and teaching experience in zoonotic diseases is required. The successful applicant will be a full participant in the MPH program, teaching graduate-level courses and developing a research program in zoonotic diseases and public health. Involvement in the veterinary undergraduate teaching program is expected.

Requests for further details should be directed to:

Office of the Dean
Western College of Veterinary Medicine
University of Saskatchewan
52 Campus Drive
Saskatoon, SK
Canada, S7N 5B4

E-mail: elaine.angielski@usask.ca
Telephone: 306-966-7448
Fax: 306-966-7314

IMMUN. & INFECTIOUS DISEASES

Are you ready to use your education and experiences to make the world a better place? Do you want to be part of a team that is doing exciting work? Then you are ready to join the team at the Institute for One World Health, the first non-profit pharmaceutical company in the US. We are a Medical Research Organization which advances global health by developing effective and affordable new medicines for infectious diseases that disproportionately affect people in the developing world.

- **Project Managers**
- **Director Clinical Operations**
- **Toxicologist**
- **Biostatistician**
- **Clinical Research Associates (CRAs)**

The Institute for One World Health is growing and searching for passionate and talented industry professionals to help us fulfill our mission of developing safe, effective, and affordable new medicines for people with diseases of poverty in the developing world. For a current listing of open positions in our San Francisco office please visit the employment page on our website **http://www.oneworldhealth.org**.

iOWH is committed to a policy of non-discrimination and Equal Opportunity for all qualified applicants without regard to race, color, sex, national origin, age, disability, veteran status or ancestry.

POSITIONS OPEN

Fluidigm

SENIOR APPLICATIONS DEVELOPMENT SCIENTIST
Job 2006-17-SCI

Fluidigm seeks a pragmatic winner in the laboratory to develop homogeneous fluorescent assays and integrated fluidic circuits for the detection of rare mutants in an advanced microfluidic format for the Fluidigm BioMark instrument platform. Requires a Ph.D. in molecular biology, biochemistry, or chemistry; over five years of experience in assay development and commercialization; experience designing homogeneous fluorescent PCR assays to detect rare mutations; the ability to independently run experiments, analyze data, interpret results, modify procedures, and maintain records of experiments; success developing/designing procedures for commercial customers; and knowledge of statistics. E-mail resume and cover letter to **e-mail: jobs@fluidigm.com.** View complete job description at **website: http://www.fluidigm.com.** *Equal Opportunity Employer.*

CHAIR OF BIOCHEMISTRY AND MOLECULAR BIOLOGY
Uniformed Services University of the Health Sciences

The Uniformed Services University seeks applications for the position of Chair of the Department of Biochemistry and Molecular Biology, a tenured position within the F. Edward Hébert School of Medicine. Candidates, *who must be U.S. citizens or permanent residents,* should have an outstanding record of accomplishments, including an internationally recognized research program in biochemistry or a related discipline, and leadership skills to oversee the research programs of the Department and to direct the teaching of biochemistry in the School of Medicine. Salary and benefits will be based on federal government pay scales for senior scientists. Further information on the position can be obtained from the Search Committee; the Department website can be found at **website: http://bio.usuhs.mil.** We welcome nominations of qualified persons. Applications should be sent to:

Brian M. Cox, Ph.D.
Chair, Biochemistry Search Committee
Department of Pharmacology
Uniformed Services University
4301 Jones Bridge Road
Bethesda, MD 20814-4799
E-mail: bcox@usuhs.mil

The University is an Equal Opportunity Employer committed to excellence through diversity.

POSTDOCTORAL RESEARCH POSITIONS
Molecular Immunology of Infectious Diseases

The U.S. Army Medical Research Institute of Infectious Diseases (USAMRIID) in Frederick, Maryland, has research appointments available for highly motivated and qualified candidates with a Ph.D. or M.D. and zero to five years of relevant postgraduate experience. Studies include cell biology of intracellular bacteria, innate immune sensing, novel vaccine and therapeutic strategies directed toward Centers for Disease Control and Prevention category A, B pathogens. Stipends are highly competitive and commensurate with experience. *U.S. citizenship or permanent residence status required.* To apply, please forward a cover letter and curriculum vitae to: **Dr. Robert G. Ulrich, Laboratory of Molecular Immunology, e-mail: ulrich@ncifcrf.gov** or **e-mail: robert.ulrich@amedd.army.mil.**

POSITIONS OPEN

FACULTY POSITIONS
Massachusetts Institute of Technology

The Department of Earth, Atmospheric, and Planetary Sciences at MIT invites applicants to fill multiple faculty positions in the geological sciences. We seek individuals with a breadth of research interests, a strong interest in field-based observation, and a commitment to interdisciplinary studies. Particular attention will be given to candidates in the areas of structure and tectonics, metamorphic petrology, igneous petrology/geochemistry, surface processes, and low-temperature geochronology. Strong preference will be given to candidates at the junior faculty level.

Interested individuals should send curriculum vitae, one-page descriptions of research and teaching plans, and the names of three potential professional references to: **Professor Maria T. Zuber, Head, Attention: Geology Faculty Search, Department of Earth, Atmospheric, and Planetary Sciences, Massachusetts Institute of Technology, 77 Massachusetts Avenue, 54-918, Cambridge, MA 02139-4307,** or by **e-mail: mtz@mit.edu. Fax: 617-253-7651.**

MIT is an Equal Opportunity/Affirmative Action Employer; applications from women and underrepresented minority candidates are encouraged. MIT is a nonsmoking environment.

DIRECTOR
Biomedical Nuclear Magnetic Resonance Laboratory, Department of Radiology
Dartmouth Medical School

Appointment will be made at the **ASSISTANT, ASSOCIATE,** or **PROFESSORIAL** level. Requires expert knowledge in techniques and applications of in vivo nuclear magnetic resonance (NMR). Goals include: developing an independent externally funded high quality research program utilizing NMR; directing multi-user small animal NMR facility of the Department of Radiology, a 7T system with a Varian Console and collaborating with other basic and clinical investigators.

We will begin consideration of completed applications on June 1, 2006.

Submit curriculum vitae and three references with contact information to:

Harold M. Swartz, M.D., Ph.D.
Dartmouth Medical School, 702 Vail
Hanover, NH 03755
Fax: 603-650-1717
E-mail: harold.swartz@dartmouth.edu

Equal Opportunity/Affirmative Action Employer.

Department of Pathology at Columbia University Medical Center seeks candidate at level of **STAFF ASSOCIATE** or **SENIOR STAFF ASSOCIATE** to manage robotic screening facility **(website: http://www.ColumbiaMNC.org).**

Candidate will screen collections of chemical compounds and viral vectors in cell-based and other biological assays. B.S. with four to eight years or M.S. with two to six years of relevant experience required. Send resume to **Dr. Chris Henderson** at **e-mail: ch2331@columbia.edu.**

We are an Affirmative Action/Equal Opportunity Employer.

The laboratory of **Mani Pashmforoush, M.D., Ph.D.,** at University of Southern California's Institute for Genetic Medicine is interested in discovering the transcriptional regulation of cardiac development. A funded **POSTDOCTORAL POSITION** is available immediately. Experience in developmental biology techniques including in-situ hybridization, immuno-histochemistry, DNA cloning, and mouse embryo manipulation is preferred. Applicants are requested to e-mail curriculum vitae to **e-mail: mpashmfo@usc.edu.**

AWARDS

RANBAXY RESEARCH AWARDS 2005

RESEARCH FOR LIFE
RANBAXY
SCIENCE FOUNDATION

Nominations are invited from Heads of Research Institutions, Universities and Medical & Pharmaceutical Colleges, for the Ranbaxy Research Awards-2005. There are four Awards of Rs. 1 lakh each, for excellence in original research, in Medical and pharmaceutical Sciences.

Medical Sciences
One Award each for Basic Research, Medical Research and Clinical Research.

Pharmaceutical Sciences
One Award

The sponsored work of Indian scientists, both in India and abroad, together with their bio-data, research achievements, awards received in the past and papers published, may be forwarded (in 12 bound sets) to the Ranbaxy Science Foundation by July 1, 2006.

Details of the procedure are being circulated to nominators and are also available from the office of the Foundation and on **our Website**. A panel of judges, comprising eminent scientists, will review the research work. Non-resident Indian scientists are also eligible for these awards.

Dr. O.P. Sood
Member-Governing Council
RANBAXY SCIENCE FOUNDATION
77B, Sector 18, IFFCO Road, Udyog Vihar Industrial Area, Gurgaon-122 015 (Haryana) India
Phone : 91-124-2341477 (D) 2342001-10, 5012501-10
Fax : 91-124-2342018, 2342017
E-mail : omprakash.sood@ranbaxy.com
Website : http://www.ranbaxysciencefoundation.com

Max Planck Institute for Demographic Research

International Max Planck Research School for Demography

The Max Planck Institute for Demographic Research intends to foster interdisciplinary research in biodemography by promoting early career development.

For this purpose it organizes a

Summer School on Biodemography

Date: 24th July – 17th August 2006

Location: Max Planck Institute for Demographic Research, Rostock, Germany

Content and organization: Biodemography is a new branch of demography concerned with understanding the complementary biological and demographic determinants of and interactions between birth and death processes that shape individuals, cohorts and populations. The Summer School on Biodemography is divided into two lecture series and an international research workshop. In the first lecture series James Carey and James Vaupel give an introduction to the principles of biodemography, based primarily on a book in progress by Carey and Vaupel. The second lecture series addresses matrix methods in biodemography and is presented by Hal Caswell. The lecture series begin on 24th July and end on 11th August 2006. Instruction is given in the form of two two-hour lectures every day from Monday to Friday. The research workshop titled "2nd International Workshop on the Evolutionary Demography of Aging" focuses on the ultimate evolutionary determinants of age patterns of mortality across species, and will be held after the lecture series end, for three full days, 15th-17th August 2006.

Application: Advanced doctoral students and young research scientists (i.e., dissertation completed within the last three years) are encouraged to apply. Applicants should have a strong interest in biology and understand elementary calculus, basic matrix algebra, and introductory probability and statistics. Scholarships are available.
Visit **www.demogr.mpg.de/school** for more information and application instructions. Application deadline is **20th May 2006**. Review of applications will continue until all student positions have been filled.

MAX PLANCK SOCIETY

POSITIONS OPEN

The laboratory of **Dr. Atul Butte** in Stanford Medical Informatics is seeking highly motivated **POSTDOCTORAL FELLOWS** to develop and study novel bioinformatics methods in translational bioinformatics.

Ideal candidates will have an M.D. or Ph.D. with a strong background in bioinformatics, biostatistics, and genomics, and a good publication record. Experience with biological databanks and programming experience with Linux, Perl, or Java (or equivalent), and databases such as MySQL is required. Strong problem-solving skills, creative thinking, and the ability to build new software applications are required. Applicants must possess good communication skills and be fluent in both spoken and written English. A background in molecular biology or medicine will be a strong plus. Prior experience with microarray analysis, XML, the R statistical package, knowledge representation, or parallel computing platforms is also a plus. This exciting work will be guided by multidisciplinary collaborations with top scientists in stem-cell, immunology, and transplantation research at Stanford.

To apply, please send your curriculum vitae, a brief statement of research interests, and contact information for three references to **Julie Schnitzer, e-mail: julie.schnitzer@stanford.edu, telephone: 650-724-4381.**

CHIEF MEDICAL OFFICER

Highly intelligent individual with exceptional communication skills sought by prominent Manhattan family to research and coordinate family medical and healthcare issues. Act as liaison with leading medical researchers and consultants in academia and industry, with full responsibility for technical, financial, and administrative functions. Considerable weight given to evidence of unusual academic or other intellectual distinction. Ph.D. or M.D. required, clinical experience a plus but not essential. Possible entrepreneurial opportunities involving delivery of ultrahigh-end medical care to other, similar families. Full- time position. Excellent compensation with significant upside potential and management possibilities. Resume to **e-mail: fmc4@spsfind.com.**

POSTDOCTORAL RESEARCH POSITION

Position is available in the Laboratory of Cellular and Molecular Cerebral Ischemia to study neuronal, vascular, and inflammatory mediators of oxidative stress and cellular plasticity (**K. Maiese, F. Li, and Z.Z. Chong,** *JAMA* **293:** 90-95, 2005, **Z.Z. Chong, F. Li, and K. Maiese,** *Prog. Neurobiol.* **75:** 207-246, 2005). Expertise in molecular biology with in vitro and in vivo experimental models is desired. Please forward curriculum vitae and three references to: **Kenneth Maiese, M.D., Neurology, 8C-1 UHC, Wayne State University, 4201 Street Antoine, Detroit, MI 48201, fax: 313-966-0486, e-mail: kmaiese@med.wayne.edu.** *Wayne State University is an Equal Opportunity/Affirmative Action Employer.*

COMPUTATIONAL CELL BIOLOGY
Virginia Tech

A two-year **POSTDOCTORAL POSITION** is available immediately to conduct research in the area of mammalian cell cycle regulation in collaboration with **Professor John Tyson.** The work involves modeling molecular regulatory pathways using nonlinear ordinary differential equations. Candidates must have a Ph.D. degree, experience in mathematical modeling, and an interest in applying models to problems in the molecular biology of cancer. For additional details and to apply online, see **website: http://www.jobs.vt.edu** (posting number 060374). *Virginia Tech is an Equal Opportunity Employer.*

A **POSTDOCTORAL POSITION** is available in Purdue University to study signaling mechanisms of cell cycle, especially functions of Polo kinases in mammalian cells. Ideal applicants should have Ph. D. in cell biology, and experience in signal transduction is preferred. Please send resumes to **Dr. Xiaoqi Liu** via **e-mail: liu8@purdue.edu.** *Purdue University is an Equal Opportunity, Equal Acess, Affirmative Action Employer.*

POSITIONS OPEN

POSTDOCTORAL TRAINING
Clinical/Translational Biodefense and Emerging Infectious Disease Research

Positions supported by the NIH/National Institute of Allergy and Infectious Disease Region VIII Regional Center for Excellence in Biodefense grant are available at the University of Colorado at Denver and Health Sciences Center (UCDHSC) for advanced postdoctoral training leading to careers in biodefense-related clinical/translational research. Candidates should have Ph.D., M.D., M.D./Ph.D., D.V.M, or D.V.M./Ph.D. degrees, demonstrated competency and productivity in research, and strong interest in obtaining training in translational research involving select agents and/or emerging infectious diseases. Applicants pursuing biodefense research *must be U.S. citizens or permanent residents of the United States,* and appointment is contingent on receiving federal authorization to work with select agents at UCDHSC. Positions are available immediately, starting dates are flexible, and successful candidates are eligible for support for up to two years from this funding source. The research facilities and the training environment at UCDHSC are excellent. Compensation is determined by NIH policies for postdoctoral training. To apply send curriculum vitae and bibliography, names of three professional references with contact information, and a cover letter describing both past research experience and future career goals in biodefense/emerging infectious disease-related research. Send application materials to: **Randall K. Holmes, M.D., Ph.D., UCDHSC Department of Microbiology, Mail Stop 8333, P.O. Box 6511, Aurora, CO 80045,** or **e-mail: randall.holmes@uchsc.edu.** *The University of Colorado at Denver and Health Sciences Center is committed to diversity and equality in education and employment.*

RESEARCH ASSOCIATE
Cell Biology

The Section of Nephrology at the University of Chicago **(website: http://nephrology.bsd.uchicago.edu)** is seeking a Ph.D. scientist experienced in cell biology for a Research Associate position; academic rank and salary will be commensurate with previous experience and accomplishments. The primary activity of a Research Associate is academic research in association with a faculty member or team. Studied will be a diversity of cultured renal cells using microscopic, biochemical, molecular biologic and genomic approaches. At least five years of experience in the study of cultured cells, including with imaging, signal transduction, transfection, and epigenetic aspects is required. Our ongoing work is in immunopathology, although experience in this area is not essential. Substantial resources are in place for this work, including a new confocal microscopy system and the Sectional-operated Functional Genomics Facility **(website: http://fgf.bsd.uchicago.edu).** Send curriculum vitae and names of three references via e-mail to: **Dr. Richard Quigg, Chief, Section of Nephrology, e-mail: rquigg@uchicago.edu.** *The University of Chicago is an Affirmative Action/Equal Opportunity Employer.*

SCIENTIST. Research with Master's or foreign equivalent in pharmaceutical science and one year of experience to develop generic prescription (oral solid or liquid) dosage forms as per current good manufacturing practice (cGMP) requirements. Prepare chemicals, manufacturing, and controls for submission of Abbreviated New Drug Applications. Prepare protocols and write reports. Formulate oral solid dosage forms using drug delivery technologies. Perform scale-up studies based on Scale-Up and Post-Approved Changes (SUPAC) guidance. Review in vivo clinical study reports for FDA submissions. One year of experience as Drugs Inspector is acceptable. Mail resumes to: **Accumed Inc., 2572 Brunswick Pike, Lawrenceville, NJ 08648.** Job location: Lawrenceville, New Jersey. Human Resources Department. *Equal Opportunity Employer.*

POSITIONS OPEN

POSTDOCTORAL RESEARCH POSITIONS
Protein Biophysics of Infectious Diseases

The U.S. Army Medical Research Institute of Infectious Diseases (USAMRIID) in Frederick, Maryland has research appointments available for highly motivated and qualified candidates with a Ph.D. or M.D. and zero to five years of relevant postgraduate experience. Studies include developing protein interaction networks (interactomes) for Centers for Disease Control and Prevention category A, B pathogens and discovery of novel protein assemblies. Prior experience in analytical methods for measuring protein-protein interactions desired. Stipends are highly competitive and commensurate with experience. *U.S. citizenship or permanent residence status required.* To apply, please forward a cover letter and curriculum vitae to: **Dr. Robert G. Ulrich, Laboratory of Molecular Immunology, e-mail: ulrich@ncifcrf.gov** or **e-mail: robert.ulrich@amedd.army.mil.**

MARKETPLACE

TRANSFECTION

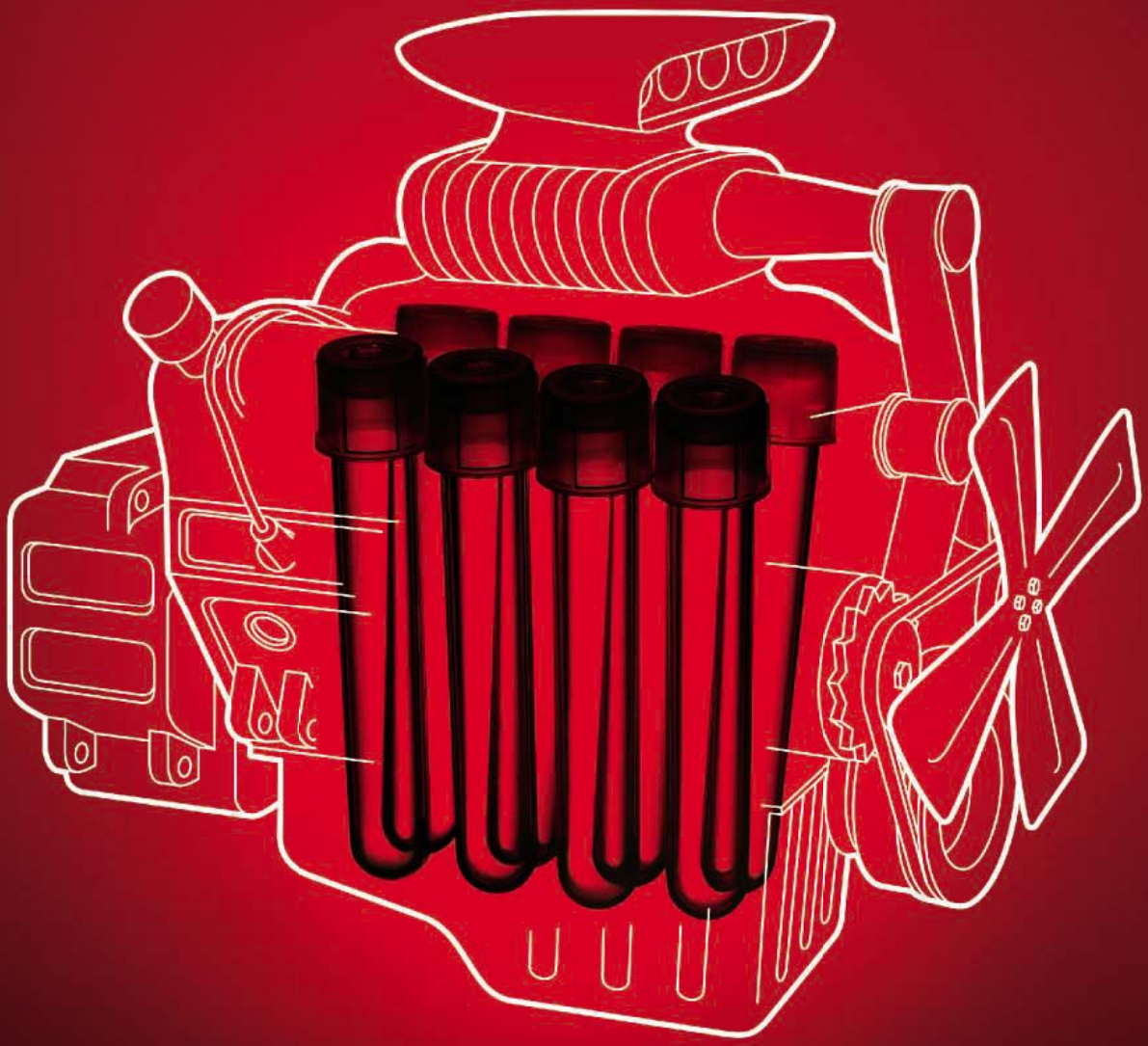

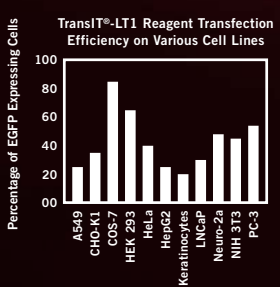

POWER YOUR RESEARCH

***Trans*IT®-LT1 Transfection Reagent from Mirus Bio. Efficiency at its peak.** Get powerful plasmid delivery and expression without sacrificing cell viability. Invented by Mirus Bio scientists to work with a broad range of cell types, our low-toxicity reagent delivers accurate results in two simple steps. Keep cells healthy and research moving forward with transfection technology from the pioneers in gene delivery. Because your research begins at the bench — it doesn't end there.

Mirus®

It All Begins at the Bench

Visit mirusbio.com to view our extensive citation database.